UNIVERSIDADE FEDERAL DE CIÊNCIAS DA SAÚDE DE PORTO ALEGRE – UFCSPA
CURSO DE PÓS-GRADUAÇÃO EM BIOCIÊNCIAS

Jeferson Gustavo Henn

Avaliação da eficácia de uma nanoemulsão de temozolomida e da influência de co e pré-tratamentos com ferroceno em linhagens celulares de glioblastoma humano

Porto Alegre
2023

Jeferson Gustavo Henn

Avaliação da eficácia de uma nanoemulsão de temozolomida e da influência de co e pré-tratamentos com ferroceno em linhagens celulares de glioblastoma humano

Tese submetida ao Programa de Pós-Graduação em Biociências da Fundação Universidade Federal de Ciências da Saúde de Porto Alegre como requisito para a obtenção do grau de Doutor

Orientadora: Dra. Dinara Jaqueline Moura

Porto Alegre
2023

Catalogação na Publicação

Henn, Jeferson Gustavo
Avaliação da eficácia de uma nanoemulsão de temozolomida e da influência de co e pré-tratamentos com ferroceno em linhagens celulares de glioblastoma humano / Jeferson Gustavo Henn. -- 2023.
175 p. : 30 cm.

Tese (doutorado) -- Universidade Federal de Ciências da Saúde de Porto Alegre, Programa de Pós-Graduação em BioCiências, 2023.

Orientador(a): Dinara Jaqueline Moura.

1. Glioblastoma. 2. Temozolomida. 3. Nanoemulsão. 4. Ferroceno. 5. Espécies reativas de oxigênio. I. Título.

Sistema de Geração de Ficha Catalográfica da UFCSPA com os dados fornecidos pelo(a) autor(a).

INSTITUIÇÕES E FONTES FINANCIADORAS

Este trabalho foi realizado no Laboratório de Genética Toxicológica da Universidade Federal de Ciências da Saúde de Porto Alegre, e no *Biological Research Institute* e *Materials Research Institute* da *Technological University of the Shannon: Midlands Midwest,* Athlone, Irlanda. O projeto teve suporte financeiro da Fundação de Amparo à Pesquisa do Estado do Rio Grande do Sul (FAPERGS), da Coordenação de Aperfeiçoamento de Pessoal de Nível Superior (CAPES) e do Conselho Nacional de Desenvolvimento Científico e Tecnológico (CNPq).

Dedico este trabalho aos meus pais, Maria e Nestor, por sempre garantirem que eu tivesse a melhor educação possível e que, mesmo muitas vezes não entendendo as minhas escolhas, jamais deixaram de me apoiar.

AGRADECIMENTOS

À minha orientadora e amiga Dinara, a quem eu devo boa parte do que sei e sou profissionalmente. Obrigado por ter me aceito como teu aluno, por ter me lapidado, e por ter me proporcionado a liberdade de escolha durante esta trajetória acadêmica.

À profa. Jenifer, por ter me aberto as portas do Lab GenTox, e por ser uma inspiração científica, e à profa. Tanira, pelo auxílio incondicional neste trabalho.

Ao Lab GenTox, que me apresentou amigos que levarei para a vida toda. Um abraço especial à Adri, Bru's, Cris, Dani, Fran, Helena, Jú, Michi, Natalia, Nina, Paulinha, Vick's, e ao Juli, Pablito e Rick, por todas as trocas de experiências, pelos almoços, cafés, sorvetes, sushis e rolês aleatórios. Aos melhores parceiros científicos que eu pude ter: Matheus (meu braço direito e esquerdo), Ana Moira, Luiza e Nathi, muitíssimo obrigado pela amizade, por todos estes anos de convivência, por dividirem a bancada comigo, por tanta troca e cumplicidade. Desejo todo o sucesso do mundo a vocês.

Aos amigos que fiz na academia Kyokushin, por terem me apresentado ao Margot, Opinião e às cervejadas, e por terem feito de POA uma das melhores fases da minha vida. É sempre um prazer enorme reencontrá-los. Torço pelo sucesso e pela felicidade de cada um de vocês.

Bibi, Gui, Gugu, Titi e Yu: obrigado por compartilharem tanto comigo nestes quase 4 anos de 'Irlandinha'. A vida aqui tem mais graça com vocês por perto. Que o futuro nos reserve ainda mais oportunidades de desvendar esse mundão juntos. À Vivi e à Marina, pelas risadas em meio ao 'ranço' e ao desespero dos experimentos malsucedidos, pelas junções na cozinha, no centro ou até no Lidl. Desejo um mundo de realizações a vocês. À Emma, minha irlandesa com alma brasileira: obrigado por todo o apoio e pelos momentos tanto no lab como nos pubs.

Ao meu amigo Léo, que mesmo estando longe foi o maior responsável por manter minha sanidade mental durante estes anos, seja me xingando, ou com intermináveis e hilárias videochamadas, com os mais variados assuntos. À Vanessa, minha irmã da vida, pelos anos de convivência em POA com a Phoebe, minha sobrinha de 4 patas. É muito bom saber que continuamos perto, agora na

Europa. Espero que possamos desfrutar cada vez mais de momentos juntos, como nos velhos tempos.

Às agências de fomento FAPERGS, CAPES e CNPq, pelo apoio financeiro deste projeto. Ao professor Michael Nugent, por ter proporcionado minha vinda à Irlanda e minha inserção no seu grupo de pesquisa.

Aos meus amigos e familiares de Sinimbu e Santa Cruz, que mesmo com a distância sempre torceram por mim.

Por fim, agradeço aos meus pais, Maria e Nestor, pela vida, pelos ensinamentos, por todo o estímulo, por nunca terem deixado me faltar nada, e por me mostrarem que desistir jamais está nos planos. Se cheguei até aqui, boa parte se deve a vocês, e essa conta eu jamais conseguirei pagar. Obrigado por tudo! Amo vocês!

“Quando a educação não é libertadora,
o sonho do oprimido é ser o opressor.”
Paulo Freire

SUMÁRIO

LISTA DE ABREVIATURAS, SÍMBOLOS E UNIDADES

BER: reparo por excisão de bases (do inglês *base excision repair*)

BHE: barreira hematoencefálica

DDS: sistema de entrega de fármacos (do inglês *drug delivery system*)

DNA: do inglês *deoxyribonucleic acid*

ERK1/2: do inglês *extracellular signal-regulated kinase 1/2*

Fc: ferroceno

FDA: do inglês *U.S. Food and Drug Administration*

GB: glioblastoma

H_2O_2: peróxido de hidrogênio

HR: recombinação homóloga (do inglês *homologous recombination*)

HPMA: *N*-(2-hidroxipropil)-metacrilamida

IARC: do inglês *International Agency for Research on Cancer*

IDH: isocitrato desidrogenase

INCA: Instituto Nacional do Câncer

MGMT: O^6-metilguanina-DNA metiltransferase

MMR: reparo por mal pareamento do DNA (do inglês *mismatch repair*)

MTIC: 3-metil-(triazen-1-il)imidazol-4-carboximida

NADPH: do inglês *nicotinamide adenine dinucleotide phosphate*

NE: nanoemulsão

NHEJ: reparo por junção de extremidades não-homólogas (do inglês *non-homologous end joining*)

nm: nanômetro

NP: nanopartícula

·OH: radical hidroxila

OMS: Organização Mundial da Saúde

O^6-MG: O^6-metilguanina

PEG: polietilenoglicol

PI3K/AKT: do inglês *phosphoinositide 3-kinase/protein kinase B*

QD: do inglês *quantum dots*

RNA: do inglês *ribonucleic acid*

ROS: espécies reativas de oxigênio (do inglês *reactive oxygen species*)

SNC: sistema nervoso central

TMZ: temozolomida

WHO: do inglês *World Health Organization*

LISTA DE FIGURAS E TABELAS

RESUMO

O glioblastoma é um glioma de grau IV, ocorrendo predominantemente em adultos e com características altamente agressivas. O tratamento convencional para este tipo tumoral compreende ressecção cirúrgica, seguida de radioterapia combinada com quimioterapia utilizando temozolomida. Estas abordagens terapêuticas desempenham um papel essencial na gestão clínica da doença, embora ainda resultem em um prognóstico desfavorável, com uma média de sobrevida global de apenas 14 a 19 meses. Isto ocorre principalmente devido à natureza inoperável da maioria dos tumores e à resistência crescente à quimioterapia quando estes são diagnosticados em estágios avançados, o que justifica a necessidade pela busca de novas moléculas e estratégias terapêuticas para o seu tratamento. O recente progresso na área da nanotecnologia, com o desenvolvimento de sistemas de entrega de fármacos como as nanoemulsões, e a ação sensibilizante tumoral e geradora de espécies reativas de oxigênio do ferroceno, têm trazido novas possibilidades à complementação da quimioterapia em diversos tipos de câncer, aumentando a eficácia dos tratamentos. Neste contexto, esta tese apresenta dois capítulos abordando (i) as diferentes nanoestruturas já desenvolvidas para a entrega de moléculas no tratamento do câncer, como estas conseguem atingir o ambiente tumoral e aumentar a toxicidade nos tecidos-alvo, e as barreiras que estes sistemas enfrentam para alcançar resultados positivos, bem como (ii) o desenvolvimento, a caracterização e a avaliação da citotoxicidade de uma nanoemulsão contendo temozolomida e sua combinação com ferroceno em linhagens celulares de glioblastoma humano. A caracterização físico-química da nanoemulsão revelou a presença da temozolomida na interface do sistema, permitindo sua rápida liberação. Em combinação com o ferroceno, reduziram a viabilidade celular em tratamentos agudos e em regime de dois ciclos, aumentando a sensibilidade à temozolomida da linhagem celular T98G por meio da alteração do potencial da membrana mitocondrial, com uma indução de espécies reativas de oxigênio, com consequente morte celular. Estes resultados demonstraram a eficácia do uso de uma nanoemulsão contendo temozolomida e sua combinação com ferroceno como uma efetiva abordagem ao tratamento do glioblastoma. Além

disso, o rápido desenvolvimento da nanomedicina e o constante melhoramento das técnicas relacionadas apontam para um futuro promissor no tratamento de diversos tipos de câncer com um possível aumento da qualidade de vida destes pacientes.

Palavras-chave: *Glioblastoma. Temozolomida. Nanomedicina. Nanoemulsão. Ferroceno. Espécies reativas de oxigênio.*

ABSTRACT

Glioblastoma is a grade IV glioma, occurring predominantly in adults and with highly aggressive characteristics. Its conventional treatment involves surgical resection followed by combined radiotherapy and chemotherapy using temozolomide. These therapeutic approaches play an essential role in the clinical management of the disease, although they still result in a poor prognosis, with an average overall survival of only 14 to 19 months. This is mainly due to the inoperable nature of most tumors and the increasing resistance to chemotherapy when diagnosed at advanced stages, justifying the need to search for new molecules and therapeutic strategies for its treatment. Recent progress in the field of nanotechnology, with the development of drug delivery systems such as nanoemulsions, and the tumor-sensitizing and reactive oxygen species generating action of ferrocenes, have brought new possibilities for complementing chemotherapy in various types of cancer, increasing treatment effectiveness. In this context, this thesis presents a compilation of two chapters addressing (i) the different nanostructures already developed for the delivery of molecules in cancer treatment, how they can reach the tumor environment and increase toxicity in target tissues, and the barriers these systems face to achieve positive results, as well as (ii) the development, characterization, and evaluation of the cytotoxicity of a nanoemulsion containing temozolomide and its combination with ferrocene in human glioblastoma cell lines. The physicochemical characterization of the nanoemulsion revealed the presence of temozolomide at the system interface, allowing its rapid release. In combination with ferrocene, it reduced cell viability in acute treatments and in a two-cycle regimen. This reduction in viability in the T98 cell line appears to be associated with changes in mitochondrial membrane potential, increasing the generation of reactive oxygen species, therefore leading to cell death. These results demonstrated the effectiveness of using a nanoemulsion containing temozolomide and its combination with ferrocene as an effective approach to glioblastoma treatment. Furthermore, the rapid development of nanomedicine and ongoing improvements in related

techniques point to a promising future in the treatment of various types of cancer and the improvement of the quality of life for these patients.

Keywords: *Glioblastoma. Temozolomide. Nanomedicine. Nanoemulsion. Ferrocene. Reactive oxygen species.*

1 INTRODUÇÃO

O câncer é caracterizado pelo crescimento desordenado de células anormais, apresentando desorganização parenquimal de tecidos e órgãos e o consequente comprometimento fisiológico do sistema acometido. A etiologia da doença envolve diversas características, como a ocorrência de danos ao DNA e o estresse replicativo, que geralmente geram algum tipo de instabilidade genômica, bem como desordens no sistema imunológico, o aporte angiogênico e a recorrência de tumores em razão da invasão tecidual e metástase (Negrini et al., 2010).

Considerando a diversidade de tipos celulares presentes no conjunto tumoral, a comunidade científica enfrenta um desafio significativo não apenas na compreensão abrangente das vias afetadas, mas também na busca por abordagens terapêuticas que alcancem eficácia com taxas reduzidas de efeitos colaterais. Esse desafio é facilmente evidenciado quando observados os dados epidemiológicos da doença em anos recentes. Conforme a *World Health Organization* (WHO), o câncer foi responsável por quase 10 milhões de mortes em 2020, o que representa em torno de uma em cada seis mortes, desta forma ocupando o 2º lugar entre as principais causas de morte no mundo, atrás apenas das doenças cardiovasculares (Bray et al., 2018; WHO, 2020). De acordo com a *International Agency for Research on Cancer* (IARC, 2020), para o período entre 2020 e 2040, é esperado um total de 30,2 milhões de novos casos de câncer em todo o mundo, representando um aumento de aproximadamente 60% em relação ao número atual, além de 19,3 milhões de óbitos.

No Brasil, no ano de 2020, foram registrados 552.212 novos casos de câncer e ocorreram 259.949 mortes relacionadas a essa doença (Bray et al., 2018). Conforme dados do Instituto Nacional do Câncer (INCA, 2020), as estimativas para o Brasil nos anos de 2020 a 2022 previam cerca de 625 mil novos casos, com uma projeção de aumento de até 50% até 2025, principalmente devido ao envelhecimento e ao crescimento da população. Estimativas indicam que a incidência de câncer deverá aumentar em quase 80% até 2040, acompanhada por um crescimento de 83% nas taxas de mortalidade. Em geral, a incidência e a letalidade do câncer estão em ascensão globalmente, impulsionadas tanto pelo envelhecimento quanto pelo aumento populacional, bem como pelas mudanças

nos padrões de risco da doença, especialmente aqueles relacionados ao desenvolvimento socioeconômico (Rezende et al., 2019).

Ao se concentrar exclusivamente nos tumores que afetam o sistema nervoso central (SNC), os gliomas representam 28% de todos os tumores primários cerebrais e 80% dos tumores malignos deste sistema (Ostrom et al., 2015). De maneira geral, o termo "glioma" engloba uma variedade de tumores gliais, tanto benignos quanto malignos e, apesar de sua incidência relativa ser baixa, apresentam um prognóstico desfavorável e impacto negativo na qualidade de vida e função cognitiva dos pacientes (Guntuku et al., 2016). Estes tumores são categorizados com base em sua histopatologia, e os astrocitomas de grau IV, conhecidos como glioblastomas (GBM), são os mais agressivos (R. Chen et al., 2017), representando a maioria dos casos entre todos os gliomas e apresentando-se como a forma mais severa e com o prognóstico mais desfavorável (Bray et al., 2018).

1.1 Glioblastoma

Os GB, também conhecidos como gliomas de grau IV, possuem uma alta prevalência, compreendendo 45% dos tumores malignos que afetam o SNC (Bush et al., 2017). Essa variante tumoral é histologicamente definida como astrocitoma e sua classificação molecular ocorre com base no status da enzima isocitrato desidrogenase (IDH) e na metilação do promotor da enzima O^6-metilguanina-DNA metiltransferase (MGMT) (Louis et al., 2021; Yeon Nam & de Groot, 2017). A enzima IDH do tipo selvagem é frequentemente encontrada em níveis excessivos no GB (Calvert et al., 2017), e desempenha um papel significativo na geração de NADPH, exibindo uma atividade enzimática superior a outras enzimas envolvidas na produção deste cofator, principalmente através de sua ação de descarboxilação oxidativa. Essa característica impulsiona a progressão do tumor e promove a resistência à morte celular ao favorecer a síntese eficaz de ácidos graxos, bem como a participação em mecanismos de hipóxia mediados pela geração de espécies reativas de oxigênio (ROS) (Alzial et al., 2022).

O GB se caracteriza por sua natureza difusa, embora sua etiologia e fisiopatologia completas ainda não estejam plenamente compreendidas. Apesar de ser possível ocorrer em qualquer faixa etária, é importante destacar que a incidência aumenta com o envelhecimento, sendo a idade média do diagnóstico em torno dos 65 anos (Le Rhun et al., 2019). Após o diagnóstico, a taxa de sobrevida em longo prazo é baixa, com apenas 4 a 5% dos pacientes sobrevivendo por mais de 5 anos. Mesmo com os avanços recentes nas estratégias terapêuticas, a média de sobrevida após diagnóstico e com tratamento gira em torno de 15 meses (Batash et al., 2017). Por conseguinte, apesar da aplicação de todas as abordagens de tratamento disponíveis, essa doença continua sendo praticamente intratável.

Atualmente, a abordagem padrão de tratamento para pacientes com GB consiste em uma combinação de ressecção cirúrgica, radioterapia e quimioterapia adjuvante. Contudo, devido à alta capacidade de infiltração do tecido normal pelo tumor, a completa ressecção se torna praticamente inviável e, mesmo quando realizada, a taxa de recorrência é elevada uma vez que células invasivas remanescentes acabam originando novos tumores próximos à região original. Avaliar a extensão da ressecção e ponderar os benefícios em relação aos riscos da cirurgia são desafios complexos. Embora haja uma tendência geral de maiores taxas de ressecção estarem associadas a uma melhor sobrevida, é crucial uma análise criteriosa para entender como essa melhora na sobrevivência se compara aos potenciais déficits neurológicos que podem surgir após a cirurgia (Morás et al., 2021).

Neste contexto, as limitações da cirurgia sugerem a necessidade de abordagens terapêuticas combinadas, como a radioterapia por radiação ionizante (J. Wang et al., 2018) que gera quebras de fita simples e dupla e ligações cruzadas na molécula de DNA, além de danos indiretos por meio da geração de ROS (Morás et al., 2021). A radiação, no entanto, não apenas reduz a proliferação e metástase das células cancerosas, mas também pode geneticamente alterar os tecidos normais, causando prejuízos às células não tumorais (J. Wang et al., 2018). Além disso, as células tumorais podem adaptar suas respostas à radiação ao se utilizarem de sua condição ambiental de hipóxia, reduzindo o fornecimento de oxigênio e limitando a produção de ROS. Similarmente, as células tumorais podem

fortalecer suas defesas antioxidantes para neutralizar moléculas oxidativas antes que causem dano celular (Morás et al., 2021).

Por fim, a quimioterapia é o terceiro componente terapêutico empregado em conjunto com as abordagens já mencionadas. O fármaco mais comumente utilizado é a temozolomida (TMZ), um pró-fármaco da classe de agentes alquilantes, cujo mecanismo de ação baseia-se na transferência do seu grupo alquil eletrofílico para o sítio mais nucleofílico do DNA. A inclusão da TMZ no protocolo de tratamento de GB recém-diagnosticados, sem dúvida, melhorou a sobrevida dos pacientes. Entretanto, sua administração sistêmica apresenta desvantagens significativas, como efeitos adversos gastrointestinais e hematológicos. Ademais, sua eficácia clínica é limitada pela necessidade de doses sistêmicas mais altas para alcançar efeitos terapêuticos no cérebro, e diversos mecanismos de resistência estão associados ao fracasso do tratamento, incluindo mecanismos de reparo do DNA e a presença da barreira hematoencefálica (BHE) (Miranda et al., 2017; Morás et al., 2021; Strobel et al., 2019).

1.2 Temozolomida

A TMZ é um derivado imidazotetrazina, resultante da modificação do agente alquilante dacarbazina, sendo comumente conhecida pelo seu nome comercial Temodal®. A descoberta de sua ação antitumoral ocorreu em 1987 (Lee, 2016; Stevens et al., 1987) e desde sua aprovação em 2005 pela *Food and Drug Administration* (FDA) (Stupp et al., 2005) tem sido amplamente utilizada como tratamento quimioterápico de primeira linha para pacientes com GB.

A administração da TMZ é predominantemente oral, e sua absorção ocorre no intestino delgado, seguida de uma hidrólise espontânea no meio intracelular, gerando o metabólito reativo e alquilante 3-metil-(triazen-1-il)imidazol-4-carboximida (MTIC). O MTIC, por sua vez, penetra no núcleo das células e adiciona grupos metil às bases do DNA, especificamente nas posições N3 da adenina e N7 e O6 da guanina. As metilações na guanina levam à incorporação errônea de uma timina durante o processo de replicação, resultando em danos nas fitas do DNA e morte celular por apoptose.

Entretanto, suas propriedades eletroquímicas levam a diferentes taxas de metilação, com maior frequência (cerca de 90%) e menor grau de citotoxicidade nas posições N3 da adenina e N7 da guanina, fato este relacionado à ação do mecanismo de reparo por excisão de bases (BER). Apenas 5 a 10% das metilações ocorrem na posição O6 da guanina, resultando no estabelecimento de uma O^6-metilguanina (O^6-MG) ao DNA, uma lesão altamente citotóxica e mutagênica. Neste caso, a via de reparo por mal pareamento do DNA (MMR) é ativada, mas ela só atua no reparo da fita de DNA recém-sintetizada, mantendo a metilação na fita molde. Isso acaba por gerar ciclos fúteis de substituição, aumento do gasto energético e a potencial parada da forquilha de replicação, levando a célula à morte por apoptose (Figura 1) (Erasimus et al., 2016; Morás et al., 2021; Ortiz et al., 2021; Wesolowski et al., 2010).

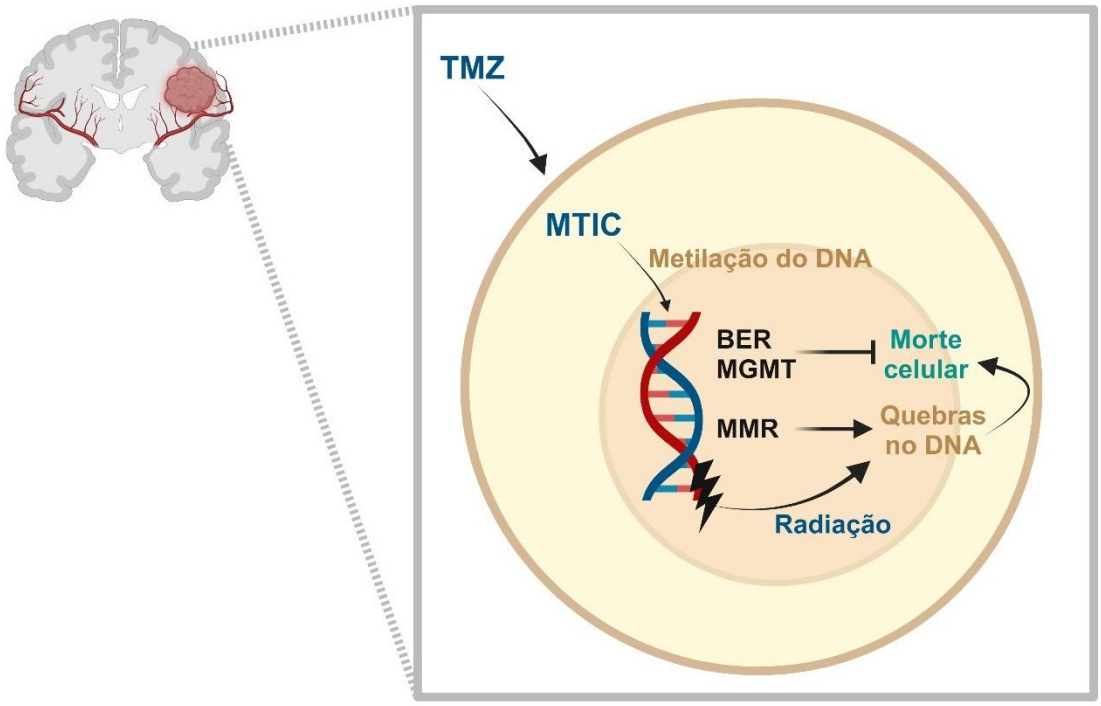

Figura 1: Mecanismo de ação da temozolomida. A temozolomida (TMZ) é convertida intracelularmente na sua forma ativa imidazólica (MTIC), que transfere de seu grupo alquil eletrofílico para o átomo mais nucleofílico do DNA. Na ausência e/ou ineficácia dos mecanismos de reparo de DNA, os danos gerados por esta metilação acabam levando a célula à morte por apoptose. **Fonte:** adaptado de Morás et al. (2021), com o auxílio da ferramenta BioRender. **Abreviaturas:** BER (reparo por excisão de bases); MGMT (O6-metiguanina-DNA metiltransferase); MMR (reparo por mal pareamento do DNA).

Não obstante, muitos pacientes não respondem ao tratamento com TMZ devido à influência de seu perfil genético, que afeta a resposta do organismo ao quimioterápico. Isso se relaciona à ação de diferentes vias de sinalização e reparo do DNA, que reconhecem e corrigem erros na molécula a fim de evitar o seu colapso e a parada do ciclo celular. Tais vias estão comumente superativadas em células tumorais, que as usam para sobreviver em condições de instabilidade genômica, consequentemente contribuindo para a resistência a diversos quimioterápicos e piora do prognóstico dos pacientes (Lee, 2016).

O GB se utiliza de várias vias para reparar os danos causados ao DNA pela TMZ: os já mencionados BER e MMR, além do reparo direto pela enzima O^6-metiguanina-DNA metiltransferase (MGMT), o reparo por recombinação homóloga (HR) e o reparo por junção de extremidades não-homólogas (NHEJ). De um modo geral, as lesões menos citotóxicas são frequentemente reparadas pela via BER, que envolve uma série de etapas de quebras, clivagens e polimerização da fita de DNA. As lesões do tipo O^6-MG são reparadas em um passo pela enzima MGMT, especialmente em pacientes com alta expressão do gene codificante desta enzima. Além do mais, as quebras duplas também podem ser reparadas pelas vias HR, uma via livre de erros, mas que depende da ressecção de extremidades do DNA e disponibilidade de uma fita molde para a ressíntese, ou via NHEJ, que repara o dano pela simples remoção e junção das extremidades, sendo por esta razão mais propensa a erros (Figura 2) (Erasimus et al., 2016).

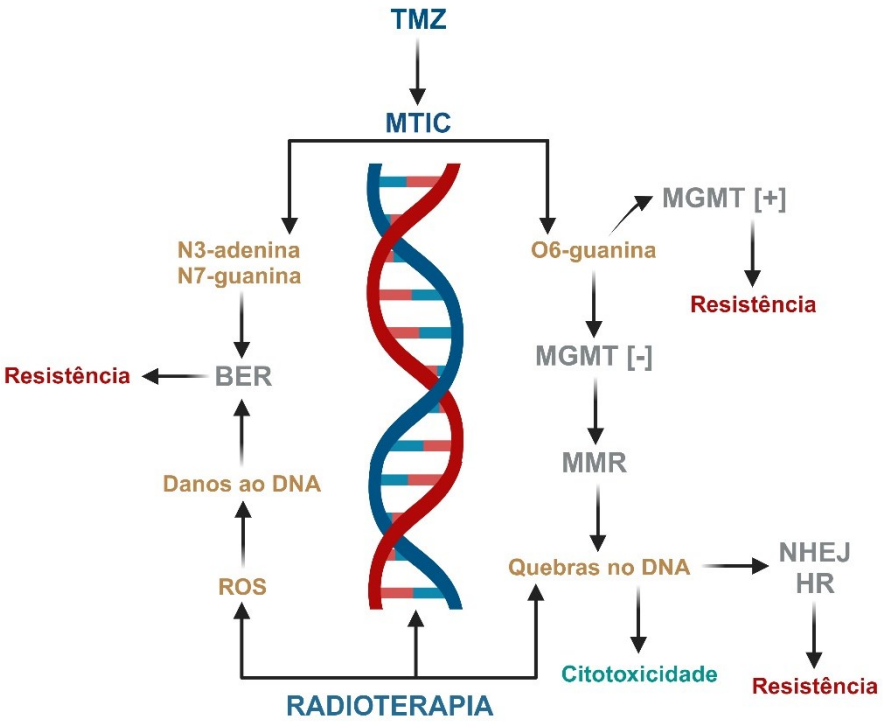

Figura 2: Vias de reparo de DNA relacionadas ao tratamento com temozolomida e radioterapia. Aproximadamente 90% das lesões causadas pela forma ativa imidazólica (MTIC) da temozolomida (TMZ) ocorrem nas posições N3 da adenina e N7 da guanina, enquanto apenas 5 a 10% atingem a porção O6 da guanina. A radioterapia causa danos ao DNA por meio de quebras ou da geração de espécies reativas de oxigênio (ROS). De um modo geral, cada uma destas lesões pode ser reparada por vias específicas de reparo (BER, MGMT, MMR, NHEJ e HR), induzindo resistência ao tratamento. **Fonte**: adaptado de Morás et al. (2021), com o auxílio da ferramenta BioRender. **Abreviaturas:** BER (reparo por excisão de bases); HR (recombinação homóloga); MGMT (O6-metiguanina-DNA metiltransferase); MMR (reparo por mau pareamento do DNA); NHEJ (reparo por junção de extremidades não-homólogas).

No contexto dos tumores cerebrais, a localização anatômica desempenha um papel significativo na resistência ao tratamento. A BHE, composta de uma complexa rede angiogênica e junções celulares extremamente apertadas e restritivas, dificulta a entrega de moléculas em níveis terapêuticos, desta forma restringindo a eficácia da quimioterapia (Morás et al., 2021; Ortiz et al., 2021). Logo, apesar da TMZ constituir o padrão-ouro para o tratamento do GB, diversos obstáculos como a natureza invasiva do tumor e sua resistência inerente e adquirida podem levar a resultados insatisfatórios. Tais complexidades ressaltam a urgência em se desenvolver novas estratégias terapêuticas para melhorar a eficácia do tratamento desta doença.

1.3 Ferroceno

O ferroceno (Fc) foi acidentalmente descoberto no início dos anos 1950, através de uma reação entre C_5H_5BrMg e $FeCl_3$ (Peter & Aderibigbe, 2019). Este composto organometálico do tipo metaloceno apresenta uma estrutura constituída por dois anéis ciclopentadienil ligados em posições opostas a um átomo metálico central de ferro (Fe) (Figura 3) e, devido às suas propriedades eletrônicas favoráveis e fácil funcionalização, tem sido amplamente utilizado na ciência dos materiais. Ademais, sua estrutura única, aliada a propriedades de permeação de membrana, estabilidade em ambientes aquosos e aeróbicos, e baixa toxicidade, despertaram interesse da comunidade científica para possíveis aplicações biológicas. Desde então, tem sido incorporado em estruturas contendo compostos bioativos para potencializar suas atividades ou descobrir novas propriedades terapêuticas. Suas aplicações já demonstraram atividades antifúngica, antibacteriana, antimalárica, anticancerígenas e supressoras do vírus da imunodeficiência humana (Atmaca et al., 2017; Ornelas, 2011).

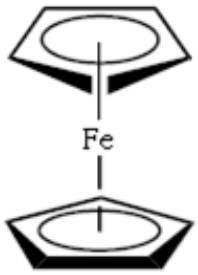

Figura 3: Representação esquemática do composto ferroceno. O ferroceno e seus derivados são compostos organometálicos do tipo metaloceno, e consistem em dois anéis ciclopentadienil opostamente ligados a um átomo central de ferro (Fe). **Fonte:** elaboração própria.

O mecanismo de ação do Fc e seus derivados parece estar centrado no átomo de Fe, que é transportado no plasma pela transferrina e armazenado nas células retículo-endoteliais do fígado, baço e da medula óssea sob as formas de ferritina e hemossiderina. Essa estocagem é fundamental para evitar a presença do Fe na sua forma livre, uma vez que esta, quando em contato com o oxigênio circulante, pode induzir a síntese anômala de ROS, que podem causar danos a proteínas, lipídios e ao DNA (Grotto, 2008). Por outro lado, sabe-se que células

tumorais frequentemente apresentam níveis elevados de ROS devido ao hipermetabolismo necessário à sua proliferação, especialmente o peróxido de hidrogênio (H_2O_2), que gera radicais hidroxila (·OH) através da reação de Fenton, um processo em que o Fe^{2+} desempenha papel crucial. Neste contexto, o Fc pode ser utilizado como fonte exógena de Fe^{2+}, potencializando a catálise de H_2O_2 e a geração de radicais ·OH que, devido ao curto tempo de meia-vida, acabam gerando danos específicos às células tumorais, poupando as células saudáveis adjacentes (Murillo et al., 2022).

O Fc exibe propriedades redox interessantes, e sua estabilidade é assegurada pela regra dos 18 elétrons. Entretanto, ao sofrer oxidação, percebe-se a formação de um cátion correspondente, que possui um elétron desemparelhado em um de seus orbitais. Desta forma, o equilíbrio intracelular entre Fe^{2+} e Fe^{3+} pode ser exogenamente modulado pelo Fc através de transferências eletrônicas rápidas e reversíveis, gerando radicais livres e, potencialmente, contribuir para a geração de mais danos às células tumorais (Figura 4) (Köpf-Maier et al., 1984; Murillo et al., 2022; Neuse, 2008). A nível molecular, este composto também já demonstrou a capacidade de suprimir a viabilidade celular e inibir as vias de sinalização PI3K/AKT e ERK1/2, que são cruciais para a promoção da tumorigênese (Atmaca et al., 2017; Tian et al., 2016).

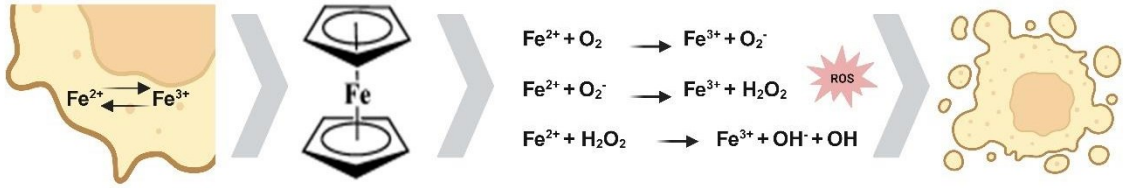

Figura 4: Representação esquemática do mecanismo de ação do ferroceno no ambiente intracelular. Em situações fisiológicas, Fe^{2+} e Fe^{3+} encontram-se em equilíbrio no interior da célula. O ferroceno pode atuar como fonte exógena de Fe^{2+}, que via reação de Fenton gera o radical hidroxila, e eventualmente levando a célula à morte por apoptose. **Fontes:** elaboração própria com o auxílio da ferramenta BioRender; Ornelas, 2011.

Contudo, apesar dos resultados promissores evidenciando a atividade supressora tumoral do Fc, ainda há carência de dados concretos sobre sua interação com agentes quimioterápicos diversos, bem como seu comportamento em relação a tumores cerebrais devido à presença da BHE. Dada a contínua necessidade de se encontrar alternativas terapêuticas para o câncer e os desafios

clínicos associados, é crucial aprofundar o estudo deste composto, buscando novos caminhos de tratamento para diferentes tipos de câncer, especialmente os de alta letalidade, como o GB. Adicionalmente, os obstáculos impostos pelo microambiente tumoral, acrescidos da BHE no caso do GB, requerem o uso de sistemas de entrega de fármacos (DDS) diretamente ao tumor, com o intuito de aumentar a eficácia terapêutica e, ao mesmo tempo, reduzir os efeitos colaterais.

1.4 Sistemas de entrega de fármacos para o tratamento do câncer

Os DDS são empregados principalmente para obter controle preciso em termos de tempo e local durante a administração de fármacos e/ou agentes biológicos (Pillai & Panchagnula, 2001). De um modo geral, estes sistemas permitem que moléculas tenham seus perfis de liberação modulados e que sejam liberadas de maneira sítio-específica por meio de nanocarreadores com tamanhos variando entre 1 e 500 nm, melhorando a segurança e eficácia do tratamento, e a adesão do paciente em razão da minimização dos efeitos colaterais e do melhor manejo dos esquemas de administração (Wakaskar, 2018; Whittlesey & Shea, 2004). Tais modificações são atingidas por meio de alterações do perfil farmacocinético intrínseco das moléculas pelas propriedades da matriz do sistema, incluindo sua composição e suas características de superfície. Além disso, os DDS possibilitam a administração de fármacos potentes, mas de natureza instável, com mínimas flutuações de doses, garantindo a uniformização prolongada da sua concentração plasmática aliada a uma menor incidência de toxicidade sistêmica (Berkland et al., 2002).

Para uma aplicação eficaz destes sistemas, é essencial compreender as características tanto do fármaco quanto da matriz escolhida, uma vez que modificações nestes parâmetros serão determinantes na taxa de liberação de uma molécula. Além disso, o tecido-alvo no qual o DDS deve atuar influencia na escolha da matriz, dos fármacos e do sistema, evidenciando que uma abordagem multifacetada é fundamental para o sucesso na administração de moléculas por meio de DDS (Allen & Cullis, 2004; Hicks et al., 1985).

Ao permitirem a combinação de diferentes materiais e técnicas, estas nanoestruturas também toleram o carreamento e a conjugação de moléculas que são incompatíveis aos sistemas de administração convencionais, bem como as protegem da degradação precoce. Da mesma forma, os DDS facilitam o encapsulamento de moléculas de baixa solubilidade, a modificação dos seus alvos, o aumento de sua interação com membranas e sua passagem por barreiras celulares (Bertrand et al., 2014).

Recentemente, as estratégias de DDS vêm desempenhando um papel crucial na transformação de moléculas promissoras em terapias eficazes, e a versatilidade destes sistemas permite o acompanhamento da evolução do panorama de novas terapias contra o câncer (Allen & Cullis, 2004; Hicks et al., 1985; Vargason et al., 2021a). Atualmente, estas nanoestruturas podem se apresentar de diferentes formas e com os mais variados materiais, incluindo lipossomas, micelas, exossomas, nanopartículas (NPs) poliméricas, conjugados poliméricos e NPs inorgânicas (Figura 5), que serão brevemente discutidas a seguir (informações mais detalhadas podem ser consultadas na Seção 3.1 desta tese). Sistemas mais simples, como as nanoemulsões – foco principal deste estudo – também são amplamente utilizados, e serão abordados numa seção à parte.

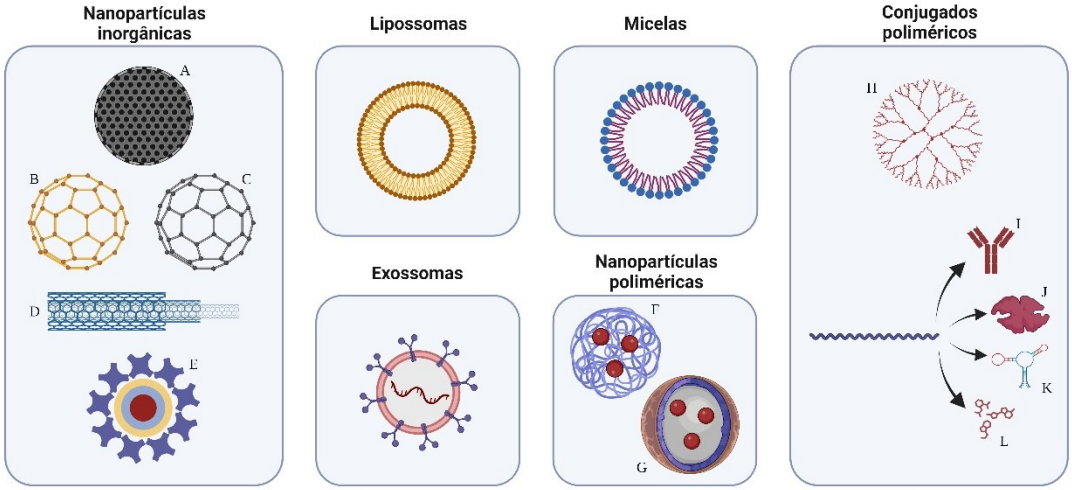

Figura 5: Representação esquemática dos diferentes tipos de nanoestruturas utilizados em sistemas de entrega de fármacos. Legenda: sílica (A), ouro (B), prata (C), nanotubo de carbono (D), *quantum dots* (E), nanocápsula (F), nanoesfera (G), dendrímero (H), polímero-anticorpo (I), polímero-proteína (J), polímero-aptâmero (K), e polímero-fármaco (L). **Fonte:** elaboração própria com o auxílio da ferramenta BioRender.

Os lipossomas são formados por vesículas fosfolipídicas medindo a partir de 50 nm, e são amplamente utilizados em aplicações biomédicas em razão da habilidade em comportar moléculas hidrofóbicas na sua bicamada lipídica e encapsular compostos hidrofílicos no seu núcleo (Anselmo & Mitragotri, 2019; Chaturvedi et al., 2018). Lipossomas catiônicos também podem ser eletrostaticamente ligados a ácidos nucleicos, e sua composição semelhante à membrana celular garante um elevado grau de compatibilidade em comparação a nanocarreadores sintéticos, minimizando efeitos antigênicos e tóxicos. Entretanto, desafios como o tempo prolongado de circulação no plasma, a instabilidade por ação da oxidação fosfolipídica, o processo de esterilização e limitações no controle de liberação de moléculas constituem fatores limitantes no seu uso terapêutico (Li et al., 2017; Pérez-Herrero & Fernández-Medarde, 2015). Tais problemas podem ser contornados por modificações estruturais e físico-químicas, utilizando polímeros para aumentar e/ou estabilizar a taxa de liberação, modular o tempo de circulação no plasma, e permitir o encapsulamento de ácidos nucleicos para transfecção celular, bem como a ligação com anticorpos para imunoterapia (Pérez-Herrero & Fernández-Medarde, 2015; Torchilin, 2005).

Diversos estudos *in vitro* e *in vivo* têm demonstrado a eficácia de sistemas lipossomais no tratamento de diversos tumores, sendo os sistemas responsivos ao pH os mais promissores. Notavelmente, formulações como o Doxil®, o primeiro nanocarreador aprovado pelo FDA em 1995, têm sido ferramentas fundamentais na quimioterapia ao utilizarem brechas na vasculatura tumoral para atingir estas células de maneira mais eficaz que outras NPs (Chaturvedi et al., 2018; Qiu et al., 2017; Torchilin, 2005).

As micelas são nanocarreadores coloidais, anfifílicos, com tamanhos entre 5 e 200 nm, customizadas para a liberação controlada e lenta de fármacos. Sua estrutura compreende um núcleo hidrofóbico e uma camada externa com polaridade suficiente para se dispersar em meio aquoso (Bregoli et al., 2016; Lee Ventola, 2017; Rizwanullah et al., 2018). Desenhadas para melhorar a solubilidade e biodisponibilidade de fármacos, as micelas normalmente apresentam um núcleo composto de óxido de polifenileno ou lipídeos, sustentados por forças de van der

Waals, e uma superfície hidrofílica coberta de polímeros, garantindo proteção e circulação plasmática prolongada (Elkhodiry et al., 2016; Li et al., 2017).

Micelas contendo doxorrubicina já demonstraram atividade antitumoral *in vitro* para o tratamento de câncer oral, bem como micelas poliméricas carreando cisplatina se mostraram capazes de diminuir quadros de nefrotoxicidade, enquanto aumentavam a liberação linfática do fármaco. Além disso, este sistema encontrou aplicações na entrega de microRNAs para atingir tumores, modulando a autofagia, a proliferação e a invasão celular. Apesar de sua versatilidade, preocupações com a estabilidade deste sistema surgem devido a fatores como a baixa concentração micelar crítica, que pode ser resolvida pela conjugação com estruturas poliméricas, aumentando a estabilidade e o acúmulo tumoral por meio do *enhanced permeability and retention effect*, justificando assim seu uso na quimioterapia (Elkhodiry et al., 2016; Endo et al., 2013; Lasic & Needhamt, 1995; Saiyin et al., 2014).

Os exossomas compreendem um subtipo de vesículas extracelulares com tamanhos entre 30 e 150 nm, e originam-se da exocitose de endossomos para o meio extracelular (Couto et al., 2018; Greening et al., 2015). Estas estruturas são secretadas por diversos tipos celulares, incluindo células imunológicas, tumorais, neuronais, endoteliais e fibroblastos, e consistem em uma bicamada lipídica com a capacidade de carrear e transferir proteínas, ácidos nucleicos e outras moléculas, além de transmitir informações a células adjacentes e modular seu comportamento mediantes modificações moleculares (Greening et al., 2015; Lim & Kim, 2019). Diferentemente de lipossomas e micelas, os exossomas oferecem vantagens únicas em razão da sua biocompatibilidade e origem natural. Tal característica reduz as chances de serem precocemente fagocitados, aumentando sua capacidade de penetração no ambiente tumoral, bem como permitindo a eles desempenharem importantes funções na modulação da resposta imune, reciclagem e comunicação celular (Greening et al., 2015; Kalluri, 2016).

As nanopartículas poliméricas são sistemas coloidais sólidos capazes de dissolver, apreender, encapsular ou adsorver agentes terapêuticos em uma matriz polimérica biodegradável e biocompatível. A versatilidade destas nanoestruturas permite a associação de moléculas de diferentes naturezas físico-químicas, e sua apresentação se dá particularmente em duas diferentes formas: as nanocápsulas,

compostas de uma vesícula com uma cavidade oleosa ou aquosa, contendo o fármaco e envolta por uma membrana polimérica, e as nanoesferas, uma matriz polimérica na qual o fármaco encontra-se amplamente disperso (Letchford & Burt, 2007; Parveen & Sahoo, 2008; Prabhu et al., 2015). Sua composição envolve tanto polímeros naturais, como a quitosana e a albumina, quanto sintéticos, como o álcool polivinílico, ácido poliacrílico, poli(ácido lático-*co*-ácido glicólico) e a poli(Ɛ-caprolactona), onde sua preparação se dá por métodos como evaporação do solvente, polimerização em emulsão, e diálise (Banik et al., 2016; El-Say & El-Sawy, 2017).

A grande variedade de polímeros que podem ser usados como veículos na produção de DDS requer um minucioso estudo de suas propriedades mecânicas e físico-química previamente à sua utilização. A exemplo, polímeros com perfis de resistência, rigidez e dureza bem definidos apresentam vantagens na modulação da cinética de degradação destes materiais, e consequentemente no perfil de liberação das moléculas carreadas, enquanto o caráter hidrofóbico ou hidrofílico destes materiais influenciará na solubilidade, toxicidade e no perfil de liberação (Bhatia, 2016). Atualmente, NPs poliméricas já são encontradas em medicamentos como o Abraxane®, que utiliza a albumina como carreadora do fármaco paclitaxel no tratamento de tumores metastáticos de mama, e o Eligard®, composto de um polímero sintético contendo acetato de leuprorrelina para o tratamento de tumores de próstata (Banik et al., 2016; Lee Ventola, 2017).

De maneira similar, polímeros hidrofílicos e anfifílicos também podem ser conjugados com diferentes moléculas através de ligações covalentes, com o intuito de melhorar a efetividade terapêutica e minimizar efeitos colaterais (Ekladious et al., 2019; Lomkova et al., 2016; Pang et al., 2014). Estas combinações podem se apresentar na forma de dendrímeros e polímeros ligados a fármacos, proteínas, anticorpos ou aptâmeros, e têm demonstrado efeitos positivos no prolongamento da circulação do conjugado no plasma, e na sua solubilidade e biodisponibilidade, evitando assim a liberação imediata nos tecidos-alvo (Chang et al., 2016; Lomkova et al., 2016). Polímeros como o polietilenoglicol (PEG) e o *N*-(2-hidroxipropil)-metacrilamida (HPMA) já foram conjugados a proteínas e doxorrubicina, respectivamente. Enquanto o conjugado PEG-adenosina desaminase evoluiu para

o produto veterinário Adagen®, a combinação HPMA-doxorrubicina esbarrou em requisitos como eficácia terapêutica em razão do baixo acúmulo no ambiente tumoral (Banerjee et al., 2012; Seymour et al., 2009).

Por fim, o grupo das NPs inorgânicas engloba uma gama de estruturas que incluem NPs de ouro, prata, sílica e magnéticas, nanotubos de carbono e *quantum dots* (QDs), e têm recebido atenção especial no campo do tratamento do câncer em razão de suas propriedades físico-químicas e características de superfície peculiares (F. Wang et al., 2016; F. Yang et al., 2012; Yezhelyev et al., 2009). As NPs de ouro, com tamanhos e formas variados, exibem ressonância plasmônica de superfície, permitindo a conversão de luz em calor para hipertermia localizada e erradicação de células cancerígenas. Efeitos similares podem ser vistos no uso de NPs magnéticas, como as de óxidos de ferro, que geram efeitos térmicos quando expostas a um campo magnético. NPs de ferro responsivas à ablação termal já se encontram aprovadas para o tratamento de GB, sob o nome comercial de NanoTherm® (Mukerjee et al., 2012; Tran et al., 2017; Xu et al., 2018; Yezhelyev et al., 2009). As NPs de prata, conhecidas pela sua maior estabilidade, condutividade e propriedades catalíticas, possuem potencial terapêutico por meio de atividades antiangiogênicas e antiproliferativas, embora também tenham demonstrado citotoxicidade não-seletiva devido à sua capacidade de penetrar em diversos tecidos (Greulich et al., 2011; Jeyaraj et al., 2013). As NPs de sílica, particularmente aquelas de sílica mesoporosa, servem como reservatórios para a administração controlada de fármacos devido ao seu tamanho de poro personalizado (Vallet-Regi et al., 2001; Y. Yang & Yu, 2016).

Os nanotubos de carbono, hidrofóbicos e organizados em camadas com diâmetros de 1 a 4 nm, apresentam propriedades como baixo peso, estabilidade mecânica, elevada capacidade de carreamento, e boa condutividade termal e elétrica, permitindo a incorporação de fármacos, RNA e anticorpos, que por sua vez podem ser liberados diretamente no citoplasma graças à capacidade de penetração do ‘tipo agulha’ destas estruturas. Por outro lado, a baixa solubilidade dos nanotubos pode aumentar sua toxicidade (Chaturvedi et al., 2018; Markman et al., 2013; F. Yang et al., 2012). Por último, os QDs constituem nanocristais ou NPs semicondutoras de 2 a 10 nm, com características fluorescentes, e atuam como

transportadores teragnósticos versáteis, capazes de detectar proteínas e peptídeos superexpressos e aumentar a geração de ROS e consequente apoptose celular (Chaturvedi et al., 2018; Probst et al., 2013; Xu et al., 2018).

1.4.1 Nanoemulsões

As nanoemulsões (NE) são dispersões coloidais transparentes/translúcidas e heterogêneas de duas substâncias líquidas imiscíveis (óleo e água), onde um líquido está disperso no outro por meio da ação de agentes surfactantes, formando um sistema com tamanho de gotículas tipicamente entre 20 e 200 nm (Pavoni et al., 2020; Shaker et al., 2019). Suas principais características são a estabilidade termodinâmica e cinética (ausência de aparente floculação ou coalescência), e a distribuição uniforme do tamanho das gotículas, o que garante a elas propriedades físico-químicas e biológicas diferentes de outras emulsões com tamanho de gotículas superior a 500 nm (Rai et al., 2018).

Com base em sua composição, uma NE pode ser classificada em três diferentes tipos: óleo em água, onde a fase oleosa está dispersa numa fase aquosa contínua; água em óleo, onde a fase aquosa está dispersa numa fase oleosa contínua; e bicontínua, onde microdomínios compostos de fases oleosa e aquosa encontram-se interdispersos no sistema (Rai et al., 2018). Os componentes básicos da sua fase oleosa incluem triglicerídeos de cadeia média, ácidos graxos, solventes orgânicos, emulsificantes, enquanto a fase aquosa compõe-se de água e surfactante (Nastiti et al., 2017), este último de caráter comumente não-iônico e com considerável capacidade de reduzir a tensão superficial, evitando assim a agregação das gotículas e aumentando a permeação do sistema (Harwansh et al., 2019; Pavoni et al., 2020).

As NE do tipo óleo em água (Figura 6) são as mais comuns, e podem ser obtidas por meio de diversas metodologias, que incluem o uso de microfluidizador e ultrassom, a emulsão espontânea, inversão de fase, homogeneização por alta pressão, e o método por deslocamento de solvente (Beck-Broichsitter et al., 2010; Fathi et al., 2012; Nastiti et al., 2017; Singh et al., 2017). Este último método constitui-se de um processo rápido, reprodutível e econômico, e requer o uso de

solventes orgânicos anfifílicos e miscíveis em água, como a acetona. Sua metodologia consiste na adição progressiva da fase oleosa, contendo o solvente orgânico, à fase aquosa, sob agitação constante e temperatura apropriada, levando à formação de partículas coloidais em suspensão por meio de fenômenos hidrodinâmicos interfaciais entre as duas fases (Beck-Broichsitter et al., 2010).

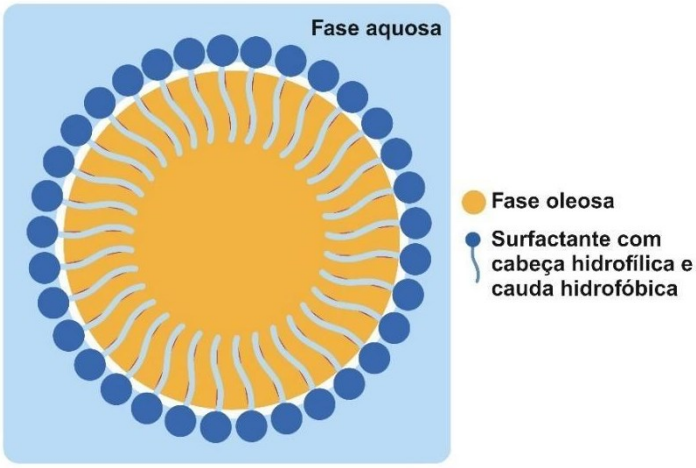

Figura 6: Representação esquemática de uma gotícula de nanoemulsão do tipo óleo em água. **Fonte:** figura elaborada pelo autor com o auxílio da ferramenta BioRender.

Estudos pré-clínicos e clínicos têm demonstrado a alta eficácia do uso de NE no carreamento de diversas moléculas com atividade antitumoral, tanto naturais como sintéticas, principalmente contra tumores do trato gastrointestinal e sistema reprodutor, bem como de pele, cérebro, mama, pulmão e leucemia (Tabela 1).

Tabela 1: Ensaios pré-clínicos e clínicos utilizando nanoemulsões contendo moléculas para o tratamento do câncer.

Molécula carreada	Tipo de câncer	Fase do estudo	Resultados e/ou status	Referência
Campferol	Glioma	Pré-clínica	Redução do crescimento tumoral	(Colombo et al., 2018)
7-cetocolesterol	Melanoma	Pré-clínica	Redução de 50% dos tumores e aumento da área necrótica	(Natesan et al., 2017)
Curcumina	Próstata	Pré-clínica	Aumento da citotoxicidade; parada do ciclo celular e aumento da apoptose	(Guan et al., 2017)
DHA-SBT-1214	Pâncreas	Pré-clínica	Inibição do crescimento tumoral induzido por células-tronco	(Ahmad et al., 2017)

Didodecil-metotrexato	Leucemia	Pré-clínica	Aumento da ação do metotrexato quanto comparada à sua versão não esterificada	(Botchkina et al., 2010)
Licopeno	Cólon	Pré-clínica	Redução dos níveis de proteínas relacionadas à progressão do ciclo celular; aumento da apoptose e redução da migração celulares	(Sánchez-López et al., 2019)
Paclitaxel	Ovário	Pré-clínica	Redução dos níveis de proteínas relacionadas à progressão do ciclo celular; aumento do estresse mitocondrial	(Cronin et al., 2010)
Paclitaxel	Pulmão	Pré-clínica	Inibição do crescimento tumoral	(Sánchez-López et al., 2019)
Ácido 5-aminolevulínico	Células basais	Clínica	Ativo, sem recrutamento	(Sánchez-López et al., 2019)
Curcumina	Mama	Clínica	Ativo, em recrutamento	(Sánchez-López et al., 2019)
Paclitaxel	Mama	Clínica	Fase I	(Graván et al., 2023)

Em comparação a outras emulsões convencionais, as NE exibem uma série de vantagens como elevada estabilidade, rápida absorção via internalização nos enterócitos e a habilidade em melhorar a solubilidade de moléculas, consequentemente aumentando sua biodisponibilidade. Além disso, o incremento da área interfacial entre as fases oleosa e aquosa das NE confere a elas uma alta capacidade de solubilização de compostos, tanto hidrofóbicos quanto hidrofílicos, enquanto características como a carga superficial, o tamanho menor das gotículas e a estabilidade cinética agem contra efeitos indesejáveis, como sedimentação, floculação e coalescência (Rai et al., 2018). Por fim, NE capazes de carrear moléculas bioativas adsorvidas em sua interface podem oferecer rápida liberação e início da ação farmacológica, bem como ser combinadas com outras moléculas de liberação lenta numa abordagem sinérgica, permitindo assim esquemas de tratamento com dose de ataque, somados a uma ação mais prolongada, fator importante na terapia de tumores localizados em áreas de difícil acesso, como os tumores cerebrais (D. Chen et al., 2023; Heravi Shargh et al., 2021).

O câncer, uma enfermidade complexa e diversificada, continua a desafiar a eficácia terapêutica, mesmo com avanços notáveis. Diante do aumento previsto

dos casos e das taxas alarmantes de mortalidade, é evidente a necessidade de abordagens mais efetivas. O GB, notório por sua resistência a tratamentos e prognóstico desfavorável, destaca a urgência de soluções inovadoras, e a pesquisa com o Fc, explorando seu efeito na potencialização da quimioterapia e na entrega direcionada de medicamentos, desponta como uma promissora estratégia. Aliado a isto, os sistemas de entrega de fármacos, desde lipossomas a nanoemulsões, desempenham um papel crucial nesse cenário, oferecendo soluções multifacetadas para os desafios terapêuticos. Por fim, a versatilidade desses sistemas tem potencial para moldar terapias mais eficazes e inovadoras, abrindo caminho para novos avanços na luta contra o câncer.

2 OBJETIVOS

2.1 Objetivo geral

Desenvolver, caracterizar e avaliar a eficácia de uma nanoemulsão contendo temozolomida e o efeito de pré e cotratamentos com ferroceno em linhagens celulares de glioblastoma humano.

2.2 Objetivos específicos

1 – Investigar o uso de sistemas de entrega de fármacos no tratamento do câncer, por meio da elaboração de um artigo de revisão.

2 – Desenvolver e caracterizar uma nanoemulsão do tipo óleo em água, contendo temozolomida.

3 – Avaliar a eficácia desta nanoemulsão e do ferroceno em esquemas de mono e cotratamento agudos em linhagens de glioblastoma humano.

4 – Avaliar a eficácia da nanoemulsão contendo temozolomida com e sem esquemas de pré e cotratamento com ferroceno em linhagens de glioblastoma humano, simulando uma abordagem clínica de tratamento.

3 ARTIGOS CIENTÍFICOS

3.1 Capítulo 1: Cancer nanomedicine: recent developments in drug delivery systems and strategies to overcome eventual barriers to achieve a better outcome

Artigo científico submetido à *revista Journal of Drug Delivery Science and Technology* (fator de impacto 5).

Observação: as figuras foram inseridas junto ao texto para facilitação da leitura, e a paginação segue a ordem geral da tese.

Cancer nanomedicine: recent developments in drug delivery systems and strategies to overcome eventual barriers to achieve a better outcome

Jeferson Gustavo Henn[ab], Tanira Alessandra Silveira Aguirre[c], Michael Nugent[b], Dinara Jaqueline Moura[a]*

[a] Laboratório de Genética Toxicológica, Universidade Federal de Ciências da Saúde de Porto Alegre, Porto Alegre, Rio Grande do Sul, Brazil, 90050-170
[b] Materials Research Institute, Technological University of the Shannon: Midlands Midwest, Athlone, Co. Westmeath, Ireland, N37HD68
[c] Laboratório de Farmacociências, Universidade Federal de Ciências da Saúde de Porto Alegre, Porto Alegre, Rio Grande do Sul, Brazil, 90050-170

*Corresponding author. Address: Universidade Federal de Ciências da Saúde de Porto Alegre, 245 Sarmento Leite Street, Lab. 714, Porto Alegre, Rio Grande do Sul, Brazil, 90050-170.
Email: dinaram@ufcspa.edu.br (Dinara Jaqueline Moura)

Graphical abstract

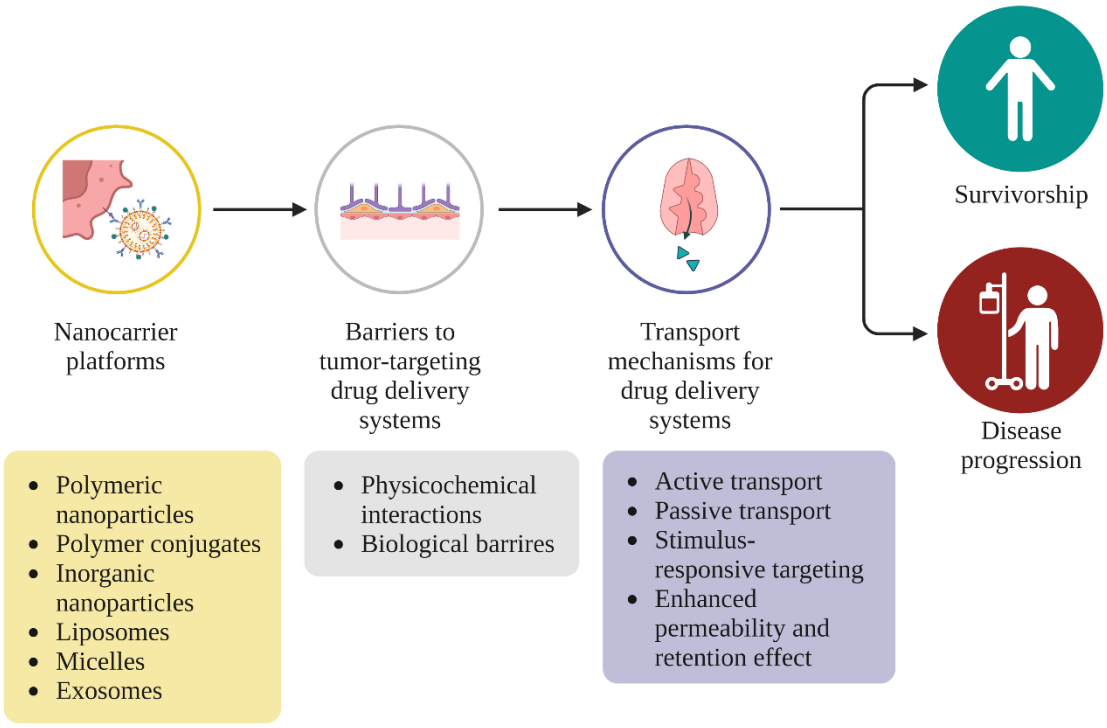

ABSTRACT

Cancer has been a global challenge given the number of limitations of current therapies, such as multi-drug resistance, high levels of toxicity, side effects, the tumor microenvironment, and the lack of cell-targeted approaches. Over the past decades, several strategies using nanotechnological structures for drug delivery systems have been developed to provide targeted and controlled release of drugs for *in situ* anticancer therapies. These nanostructures are made of different types of biocompatible materials, ranging from polymeric to organic and inorganic nanoparticles, thus allowing them to interact with different cells, membranes, and receptors, as well as to conjugate molecules with the most diverse physicochemical characteristics. Moreover, these structures can potentially overcome the drawbacks of systemic therapy, taking advantage of the organism's biological mechanisms to increase therapeutic efficacy while reducing systemic toxicity. In this review, we focus on nanostructures as drug delivery systems for cancer treatment, how they can reach tumor cells and improve *in situ* toxicity, and the barriers they may face to achieve a positive outcome. Overall, several nanoproducts have been developed to treat different types of cancers, and most of the current nanomedical approaches focus on the ability to target tumor cells by improving drug delivery rates and combining different molecules, therefore potentially reducing side effects. On the other hand, concerns regarding individual characteristics of patients, tumor barrier mechanisms, and the potential toxicity of non-biological materials are still challenges to be addressed. Nonetheless, the rapid development of nanomedicine and the constant improvement of related techniques point to a promising future in the treatment of cancer and in improving the quality of life of patients.

Keywords: *cancer; nanotechnology; nanocarriers; drug resistance; local delivery; targeted therapy*

1. Introduction

Cancer is a multifactorial and complex set of diseases characterized by abnormal and uncontrolled cell growth, presenting tissue and organ parenchymal disorganization that leads to a physiological impairment of the affected organism [1]. Etiologically, this disease involves several features such as DNA damage and replicative stress – which may lead the cells to some genomic instability – as well as immunological disorders, increased angiogenic support, and recidivism due to tissue invasion and metastasis [2,3].

According to the World Health Organization, in 2020, there were around 19.2 million new worldwide cancer cases and 9.9 million deaths. For 2040, the estimated number of new cases is around 29.5 million, representing an increase of 63.4% [4]. This makes cancer the second leading cause of death, reinforcing it as an imminent public health problem and justifying the constant search for new therapies and treatment approaches [5].

Conventional cancer treatment usually includes a triad composed of surgical resection, chemotherapy, and radiotherapy. However, tumor resection is, in several cases, a dangerous procedure that may cause several damages to the patient, depending on the location and the extension of the tumor. Besides, radiotherapy also has its complications since it may cause skin irritation and adverse effects on healthy tissues adjacent to the tumor site. Finally, even with all the improvements that have been made in the last few years, chemotherapy drugs still have limited effects and poor pharmacokinetics, causing toxicity not only to nearby healthy cells but also to the entire organism due to their lack of specificity [5,6].

Recently, some of these flaws have been overcome by the advent of cancer immunotherapy. This approach harnesses the patient's immune system to target tumor cells by binding to specific tumor antigens, hence increasing the immune system's ability to identify, inhibit, and kill those neoplastic cells [7]. Although promising, immunotherapy still faces some challenges, such as the understanding of the dominant drivers of cancer immunity, primary versus secondary immune escape, and organ-specific tumor immune features, as well as the elucidation of the benefits of endogenous versus synthetic immunity and the need for highly patient-personalized approaches that lead to high-cost treatment [7,8].

In addition, most drugs face other major problems related to chemoresistance, allowing cancer cells to evade and survive to different treatments. This can be achieved by

using molecular mechanisms that reduce drug availability through changes in the pH of the tumor microenvironment (TME), promoting epithelial-mesenchymal transition, and/or overexpressing oncogenic signaling pathways [9].

Furthermore, TME is by itself a significant physical barrier to cancer therapies. It includes subpopulations of malignant cells with different genetic backgrounds, healthy cells and blood, immune, and endothelial cells that work like scaffolds for the tumor, not to mention the high vascularization at the site, which gives extra oxygen supply to maintain the tumor's high metabolic rate [10]. Moreover, all these characteristics give the tumor a more rigid consistency, and this leads us to other important roles of oxygen supply on TME: the high replicative rate of peripheral tumor cells and the reduced oxygen rate in the central region of the tumor, generating a state of hypoxia that activates inflammatory pathways and downregulates tumor suppressor proteins such as p53 [9-11].

To overcome these issues, several nanotechnological approaches applied to medicine have been developed in the last few years, transforming nanomedicine into a wide-ranging field that comprehends physicochemical, biological, and engineering principles to obtain structures with a size range of 1-500 nm [12]. By joining different materials and techniques, these nanostructures may be able to facilitate the combination of different molecules and protect them from earlier degradation. These techniques may also facilitate the encapsulation of drugs that are insufficiently soluble, modification of their targets, enhancement of the interaction with cell membranes, circumventing organ barriers, and providing a drug delivery system (DDS) directly to the tumor site, thereby enabling the utilization of lower doses and avoiding adverse effects [13].

One of the most significant advantages of nanostructures is the wide range of different materials and approaches that can be used to obtain them. They may involve polymeric nanoparticles (PNPs), polymer conjugates, inorganic nanoparticles (INPs), liposomes, micelles, exosomes, carbon nanotubes, and quantum dots (QDs) (Figure 1). The choice of material to be used will depend on factors such as physicochemical interactions between the molecule of interest and the material, the route of administration, the location of the therapeutic target, and the mechanism of targeting [14,15]. Moreover, the development of these nanotechnologies has been supported over the past years by various strategies that enhance their functionalities, either by surface modifications, physical properties, or controlled release [16].

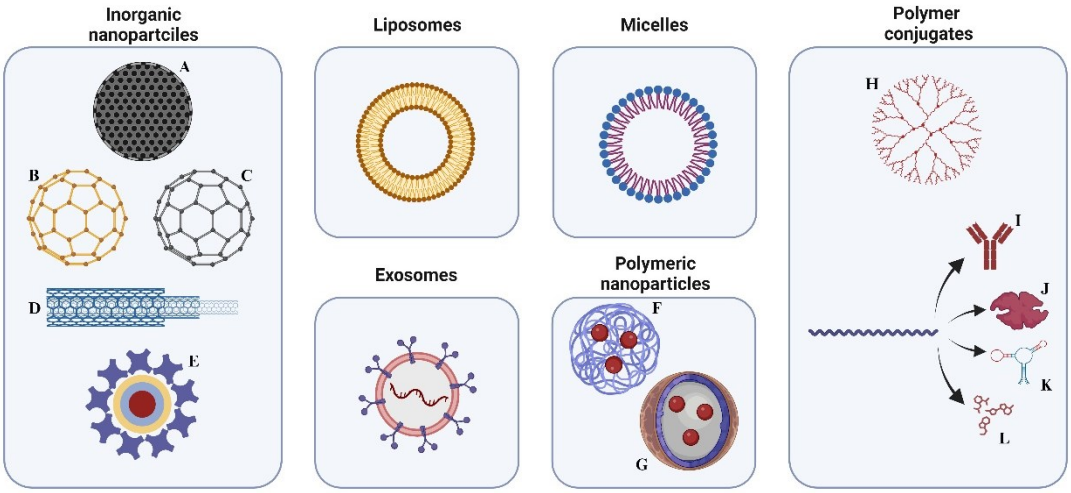

Fig. 1: Schematic representation of the different types of nanostructures for DDS. Inorganic nanoparticles: gold (A), silica (B), silver (C), carbon nanotube (D), and quantum dots (E). Polymeric nanoparticles: nanocapsule (F) and nanosphere (G). Polymer conjugates: polymer-antibody (H), polymer-protein (I), polymer-aptamer (J), polymer-drug (K), and dendrimer (L). Exosome (M). Liposome (N). Micelle (O).

In short, nanomedicine applied to cancer diagnosis, prevention, and treatment can be structured in three major aspects: the nanocarrier platforms, the common barriers that hamper cancer chemotherapy, and the transport and cell targeting mechanisms to overcome these barriers. Thus, this work proposes to review, update, and discuss all these features and demonstrate how to overcome them by using rational DDS approaches (as schematized in Supplementary Information Fig. S1).

2. Nanocarrier platforms

2.1 Polymeric nanoparticles

PNPs are solid colloidal systems that allow the dissolution, entrapment, encapsulation, or adsorption of therapeutic agents onto the polymer matrix. These drug carriers are biocompatible and biodegradable, as well as highly versatile in terms of the drug classes that can be associated with them. PNPs can be obtained in different structures depending on the process of formation, resulting in nanocapsules, a single vesicular polymeric membrane involving the drug confined in an oily or aqueous cavity, or nanospheres, a matrix in which the drug is dispersed all over the particles [17-19].

The production of PNPs involves several types of synthetic and/or natural polymers. Among the natural ones, chitosan and albumin-based PNPs are the most well-known. Synthetic polymers used to prepare PNPs include molecules such as poly(vinyl alcohol) (PVA), poly(lactide-co-glycolide) (PLGA), poly(acrylic acid) (PAA), polylactide (PLA),

polyglycolide, poly(ε-caprolactone) (PCL), poly(D,L-lactide), PLGA-polyethylene glycol (PLGA-PEG), polyamidoamine (PMAM), and polyethylene oxide (PEO) [18,19]. The preparation methods include solvent evaporation, emulsion polymerization, conventional emulsion polymerization, surfactant-free emulsion polymerization, and dialysis [20,21].

Numerous *in vitro* and *in* vivo studies have been carried out using PLGA systems. Moreno et al. formulated PLGA nanoparticles (NPs) containing cisplatin and verified their cytotoxicity in DHD/K12PROb rat cells obtained from colon adenocarcinoma. The results revealed that the formulation offered a controlled release of cisplatin, inducing more effective apoptosis when compared to the free-form drug [22]. In the same way, doxorubicin and tamoxifen-loaded PLGA NPs presented higher drug payloads to MDA-MB-231 human and C1271 murine breast cancer cells, respectively [23,24], and doxorubicin NPs had a synergistic effect along with photothermal treatment in HeLa human cervical carcinoma cells [25]. Regarding pancreatic carcinoma, Papa et al. used gemcitabine-loaded PLGA NPs in PANC1 human pancreatic carcinoma cells and observed increased amounts of cytotoxicity and apoptosis [26], and similar results were found in U87MG human glioma cells treated with 5-fluorouracil (5-FU) PLGA NPs [27].

Concerning *in vivo* models, Han et al. revealed that cisplatin PLGA-mPEG NPs administered in IRC and BALB/c mice were highly stable and showed a median lethal dose (LD_{50}) of more than 100 mg/kg, which was much higher than its free-form [28], and the same formulation was also efficient in rat glioblastoma models, with satisfactory delivery across the blood-brain barrier (BBB) [29]. Cisplatin PLGA NPs injected in a DHD/K12PROb colon adenocarcinoma nude mouse model showed no toxicity signs and reduced tumor volume [30].

Chitosan and PEG were similarly used to obtain PNPs loaded with 5-FU. Studies using mouse hepatic cancer models revealed that the formulation was able to reduce the tumor growth rate via the p53 apoptosis pathway, as well as reduce the side effects and immunosuppression of the conventional treatment [31,32]. Using PBLG-PEG NPs containing 5-FU in a Balb/c nude mouse model implanted with LoVo colon cancer or Tca8113 oral squamous carcinoma cells, Li et al. displayed that both models presented slower tumor growth and prolonged tumor doubling times [33].

Currently, PNPs are being used in several preclinical assays and clinical trials for cancer therapy; however, only a few of them have completed all requirements for Food and

Drug Administration (FDA) approval for commercialization. Nevertheless, most of them are in the advanced stages of clinical studies or already approved, offering a variety of future possibilities in the chemotherapy field (Table 1).

Table 1: Examples of current clinical trials using polymeric nanoparticles for cancer therapy.

PNP	Commercial drug (sponsor)	Generic name	Indications	Status	Ref.
Albumin	ABI-008 (Abraxis/Celgene)	Docetaxel	Metastatic breast and prostate cancer	Phase II	[34]
Albumin	ABI-009 (Abraxis/Celgene)	Nab-sirolimus	Solid tumors, bladder cancer	Phase II	[34]
Albumin	ABI-011 (Abraxis/Celgene)	Thiocolchicine dimer	Solid tumors, lymphoma	Phase I	[34]
Albumin	Abraxane (Abraxis/Celgene)	Paclitaxel	Metastatic breast cancer and various other tumors	Approved	[21]
Polyamino acid-PEG	NC-6004 Nanoplatin (Nanocarrier)	Cisplatin	Advanced solid tumors, lung, biliary, bladder, and pancreatic cancers	Phase II	[37]
Polyamino acid-PEG	NC-4016 DACH-Platin micelle (Nanocarrier)	Oxaliplatin	Advanced solid tumors or lymphomas	Phase I	[37]
PIHCA	Transdrug (Onxeo)	Doxorubicin	Hepatocellular carcinoma	Phase III	[21]
PLGA-PEG	BIND-014 (Bind Therapeutics)	Docetaxel	Metastatic castration-resistant prostate and non-small cell lung cancers	Phase II	[35]
PLGH	Eligard (TOLMAR Pharmaceuticals)	Leuprolide acetate	Prostate cancer	Approved	[38]

PNP: polymeric nanoparticle; PIHCA: poly(isohexylcyanoacrylate); PLGA: poly(lactic-co-glycolic acid); PEG: polyethylene glycol; PLGH: DL-lactide-co-glycolide.

2.2 Polymer conjugates

The conjugation of macromolecular polymers with drugs, proteins, and their derivatives is an interesting platform for DDS as it allows therapeutic agents to be covalently bound to hydrophilic or amphiphilic polymers instead of being encapsulated as in a PNP [39-41]. This nanoscale system may be able to prolong drug circulation time in the blood

and improve its solubility and bioavailability, reducing the occurrence of side effects and burst release (expect at the target tissue) [40,42].

Most polymer conjugates use *N*-(2-hydroxypropyl)-methacrylamide (HPMA) copolymers, polyethylenimine (PEI), polyglutamic acid (PGA), PAA, PCL, PEG, PLA, PLGA dextran, or hyaluronic acid (HA), and they can be bound to one or more drugs, proteins, antibodies, or aptamers, acquiring different structures such as dendrimers, polymer-drug, polymer-protein, polymer-antibody, and polymer-aptamer conjugates, with many of them already launched in the market [39,42-44].

Proteins and antibodies conjugated to PEG have been well-known in the pharmaceutical industry since the 1990s, when Adagen®, a PEG-adenosine deaminase conjugate, was approved by the FDA for the treatment of ADA-SCID (severe immunodeficiency caused by hereditary deficiency of the adenosine deaminase enzyme) [45]. In the cancer field, this strategy allowed several companies to start different clinical developments, including drug-polymer conjugates. The first drug-polymer conjugate to progress in clinical trials was a HPMA-doxorubicin formulation, which in preclinical assays showed a higher improvement in plasma half-life and antitumor activity and a lower toxicity. However, clinical trials failed after only a few patients presented tumor drug accumulation, with minimal efficacy [46].

Lastly, dendrimers are unimolecular, three-dimensional, and highly branched polymeric structures. They present a central core with radiating blocks in branched units, which give them a precise shape with low dispersity [39,47]. One of the main advantages of dendrimers is their ability to penetrate through intestinal membranes, which is frequently a limitation to oral drug administration due to the permeability barriers in the gastrointestinal tract [41]. The first dendrimer to receive commercial approval was SPL7013 (VivaGel), a poly(L-lysine) topical microbicide to treat bacterial vaginosis. However, the most widely used polymer is poly-amidoamine (PMAM), a cationic amine-terminated and non-biodegradable molecule, which makes it difficult to use in medicine [39]. Despite this, some drug-dendrimer formulations are currently under study (Table 2).

Table 2: Examples of current clinical trials using polymer conjugates for cancer therapy.

Conjugate	Commercial drug (sponsor)	Generic name	Indications	Status	Ref.
PEG-protein	Calaspargase pegol (Shire)	Asparaginase	Acute lymphoblastic	Phase II	[48]

			leukemia, lymphoblastic lymphoma		
PEG-protein	Pegilodecakin (ARMO BioSciences)	IL-10	Pancreatic cancer	Phase I	[50]
PEG-protein	Pegargiminase (Polaris Group)	Arginine deiminase	Mesothelioma	Phase I	[51]
PEG-protein	BCT-100 (Bio-Cancer Treatment International)	Arginase-1	Acute myeloid leukemia	Phase II	[52]
PEG-protein	NKTR-214 (Nektar Therapeutics)	IL-2	Solid tumors	Phase II	[53]
PEG-aptamer	Olaptesed pegol (Noxxon Pharma)	Anti-CXCL12 aptamer	Colorectal and pancreatic cancers	Phase I/II	[54]
SMA-drug	SMANCS (Astellas Pharma)	Neocarzinostatin	Liver and renal cancers	Approved	[55]
PGA-drug	Opaxio (CTI BioPharma)	Paclitaxel	Ovarian, peritoneal, and fallopian tube cancers	Phase III	[56]
Dextran-drug	OsteoDex (DexTech Medical)	Alendronate	Prostate cancer	Phase II	[57]
PEG-drug	NKTR-262 (Nektar Therapeutics)	TLR7/TLR8 agonist	Solid tumors	Phase I/II	[39]
PEG-drug	DFP-13318 (ProLynx)	SN-38	Solid tumors	Phase I	[58]
PEG-polylysine dendrimer	DEP docetaxel (Starpharma)	Docetaxel	Solid tumors	Phase II	[39]
PEG-polylysine dendrimer	DEP cabazitaxel (Starpharma)	Cabazitaxel	Solid tumors	Phase II	[39]

PEG: polyethylene glycol; IL-10: interleukin-10; IL-2: interleukin-2; SMA: poly(styrene-co-maleic acid); PGA: polyglutamic acid; TLR7: toll-like receptor 7; TLR8: toll-like receptor 8.

2.3 Inorganic nanoparticles

INPs comprise structures such as gold, silver, gadolinium, hafnium, magnetic, and silica NPs, as well as carbon nanotubes and QDs. In common, all of them are quickly developed, and they have physicochemical properties and surface engineering that guarantee exceptional biocompatibility [59]. In contrast with PNPs, inorganic nanomaterials with biomedical applications were recently developed and have already shown significant impacts on cancer therapy [60,61] (Table 3).

Table 3: Examples of current clinical trials using inorganic nanoparticles for cancer therapy.

INP	Commercial drug (sponsor)	Generic name	Indications	Status	Ref.
Gd-chelate-based NP	AGuIX (National Cancer Institute, France)	Polysiloxane	Advanced cervical cancer	Phase I	[37]
Gold NP	NU-0129 (Northwestern)	Nucleic acids	Glioblastoma	Phase I	[37]
Gold NP	CYT-6091 (National Institutes of Health Clinical Center)	Tumor necrosis factor-α	Pancreatic, melanoma, soft tissue sarcoma, ovarian, and breast cancers	Phase I	[94]
Hafnium oxide NP	NBTXR3 (PEP503) (Nanobiotix)	NPs stimulated with external radiation to enhance tumor cell death via electron production	Advanced squamous cell carcinoma	Phase I/II	[95]
Iron NP	Magnablate (University College London Hospitals)	Iron NP. Magnetic-field responsive to thermal ablation	Prostate cancer	Phase I	[96]
Iron NP	NanoTherm (MagForce Nanotechnologies)	Iron NP responsive to thermal ablation	Glioblastoma	Approved	[97]
Silica NP	AuroLase (Nanospectra Biosciences)	Silica-gold nanoshells coated with PEG, laser-responsive	Thermal ablation of head / neck cancer and metastatic lung tumors	Finished	[96]

NP: nanoparticle; Gd: gadolinium; PEG: polyethylene glycol.

Gold NPs are synthesized under different substrates and methodologies, with sizes ranging from 1 to 100 nm and shapes going from nanospheres and nanocages to nanorods and nanostars. These NPs are very interesting due to their peculiar surface plasmon resonance, which converts light into heat, causing local hyperthermia and hence killing cancer cells [62,63]. Moreover, gold is a metal that can be conjugated with a large variety of molecules, and along with the fact that it shows low toxicity and high stability [64], several *in vitro* and *in vivo* antitumor studies have been carried out, especially using phytochemical molecules. Chen et al. synthesized gold NPs conjugated with epigallocatechin-3-gallate (EGCG) to test their activity against B16F10 murine melanoma cells, and the results revealed a 4.9-fold increased efficacy when compared to EGCG free-form. Comparable results were observed in tumor growth rate in a murine melanoma model [65]. In the breast cancer field, Kondath et al. and Raghavan et al. tested the anticancer effects of morin and kaempferol in MCF-7 human cell line models, respectively. Morin-gold NPs revealed high cytotoxicity levels when administered in MCF-7 cells and showed a biocompatible profile

when tested in HBL-100 normal human blood cells. Analogous results were found in kaempferol-gold NPs administration, where cell viability was reduced in a dose and time-dependent manner, probably by inducing apoptotic pathways [66,67].

Similarly, silver NPs have interesting properties of stability, conductivity, and catalysis, making them a real focus on cancer treatment since they can internalize into mammalian cells by endocytosis and distribute their content to the cytoplasm and nucleus. Additionally, their small size also makes them able to cross the BBB, although some physicochemical properties may cause cytotoxicity to both normal and cancer cells [68,69]. *In vitro* antitumor activity of NPs has been analyzed against numerous types of cancer, with remarkable antiangiogenic and anti-proliferative properties [70,71]. Jeyaraj et al. and Gurunathan et al. carried out studies using biologically synthesized silver NPs from *Sesbania grandiflora* and *Bacillus funiculus* against MCF-7 and MDA-MB-231 human breast cancer cells, respectively. Results showed increased cytotoxicity in both cell lines, with noticeable effects on DNA damage, apoptosis pathways, and oxidative stress [69,72]. Also, Vasanth et al. tested the anticancer activity of *Moringa oleifera* silver NPs on HeLa human cervical carcinoma cells. They showed outstanding anticancer activity, probably due to oxidative stress followed by cell growth inhibition due to apoptosis induction [73].

Silica-based NPs, mainly mesoporous silica NPs, have been investigated as promising candidates for tumor target systems due to their ability to accept organic molecules and to act as a suitable reservoir for controlled DDS. As their main characteristics, they can be very strictly pore-sized and have a specific pore volume and surface area that support a high drug payload [74,75].

Mesoporous silica NPs containing doxorubicin and L-arginine as a nitric oxide donor were used, respectively, by Huang et al. and Zhang et al., in *in vitro* and *in vivo* pancreatic carcinoma models. The first study observed that MiaPaCa-2 human pancreatic carcinoma cells treated with the NPs had higher cytotoxicity levels than the free drug treatment. The formulation was fully functional to effectively deliver the drug in the SCID mouse model. The second one revealed that PANC-1 human pancreatic carcinoma cells treated with the NPs together with ultrasound-triggered release had increased levels of p53 and caspase-3 protein levels, indicating DNA damage followed by apoptosis. *In vivo* experiments also showed an interesting inhibition of tumor growth in nude mice [76,77]. Giménez et al. loaded safranin-O and doxorubicin into PEG-capped mesoporous silica NPs to test them against

HeLa human cervical carcinoma cells in a glutathione (GSH)-dependent model (which has a higher concentration and more reductive properties inside tumors) and exposed that the system can be retained closed at low GHS levels, allowing the drug release only at high GSH concentrations [78].

Magnetic materials are well known and have been functionally introduced in several areas. The interest in using them with biomedical prospects is because they can generate significant thermal effects in a magnetic field [61]. To date, Fe_3O_4 and other iron oxides are the main components of magnetic NPs due to their low toxicity and well-known metabolism routes. Despite being more common as contrast agents, they have been lately investigated as potential antitumor target systems [60].

Singh et al. used PLGA-magnetic NPs for the co-delivery of hydrophilic (carboplatin) and hydrophobic (paclitaxel and rapamycin) drugs in *in vitro* models using MCF-7 human breast cancer and PANC-1 human pancreatic carcinoma cells. Their results displayed improved cellular uptake and an increased synergistic effect of the conjugated system compared to free drugs [79]. Kohler et al. treated 9L rat glioma cells with methotrexate-PEG magnetic NPs and observed increased cytotoxicity compared to empty NPs or free-drug, along with augmented cytoplasm retention, allowing extended tumor imaging over the therapeutic time course [80]. *In vivo* assays were conducted by Alexiou et al. using VX-2 squamous carcinoma cells implanted on a New Zealand white rabbit model and intra-arterially treated with magnetic NPs bound to mitoxantrone, resulting in a complete and permanent remission of the tumor in comparison with the negative control and intravenous administration groups [81].

Carbon nanotubes can be classified into single- and multiwalled versions and display inherent properties such as ultralight weight, mechanical strength, large internal volume, and pronounced electrical and thermal conductivities. These nanosystems have acquired increased attention in cancer nanomedicine in the last twenty years because of their versatile profiles, allowing the incorporation and establishment of several DDS containing from drugs and small interfering RNA to proteins and antibodies [15,60,64]. Structurally, carbon nanotubes are hydrophobic self-assembling sheets of atoms organized in a tube shape with a diameter between 1 and 4 nm, giving them the ability to cross cells using “needle-like penetration”, and therefore deliver their content into the cytoplasm. On the other hand, these nanostructures are non-dispersible in all solvents, which increases cytotoxicity levels and

requires structural chemical modifications to convert them into water-dispersible carriers, allowing the inclusion of different chemotherapeutic drugs [35,82].

Two *in vitro* studies using A549 human lung carcinoma cells looked for the phytochemical anticancer properties of carbon nanotubes containing betulinic acid and silibinin, and in both cases the cytotoxicity effects were higher than the free-drug treatments and showed no toxicity against normal cell lines [83,84]. Paclitaxel was also PEG-functionalized into carbon nanotubes and tested in HeLa human cervical carcinoma and MCF-7 human breast cancer cells, showing high efficacy to kill both cell lines with a lower IC_{50} than free-drug [85]. Similar effects were observed *in vitro* and *in vivo* by using cisplatin carbon nanotubes bound to the specific receptor ligand EGF (epidermal growth factor) against HNSCC neck squamous carcinoma cells and mice xerographically implanted with the same cell line overexpressing the EGF receptor. In both experiments, the nanosystems could selectively and efficiently target cells overexpressing the receptors, killing most of the tumor cells [86].

Finally, QDs are 2-10 nm-sized semiconductors and fluorescent NPs or nanocrystals, composed of groups II-VI or III-V elements such as sulfides, selenides, tellurides, and carbon (silicon). By carrying properties such as small size, versatile surface chemistry, narrow emission profile, high photostability and brightness, and sensitivity to the microenvironment, QDs are worthy candidates as DDS in biological systems [15,63,87]. Their fluorescent characteristics allow them to act as probes with intense signal emission, making these NPs an emerging theragnostic system. Besides, they can also act as photosensitizers and, once combined with a specific wavelength of light and oxygen, generate reactive oxygen species inside tumors, leading the cells to trigger the apoptotic pathway [88]. For example, QDs have been used to target specific overexpressed proteins, peptides, and receptors and therefore detect early stages of pancreatic, ovarian, and breast cancer [89-91].

Nurunnabi et al. conducted *in vitro* and *in vivo* studies using QDs micelles loaded with herceptin and tested them against SK-BR3 human breast cancer and KB human nasopharyngeal epidermoid cancer cells, as well as in SKH1 mice injected with MDA-MB-231 human breast cancer cells. Results revealed an increased cytotoxicity dose and time-dependent effect in cell lines and an *in vivo* antitumor effect, with shrinkage of the tumor volume and inhibition of tumor growth [92]. Bagalkot et al. carried out assays with QD-

aptamer conjugates containing doxorubicin (which is fluorescent) and capable of recognizing the extracellular domain of the prostate-specific membrane antigen to treat LNCaP human prostate adenocarcinoma cells. They showed that the formulation was not only able to specifically detect and bind to the tumor cells but also intracellularly release the drug and, as a result, provide images of the tumor cells [93].

2.4 Liposomes

Liposomes are ≥ 50 nm-sized phospholipidic vesicles and the most common form of lipid-based nanostructure with biomedical applications, being able to contain hydrophobic therapeutic agents at their lipid bilayer and hydrophilic agents inside them. Consequently, cationic liposomes can also be electrostatically bound to anionic nucleic acids. They can often be classified as multilamellar vesicles, small unilamellar vesicles, large unilamellar vesicles, long-circulating liposomes, and immunoliposomes [15,98].

As a main advantage, liposomes have a composition that assembles to the cell membrane, making them more biocompatible than other nanocarriers with synthetic materials, avoiding antigenic and toxic effects, therefore being one of the most common nanocarriers. Also, their structure protects drugs from early degradation and other microenvironmental hazards, not to mention that they are a suitable way to carry hydrophobic agents. On the other hand, these features may lead to some limitations, such as long-time circulation in the blood, poor stability due to phospholipid oxidation, difficulties in sterilization, and limited drug release control [35,99].

These problems can be easily solved by making structural and physicochemical modifications using polymers to enhance stability and drug release rates [35]. In detail, liposome surface modifications can range from the attachment of specific ligands for targeted purposes to the attachment of hydrophilic polymers for long-circulation profiles, the attachment of label carriers for drug delivery monitoring or diagnostic imaging, the incorporation of positively charged polymers or lipids for DNA binding to allow cell transfection, and the attachment of antibodies and antigens for immunoassays [100].

Several *in vitro* and *in vivo* studies have been carried out using liposome systems for chemotherapeutic encapsulation. One of the most promising approaches is pH-sensitive liposomes, which can release drugs only inside tumors due to their particular pH environment, avoiding early degradation and side effects [101]. Banerjee et al. developed

poly(styrene-co-maleic acid)-based liposomes for 5-FU cytosolic delivery and applied them in HT-29 colon cancer cells. As a main result, they increased intracellular drug availability, resulting in enhanced apoptosis [102]. Another study using folate receptor-targeted liposomes containing cytarabine showed efficient intracellular drug and gene delivery in KB human oral cancer cells, enhanced cytotoxicity, and a decreased IC_{50} value [103].

Mo et al. tested liposomes based on zwitterionic oligopeptide lipids containing temsirolimus in both *in vitro* and *in vivo* models against renal carcinoma, and they revealed a significantly higher antiproliferative and apoptotic induction in A498 human carcinoma cells, which was confirmed in the xenograft cancer model [104]. Looking for doxorubicin-triggered release, Ishida et al. and Paliwal et al. established pH-sensitive liposomes to treat lymphoma and breast cancer, respectively, *in vitro* and *in vivo*. Narnalwa human Burkitt's lymphoma cells presented higher cytotoxicity when treated with liposomes targeted to their CD19 epitope. The same model applied to the murine model corroborated their efficacy, even though rapid drug release and clearance were observed. In the breast cancer models, estrogen-anchored liposomes containing the drug showed increased intracellular uptake in ER-positive MCF-7 cancer cells, with nuclear drug localization and cytotoxicity by reactive oxygen species generation. Balb/c mice implanted with DMBA cancer cells and intravenously treated with the formulations exhibited tumor suppression by intracellular drug trafficking [105,106].

Among all nanomedicines, the liposomal formulation Doxil® became the first nanosystem approved by the FDA in 1995 and consisted of doxorubicin for the treatment of Kaposi's sarcoma [36]. Other liposomal systems have been developed and extensively used in chemotherapy and immunotherapy (Table 4), since they can take advantage of the leaked character of tumor blood vessels and therefore target cancer cells more easily than other NPs [15,100,107].

Table 4: Examples of current clinical trials using liposomes for cancer therapy.

Commercial drug (sponsor)	Generic name	Indications	Status	Ref.
Aroplatin (L-NDDP) (Aronex)	DACH platin	Colorectal cancer, solid malignancies	Phase I/II	[108]
ATI-1123 (Azaya Therapeutics)	Docetaxel	Solid tumors	Phase I	[34]
DaunoXome (Galen)	Daunorubicin	Kaposi's sarcoma	Approved	[34]
2B3-101 (to-BBB)	Doxorubicin	Brain metastasis of breast cancer	Phase I/II	[109]

Doxil / Caelyx (Johnson & Johnson)	Doxorubicin	Kaposi's sarcoma, ovarian, breast cancers, multiple myeloma	Approved	[110]
EGFR antisense DNA liposomes (University of Pittsburgh)	EGFR antisense DNA	Head / neck cancer	Phase I	[111]
LEM-ETU (Insys Therapeutics)	Mitoxantrone	Leukemia, breast, stomach, liver, and ovarian cancers	Phase I	[112]
Lipo-Dox (Taiwan Liposome)	Doxorubicin	Kaposi's sarcoma, ovarian cancer, breast cancer	Approved	[113]
Lipo-MERIT (BioNTech SE)	Naked RNA-drug products	Cancer vaccine for advanced melanoma	Phase I	[37]
Lipoplatin (Regulon)	Cisplatin	Non-small-cell lung cancer	Phase III	[114]
Liposomal Annamycin (Moleculin Biotech)	Annamycin	Soft-tissue sarcomas with pulmonary metastases	Phase I/II	[37]
Marqibo (Talon)	Vincristine	Acute lymphoid leukemia	Approved	[115]
Mepact (Takeda)	Mifamurtide MTP-PE	Osteosarcoma	Approved	[116]
Myocet (Cephalon)	Doxorubicin	Breast cancer	Approved	[117]
ThermoDox (Celsion)	Doxorubicin	Unresectable hepatocellular carcinoma	Phase III	[118]
Vyxeos CPX-351 (Jazz Pharmaceuticals)	Cytarabine / daunorubicin	Acute myeloid leukemia	Approved	[37]

DACH: diaminocyclohexane; MTP-PE: muramyl tripeptide phosphatidylethanolamine; EGFR: epidermal growth factor receptor; DNA: deoxyribonucleic acid; RNA: ribonucleic acid.

2.5 Micelles

Micelles are colloidal amphiphilic nanocarriers, 5-200 nm-sized and finely customized to allow slow and controlled drug release. They are structurally designed with an internal hydrophobic core and an external shell with enough polarity to dissociate in aqueous solutions. The development of these NPs is a usual technique to overcome poor drug solubility and therefore increase their bioavailability [36,38,64].

Usually, the core contains polyphenylene oxide or lipids in its composition, which are maintained by van der Waals forces, while the external hydrophilic surface is sustained by hydrogen bonds and covered by PEG; nonetheless, PLA, PGA, and other polymers may be used, all of them affording protection and prolonged blood circulation [99,119]. Two of the most important and crucial factors in micelle formation are the critical micelle temperature and the critical micelle concentration (CMC), which are the specific temperature

and concentration at which micelles spontaneously assemble. CMC has a quite narrow range of concentrations that delimits changes in the physicochemical properties of amphiphilic dispersion, a central key for micelle stability. Therefore, concentrations below the CMC tend to dissolve the nanostructure, causing the premature release of the drug, whereas at the CMC, the micelle formation is viable [119,120].

Micelles have been used in *in vitro* studies, with a special focus on oral cancers. Saiyin et al. developed doxorubicin-loaded polymeric nanomicelles to treat HN-6 and CAL-27 human oral squamous carcinoma cell lines, and the outcomes indicated that the NPs could rapidly enter the cells and release the drug under the local acidic environment, inhibiting cell proliferation [121]. Similarly, Endo et al. used cisplatin-loaded polymeric nanomicelles against OSC-19, OSC-20, HSC-3, and HSC-4 human oral squamous carcinoma cell lines, with further *in vivo* application. Considering their potential antitumor activity, the authors showed and supported increased lymphatic drug delivery and a notable reduction in nephrotoxicity, extenuating the application of platinum-complexed NPs in cancer therapy [122].

Another important field for micelle application involves the incorporation of microRNAs in these nanosystems. Liao et al., Shao et al., and Wang et al. combined miRNA-32, miRNA-519a, and miRNA503 in micelles to treat prostate, hepatocellular, and osteosarcoma tumors, respectively. As results, DU145 and PC3 prostate cancer cells with downregulated miRNA-32 showed high autophagy activity; SMMC-7721 and Huh7 hepatocellular carcinoma cells with downregulated miRNA-519a presented lower proliferation rates; and U2OS, Saos-2, MG63, and SW1353 osteosarcoma cell lines with overexpressed miRNA-503 significantly inhibited their proliferation and invasion, probably via IGF-1R downregulation [123-125].

Despite their apparent versatility and functionality, micelles often suffer from occasional issues, such as low stability. To increase their stability, the already mentioned CMC factor plays an important role, since if NPs are diluted below their CMC, they will dissolve and release the drug right after entering the bloodstream [119]. One of the avoidable ways to overcome these problems is to conjugate the nanocarriers to polymer structures that improve their time circulation, such as PEG and PEO, and therefore not only resist to opsonization and low stability but also enhance tumor accumulation by the enhanced

permeability and retention (EPR) effect [126], which justifies micelles application in the chemotherapy field (Table 5).

Table 5: Examples of current clinical trials using micelles for cancer therapy.

Commercial drug (sponsor)	Generic name	Indications	Status	Ref.
CriPec (Cristal Therapeutics)	Docetaxel	Solid tumors, ovarian cancer	Phase I/II	[37]
Cynviloq IG-001 (Sorrento)	Paclitaxel	Breast Cancer	Phase I/II	[37]
Docetaxel-PM (Samyang Biopharmaceuticals)	Docetaxel	Head / neck cancer, advanced solid tumors	Phase II	[37]
Genexol-PM (Samyang Biopharmaceuticals)	Paclitaxel	Brest, lung, and ovarian cancers	Approved	[127]
Imx-110 (Immix Biopharma Australia)	Stat3 / NF-κB / poly-tyrosine kinase inhibitor and low-dose of doxorubicin	Advanced solid tumors	Phase I/II	[37]
Lipotecan (TLC388) (Taiwan Liposome)	Camptothecin derivate	Liver and renal cancers	Phase I	[128]
Nanoxel (Fresenius Kaby Oncology)	Paclitaxel	Advanced breast cancer	Phase I	[129]
NC-4016 (NanoCarrier)	Oxaliplatin	Solid tumors, lymphoma	Phase I	[130]
NC-6004 (NanoCarrier)	Cisplatin	Pancreatic cancer	Phase II	[131]
NC-6300 (K-912) (NanoCarrier)	Epirubicin	Solid tumors, soft tissue sarcoma	Phase I/II	[37]
NK-012 (Nippon Kayaku)	Active metabolite of irinotecan (SN-38)	Solid tumors, small cell lung, and breast cancers	Phase II	[132]
NK-105 (Nippon Kayaku)	Paclitaxel	Gastric and breast cancers	Phase III	[133]
NK-911 (National Cancer Institute Japan / Nippon Kayaku)	Doxorubicin	Solid tumors	Phase I/II	[134]
ONM-100 (OncoNano Medicine)	Indocyanine green	Intraoperative detection of cancer	Phase II	[37]
Paclical (Oasmia Pharmaceutical)	Paclitaxel	Ovarian cancer	Phase III	[37]
SP1049C (Supratek Pharma)	Doxorubicin	Advanced adenocarcinoma	Phase II/III	[135]

Stat3: signal transducer and activator of transcription 3; NF-κB: nuclear factor kappa-light-chain-enhancer of activated B cells.

2.6 Exosomes

Exosomes are a type of extracellular vesicle ranging in size from 30 to 150 nm and derived from the exocytosis of intraluminal endosomal vesicles, which are therefore released into the extracellular space once they are fused with the plasma membrane [136,137]. They

can be secreted by almost all cell types, including endothelial, epithelial, and neuronal, as well as fibroblasts, immune cells, and tumor cells. Structurally, they are formed by a lipid bilayer, and their multicellular origin makes them able to interact, carry, and transfer a wide range of proteins, molecules, mRNA, and miRNA, delivering multifaceted sets of biological information to neighboring cells and modulating their behaviors by molecular modifications [136,138].

Although the already mentioned liposomes and micelles can well play the function of drug-loaded synthetic NPs and be opsonized in the bloodstream, these two DDS must face peculiar problems: notable toxicity and fast clearance by the mononuclear phagocyte system (MPS). Even though MPS activity can be partially circumvented or decreased by NP PEGylation, immune responses to the PEG corona can occur, and this structure may also reduce the interaction with membranes and targets, resulting in less tissue biodistribution [139].

While their complete function remains unspecified, exosomes are physiologically highly heterogeneous and typically exhibit phenotypic characteristics that resemble those of the cell that generates them. Consequently, they often end up showing roles in cell recycling, immune response modulation, enhanced tumor-cell invasion, and cell communication [136,140], and this diversity, added to their intracellular crosstalk abilities, makes them worthy candidates to surmount cell barriers, making them very useful for cancer treatment and immune regulation [141,142] (Table 6).

Table 6: Examples of current clinical trials using exosomes for cancer therapy.

Exosome origin	Sponsor	Generic name	Indications	Status	Ref.
Ascites-derived exosomes	Guangxi Medical University	Granulocyte-macrophage colony-stimulating factor	Colorectal cancer	Phase I	[143]
Dendritic cells-derived exosomes	Gustave Roussy Institute	MHC class II peptides	Melanoma	Phase I	[144]
Dendritic cells-derived exosomes	Gustave Roussy Institute	MAGE cancer antigens	Non-small cell lung cancer	Phase I	[145]
IFN-γ-dendritic cells-derived exosomes	Gustave Roussy Institute	MHC class I- and class II-restricted cancer antigens	Non-small cell lung cancer	Phase II	[146]
Mesenchymal stromal cells-derived exosomes	M.D. Anderson Cancer Center	KrasG12D siRNA (iExosomes)	Metastatic pancreatic cancer	Phase I	[147]
Plant exosomes	University of Louisville	Curcumin loaded	Colon cancer	Phase I	[147]

MHC: major histocompatibility complex; MAGE: melanoma-associated antigen; IFN-γ: interferon gamma; KrasG12D: Kirsten rat sarcoma gene (substitution – missense, position 12, G➞D); siRNA: small interfering RNA.

3. Active barriers to tumor-targeting drug delivery systems

In the last few decades, several molecular cancer mechanisms have been disclosed, increasing the understanding of this disease and establishing different and important associations with external aspects and other pathophysiological conditions [148]. On the other hand, advances in chemotherapeutic drug development have slowly been converted into major advances for patients' therapy [34], especially due to the presence of active barriers that prevent most of the drugs to reach the tumor site at therapeutic levels. One of the most well-known active barriers in cancer cells is the overexpression of ATP-binding cassette (ABC) transporters, such as P-glycoprotein. These transporters actively pump chemotherapy drugs out of cancer cells, reducing drug accumulation and effectiveness [149]. Cancer cells can also exhibit enhanced DNA repair mechanisms, which help them recover from DNA damage caused by chemotherapy and radiation therapy, as well as develop mechanisms to resist apoptosis, which is a natural process of programmed cell death [150,151]. The intratumoral heterogeneity found in the TME, which refers to the presence of various cancer cell subpopulations with different genetic and molecular characteristics, can create active barriers to treatment because not all cells respond the same way [152]. Lastly, most cancer cells possess stem cell-like properties, allowing them to self-renew and differentiate. These tumor-initiating cells can resist treatment and drive cancer progression [153].

Besides issues such as the high hydrophobicity of oral drugs (tending them to bioaccumulate and cause toxicity), non-selective targeting molecules, and tumor resistance mechanisms, some important limiting barriers to tumor DDS have been proven to be central keys for successful therapies [148,154]. Basically, they can be grouped into physicochemical, anatomical / physiological, and tumor intrinsic barriers, ranging from cellular membrane characteristics to metabolization and charge interactions [155].

3.1 Physicochemical interactions

Among all types of cancer, there are numerous possibilities for physicochemical interactions between the nanocarriers and a specific tumor. Depending on the stage of the disease and the particularities of the physiological processes and TME of each patient, these interactions may be different. To effectively deliver the chemotherapeutic drug to the tumor and have a chance to kill cancer cells, there is a long pathway through which the nanocarriers

must go. If a nanoformulation is administered by injection, this path will start at the injection site. The NP carrying the drug must follow the bloodstream to reach the tumor site and then pass through stages of extravasation from the relatively leaky regions of the tumor vasculature into the TME. Once the NPs are in the TME, they must undergo accumulation, distribution, and intracellular localization, limited by the tumor's extracellular matrix content and cell density [156-158]. The number of NPs that reach the tumor, their degree of penetration into the tissue, the uniformity of distribution, the release profile of the drug from the NP, and the binding affinity of the drug are key factors affected by physicochemical interactions. They are determinants of the success of a new nanoformulation [157]. This section intends to give an overview of how the physicochemical characteristics of nanocarriers, such as size, shape, and charge, may reflect on interactions with tumors and further uptake (Figure 2).

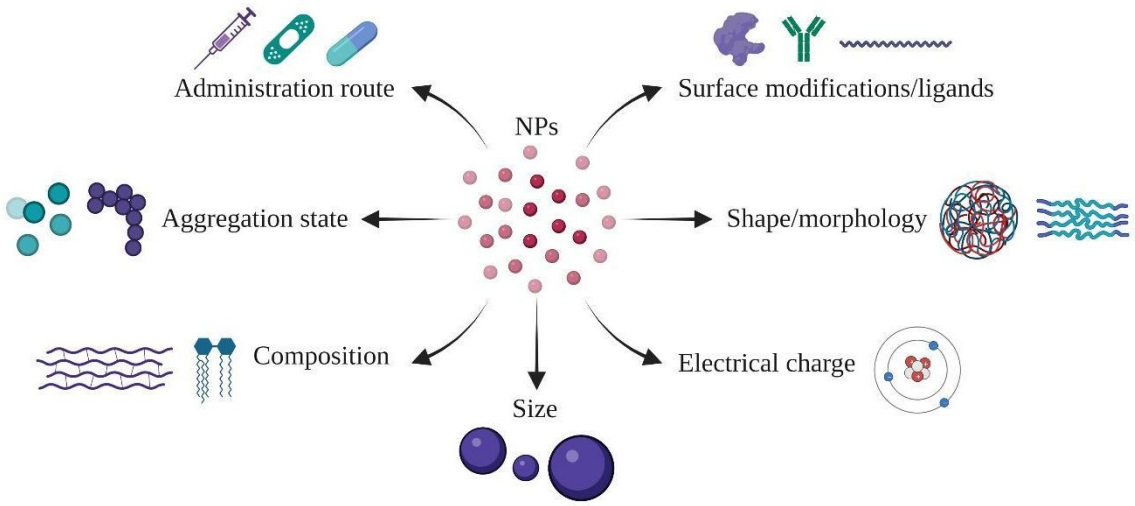

Fig. 2: Schematic representation of the different characteristics that modulate the physicochemical interactions between nanoparticles (NPs) and the target system. The administration route plays a key role in the onset of action, whereas characteristics such surface, shape, electrical charge, size, composition, and aggregation state are determinants of a successful *in situ* drug delivery.

All physicochemical characteristics evaluated will also depend on the route of administration of nanocarriers. In general, after particles are in the bloodstream, those with sizes above 100 nm will remain in circulation for longer than smaller ones. They may use the EPR effect to enable accumulation in tumor tissue. Particles with more than 200 nm may be cleared by the liver, spleen, and bone marrow, primarily by the MPS. Tiny NPs with diameters ≤ 5-6 nm are likely to be cleared by the kidney. Reduced clearance of particles will increase their chances of reaching and penetrating the tumor tissue. It was suggested

that a better penetration ratio into a tumor is seen for particles smaller than 12 nm. Thus, as there are multiple physiological barriers that a drug must overcome, some technologies exploit a responsive delivery system for solid tumors with particles that change their sizes or other characteristics to present a better penetration and accumulation profile once they enter the tumor site [159].

The platform iCluster is a polymeric clustered NP with a size of ~100 nm that undergoes a structural change to dendrimers of ~5 nm by endogenous stimuli of the TME [160]. These smaller particles extravasate into the lymphatic system and migrate into lymph nodes, inhibiting tumor metastasis [161]. NPs that reach the lymphatic system before systemic circulation can have some advantages in specific immunotherapeutic applications. Wong et al. proposed a strategy to covalently conjugate amino-PEG QDs onto a gelatine NP surface. This system initially has 100 nm NPs, and when in contact with matrix metalloproteinase-2 (MMP-2 or gelatinase A) in the TME, it is triggered by enzymatic degradation to release 10 nm QDs in tumor tissue. These QDs were used to allow easy visualization, and the authors refer to the possibility of incorporating 10 nm NPs as drug carriers [162]. Complementary studies demonstrated that a system composed of primary NPs with 20 nm that release secondary NPs with 5 nm containing the drug would be ideal for effective transport across the tumor, considering the size of the pores of the vessel wall in different tumors [157]. Another smart size-switchable nanoplatform was prepared using high-molecular-weight polymers conjugated to an MMP-2-sensitive peptide containing doxorubicin. The primary NPs have 100 nm, which release NPs with ~30 nm after extravasation from the tumor vessels in response to MMP-2 in the TME. This multistage system presented superior deep tumor accumulation results and led to more potent suppression of tumor growth and metastasis in 4T1 tumor-bearing mice compared to only primary NPs containing the same drug [163].

The size of nanocarriers is usually measured using dynamic light scattering (DLS), laser diffraction (LD), or transmission electron microscopy (TEM) techniques, individually or often combined. Except for TEM, by which the shape can be elucidated for some nanocarriers, the size measured by the other techniques usually considers structures to be spherical. The shape and structural organization of the nanocarriers can also be elucidated by other techniques, such as small-angle X-rays (SAXS), for example. The nanostructure shape strongly influences how the interaction with the cancer cell will occur, such as the

altered binding kinetics and dynamics of ligand-receptor interactions and the retention profile of drugs inside a tumor. Usually, studies compare spherical nanostructures to alternative shapes. However, it is interesting to maintain similar sizes to ensure that differences are due to shape only. Research converges on explanations based on the area of contact between the nanostructure and cells to explain the differences observed. A spherical NP may have limited contact; on the other hand, other structures can have multiple areas of contact and binding sites [159].

Tubular polymersomes (TP, 60 nm diameter and 240 nm length) were compared to spherical polymersomes (SP, 60 and 240 nm), both formed of the amphiphilic diblock copolymer PMPC-PDPA. The kinetics of cellular internalization on a cancer-cell line (FaDu) were different among these structures, being delayed for TP [164]. Furthermore, SP entered the cell cytosol, while TP were found within the cytosol and associated with the cellular surface. Cancer-cells activate different molecular pathways depending on the nanostructure's shape. This difference led to a higher toxicity of TP towards FaDu cells when compared to SP, both containing doxorubicin [165]. Another study compared two nanostructures formed by the DNA aptamer AS1411 conjugated to ~44 nm gold nanostars (AS1411-AuNS) or to ~50 nm spherical gold NPs (AS1411-50NPs) in terms of targeted ligand-receptor interactions on cancer cells in an in vitro model [166,167]. AS1411 is a tumor-targeting ligand that binds to nucleolin at the cell surface and is then transported to a perinuclear region to induce cell apoptosis. AS1411-AuNS exhibited better results in terms of velocity under directed diffusion and translational motion during restricted diffusion compared to AS1411-50NPs on nucleolin-expressing cells. Therefore, the shape of nanostructures influenced the dynamics of targeting nucleolin [166].

Similar to size switchable platforms, shape transformable NP systems that can change from one format to another may be interested in improving blood circulation time and tumor penetration. One example is a NP formed by the self-assembling of a linear triblock molecule containing a photosensitizer for photodynamic therapy, a chemotherapeutic drug, and an MMP-2-responsive peptide. Further, coating with polyethylene glycol-histidine was carried out to give a negative charge to the system. The final nanostructures were spherical (76.7 ± 5.2 nm) and could transform into nanofibers (~2000 nm) following the enzymolysis by MMP-2 at an acidic pH. Compared with control spherical NPs, the particles that changed to nanofibers increased tumor retention and had the

best capacity to promote tumor apoptosis in a BALB/c nude mouse 4T1 breast cancer model. The same work proposed a switch on NPs' charge from negative to positive. Once in the presence of the acidic pH of the TME, the histidine present in the coating is protonated, and the cationic primary NP is exposed. Positively charged NPs demonstrated a 1.33-fold increase in tumor penetration measured in the multicellular spheroids model compared to negatively charged NPs [168].

Positively charged nanostructures could have higher internalization and cellular uptake than negatively charged ones. The positive charge also promotes deeper penetration in tumors through caveolae-mediated endocytosis mechanisms. Most proteins in the blood are negatively charged at the physiological pH; therefore, negatively charged nanostructures tend to have a longer blood circulation than positive ones [168,169]. Therefore, in view of obtaining a balance among the best physicochemical characteristics and biological outcomes, researchers have invested in these switchable charged nanocarriers. Nanotechnology applied to cancer immunotherapy holds promise for treating several cancer types and can show improved results with combined engineered characteristics. Poly(ε-caprol actone)-poly(L-arginine) micelles loaded with indoleamine 2,3-dioxygenase 1 siRNA (IDO1 siRNA) and mitoxantrone have a positive charge. These NPs were coated with poly(ethylene glycol)-poly(L-lysine)-2,3-dimethylmaleic anhydride through electrostatic interactions and acquired a negative charge. Within the TME acidic pH, the large-sized NPs with a negative charge switched into smaller and positive particles to enhance tumor penetration and cellular uptake, showing an antitumor immune response in an *in vivo* animal model [170].

3.2 Biological barriers

Tumors possess a range of physiological defensive mechanisms that allow them to resist conventional treatments and, in combination with the complexity of the biological system, form an obstacle to approaches aiming to the delivery of drugs to specific sites. Hence, the ability to design nanocarriers layered with specific attributes is a key to a successful DDS, as this would allow them to execute sequential functions to cross these defensive barriers one at a time [171]. In this section, we discuss the different types of biological barriers and their influence when it comes to DDS.

The extracellular matrix (ECM) is a complex network of proteins and other molecules that provides structural support to cells and tissues. It plays an important role in cell adhesion, migration, proliferation, and differentiation. However, the ECM can also act as a barrier to drug penetration, as its composition and density can limit the diffusion of molecules into the tumor tissue, thus reducing the effectiveness of certain therapies [172]. As an example, Heldin et al. investigated the effect of the ECM on the delivery of paclitaxel, and they found that the ECM significantly reduced the penetration of paclitaxel into tumor cells, which could explain the resistance of some tumors to this drug [173], and Tiwari et al. revealed a similar loss of delivery effectiveness of topical drugs for the treatment of skin diseases [174]. On the other hand, strategies such as the use of ECM-degrading enzymes or the modification of drugs to improve their penetration through the ECM have already been studied. They could be deemed approaches to enhance drug delivery ratios [175]. Opsonisation is also a major obstacle characterized by the binding of specific blood serum proteins (opsonins) to nanocarriers, which become enclosed, signaled, and more easily detected by phagocytes, leading the NPs to early degradation [176].

Tumor blood vessels can also play a significant role in limiting drug penetration into solid tumors. The abnormal and disorganized architecture of tumor blood vessels can lead to poor perfusion and altered blood flow, creating a barrier to drug delivery. In addition, tumor-associated macrophages and other immune cells can accumulate around blood vessels, further restricting drug access to tumor cells [177]. Such a finding has already been shown by Cassetta et al. when they studied the influence of tumor-associated macrophages on drug delivery in a mouse model of breast cancer, revealing that the macrophages accumulated around tumor blood vessels and created a physical barrier to the penetration of chemotherapeutic drugs [178]. In another study, Friedrich et al. used a combination of imaging and mathematical modeling to study drug distribution in solid tumors. The results showed that tumors' chaotic and disordered blood vessel networks created non-uniform drug distributions, with some regions of the tumor receiving little or no drug exposure [179]. The importance of understanding the complex interactions between tumor blood vessels, tumor cells, and the surrounding microenvironment in developing effective cancer therapies is evident. Thus, developing strategies to overcome these barriers, such as improving blood vessel function or using combination therapies to target both tumor cells and the surrounding microenvironment, may be necessary to improve treatment outcomes.

Another barrier to DDS is the presence of drug efflux transporters on the cell surface. They play an important role in removing drugs and other molecules from cells and are often overexpressed in tumors, where they can act as a barrier to drug penetration by actively pumping drugs out of cells before they can exert their therapeutic effects [149]. As an alternative, the development of strategies to overcome these barriers, such as using efflux transporter inhibitors or modifying drugs to reduce their susceptibility to efflux transporters, has already been considered [180].

Because of their ability to self-renew, differentiate into various cell types, and resist chemotherapy and radiation, cancer stem cells (CSCs) – a subset of cancer cells that are thought to be responsible for tumor initiation, progression, and resistance to therapy – are also a significant barrier to drug penetration in cancer treatment [181]. This resistant profile is supported by elevated levels of drug efflux transporters and DNA repair enzymes [182], turning CSCs into a frontline defensive mechanism, reinforcing the importance of targeting these cells with novel drug combinations to improve overall treatment outcomes.

The immune system can act as a barrier to drug penetration in cancer treatment, particularly in the case of immunotherapies that rely on activating the patient's own immune system to fight cancer cells. It can not only recognize and eliminate cancer cells but also develop resistance to immunotherapies and limit their effectiveness, allowing cancer cells to evade immune surveillance and proliferate unchecked [151]. This has already been reported in studies involving immunotherapy in melanoma, in which the presence of regulatory T cells was associated with reduced response to the treatment [183], and in chemotherapy in breast cancer, where macrophages were recruited to tumors in response to the treatment, promoting drug resistance by producing signaling molecules that protected cancer cells from chemotherapy-induced cell death [184]. Understanding the complex interactions between cancer cells and the immune system to develop more effective treatments and possibly using combination therapies to target these cells may be crucial for developing more effective therapies that can overcome this barrier.

Lastly, tumors also take advantage of their interactions with surrounding areas, creating an environment with a particular composition. This structure, known as the tumor microenvironment (TME), plays a critical role in cancer progression and response to treatment. It is composed of various non-cancerous cells, such as immune cells, fibroblasts, endothelial cells, and extracellular matrix components (Figure 3). It can either promote or

inhibit cancer growth, invasion, and metastasis, depending on its composition and interactions with cancer cells [185,186].

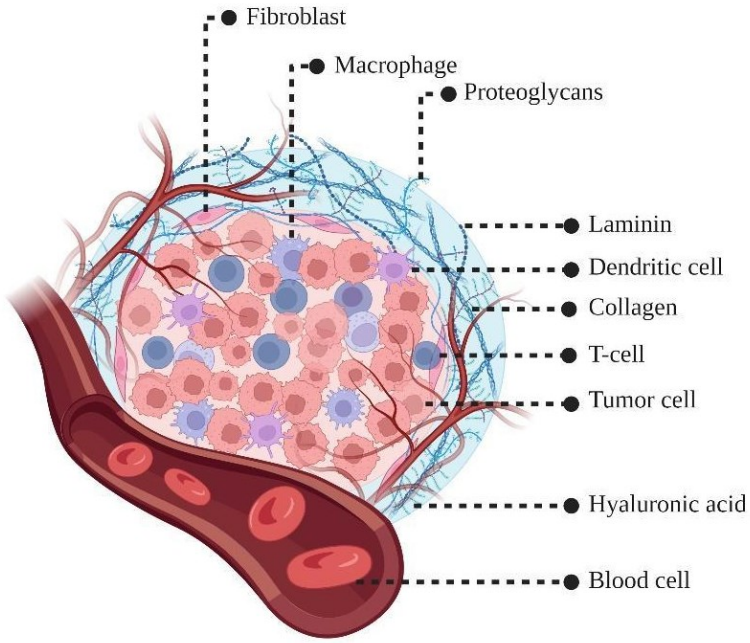

Fig. 3: Schematic representation of the tumor microenvironment and its composition. This ecosystem that surrounds the cancer cells constantly interacts and influence the tumor growth, invasion, and metastasis.

When promoting cancer growth, the TME can create a hostile environment for drug delivery with low pH, hypoxia, and high interstitial fluid pressure, contributing to drug resistance [187]. Also, cancer cells can interact with the immune system within the TME, which inhibits the infiltration and activation of immune cells, particularly T cells [188,189]. Therefore, cancer treatments that target the TME have shown promise in preclinical and clinical studies. These treatments aim to modify the TME to enhance the efficacy of conventional therapies, such as chemotherapy and radiation therapy, or to directly target the TME components that promote cancer growth and metastasis.

Currently, numerous DDS strategies and cancer treatments are under investigation to address the diverse biological barriers that hamper effective therapy. As examples, NPs and liposomes have demonstrated a high ability to evade ECM, TME, and tumor blood vessels through their unique physicochemical properties such as size, geometry, compositions and / or stiffness [190], whereas antibody-drug conjugates containing brentuximab vedotin and trastuzumab emtansine have shown promise in targeting a wide range of cancer types via immune system [191,192]. Likewise, the field of immunotherapy has witnessed remarkable

advancements, with therapies like immune checkpoint inhibitors (e.g., pembrolizumab and nivolumab) and adoptive cell therapies, including CAR-T cell therapy [193,194]. These treatments reinvigorate the immune system to recognize and attack cancer cells, effectively overcoming immunosuppressive barriers within the tumor microenvironment. Furthermore, advances in gene editing and RNA-based therapies hold potential to target genetic and molecular barriers associated with cancer, offering a personalized and highly precise approach to treatment [195,196]. The next section will give more details on the transport mechanisms and targeted strategies involved in chemotherapy DDS and how they can be used to improve treatment outcomes.

4. Targeted strategies and transport mechanisms for chemotherapy drug delivery systems

Cancer is a complex and challenging disease, and drug delivery strategies that specifically target cancer cells while minimizing toxicity to healthy tissues are essential for effective treatment. Generally, a tumor-targeting DDS needs to be functionalized to allow the increase of molecule adsorption, tumor-site delivery rates, cellular uptake, and controlled release [197], and most of these outcomes depend on the transport mechanisms they use to reach the tumor site and the way they will bind to the tumor cell, which generally involves overexpressed cell receptors.

Many different types of receptors can be overexpressed in tumor cells, and these receptors can be targeted for cancer therapy. The epidermal growth factor receptor (EGFR) is often overexpressed in a variety of cancers, including lung, colorectal, and breast cancer. Drugs like erlotinib and cetuximab target EGFR to inhibit its signaling and slow cancer growth [198,199]. The human Epidermal growth factor receptor 2 (HER2) overexpression is common in some breast and gastric cancers, and drugs such as trastuzumab are already being used to target HER2-positive tumors [200,201]. The vascular endothelial growth factor receptor (VEGFR) is often upregulated in tumors, and drugs such as bevacizumab target this receptor to inhibit tumor angiogenesis [202,203]. The programmed death-1 (PD-1) and programmed death Ligand-1 (PD-L1) are overexpressed in various cancers and are targeted by immune checkpoint inhibitors such as pembrolizumab and nivolumab, which help the immune system recognize and attack cancer cells [204-206]. The androgen receptor (AR), estrogen receptor (ER), and progesterone receptor (PR) are overexpressed in prostate cancer and / or breast cancer, and drugs such as enzalutamide, abiraterone, tamoxifen, and / or

aromatase inhibitors target these receptors to block hormone-driven tumor growth [207-210]. Tyrosine kinase receptors are also targeted in cancer therapy, especially by using drugs such as imatinib and vandetanib for chronic myeloid leukemia and thyroid cancer, respectively [211-212]. Finally, folate and transferrin receptors, as well as integrins can also be found upregulated in cancer cells and may be used as targets for a more effective therapy outcome [213-215].

Transport mechanisms are crucial for drug delivery systems because they determine how drugs are delivered to their target sites in the body, and their effectiveness enables drugs to reach their intended targets while avoiding other areas of the body where they may cause harm [216]. These mechanisms can be intrinsic to the organism, such as the active and passive transports, and target-related, such as stimulus-responsive targeting and the EPR effect. This section aims to give an overview of the different cell transport mechanisms that can affect and/or interact with DDS (Figure 4) and how they can be used to increase *in situ* drug delivery rates.

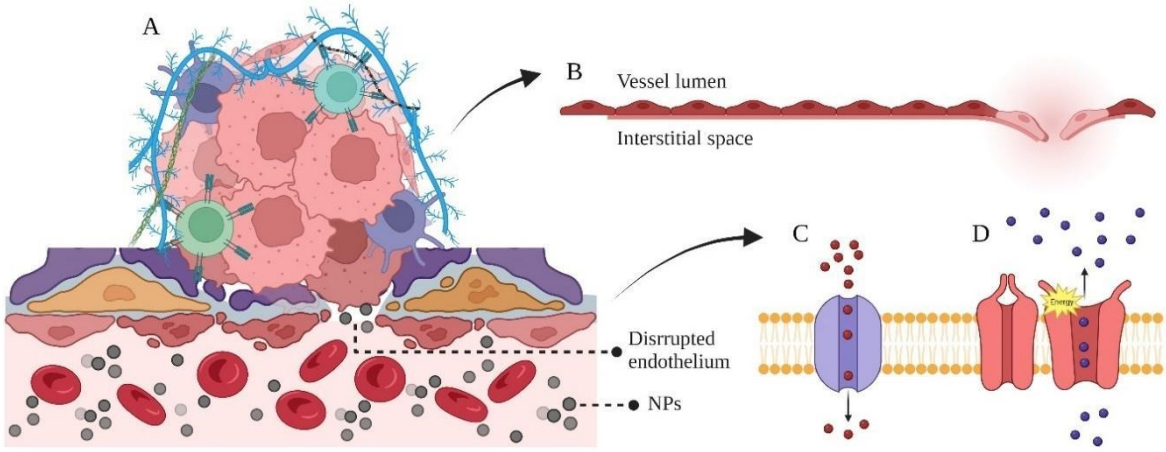

Fig. 4: Schematic representation of the different transport mechanisms for chemotherapy drug delivery systems. The EPR effect tends to enhance the accumulation of nanocarriers in the tumor tissue due to abnormal vessels architecture (A), and this delivery can be also improved by stimulus-responsive mechanisms causing a transient disruption of the endothelium (B), or passive (C) and active (D) transports.

4.1 Active transport

Active transport is a mechanism by which substances are transported across biological membranes against their concentration gradients, requiring energy expenditure. It is a critical process for many physiological functions in the body, including the uptake and elimination of drugs. Tumor cells often exhibit altered expression or activity of active

transporters, leading to increased uptake or efflux of drugs and altered pharmacokinetics. This can affect the efficacy of anticancer drugs and contribute to drug resistance [217,218].

One example of a drug that uses active transport is the tyrosine kinase inhibitor imatinib, which is transported into cells by the organic cation transporter 1 (OCT1). Reduced expression or activity of OCT1 has been associated with resistance to imatinib in chronic myeloid leukemia and gastrointestinal stromal tumors [219]. Similarly, the use of P-glycoprotein (an overexpressed protein in many cancer cells and responsible for pumping chemotherapy drugs out of the cell, leading to drug resistance) inhibitors, such as verapamil, can prevent the efflux of chemotherapy drugs and increase their accumulation in cancer cells, leading to improved therapeutic efficacy [220,221].

Finally, the use of antibody-drug conjugates (ADCs) can also take advantage of the active transport system. ADCs are composed of a monoclonal antibody that recognizes a specific antigen on cancer cells linked to a cytotoxic drug. The antibody targets the cancer cell, and the drug is transported into the cell via endocytosis. Once inside the cell, the drug is released and kills the cancer cell. ADCs have shown promising results in clinical trials for the treatment of various types of cancer, such as breast cancer and lymphoma. Finally, the multidrug resistance-associated protein family, breast cancer resistance protein, and the solute carrier family member SLC22A18 have also been implicated in tumor drug resistance [222,223].

4.2 Passive transport

Passive transport is a process by which substances are transported across biological membranes down their concentration gradients without the requirement of energy expenditure, playing a significant role in the distribution of drugs to tumors and their subsequent pharmacokinetics [217,218]. In cancer treatment, passive transport is often exploited to deliver drugs to cancer cells. This is because cancer cells have a higher demand for nutrients and oxygen compared to normal cells, leading to a higher concentration of these molecules in their immediate vicinity. By exploiting the passive transport process, drugs can be designed to specifically target cancer cells and enter them more easily, leading to more effective treatment [224,225].

For example, the liposomal formulation of doxorubicin can accumulate in tumor tissues due to its EPR effect, where it preferentially extravasates and accumulates in the

tumor tissue through passive diffusion. Doxorubicin is released from the liposomes and can exert its cytotoxic effects on tumor cells [226,227]. Similar approaches have been used to deliver other drugs, such as cisplatin and methotrexate [228,229].

Passive transport can also play a role in the uptake of small molecule tyrosine kinase inhibitors (TKIs) in tumors. Many TKIs are hydrophobic and can passively diffuse into cells, although their specificity for target kinases can be affected by transporter expression [230]. Finally, another example of passive transport in cancer treatment is the use of NPs. They can be designed to selectively accumulate in cancer cells due to their EPR effect (which will be further discussed). This effect is because tumor blood vessels have large pores that allow for the accumulation of NPs, while normal blood vessels do not. Once inside the cancer cells, NPs can release drugs or be used for imaging or therapy [231].

4.3 Stimulus-responsive targeting

Also known as triggered drug transport, stimulus-responsive targeting is a promising approach for targeted drug delivery to tumors, where drug release is controlled by a specific stimulus in the TME. This approach can enhance drug efficacy while reducing off-target toxicity [232].

One example of a stimulus for triggering drug release in tumors is pH. The TME is typically more acidic than healthy tissues due to the production of lactic acid by tumor cells and poor perfusion. This pH difference can be exploited to design pH-responsive drug delivery systems, such as polymeric NPs and liposomes. These systems can be engineered to release their payload in response to the lower pH in the TME, resulting in targeted drug delivery to tumor cells [233].

Another stimulus that can be used to activate drug transport is light. Light-responsive NPs can be designed to release their drug payload upon exposure to a specific wavelength of light, allowing for localized drug delivery to tumors. Photodynamic therapy (PDT) is an example of a light-triggered drug delivery approach used to treat cancer. In PDT, a photosensitizing agent is administered to the patient, which accumulates in tumor tissues. Upon exposure to light of a specific wavelength, the photosensitizer is activated, generating reactive oxygen species that can kill tumor cells [234,235].

Magnetic fields can also be used as a stimulus for triggering drug delivery to tumors. Magnetic NPs can be functionalized with a drug and targeted to tumor tissues using an

external magnetic field. The magnetic field can then be used to control the release of the drug at the tumor site [236].

4.4 The enhanced permeability and retention effect

The EPR effect is observed in tumors where leaky blood vessels and a lack of lymphatic drainage lead to the accumulation of macromolecules and NPs in the tumor tissue. This effect has been exploited for the development of tumor-targeted drug delivery systems [237].

Several studies have demonstrated the potential of the EPR effect for delivering various types of therapeutics to tumors. For example, a study by Maeda et al. showed that the EPR effect could be utilized to selectively deliver liposomes loaded with doxorubicin to solid tumors in mice [237]. Similarly, a study by Peer et al. demonstrated the selective accumulation of polymeric NPs in tumors due to the EPR effect, resulting in improved efficacy and reduced toxicity of the loaded drug [238].

In addition to liposomes and PNPs, other drug delivery systems have also been shown to take advantage of the EPR effect. For example, PEGylated gold NPs have been shown to accumulate in tumors due to the EPR effect and can be used for photothermal therapy and drug delivery. While the EPR effect has shown promise for the targeted delivery of drugs to tumors, several limitations exist, such as heterogeneity in the EPR effect across different tumor types and individuals [239]. Nonetheless, ongoing research is focused on optimizing the design of drug delivery systems to maximize the potential of the EPR effect for tumor targeting.

5. Prospects, benefits, and limitations in the clinical application of nanomaterials for cancer treatment

The clinical potential of nanomaterials in the treatment of cancer is undeniably promising. Nanomedicine has revolutionized the field of oncology by offering innovative strategies to improve drug delivery, enhance therapeutic efficacy, and reduce the adverse effects associated with conventional cancer treatments, mainly due to the development of NPs that have emerged as key players in the development of targeted DDS [240,241]. Their ability to encapsulate and transport chemotherapeutic agents to specific tumor sites while minimizing exposure to healthy tissues has the potential to transform cancer therapy.

Moreover, functionalized nanocarriers can enable precise control over drug release kinetics, ensuring a sustained therapeutic effect [242].

Several of these DDS have already been used to deliver and target tumor cells, hence giving us a good overview of their benefits. As examples, liposomes have shown to be very versatile in terms of biocompatibility, allowing for the encapsulation of both hydrophilic and hydrophobic drugs, which enhances drug solubility and bioavailability [243]. PNPs such as PLGA-based systems, offer controlled and sustained drug release, improved drug stability, and the potential to target specific tissues or cells, whereas INPs such as gold nanoparticles, offer unique properties for applications in cancer therapy, such as hyperthermia-based treatment and imaging [244,239]. Lastly, carbon nanotubes and QDs provide versatility for cancer therapy, allowing for drug delivery, imaging, and potential early cancer detection, and exosomes are natural carriers that can be engineered for cancer therapy. They offer the potential for cell recycling, immune modulation, and communication between cells for targeted therapy [245,246].

Despite the remarkable progress, several limitations must be addressed to fully harness the clinical potential of nanomaterials in cancer treatment. Challenges such as scalability, reproducibility of manufacturing processes, and regulatory hurdles remain significant barriers to clinical translation [247,248]. Achieving regulatory approval for any medical application is a complex and lengthy process that involves addressing several critical factors, such as demonstrating safety and efficacy through rigorous clinical trials. Ensuring patient safety is paramount, and robust clinical data is essential to confirm that the product's benefits outweigh its risks. Additionally, navigating the regulatory pathways, which include rigorous preclinical and clinical testing, manufacturing consistency, and documentation requirements, can be a challenge [259,250]. Lastly, long-term safety concerns, including potential toxicities and immunological reactions, need careful evaluation to ensure patient well-being. Furthermore, the heterogeneous nature of tumors and the development of drug resistance mechanisms necessitate ongoing research into more sophisticated and personalized approaches [251].

To realize the prospects of nanomaterials in cancer therapy, concerted efforts are needed to address these limitations. Research should focus on optimizing nanomaterial design, streamlining scalable manufacturing processes, and navigating the complex regulatory landscape [252]. Lastly, the integration of advanced imaging and diagnostic

modalities with therapeutic nanocarriers holds great promise for real-time monitoring of treatment responses and personalized medicine [253].

6. Conclusions

Cancer is a complex and multifactorial global health challenge, requiring exploration beyond traditional treatments such as surgery, chemotherapy, and radiotherapy due to their limitations and side effects. The potential of cancer immunotherapy, which harnesses the immune system to combat tumors, is promising but faces obstacles related to tumor diversity, personalized care, and cost. Additionally, the development of chemoresistance and the complex tumor microenvironment pose significant barriers to effective cancer therapy, complicating drug delivery and efficacy.

Nanotechnology has emerged as a promising solution to these challenges by allowing precise engineering of nanostructures for drug delivery. These nanocarriers, utilizing various materials and techniques, offer improved drug stability, solubility, and target specificity, potentially reducing adverse effects. Moreover, surface modifications and controlled release strategies enhance their functionality, offering a multifaceted approach to advance cancer diagnosis, prevention, and treatment. As examples, PNPs can effectively encapsulate and deliver drugs, even crossing barriers such as the BBB. While many have reached clinical studies, challenges like FDA approval, personalized medicine, scalability, and cost-effectiveness persist. Polymer conjugates have mixed success, needing refinement for better tumor accumulation. INPs show potential for hyperthermia-based cancer therapy but need more research for safety and stability. Carbon nanotubes and QDs offer versatility and early cancer detection. Liposomes face stability challenges, while micelles solve solubility but face dilution issues, and exosomes hold promise in cell recycling, immune modulation, and communication.

In summary, the field of nanomedicine presents exciting prospects for revolutionizing cancer therapy by confronting numerous daunting challenges. While our understanding of cancer mechanisms and the development of innovative chemotherapeutic drugs are advancing, we must not underestimate the critical barriers that hinder the efficacy of tumor-targeting DDS. These barriers are complex, encompassing physicochemical, anatomical/physiological, and intrinsic tumor factors that pose substantial impediments to the success of DDS.

Although transport mechanisms like active and passive transport, stimulus-responsive targeting, and the EPR effect offer exciting possibilities for targeted drug delivery, formidable challenges in scalability, manufacturing consistency, regulations, and long-term safety persist. Success hinges on comprehensive efforts to optimize nanomaterial design, refine manufacturing, and navigate complex regulations to ensure the benefits of nanomedicine outweigh the risks. Furthermore, integrating advanced imaging and diagnostics with therapeutic nanocarriers holds potential for personalized cancer treatment. Overcoming these multifaceted barriers is imperative for realizing the full clinical potential of nanomaterials in the battle against cancer.

Overall, the evolution of nanomedicine for cancer treatment has been characterized by a progression from drug delivery to imaging and diagnosis to targeted therapy. As the field continues to advance, we will likely see even more sophisticated and effective nanoscale devices and therapies for cancer treatment. Despite the potential benefits of nanomedicine, there are also challenges to be addressed, such as toxicity, regulatory issues, and the need for more robust clinical trials to demonstrate efficacy. However, with continued research and development, nanomedicine has the potential to revolutionize cancer treatment and improve patient outcomes.

Declaration of competing interest

None.

Acknowledgements

This work was supported in parts by grants and/or scholarships from FAPERGS (Fundação de Apoio à Pesquisa do Rio Grande do Sul, Brazil), CAPES (Coordenação de Aperfeiçoamento de Pessoal de Nível Superior, Brazil) and CNPq (Conselho Nacional de Desenvolvimento Científico e Tecnológico, Brazil). The figures were created with BioRender.com.

CRediT authorship contribution statement

Jeferson Gustavo Henn: conceptualization, data curation, formal analysis, investigation, methodology, project administration, validation, visualization, writing – original draft, and writing – review & editing. **Tanira Alessandra Silveira Aguirre**: data curation, formal

analysis, investigation, validation, and writing – review & editing. **Michael Nugent**: resources, validation, and writing – review & editing. **Dinara Jaqueline Moura**: funding acquisition, project administration, resources, supervision, validation, and writing – review & editing.

All authors reviewed the final manuscript.

Declaration of Generative AI and AI assisted technologies in the writing process

The authors declare that no Generative AI and AI assisted technologies were used in the writing process.

References:

[1] Druker B. Imatinib: A Viewpoint by Brian J. Druker. *Drugs* (2001). https://doi.org/10.2165/00003495-200161120-00009.

[2] Negrini S.; Gorgoulis V.G; Halazonetis T.D. Genomic instability – an evolving hallmark of cancer. *Nat. Rev. Mol. Cell Biol.* (2010). https://doi.org/10.1038/nrm2858.

[3] Junttila M.R.; De Sauvage F.J. Influence of tumour micro-environment heterogeneity on therapeutic response. *Nature* (2013). https://doi.org/10.1038/nature12626.

[4] Globocan Observatory, World Cancer Today. *Int. Agency Res. Cancer* (2020). Available at https://gco.iarc.fr/today/home (2023).

[5] Bor G.; Azmi I.D.M.; Yaghmur A. Nanomedicines for cancer therapy: Current status, challenges and future prospects. *Ther. Deliv.* (2019). https://doi.org/10.4155/tde-2018-0062.

[6] Arruebo M.; Vilaboa N.; Sáez-Gutierrez B.; Lambea J.; Tres A.; Valladares M.; González-Fernández A. Assessment of the evolution of cancer treatment therapies. *Cancers (Basel)* (2011). https://doi.org/10.3390/cancers3033279.

[7] Peterson C.; Denlinger N.; Yang Y. Recent Advances and Challenges in Cancer Immunotherapy. *Cancers (Basel)*. (2022). https://doi.org/10.3390/cancers14163972.

[8] Hedge, P.S.; Chen D.S. Top 10 Challenges in Cancer Immunotherapy. *Immunity*. (2020). https://doi.org/10.1016/j.immuni.2019.12.011.

[9] Yeldag G.; Rice A.; Hernández A. del R. Chemoresistance and the self-maintaining tumor microenvironment. *Cancers (Basel)* (2018). https://doi.org/10.3390/cancers10120471.

[10] Linton S.S.; Sherwood S.G.; Drews K.C.; Kester M. Targeting cancer cells in the tumor microenvironment: Opportunities and challenges in combinatorial nanomedicine. *Wiley Interdiscip. Rev. Nanomedicine Nanobiotechnology* (2016). https://doi.org/10.1002/wnan.1358.

[11] Roma-Rodrigues C.; Mendes R.; Baptista P.V.; Fernandes A.R. Targeting tumor microenvironment for cancer therapy. *Int. J. Mol. Sci.* (2019). https://doi.org/10.3390/ijms20040840.

[12] Wakaskar R.R. Promising effects of nanomedicine in cancer drug delivery. *J. Drug Target* (2018). https://doi.org/10.1080/1061186x.2017.1377207.

[13] Bertrand N.; Wu J.; Xu X.; Kamaly N.; Farokhzad O.C. Cancer nanotechnology: The

impact of passive and active targeting in the era of modern cancer biology. *Advanced Drug Delivery Reviews* (2014). doi:10.1016/j.addr.2013.11.009.

[14] Arranja, A.G., Pathak, V., Lammers, T. & Shi, Y. Tumor-targeted nanomedicines for cancer theranostics. *Pharmacol.* (2017). https://doi.org/10.1016/j.phrs.2016.11.014.

[15] Chaturvedi V.K.; Singh A.; Singh V.K.; Singh M.P. Cancer Nanotechnology: A New Revolution for Cancer Diagnosis and Therapy. *Curr Drug Metab.* (2019). https://doi.org/10.2174/1389200219666180918111528.

[16] Song W.; Anselmo A.C.; Huang L. Nanotechnology intervention of the microbiome for cancer therapy. *Nat. Nanotechnol.* (2019). https://doi.org/10.1038/s41565-019-0589-5.

[17] Letchford K.; Burt H. A review of the formation and classification of amphiphilic block copolymer nanoparticulate structures: micelles, nanospheres, nanocapsules and polymersomes. *Eur. J. Pharm. Biopharm.* (2007). https://doi.org/10.1016/j.ejpb.2006.11.009.

[18] Parveen S.; Sahoo S.K. Polymeric nanoparticles for cancer therapy. *J. Drug Target* (2008). https://doi.org/10.1080/10611860701794353.

[19] Prabhu R.H.; Patravale V.B.; Joshi M.D. Polymeric nanoparticles for targeted treatment in oncology: Current insights. *Int. J. Nanomedicine* (2015). https://doi.org/10.2147/ijn.s56932.

[20] El-Say K.M.; El-Sawy H.S. Polymeric nanoparticles: Promising platform for drug delivery. *Int. J. Pharm.* (2017). https://doi.org/10.1016/j.ijpharm.2017.06.052.

[21] Banik B.L.; Fattahi P.; Brown J.L. Polymeric nanoparticles: The future of nanomedicine. *Wiley Interdiscip. Rev. Nanomedicine Nanobiotechnology* (2016). https://doi.org/10.1002/wnan.1364.

[22] Moreno D.; de Ilarduya C.T.; Bandrés E.; Buñuales M.; Azcona M.; García-Foncillas J.; Garrido M.J. Characterization of cisplatin cytotoxicity delivered from PLGA-systems. *Eur. J. Pharm. Biopharm.* (2008). https://doi.org/10.1016/j.ejpb.2007.08.006.

[23] Betancourt T.; Brown B.; Brannon-Peppas L. Doxorubicin-loaded PLGA nanoparticles by nanoprecipitation: Preparation, characterization and in vitro evaluation. *Nanomedicine* (2007). https://doi.org/10.2217/17435889.2.2.219.

[24] Jain A.K.; Swarnakar N.K.; Godugu C.; Singh R.P.; Jain S. The effect of the oral administration of polymeric nanoparticles on the efficacy and toxicity of tamoxifen. *Biomaterials* (2011). https://doi.org/10.1016/j.biomaterials.2010.09.037.

[25] Park H.; Yang J.; Lee J.; Haam S.; Choi I-H.; Yoo K-H. Multifunctional nanoparticles for combined doxorubicin and photothermal treatments. *ACS Nano* (2009). https://doi.org/10.1021/nn900215k.

[26] Papa A-L.; Basu S.; Sengupta P.; Benerjee D.; Sengupta S.; Harfouche R. Mechanistic studies of Gemcitabine-loaded nanoplatforms in resistant pancreatic cancer cells. *BMC Cancer* (2012). https://doi.org/10.1186/1471-2407-12-419.

[27] Nair K. L.; Jagadeeshan S.; Nair S.A.; Kumar G.S.V. Biological evaluation of 5-fluorouracil nanoparticles for cancer chemotherapy and its dependence on the carrier, PLGA. *Int. J. Nanomedicine* (2011). https://doi.org/10.2147/ijn.s20165.

[28] Cheng L.; Jin C.; Lv W.; Ding Q.; Han X. Developing a highly stable PLGA-mPEG nanoparticle loaded with cisplatin for chemotherapy of ovarian cancer. *PLoS One* (2011). https://doi.org/10.1371/journal.pone.0025433.

[29] Wohlfart S.; Khalansky A.S.; Gelperina S.; Maksimenko O.; Bernheuther C.; Glatzel M.; Kreuter J. Efficient chemotherapy of rat glioblastoma using doxorubicin-loaded

PLGA nanoparticles with different stabilizers. *PLoS One* (2011). https://doi.org/10.1371/journal.pone.0019121.

[30] Moreno D.; Zalba S.; Navarro I.; Tros de Ilarduya C.; Garrido M.J. Pharmacodynamics of cisplatin-loaded PLGA nanoparticles administered to tumor-bearing mice. *Eur. J. Pharm. Biopharm.* (2010). https://doi.org/10.1016/j.ejpb.2009.10.005.

[31] Cheng M.R.; Li Q.; Wan T.; He B.; Han J.; Chen H-X; Yang F-X.; Wang W.; Xu H-Z.; Ye T.; Zha B-B. Galactosylated chitosan/5-fluorouracil nanoparticles inhibit mouse hepatic cancer growth and its side effects. *World J. Gastroenterol.* (2012). https://doi.org/10.3748%2Fwjg.v18.i42.6076.

[32] Cheng M.; He B.; Wan T.; Zhu W., Han J.; Zha B.; Chen H.; Yang F.; Li Q.; Wang W.; Xu H.; Ye T. 5-Fluorouracil Nanoparticles Inhibit Hepatocellular Carcinoma via Activation of the p53 Pathway in the Orthotopic Transplant Mouse Model. *PLoS One* (2012). https://doi.org/10.1371/journal.pone.0047115.

[33] Li S.; Wang A.; Jiang W.; Guan Z. Pharmacokinetic characteristics and anticancer effects of 5-Fluorouracil loaded nanoparticles. *BMC Cancer* (2008). https://doi.org/10.1186/1471-2407-8-103.

[34] Wicki A.; Witzigmann D.; Balasubramanian V.; Huwyler J. Nanomedicine in cancer therapy: Challenges, opportunities, and clinical applications. *J. Control. Release* (2015). https://doi.org/10.1016/j.jconrel.2014.12.030.

[35] Pérez-Herrero E; Fernández-Medarde A. Advanced targeted therapies in cancer: Drug nanocarriers, the future of chemotherapy. *Eur. J. Pharm. Biopharm.* (2015). https://doi.org/10.1016/j.ejpb.2015.03.018.

[36] Bregoli L.; Movia D.; Gavigan-Imedio J.D.; Lysaght J.; Reynolds J.; Prina-Mello A.P. Nanomedicine applied to translational oncology: A future perspective on cancer treatment. *Nanomedicine Nanotechnology, Biol. Med.* (2016). https://doi.org/10.1016/j.nano.2015.08.006.

[37] Anselmo A.C.; Mitragotri S. Nanoparticles in the clinic: An update. *Bioeng. Transl. Med.* (2019). https://doi.org/10.1002%2Fbtm2.10143.

[38] Ventola C.L. Progress in nanomedicine: Approved and investigational nanodrugs. *P T*. (2017). http://www.ncbi.nlm.nih.gov/pmc/articles/pmc5720487/.

[39] Ekladious I.; Colson Y.L.; Grinstaff M.W. Polymer–drug conjugate therapeutics: advances, insights and prospects. *Nat. Rev. Drug Discov.* (2019). https://doi.org/10.1038/s41573-018-0005-0.

[40] Lomkova E.A.; Chytil P.; Janoušková O.; Mueller T.; Lucas H.; Filippov S.K.; Trhlíková O.; Aleshunin P.A.; Skorik Y.A.; Ulbrich K.; Etrycj T. Biodegradable Micellar HPMA-Based Polymer-Drug Conjugates with Betulinic Acid for Passive Tumor Targeting. *Biomacromolecules* (2016). https://doi.org/10.1021/acs.biomac.6b00947.

[41] Pang X.; Yang X.; Zhai G. Polymer-drug conjugates: Recent progress on administration routes. *Expert Opin. Drug Deliv.* (2014). https://doi.org/10.1517/17425247.2014.912779.

[42] Chang M.; Zhang F.; Wei T.; Zuo T.; Guan Y.; Lin G.; Shao W. Smart linkers in polymer-drug conjugates for tumor-targeted delivery. *J. Drug Target.* (2016). https://doi.org/10.3109/1061186x.2015.1108324.

[43] Duro-Castano A.; Movellan J.; Vicent M.J. Smart branched polymer drug conjugates as nano-sized drug delivery systems. *Biomater. Sci.* (2015). https://doi.org/10.1039/C5BM00166H.

[44] Sun H.; Zu Y. Aptamers and their applications in nanomedicine. *Small*. (2015). https://doi.org/10.1002/smll.201403073.

[45] Banerjee S.S.; Aher N.; Patil R.; Khandare J. Poly(ethylene glycol)-Prodrug Conjugates: Concept, Design, and Applications. *J. Drug Deliv.* (2012). https://doi.org/10.1155/2012/103973.

[46] Seymour L.W.; Ferry D.R.; Kerr D.J.; Rea D.; Whitlock M.; Poyner R.; Boivin C.; Hesslewood S.; Twelves C.; Blackie R.; Schatzlein A.; Jodrell D.; Bissett D.; Calvert H.; Lind M.; Robbins A.; Burtles S.; Duncan R.; Cassidy J. Phase II studies of polymer-doxorubicin (PK1, FCE28068) in the treatment of breast, lung and colorectal cancer. *Int. J. Oncol.* (2009). https://doi:10.3892/ijo_00000293.

[47] Pang X.; Jian Y.; Xiao Q.; Leung A.W.; Hua H.; Xu C. PH-responsive polymer-drug conjugates: Design and progress. *J. Control. Release* (2016). https://doi.org/10.1016/j.jconrel.2015.12.024.

[48] Angiolillo A.L.; Schore R.J.; Devidas M.; Borowitz M.J.; Carroll A.J.; Gastier-Foster J.M.; Heerema N.A.; Keilani T.; Lane A.R.; Loh M.L.; Reaman G.H.; Adamson P.C.; Wood B.; Wood C.; Zheng H.W.; Raetz E.A.; Winick N.J.; Carroll W.L.; Hunger S.P. Pharmacokinetic and pharmacodynamic properties of calaspargase pegol Escherichia coli L-asparaginase in the treatment of patients with acute lymphoblastic leukemia: Results from children's oncology group study AALL07P4. *J. Clin. Oncol.* (2014). https://doi:10.1200/JCO.2014.55.5763.

[49] Hingorani S.R.; Zheng L.; Bullock A.J.; Seery T.E.; Harris W.P.; Sigal D.S.; Braiteh F.; Ritch P.S.; Zalupski M.M.; Bahary N.; Oberstein P.E.; Wang-Gillam A.; Wu W.; Chondros D.; Jiang P.; Khelifa S.; Pu J.; Aldrich C.; Hendifar A.E. HALO 202: Randomized phase II Study of PEGPH20 Plus Nab-Paclitaxel/Gemcitabine Versus Nab-Paclitaxel/Gemcitabine in Patients With Untreated, Metastatic Pancreatic Ductal Adenocarcinoma. *Journal of Clinical Oncology* (2018). https://doi:10.1200/JCO.2017.74.9564.

[50] Naing A.; Papadopoulos K.P.; Autio K.A. Ott P.A.; Patel M.R.; Wong D.J.; Falchook G.S.; Pant S.; Whiteside M.; Rasco D.R.; Mumm J.B.; Chan I.H.; Bendell J.C.; Bauer T.M.; Colen R.R.; Hong D.S.; Vlasselaer P.V.; Tannir N.M.; Oft M.; Infante J.R. Safety, antitumor activity, and immune activation of pegylated recombinant human interleukin-10 (AM0010) in patients with advanced solid tumors. *J. Clin. Oncol.* (2016). https://doi:10.1200/JCO.2016.68.1106.

[51] Szlosarek, P.W.; Steele J.P.; Nolan L. *et al.* Arginine Deprivation With Pegylated Arginine Deiminase in Patients With Argininosuccinate Synthetase 1-Deficient Malignant Pleural Mesothelioma: A Randomized Clinical Trial. *JAMA Oncol.* (2017). https://doi:10.1001/jamaoncol.2016.3049.

[52] Mussai F.; Egan S.; Higginbotham-Jones J.; Perry T.; Beggs A.; Odintsova E.; Loke J.; Pratt G.; Pong U K.; Lo A.; Ng M.; Kearns P.; Cheng P.; De Santo C. Arginine dependence of acute myeloid leukemia blast proliferation: A novel therapeutic target. *Blood* (2015). https://doi:10.1182/blood-2014-09-600643.

[53] Charych D.H.; Hoch U.; Langowski J.L.; Lee S.R.; Addepalli M.K.; Kirk P.B.; Sheng D.; Liu X.; Sims P.W.; VanderVeen L.A.; Ali C.F.; Chang T.K.; Konakova M.; Pena R.L.; Kanhere R.S.; Kirksey Y.M.; Ji C.; Wang Y.; Huang J.; Sweeney T.D.; Kantak S.S.; Doberstein S.K. NKTR-214, an Engineered Cytokine with Biased IL2 Receptor Binding, Increased Tumor Exposure, and Marked Efficacy in Mouse Tumor Models. *Clin. Cancer Res.* (2016). https://doi:10.1158/1078-0432.CCR-15-1631.

[54] Ludwig H.; Weisel K.; Petrucci M.T.; Leleu X.; Cafro A.M.; Garderet L.; Leitgeb C.;

Foa R.; Greiç R.; Yakoub-Agha I.; Zboralski D.; Vauléon S.; Dümmler T.; Beyer D.; Kruschinski A.; Riecke K.; Baumann M.; Engelhardt M. Olaptesed pegol, an anti-CXCL12/SDF-1 Spiegelmer, alone and with bortezomib-dexamethasone in relapsed/refractory multiple myeloma: A Phase IIa Study. *Leukemia* (2017). https://doi:10.1038/leu.2017.5.

[55] Tsuchiya K.; Uchida T.; Kobayashi M.; Maeda H.; Konno T.; Yamanaka H. Tumor-targeted chemotherapy with SMANCS in lipiodol for renal cell carcinoma: Longer survival with larger size tumors. *Urology* (2000). https://doi:10.1016/S0090-4295(99)00537-3.

[56] Paz-Ares L.; Ross H.; O'Brien M.; Riviere A.; Gatzemeier U.; Von Pawel J.; Kaukel E.; Freitag L.; Digel W.; Bischoff H.; García-Campelo R.; Iannotti N.; Reiterer P.; Bover I.; Prendiville J.; Eisenfeld A.J.; Oldham F.B.; Bandstra B.; Singer J.W.; Bonomi P. Phase III trial comparing paclitaxel poliglumex vs docetaxel in the second-line treatment of non-small-cell lung cancer. *Br. J. Cancer* (2008). https://doi:10.1038/sj.bjc.6604372.

[57] Thellenberg-Karlsson C.; Nyman C.; Nilsson S.; Blom R.; Márquez M.; Castellanos E.; Holmber A.R. Bone-targeted novel cytotoxic polybisphosphonate conjugate in castration-resistant prostate cancer: A multicenter phase 1 study. *Anticancer Res.* (2016). https://doi:10.21873/anticanres.11249.

[58] Santi D.V.; Schneider E.L.; Ashley G.W. Macromolecular prodrug that provides the irinotecan (CPT-11) active-metabolite SN-38 with ultralong half-life, low C max, and low glucuronide formation. *J. Med. Chem.* (2014). https://doi:10.1021/jm401644v.

[59] Wang F.; Li C.; Cheng J.; Yuan Z. Recent advances on inorganic nanoparticle-based cancer therapeutic agents. *International Journal of Environmental Research and Public Health* (2016). https://doi:10.3390/ijerph13121182.

[60] Yang F.; Jin C.; Subedi S.; Lee C.L.; Wang Q.; Jiang Y.; Li J.; Di Y.; Fu D. Emerging inorganic nanomaterials for pancreatic cancer diagnosis and treatment. *Cancer Treat. Rev.* (2012). https://doi.org/10.1016/j.ctrv.2012.02.003.

[61] Yezhelyev M.; Yacoub R.; O'Regan R. Inorganic nanoparticles for predictive oncology of breast cancer. *Nanomedicine* (2009). https://doi.org/10.2217/17435889.4.1.83.

[62] Mukerjee A.; Ranjan A.P.; Vishwanatha J.K. Combinatorial Nanoparticles for Cancer Diagnosis and Therapy. *Curr. Med. Chem.* (2012). https://doi.org/10.2174/092986712801661176.

[63] Xu J.; Liao K.; Jiang H.; Zhou W. Research progress of novel inorganic nanometre materials carriers in nanomedicine for cancer diagnosis and treatment. *Artif. Cells, Nanomedicine Biotechnol.* (2018). https://doi.org/10.1080/21691401.2018.1499665.

[64] Rizwanullah M.; Amin S.; Mir S.R.; Fakhri K.U.; Rizvi M.M.A. Phytochemical based nanomedicines against cancer: current status and future prospects. *J. Drug Target.* (2018). https://doi.org/10.1080/1061186x.2017.1408115.

[65] Chen C-C.; Hsieh D-S.; Huang K-J.; Chan Y-L.; Hong P-D.; Yeh M-K.; Wu C-J. Improving anticancer efficacy of (-)-epigallocatechin-3-gallate gold nanoparticles in murine B16F10 melanoma cells. *Drug Des. Devel. Ther.* (2014). https://doi:10.2147/DDDT.S58414.

[66] Kondath S.; Raghavan B.S.; Anantanarayanan R.; Rajaram R. Synthesis and characterisation of morin reduced gold nanoparticles and its cytotoxicity in MCF-7 cells. *Chem. Biol. Interact.* (2014). https://doi:10.1016/j.cbi.2014.09.025.

[67] Raghavan B.S.; Kondath S.; Anantanarayanan R.; Rajaram, R. Kaempferol mediated

synthesis of gold nanoparticles and their cytotoxic effects on MCF-7 cancer cell line. *Process Biochem.* (2015). https://doi:10.1016/j.procbio.2015.08.003.

[68] Greulich C.; Diendorf J.; Simon T.; Eggler G.; Epple M.; Köller M. Uptake and intracellular distribution of silver nanoparticles in human mesenchymal stem cells. *Acta Biomater.* (2011). https://doi:10.1016/j.actbio.2010.08.003.

[69] Jeyaraj M.; Sathishkumar G.; Sivanandhan G.; MubarakAli D.; Rajesh M.; Arun R.; Kapildev G.; Manickavasagam M.; Thajuddin N.; Premkumar K.; Ganapathi A. Biogenic silver nanoparticles for cancer treatment: An experimental report. *Colloids Surfaces B Biointerfaces* (2013). https://doi.org/10.1016/j.colsurfb.2013.01.027.

[70] Asharani P.V.; Hande M.P.; Valiyaveettil S. Anti-proliferative activity of silver nanoparticles. *BMC Cell Biol.* (2009). https://doi.org/10.1186/1471-2121-10-65.

[71] Gurunathan S.; Lee K-J.; Kalishwaralal K.; Sheikpranbabu S.; Vaidyanathan R.; Eom S.H. Antiangiogenic properties of silver nanoparticles. *Biomaterials* (2009). https://doi.org/10.1016/j.biomaterials.2009.08.008.

[72] Gurunathan S.; Han J.W.; Eppakayala V.; Jeyaraj M.; Kim J.H. Cytotoxicity of biologically synthesized silver nanoparticles in MDA-MB-231 human breast cancer cells. *Biomed Res. Int.* (2013). https://doi.org/10.1155/2013/535796.

[73] Vasanth K.; Ilango K.; MohanKumar R.; Agrawal A.; Dubey G.P. Anticancer activity of *Moringa oleifera* mediated silver nanoparticles on human cervical carcinoma cells by apoptosis induction. *Colloids Surfaces B Biointerfaces*. (2014). http://dx.doi.org/10.1016/j.colsurfb.2014.02.052.

[74] Vallet-Regi M.; Rámila A.; Del Real R.P.; Pérez-Pariente J. A new property of MCM-41: Drug delivery system. *Chem. Mater.* (2001). https://doi.org/10.1021/cm0011559.

[75] Yang Y.; Yu C. Advances in silica based nanoparticles for targeted cancer therapy. *Nanomedicine Nanotechnology* (2016). https://doi.org/10.1016/j.nano.2015.10.018.

[76] Hwang A.A.; Lu J.; Tamanoi F.; Zink J.I. Functional nanovalves on protein-coated nanoparticles for in vitro and in vivo controlled drug delivery. *Small.* (2015). https://doi.org/10.1002/smll.201400765.

[77] Zhang K.; Xu H.; Jia X.; Chen Y.; Ma M.; Sun L.; Chen H. Ultrasound-Triggered Nitric Oxide Release Platform Based on Energy Transformation for Targeted Inhibition of Pancreatic Tumor. *ACS Nano* (2016). https://doi.org/10.1021/acsnano.6b04921.

[78] Giménez C.; de la Torre C.; Gorbe M.; Aznar E.; Sancenón F.; Murguía J.R.; Martínez-Máñez R.; Marcos M.D.; Amorós P. Gated mesoporous silica nanoparticles for the controlled delivery of drugs in cancer cells. *Langmuir* (2015). https://doi.org/10.1021/acs.langmuir.5b00139.

[79] Singh A.; Dilnawaz F.; Mewar S.; Sharma U.; Jagannathan N.R.; Sahoo S.K. Composite polymeric magnetic nanoparticles for co-delivery of hydrophobic and hydrophilic anticancer drugs and MRI imaging for cancer therapy. *ACS Appl. Mater. Interfaces* (2011). https://doi.org/10.1021/am101196v.

[80] Kohler N.; Sun C.; Fichtenholtz A.; Gunn J.; Fang C.; Zhang M. Methotrexate-immobilized poly(ethylene glycol) magnetic nanoparticles for MR imaging and drug delivery. *Small.* (2006). https://doi.org/10.1002/smll.200600009.

[81] Alexiou C.; Arnold W.; Klein R.J.; Parak F.G.; Hulin P.; Bergemann C.; Erhardt W.; Wagenpfeil S.; Lübbe A.S. Locoregional cancer treatment with magnetic drug targeting. *Cancer Res.* (2000). PMID: 11118047.

[82] Markman J.L.; Rekechenetskiy, A., Holler, E., Ljubimova, J. Y. & Angeles, L. Nanomedicine therapeutic approaches to overcome cancer drug resistance. **65**, 1866–

1879 (2013). https://doi.org/10.1016/j.addr.2013.09.019.
[83] Tan, J. M., Karthivashan G.; Arulselvan P.; Fakurazi S.; Hussein, M.Z. Characterization and in vitro studies of the anticancer effect of oxidized carbon nanotubes functionalized with betulinic acid. *Drug Des. Devel. Ther.* (2014). https://doi:10.2147/DDDT.S70650.
[84] Tan J.M.; Karthivashan G.; Arulselvan P.; Fakurazi S.; Hussein M.Z. Characterization and in vitro sustained release of silibinin from ph responsive carbon nanotube-based drug delivery system. *J. Nanomater.* (2014). https://doi:10.1155/2014/439873.
[85] Lay C.L.; Liu H.Q.; Tan H.R.; Liu Y. Delivery of paclitaxel by physically loading onto poly(ethylene glycol) (PEG)-graftcarbon nanotubes for potent cancer therapeutics. *Nanotechnology* (2010). https://doi.org/10.1088/0957-4484/21/6/065101.
[86] Bhirde A.A.; Patel V.; Gavard J.; Zhang G.; Souza A.A.; Masedunskas A.; Leapman R.D.; Weigert R.; Gutkind J.S.; Rusling J.F. Targeted killing of cancer cells in vivo and in vitro with EGF-directed carbon nanotube-based drug delivery. *ACS Nano* (2009). https://doi.org/10.1021/nn800551s.
[87] Probst C.E.; Zrazhevskiy P.; Bagalkot V.; Gao X. Quantum dots as a platform for nanoparticle drug delivery vehicle design. *Adv. Drug Deliv. Rev.* (2013). https://doi.org/10.1016/j.addr.2012.09.036.
[88] van Vlerken L.E.; Amiji M.M. Multi-functional polymeric nanoparticles for tumour-targeted drug delivery. *Expert Opinion on Drug Delivery* (2006). https://doi:10.1517/17425247.3.2.205.
[89] Chen C.; Peng J.; Xia H-S.; Yang G-F.; Wu Q-S.; Chen L-D.; Zeng L-B.; Zhang Z-L.; Pang D-W.; Li Y. Quantum dots-based immunofluorescence technology for the quantitative determination of HER2 expression in breast cancer. *Biomaterials* (2009). https://doi:10.1016/j.biomaterials.2009.02.010.
[90] Wang H.Z.; Wang H.Y.; Liang R.Q.; Ruan K.C. Detection of tumor marker CA125 in ovarian carcinoma using quantum dots. *Acta Biochim. Biophys. Sin. (Shanghai).* (2004). https://doi:10.1093/abbs/36.10.681.
[91] Yang L.; Mao H.; Cao Z.; Wang Y.A.; Peng X.; Wang X.; Sajja H.K.; Wang L.; Duan H.; Ni C.; Staley C.A.; Wood W.C.; Gao X.; Nie S. Molecular Imaging of Pancreatic Cancer in an Animal Model Using Targeted Multifunctional Nanoparticles. *Gastroenterology* (2009). https://doi:10.1053/j.gastro.2009.01.006.
[92] Nurunnabi M.; Cho K.J.; Choi J.S.; Huh K.M.; Lee Y-k. Targeted near-IR QDs-loaded micelles for cancer therapy and imaging. *Biomaterials* (2010). https://doi.org/10.1016/j.biomaterials.2010.03.057.
[93] Bagalkot V.; Zhang L.; Levy-Nissenbaum E.; Jon S.; Kantoff P.W.; Langer R.; Farokhzad O.C. Quantum Dot−Aptamer Conjugates for Synchronous Cancer Imaging, Therapy, and Sensing of Drug Delivery Based on Bi-Fluorescence Resonance Energy Transfer. *Nano Lett.* (2007). https://doi.org/10.1021/nl071546n.
[94] Libutti S.K.; Paciotti G.F.; Byrnes A.A.; Alexander Jr H.R.; Gannon W.E.; Walker M.; Seidel G.D.; Yuldasheva N.; Tamarkin L. Phase I and pharmacokinetic studies of CYT-6091, a novel PEGylated colloidal gold-rhTNF nanomedicine. *Clin. Cancer Res.* (2010). https://doi:10.1158/1078-0432.CCR-10-0978.
[95] Anselmo A.C.; Mitragotri S. Nanoparticles in the clinic. *Bioeng. Transl. Med.* (2016). https://doi:10.1002/btm2.10003.
[96] Anselmo A.C.; Mitragotri S. A Review of Clinical Translation of Inorganic

Nanoparticles. *AAPS J.* (2015). https://doi:10.1208/s12248-015-9780-2.

[97] Tran S.; DeGiovanni P-J.; Piel B.; Rai P. Cancer nanomedicine: a review of recent success in drug delivery. *Clin. Transl. Med.* (2017). https://doi.org/10.1186/s40169-017-0175-0.

[98] Namiki Y.; Fuchigami T.; Tada N.; Kawamura R.; Matsunuma S.; Kitamoto Y.; Nakagawa M. Nanomedicine for cancer: Lipid-based nanostructures for drug delivery and monitoring. *Acc. Chem. Res.* (2011). https://doi.org/10.1021/ar200011r.

[99] Li Z.; Tan S.; Li S.; Shen Q.; Wang K. Cancer drug delivery in the nano era: An overview and perspectives (Review). *Oncol. Rep.* (2017). https://doi.org/10.3892/or.2017.5718.

[100] Torchilin V.P. Recent advances with liposomes as pharmaceutical carriers. *Nat. Rev. Drug Discov.* **4**, 145–160 (2005). https://doi.org/10.1038/nrd1632.

[101] Ferreira D.D.S.; Lopes S.C.D.A.; Franco M.S.; Oliveira M.C. PH-sensitive liposomes for drug delivery in cancer treatment. *Therapeutic Delivery* (2013). https://doi:10.4155/tde.13.80.

[102] Banerjee S.; Sen K.; Pal T.K.; Guha S.K. Poly(styrene-co-maleic acid)-based pH-sensitive liposomes mediate cytosolic delivery of drugs for enhanced cancer chemotherapy. *Int. J. Pharm.* (2012). https://doi.org/10.1016/j.ijpharm.2012.07.059.

[103] Shi G.; Guo W.; Stephenson S.M.; Lee R.J. Efficient intracellular drug and gene delivery using folate receptor-targeted pH-sensitive liposomes composed of cationic/anionic lipid combinations. *J. Control. Release* (2002). https://doi.org/10.1016/s0168-3659(02)00017-2.

[104] Mo R.; Sun Q.; Li N.; Zhang C. Intracellular delivery and antitumor effects of pH-sensitive liposomes based on zwitterionic oligopeptide lipids. *Biomaterials* (2013). https://doi.org/10.1016/j.biomaterials.2013.01.030.

[105] Paliwal S.R.; Paliwal R.; Pal H.C.; Saxena A.K.; Sharma P.R.; Gupta P.M.; Agrawal G.P.; Vyas S.P. Estrogen-anchored pH-sensitive liposomes as nanomodule designed for site-specific delivery of doxorubicin in breast cancer therapy. *Mol. Pharm.* (2012). https://doi.org/10.1021/mp200439z.

[106] Ishida T.; Kirchmeier M.J.; Moase E.H.; Zalipsky S.; Allen T.M. Targeted delivery and triggered release of liposomal doxorubicin enhances cytotoxicity against human B lymphoma cells. *Biochim. Biophys. Acta - Biomembr.* (2001). https://doi.org/10.1016/S0005-2736(01)00409-6.

[107] Qiu H.; Min Y.; Rodgers Z.; Zhang L.; Wang A.Z. Nanomedicine approaches to improve cancer immunotherapy. *Wiley Interdisciplinary Reviews: Nanomedicine and Nanobiotechnology* (2017). https://doi:10.1002/wnan.1456.

[108] Dragovich T.; Mendelson D.; Kurtin S.; Richardson K.; Von Hoff D.; Hoos A.. A Phase 2 trial of the liposomal DACH platinum L-NDDP in patients with therapy-refractory advanced colorectal cancer. *Cancer Chemother. Pharmacol.* (2006). https://doi:10.1007/s00280-006-0235-4.

[109] Gaillard P.J.; Appeldoorn C.C.M.; Dorland R.; van Kregten J.; Manca F.; Vugts D.J.; Windhorst B.; van Dongen G.A.M.S.; de Vries H.E.; Maussang D.; van Tellingen O. Pharmacokinetics, brain delivery, and efficacy in brain tumor-bearing mice of glutathione pegylated liposomal doxorubicin (2B3-101). *PLoS One* (2014). https://doi:10.1371/journal.pone.0082331.

[110] Muggia F.M.; Hainsworth J.D.; Jeffers S.; Miller P.; Groshen S.; Tan M.; Roman L.; Uziely B.; Muderspach L.; Garcia A.; Burnett A.; Greco F.A.; Morrow C.P.; Paradiso L.J.; Liang L.J. Phase II study of liposomal doxorubicin in refractory ovarian cancer:

Antitumor activity and toxicity modification by liposomal encapsulation. *J. Clin. Oncol.* (1997). https://doi:10.1200/JCO.1997.15.3.987.

[111] He Y.; Zeng Q.; Drenning S.D.; Melhem M.F.; Tweardy D.J.; Huang L.; Grandis J.R. Inhibition of human squamous cell carcinoma growth in vivo by epidermal growth factor receptor antisense RNA transcribed from the U6 promoter. *J. Natl. Cancer Inst.* (1998). https://doi:10.1093/jnci/90.14.1080.

[112] Fan Y.; Zhang Q. Development of liposomal formulations: From concept to clinical investigations. *Asian J. Pharm. Sci.* (2013). https://doi.org/10.1016/j.ajps.2013.07.010.

[113] Khemapech N.; Oranratanaphan S.; Termrungruanglert W.; Lertkhachonsuk R.; Vasurattana A. Salvage chemotherapy in recurrent platinum-resistant or refractory epithelial ovarian cancer with carboplatin and Distearoylphosphatidylcholine pegylated liposomal doxorubicin (Lipo-Dox®). *Asian Pacific J. Cancer Prev.* (2013). https://doi:10.7314/APJCP.2013.14.3.2131.

[114] Stathopoulos G.P.; Antoniou D.; Dimitroulis J.; Stathopoulos J.; Marosis K.; Michalopoulou P. Comparison of liposomal cisplatin versus cisplatin in non-squamous cell non-small-cell lung cancer. *Cancer Chemother. Pharmacol.* (2011). https://doi:10.1007/s00280-011-1572-5.

[115] Rodriguez M.A.; Pytlik R.; Kozak T.; Chhanabhai M.; Gascoyne R.; Lu B.; Deitcher S.R.; Winter J.N.; Marqibo Investigators. Vincristine sulfate liposomes injection (Marqibo) in heavily pretreated patients with refractory aggressive non-Hodgkin lymphoma: Report of the pivotal phase 2 study. *Cancer* (2009). https://doi:10.1002/cncr.24359.

[116] Venkatakrishnan K.; Liu Y.; Noe D.; Mertz J.; Bargfrede M.; Marbury T.; Farbakhsh K.; Oliva C.; Milton A. Pharmacokinetics and pharmacodynamics of liposomal mifamurtide in adult volunteers with mild or moderate hepatic impairment. *Br. J. Clin. Pharmacol.* (2014). https://doi:10.1111/bcp.12261.

[117] Batist G.; Ramakrishnan G.; Rao C.S.; Chadrasekharan A.; Gutheil J.; Guthrie T.; Shah P.; Khojasteh A.; Nair M.K.; Hoelzer K.; Tkaczuk K.; Park Y.C.; Lee L.W. Reduced cardiotoxicity and preserved antitumor efficacy of liposome-encapsulated doxorubicin and cyclophosphamide compared with conventional doxorubicin and cyclophosphamide in a randomized, multicenter trial of metastatic breast cancer. *J. Clin. Oncol.* (2001). https://doi:10.1200/JCO.2001.19.5.1444.

[118] Yarmolenko P.S.; Zhao Y.; Landon C.; Spasojevic I.; Yuan F.; Needham D.; Viglianti B.L.; Dewhirst M.W. Comparative effects of thermosensitive doxorubicin-containing liposomes and hyperthermia in human and murine tumours. *Int. J. Hyperth.* (2010). https://doi:10.3109/02656731003789284.

[119] Elkhodiry M.A.; Momah C.C.; Suwaidi S.R.; Gadalla D.; Martins A.M.; Vitor R.F.; Husseini G.A. Synergistic nanomedicine: Passive, active, and ultrasound-triggered drug delivery in cancer treatment. *J. Nanosci. Nanotechnol.* (2016). https://doi.org/10.1166/jnn.2016.11124.

[120] Beltrán-Gracia E.; López-Camacho A.; Higuera-Ciapara I.; Velázquez-Fernández J.B.; Vallejo-Cardona A.A. Nanomedicine review: Clinical developments in liposomal applications. *Cancer Nanotechnology* (2019). https://doi.org/10.1186/s12645-019-0055-y.

[121] Saiyin W.; Wang D.; Li L.; Zhu L.; Liu B.; Sheng L.; Li Y.; Zhu B.; Mao L.; Li G.; Zhu X. Sequential release of autophagy inhibitor and chemotherapeutic drug with polymeric delivery system for oral squamous cell carcinoma therapy. *Mol. Pharm.*

(2014). https://doi.org/10.1021/mp5000423.
[122] Endo K.; Ueno T.; Kondo S.; Wakisaka N.; Murono S.; Ito M.; Kataoka K.; Kato Y.; Yoshizaki T. Tumor-targeted chemotherapy with the nanopolymer-based drug NC-6004 for oral squamous cell carcinoma. *Cancer Sci.* (2013). https://doi.org/10.1111/cas.12079.
[123] Liao H.; Xiao Y.; Hu Y.; Xiao Y.; Yin Z.; Liu L. microRNA-32 induces radioresistance by targeting DAB2IP and regulating autophagy in prostate cancer cells. *Oncol. Lett.* (2015). https://doi.org/10.3892%2Fol.2015.3551.
[124] Shao J.; Cao J.; Liu Y.; Mei H.; Zhang Y.; Xu W. MicroRNA-519a promotes proliferation and inhibits apoptosis of hepatocellular carcinoma cells by targeting FOXF2. *FEBS Open Bio.* (2015). https://doi:10.1016/j.fob.2015.10.009.
[125] Wang Z.; Zheng C.; Jiang K.; He J.; Cao X.; Wu S. MicroRNA-503 suppresses cell proliferation and invasion in osteosarcoma via targeting insulin-like growth factor 1 receptor. *Exp. Ther. Med.* (2017). https://doi:10.3892/etm.2017.4648.
[126] Lasic D.D.; Needham D. The "Stealth" Liposome: A Prototypical Biomaterial. *Chem. Rev.* (1995). https://doi:10.1021/cr00040a001.
[127] Lee K.S.; Chung H.C.; Im S.A.; Park Y.H.; Kim C.S.; Kim S-B.; Rha S.Y.; Lee M.Y.; Ro J. Multicenter phase II trial of Genexol-PM, a Cremophor-free, polymeric micelle formulation of paclitaxel, in patients with metastatic breast cancer. *Breast Cancer Res. Treat.* (2008). https://doi:10.1007/s10549-007-9591-y.
[128] Ghamande S.; Lin C-C.; Cho D.C.; Shapiro G.I.; Kwak E.L.; Silverman M.H.; Tseng Y.; Kuo M-W.; Mach W.B.; Hsu S-C.; Coleman T.; Yang J.C-H. A phase 1 open-label, sequential dose-escalation study investigating the safety, tolerability, and pharmacokinetics of intravenous TLC388 administered to patients with advanced solid tumors. *Invest. New Drugs* (2014). https://doi:10.1007/s10637-013-0044-7.
[129] Madaan A.; Singh P.; Awasthi A.; Verma R.; Singh A.T.; Jaggi M.; Mishra S.K.; Kulkarni S.; Kulkarni H. Efficiency and mechanism of intracellular paclitaxel delivery by novel nanopolymer-based tumor-targeted delivery system, Nanoxel^{TM}. *Clin. Transl. Oncol.* (2013).. https://doi:10.1007/s12094-012-0883-2.
[130] Ueno T.; Endo K.; Hori K.; Ozaki N.; Tsuji A.; Kondo S.; Wakisaka N.; Murono S.; Kataoka K.; Katoa Y.; Yoshizaki T. Assessment of antitumor activity and acute peripheral neuropathy of 1,2-diaminocyclohexane platinum (II)-incorporating micelles (NC-4016). *Int. J. Nanomedicine* (2014). https://doi:10.2147/IJN.S60564.
[131] Plummer R.; Wilson R.H.; Calvert H.; Boddy A.V.; Griffin M.; Sludden J.; Tilby M.J.; Eatock M.; Pearson D.G.; Ottley C.J.; Matsumura Y.; Kataoka K.; Nishiya T. A Phase I clinical study of cisplatin-incorporated polymeric micelles (NC-6004) in patients with solid tumours. *Br. J. Cancer* (2011). https://doi:10.1038/bjc.2011.6.
[132] Hamaguchi T.; Doi T.; Eguchi-Nakajima T.; Kato K.; Yamada Y.; Shimada Y.; Fuse N.; Ohtsu A.; Matsumoto S-i.; Takanashi M.; Matsumura Y. Phase I study of NK012, a novel SN-38-incorporating micellar nanoparticle, in adult patients with solid tumors. *Clin. Cancer Res.* (2010). https://doi:10.1158/1078-0432.CCR-10-0387.
[133] Kato K.; Chin K.; Yoshikawa T.; Yamaguchi K.; Tsuji Y.; Esaki T.; Sakai K.; Kimura M.; Hamaguchi T.; Shimada Y.; Matsumura Y.; Ikeda R. Phase II study of NK105, a paclitaxel-incorporating micellar nanoparticle, for previously treated advanced or recurrent gastric cancer. *Invest. New Drugs* (2012). https://doi:10.1007/s10637-011-9709-2.
[134] Matsumura Y.; Hamaguchi T.; Ura T.; Muro K.; Yamada Y.; Shimada Y.; Shirao K.; Okusaka T.; Ueno H.; Ikeda M.; Watanabe N. Phase I clinical trial and

pharmacokinetic evaluation of NK911, a micelle-encapsulated doxorubicin. *Br. J. Cancer* (2004). https://doi:10.1038/sj.bjc.6602204.

[135] Valle J.W.; Armstrong A.; Newman C.; Alakhov V.; Pietrzynski G.; Brewer J.; Campbell S.; Corrie P.; Rowinsky E.K.; Ranson M. A phase 2 study of SP1049C, doxorubicin in P-glycoprotein-targeting pluronics, in patients with advanced adenocarcinoma of the esophagus and gastroesophageal junction. *Invest. New Drugs* (2011). https://doi:10.1007/s10637-010-9399-1.

[136] Greening D.W.; Gopal S.K.; Xu R.; Simpson R.J.; Chen W. Exosomes and their roles in immune regulation and cancer. *Semin. Cell Dev. Biol.* (2015). https://doi.org/10.1016/j.semcdb.2015.02.009.

[137] Couto N.; Caja S.; Maia J.; Moraes M.C.S.; Costa-Silva B. Exosomes as emerging players in cancer biology. *Biochimie* (2018). https://doi.org/10.1016/j.biochi.2018.03.006.

[138] Lim W.; Kim H.S. Exosomes as Therapeutic Vehicles for Cancer. *Tissue Eng. Regen. Med.* (2019). https://doi.org/10.1007/s13770-019-00190-2.

[139] Batrakova E.V.; Kim M.S. Using exosomes, naturally-equipped nanocarriers, for drug delivery. *J Control Release* (2016). https://doi:10.1016/j.jconrel.2015.07.030.

[140] Kalluri R. The Biology and Function of Urine Exosomes in Bladder Cancer. *J. Clin. Invest.* (2016). https://doi.org/10.1172%2FJCI81135.

[141] Syn N.L.; Wang L.; Chow E.K.H.; Lim C.T.; Goh B.C. Exosomes in Cancer Nanomedicine and Immunotherapy: Prospects and Challenges. *Trends Biotechnol.* (2017). https://doi.org/10.1016/j.tibtech.2017.03.004.

[142] Tai Y.L.; Chen K.C.; Hsieh J.T.; Shen T.L. Exosomes in cancer development and clinical applications. *Cancer Sci.* (2018). https://doi.org/10.1111/cas.13697.

[143] Dai S.; Wei D.; Wu Z.; Zhou X.; Wei X.; Huang H.; Li G. Phase I clinical trial of autologous ascites-derived exosomes combined with GM-CSF for colorectal cancer. *Mol. Ther.* (2008). https://doi:10.1038/mt.2008.1.

[144] Escudier B.; Dorval T.; Chaput N.; André F.; Caby M-P.; Novault S.; Flament C.; Leboulaire C.; Borg C.; Amigorena S.; Boccaccio C.; Bonnerot C.; Dhellin O.; Movassagh M.; Piperno S.; Robert C.; Serra V.; Valente N.; Le Pecq J-B.; Spatz A.; Lantz O.; Tursz T.; Angevin E.; Zitvogel L. Vaccination of metastatic melanoma patients with autologous dendritic cell (DC) derived-exosomes: Results of the first phase 1 clinical trial. *J. Transl. Med.* (2005). https://doi:10.1186/1479-5876-3-10.

[145] Morse M.A.; Garst J.; Osada T.; Khan S.; Hobeika A.; Clay T.M.; Valente N.; Shreeniwas R.; Sutton M.A.; Delcayre A.; Hsu D-H.; Le Pecq J-B.; Lyely H.K. A phase I study of dexosome immunotherapy in patients with advanced non-small cell lung cancer. *J. Transl. Med.* (2005). https://doi:10.1186/1479-5876-3-9.

[146] Besse B.; Charrier M.; Lapierre V. *et al.* Dendritic cell-derived exosomes as maintenance immunotherapy after first line chemotherapy in NSCLC. *Oncoimmunology* (2016). https://doi:10.1080/2162402X.2015.1071008.

[147] Chen Y.S.; Lin E.Y.; Chiou T.W.; Harn H.J. Exosomes in clinical trial and their production in compliance with good manufacturing practice. *Tzu Chi Medical Journal* (2020). https://doi:10.4103/tcmj.tcmj_182_19.

[148] Lammers T.; Kiessling F.; Hennink W.E.; Storm G. Drug targeting to tumors: Principles, pitfalls and (pre-) clinical progress. *J. Control. Release* (2012). https://doi.org/10.1016/j.jconrel.2011.09.063.

[149] Gottesman M.M.; Fojo T.; Bates S.E. Multidrug resistance in cancer: role of ATP–dependent transporters. *Nature Reviews Cancer* (2002).

https://doi.org/10.1038/nrc706.
[150] Helleday T.; Petermann E.; Lundin C.; Hodgson B.; Sharma R.A. DNA repair pathways as targets for cancer therapy. *Nature Reviews Cancer*. (2008). https://doi.org/10.1038/nrc2342.
[151] Hanahan D.; Weinberg R.A. Hallmarks of cancer: the next generation. *Cell.* (2011). https://doi.org/10.1016/j.cell.2011.02.013.
[152] Marusyk A.; Almendro V.; Polyak K. Intra-tumour heterogeneity: a looking glass for cancer? *Nat. Ver. Cancer*. (2012). https://doi.org/10.1038/nrc3261.
[153] Visvader J.E.; Lindeman G.J. Cancer stem cells: current status and evolving complexities. *Cell Stem Cell*. (2012) https://doi.org/10.1016/j.stem.2012.05.007.
[154] Williams H.D.; Trevaskis N.L.; Charman S.A.; Shanker R.M; Charman W.N.; Pouton C.W.; Porter C.J.H. Strategies to address low drug solubility in discovery and development. *Pharmacol. Rev.* (2013). https://doi.org/10.1124/pr.112.005660.
[155] Lammers T. Improving the efficacy of combined modality anticancer therapy using HPMA copolymer-based nanomedicine formulations. *Advanced Drug Delivery Reviews* (2010). https://doi:10.1016/j.addr.2009.11.028.
[156] Nichols J.W.; Bae Y.H. Odyssey of a cancer nanoparticle: From injection site to site of action. *Nanotoday* (2012). https://doi.org/10.1016/j.nantod.2012.10.010.
[157] Stylianopoulos T.; Economides E-A.; Baish J.W.; Fukumura D.; Jain R.K. Towards Optimal Design of Cancer Nanomedicines: Multi-stage Nanoparticles for the Treatment of Solid Tumors. *Ann Biomed Eng.* (2015). https://doi.org/10.1007/s10439-015-1276-9.
[158] Sykes E.A.; Dai Q.; Sarsons C.D.; Chen J.; Rocheleau J.V.; Hwang D.M.; Zheng G.; Cramb D.T.; Rinker K.D.; Chan W.C.W. Tailoring nanoparticle designs to target cancer based on tumor pathophysiology. *PNAS* (2016). https://doi.org/10.1073/pnas.1521265113.
[159] Zein R.; Sharrouf W.; Selting K. Physical Properties of Nanoparticles That Result in Improved Cancer Targeting. Journal of Oncology (2020). https://doi.org/10.1155/2020/5194780.
[160] Li H-J.; Du J-Z.; Du X-J.; Xu C-F.; Sun C-Y.; Wang H-X.; Cao Z-T.; Yang X-Z.; Zhu Y-H.; Nie S.; Wang J. Stimuli-responsive clustered nanoparticles for improved tumor penetration and therapeutic efficacy. *PNAS* (2016). https://doi.org/10.1073/pnas.1522080113.
[161] Liu J.; Li H-J.; Luo Y-L.; Xu C-F.; Du X-J.; Du J-Z. Wang J. Enhanced Primary Tumor Penetration Facilitates Nanoparticle Draining into Lymph Nodes after Systemic Injection for Tumor Metastasis Inhibition. *ACS Nano* (2019). https://doi.org/10.1021/acsnano.9b03472.
[162] Wong C.; Stylianopoulos T.; Cui J.; Martin J.; Chauhan V.P.; Jiang W.; Popović Z.; Jain R.K.; Bawendi M.G.; Fukumura D. Multistage nanoparticle delivery system for deep penetration into tumor tissue. *PNAS* (2011). https://doi.org/10.1073/pnas.1018382108.
[163] Cun X.; Li M.; Wang S.; Wang Y.; Wang J.; Lu Z.; Yang R.; Tang X.; Zhang Z.; He Q. A size switchable nanoplatform for targeting the tumor microenvironment and deep tumor penetration. *Nanoscale* (2018). https://doi.org/10.1039/C8NR00640G.
[164] Robertson J.D.; Yealland G.; Avila-Olias M.; Chierico L.; Bandmann O.; Renshaw S.A.; Battaglia G. pH-Sensitive Tubular Polymersomes: Formation and Applications in Cellular Delivery. *ACS Nano* (2014). https://doi.org/10.1021/nn5004088.
[165] Scarpa E.; De Pace C.; Joseph A.S.; de Souza S.C,; Poma A.; Liatsi-Douvitsa E.;

Contini C.; De Matteis V.; Martí J.S.; Battaglia G.; Rizzello L. Tuning cell behavior with nanoparticle shape. *PLOS ONE* (2020). https://doi.org/10.1371/journal.pone.0240197.

[166] Choo P.; Liu T.; Odom T.W. Nanoparticle Shape Determines Dynamics of Targeting Nanoconstructs on Cell Membranes. *J. Am. Chem. Soc.* (2021). https://doi.org/10.1021/jacs.1c00850.

[167] Dam D.H.M.; Culver K.S.B.; Odom T.W. Grafting Aptamers onto Gold Nanostars Increases in Vitro Efficacy in a Wide Range of Cancer Cell Types. *Mol Pharm.* (2014). https://doi.org/10.1021/mp4005657.

[168] Jia W.; Liu R.; Wang Y.; Hu C.; Yu W.; Zhou Y.; Wang L.; Zhang M.; Gao H.; Gao X. Dual-responsive nanoparticles with transformable shape and reversible charge for amplified chemo-photodynamic therapy of breast cancer. *Acta Pharmaceutica Sinica B* (2022). https://doi.org/10.1016/j.apsb.2022.03.010.

[169] Zhang P.; Chen D.; Li L.; Sun K. Charge reversal nano-systems for tumor therapy. *Journal of Nanobiotechnology* (2022). https://doi.org/10.1186/s12951-021-01221-8.

[170] Shi M.; Zhang J.; Wang Y.; Han Y.; Zhao X.; Hu H.; Qiao M.; Chen D. Blockage of the IDO1 pathway by charge-switchable nanoparticles amplifies immunogenic cell death for enhanced cancer immunotherapy panel. *Acta Biomater.* (2022). https://doi.org/10.1016/j.actbio.2022.07.022.

[171] Sriraman S.K.; Aryasomayajula B.; Torchilin V.P. Barriers to drug delivery in solid tumors. *Tissue Barriers* (2014). https://doi.org/10.4161%2Ftisb.29528.

[172] Cox T.R.; Erler J.T. Remodeling and homeostasis of the extracellular matrix: implications for fibrotic diseases and cancer. *Dis Model Mech.* (2011). https://doi.org/10.1242/dmm.004077.

[173] Heldin C-H.; Rubin K.; Pietras K.; Ostman A. High interstitial fluid pressure - an obstacle in cancer therapy. *Nat Rev Cancer* (2004). https://doi.org/10.1038/nrc1456.

[174] Tiwari N.; Osorio-Blanco E.R.; Sonxogni A.; Esporrín-Ubieto D.; Wang H.; Calderón M. Nanocarriers for Skin Applications: Where Do We Stand? *Angew Chem Int Ed Engl.* (2021). https://doi.org/10.1002/anie.202107960.

[175] Li M.; Zhang Y.; Zhang Q.; Li J. Tumor extracellular matrix modulating strategies for enhanced antitumor therapy of nanomedicines. *Mater Today Bio.* (2022). https://doi.org/10.1016%2Fj.mtbio.2022.100364.

[176] Aggarwal P.; Hall J.B.; McLeland C.B.; Dobrovolskaia M.A.; McNeil S.E. Nanoparticle interaction with plasma proteins as it relates to particle biodistribution, biocompatibility and therapeutic efficacy. *Advanced Drug Delivery Reviews* (2009). https://doi:10.1016/j.addr.2009.03.009.

[177] Jain R.K. Normalizing tumor microenvironment to treat cancer: bench to bedside to biomarkers. *J Clin Oncol.* (2013). https://doi.org/10.1200/jco.2012.46.3653.

[178] Cassetta L.; Fragkogianni S.; Sims A.H. *et al.* Human Tumor-Associated Macrophage and Monocyte Transcriptional Landscapes Reveal Cancer-Specific Reprogramming, Biomarkers, and Therapeutic Targets. *Cancer Cell.* (2019). https://doi.org/10.1016/j.ccell.2019.02.009.

[179] Fredrich T.; Rieger H.; Chignola R.; Milotti E. Fine-grained simulations of the microenvironment of vascularized tumours. *Scientific Reports* (2019). https://doi.org/10.1038/s41598-019-48252-8.

[160] Robey R.W.; Pluchino K.M.; Hall M.D.; Fojo A.T.; Bates S.E.; Gottesman M.M. Revisiting the role of ABC transporters in multidrug-resistant cancer. *Nat Rev Cancer* (2018). https://doi.org/10.1038/s41568-018-0005-8.

[181] Clevers H. The cancer stem cell: premises, promises and challenges. *Nature Mecicine* (2011). https://doi.org/10.1038/nm.2304.
[182] Creighton C.J.; Li X.; Landis M. *et al.* Residual breast cancers after conventional therapy display mesenchymal as well as tumor-initiating features. *PNAS* (2009). https://doi.org/10.1073/pnas.0905718106.
[183] Wei S.C.; Levine J.H.; Cogdill A.P.; Zhao Y.; Anang N-N.A.S.; Andrews M.C.; Sharma P.; Wang J.; Wargo J.A.; Pe'er D.; Allison J.P. Distinct Cellular Mechanisms Underlie Anti-CTLA-4 and Anti-PD-1 Checkpoint Blockade. *Cell.* (2017). https://doi.org/10.1016/j.cell.2017.07.024.
[184] Cassetta L.; Pollard J.W. Targeting macrophages: therapeutic approaches in cancer. *Nat Rev Drug Discov.* (2018). https://doi.org/10.1038/nrd.2018.169.
[185] Anderson N.M.; Simon M.C. Tumor Microenvironment. *Curr Biol.* (2021). https://doi.org/10.1016%2Fj.cub.2020.06.081.
[186] Xiao Y.; Yu D. Tumor microenvironment as a therapeutic target in cancer. *Pharmacol Ther.* (2020). https://doi.org/10.1016%2Fj.pharmthera.2020.107753.
[187] Vaupel P.; Mayer A. Hypoxia in cancer: significance and impact on clinical outcome. *Cancer Metastasis Rev.* (2007). https://doi.org/10.1007/s10555-007-9055-1.
[188] Chen D.S; Mellman I. Elements of cancer immunity and the cancer–immune set point. *Nature* (2017). https://doi.org/10.1038/nature21349.
[189] Joyce J.A.; Fearon D.T. T cell exclusion, immune privilege, and the tumor microenvironment. *Science* (2015). https://doi.org/10.1126/science.aaa6204.
[190] Shi J.; Kantoff P.W.; Wooster R.; Farokhzad O.C. Cancer nanomedicine: progress, challenges and opportunities. *Nature Reviews Cancer* (2016). https://doi.org/10.1038/nrc.2016.108.
[191] Beck A.; Goetsch L.; Dumontet C.; Corvaïa N. Strategies and challenges for the next generation of antibody–drug conjugates. *Nature Reviews Drug Discovery* (2017). https://doi.org/10.1038/nrd.2016.268.
[192] Lambert J.M.; Morris C.Q. Antibody-Drug Conjugates (ADCs) for Personalized Treatment of Solid Tumors: A Review. *Adv Ther.* (2017). https://doi.org/10.1007/s12325-017-0519-6.
[193] Sharma P.; Allison J.P. The future of immune checkpoint therapy. *Science.* (2015). https://doi.org/10.1126/science.aaa8172.
[194] Westin J.R.; Locke F.L; Dickinson M. *et al*. Safety and Efficacy of Axicabtagene Ciloleucel versus Standard of Care in Patients 65 Years of Age or Older with Relapsed/Refractory Large B-Cell Lymphoma. *Clin Cancer Res.* (2023). https://doi.org/10.1158/1078-0432.ccr-22-3136.
[195] Le B.T.; Raguraman P.; Kosbar T.R.; Fletcher S.; Wilton S.D.; Veedu R.N. Antisense Oligonucleotides Targeting Angiogenic Factors as Potential Cancer Therapeutics. *Int J Mol Ther Nucleic Acids* (2019). https://doi.org/10.3892%2Fijo.2016.3512.
[196] Ye F.; Dewanjee S.; Li Y.; Jha N.K.; Chen Z-S.; Kumar A.; Vishakha; Behl T.; Jha S.K.; Tang H. Advancements in clinical aspects of targeted therapy and immunotherapy in breast cancer. *Molecular Cancer* (2023). https://doi.org/10.1186/s12943-023-01805-y.
[197] Chen S.; Zhao X.; Chen J.; Kuznetsova L.; Wong S.S.; Ojima I. Mechanism-Based Tumor-Targeting Drug Delivery System. Validation of Efficient Vitamin Receptor-Mediated Endocytosis and Drug Release. *Bioconjug Chem.* (2010). https://doi.org/10.1021/bc9005656.

[198] Janjigian Y.Y.; Azzoli C.G.; Krug L.M.; Pereira L.K.; Rizvi N.A.; Pietanza M.C.; Kris M.G.; Ginsberg M.S.; Pao W.; Miller V.A.; Riely G.J. Phase I/II Trial of Cetuximab and Erlotinib in Patients with Lung Adenocarcinoma and Acquired Resistance to Erlotinib. *Clinical Cancer Research*. (2011). https://doi.org/10.1158/1078-0432.CCR-10-2662.

[199] Yarden Y.; Sliwkowski M.X. Untangling the ErbB signalling network. *Nature Reviews Molecular Cell Biology*. (2001). https://doi.org/10.1038/35052073.

[200] Gajria D.; Chandarlapaty S. HER2-amplified breast cancer: mechanisms of trastuzumab resistance and novel targeted therapies. *Expert Rev Anticancer Ther.* (2011). https://doi.org/10.1586%2Fera.10.226.

[201] Slamon D.J.; Clark G.M.; Wong S.G.; Levin W.J.; Ullrich A.; McGuire W.L. Human breast cancer: correlation of relapse and survival with amplification of the HER-2/neu oncogene. *Science*. (1987). https://doi.org/10.1126/science.3798106.

[202] Ferrara N. Vascular endothelial growth factor as a target for anticancer therapy. *Oncologist*. (2004). https://doi.org/10.1634/theoncologist.9-suppl_1-2.

[203] Ferrara N.; Hillan K.J.; Novotny W. Bevacizumab (Avastin), a humanized anti-VEGF monoclonal antibody for cancer therapy. *Biochem Biophys Res Commun.* (2005). https://doi.org/10.1016/j.bbrc.2005.05.132.

[204] Hebrst R.S.; Baas P.; Kim D-W. *et al.* Pembrolizumab versus docetaxel for previously treated, PD-L1-positive, advanced non-small-cell lung cancer (KEYNOTE-010): a randomised controlled trial. *Lancet*. (2015). https://doi.org/10.1016/s0140-6736(15)01281-7.

[205] Topalian S.L.; Hodi F.S.; Brahmer J.R. *et al.* Safety, activity, and immune correlates of anti-PD-1 antibody in cancer. *N Engl J Med.* (2012). https://doi.org/10.1056/nejmoa1200690.

[206] Zhang Z.; Chen Y.; Ma M. *et al.* Significant benefit of Nivolumab treating PD-L1 positive metastatic pulmonary carcinosarcoma: a case report and literature review. *Oncotarget*. (2017). https://doi.org/10.18632%2Foncotarget.19089.

[207] de Bono J.S.; Logothetis C.J.; Molina A. *et al.* Abiraterone and increased survival in metastatic prostate cancer. *N Engl J Med.* (2011). https://doi.org/10.1056/nejmoa1014618.

[208] Scher H.I.; Fizazi K.; Saad F. *et al.* Increased survival with enzalutamide in prostate cancer after chemotherapy. *N Engl J Med.* (2012). https://doi.org/10.1056/nejmoa1207506.

[209] Bradley R.; Braybrooke J.; Gray R. *et al.* Aromatase inhibitors versus tamoxifen in premenopausal women with oestrogen receptor-positive early-stage breast cancer treated with ovarian suppression: a patient-level meta-analysis of 7030 women from four randomised trials. *Lancet Oncol.* (2022). https://doi.org/10.1016/s1470-2045(21)00758-0.

[210] Ohara M.; Akimoto E.; Noma M.; Matsuura K.; Doi M.; Kagawa N.; Itamoto T. Prognostic impact of progesterone receptor status combined with body mass index in breast cancer patients treated with adjuvant aromatase inhibitor. *Onco Lett.* (2015). https://doi.org/10.3892%2Fol.2015.3655.

[211] Ma W.; Zhu M.; Wang B. *et al.* Vandetanib drives growth arrest and promotes sensitivity to imatinib in chronic myeloid leukemia by targeting ephrin type-B receptor 4. *Mol Oncol.* (2022). https://doi.org/10.1002%2F1878-0261.13270.

[212] Mirshafiey A.; Ghalamfarsa G.; Asghari B.; Azizi G. Receptor Tyrosine Kinase and Tyrosine Kinase Inhibitors. *Innov Clin Neurosci.* (2014). PMID: 25337443.

[213] Low P.S.; Henn W.A.; Doorneweerd D.D. Discovery and Development of Folic-Acid-Based Receptor Targeting for Imaging and Therapy of Cancer and Inflammatory Diseases. *Acc Chem Res.* (2008). https://doi.org/10.1021/ar7000815.
[214] Daniels T.R.; Bernabeu E.; Rodríguez J.A.; Patel S.; Kozman M.; Chiappetta D.A.; Holler E.; Ljubimova J.Y.; Helguera G.; Penichet M.L. The transferrin receptor and the targeted delivery of therapeutic agents against cancer. *Biochem Biophys Acta*. (2012). https://doi.org/10.1016/j.bbagen.2011.07.016.
[215] Huang R.; Rofstad E.K. Integrins as therapeutic targets in the organ-specific metastasis of human malignant melanoma. *J Exp Clin Cancer Res.* (2018). https://doi.org/10.1186/s13046-018-0763-x.
[216] Mendoza C.M.L; Quintana L.E.A. Smart Drug Delivery Strategies for Cancer Therapy. *Front. Nanotechnol.* (2022). https://doi.org/10.3389/fnano.2021.753766.
[217] Wicki A.; Witzigmann D.; Balasubramanian V.; Huwyler J. Nanomedicine in cancer therapy: Challenges, opportunities, and clinical applications. *Journal of Controlled Release* (2015). http://dx.doi.org/10.1016/j.jconrel.2014.12.030.
[218] Elkhodiry M.A.; Momah C.C.; Suwaidi S.R.; Gadalla D.; Martins A.M.; Vitor R.F.; Husseini G.A. Synergistic Nanomedicine: Passive, Active, and Ultrasound-Triggered Drug Delivery in Cancer Treatment. *Journal of Nanoscience and Nanotechnology* (2016). https://doi.org/10.1166/jnn.2016.11124.
[219] Nies A.T; Koespell H.; Damme K.; Schwab M. Organic Cation Transporters (OCTs, MATEs), *In Vitro* and *In Vivo* Evidence for the Importance in Drug Therapy. *In:* Fromm M.; Kim R. (eds) Drug Transporters. Handbook of Experimental Pharmacology, vol 201. *Springer* (2011). https://doi.org/10.1007/978-3-642-14541-4_3.
[220] Zhao L.; Zhao Y.; Schwarz B.; Mysliwietz J.; Hartig R.; Camaj P.; Bao Q.; Jauch K-W.; Guba M.; Ellwart J.W.; Nelson P.J.; Bruns C.J. Verapamil inhibits tumor progression of chemotherapy-resistant pancreatic cancer side population cells. *Int J Oncol.* (2016). https://doi.org/10.3892%2Fijo.2016.3512.
[221] Seelig A. P-Glycoprotein: One Mechanism, Many Tasks and the Consequences for Pharmacotherapy of Cancers. *Front Oncol.* (2020). https://doi.org/10.3389/fonc.2020.576559.
[222] Peters C.; Brown S. Antibody–drug conjugates as novel anti-cancer chemotherapeutics. *Biosci Rep.* (2015). https://doi.org/10.1042%2FBSR20150089.
[223] Drago J.Z.; Modi S.; Chandarlapaty S. Unlocking the potential of antibody–drug conjugates for cancer therapy. *Nat Rev Clin Oncol.* (2022). https://doi.org/10.1038%2Fs41571-021-00470-8.
[224] Ganapathy V.; Thangaraju M.; Prasad P.D. Nutrient transporters in cancer: Relevance to Warburg hypothesis and beyond. *Pharmacology & Therapeutics* (2009). http://dx.doi.org/10.1016/j.pharmthera.2008.09.005.
[225] Altea-Manzano P.; Cuadros A.M.; Broadfield L.A.; Fendt S-M. Nutrient metabolism and cancer in the in vivo context: a metabolic game of give and take. *EMBO Rep.* (2020). https://doi.org/10.15252%2Fembr.202050635.
[226] Russell L.M.; Hultz M.; Searson P.C. Leakage Kinetics of the Liposomal Chemotherapeutic Agent Doxil: The Role of Dissolution, Protonation, and Passive Transport, and Implications for Mechanism of Action. *J Control Release* (2017). https://doi.org/10.1016%2Fj.jconrel.2017.11.007.
[227] dos Reis S.B.; Silva J.O.; Garcia-Fossa F.; Leite E.A.; Malachias A.; Pound-Lana G.; Mosqueira V.C.F.; Oliveira M.C.; de Barros A.L.B.; de Jesus M.B. Mechanistic

insights into the intracellular release of doxorubicin from pH-sensitive liposomes. *Biomedicine & Pharmacotherapy* (2021). https://doi.org/10.1016/j.biopha.2020.110952.

[228] Chang H-I.; Yeh M-K. Clinical development of liposome-based drugs: formulation, characterization, and therapeutic efficacy. *Int J Nanomedicine* (2012). https://doi.org/10.2147/ijn.s26766.

[229] Martinho N.; Santos T.C.B.; Florindo H.F.; Silva L.C. Cisplatin-Membrane Interactions and Their Influence on Platinum Complexes Activity and Toxicity. *Front Physiol.* (2018). https://doi.org/10.3389%2Ffphys.2018.01898.

[230] Honeywell R.J.; Hitzerd S.; Kathmann I.; Peters G.J. Transport of six tyrosine kinase inhibitors: active or passive? *ADMET and DMPK* (2016). https://doi.org/10.5599/admet.4.1.275.

[231] Wilhelm S.; Tavares A.J.; Dai Q.; Ohta S.; Audet J.; Dvorak H.F.; Chan W.C.W. Analysis of nanoparticle delivery to tumours. *Nature Reviews Materials* (2016). https://doi.org/10.1038/natrevmats.2016.14.

[232] Fang Z.; Shen Y.; Gao D. Stimulus-responsive nanocarriers for targeted drug delivery. *New J. Chem.* (2021). https://doi.org/10.1039/D0NJ05169A.

[233] Lee E.S.; Gao Z.; Bae Y.H. Recent progress in tumor pH targeting nanotechnology. *J Control Release* (2008). https://doi.org/10.1016/j.jconrel.2008.05.003.

[234] Torchilin V. Multifunctional and stimuli-sensitive pharmaceutical nanocarriers. *European Journal of Pharmaceutics and Biopharmaceutics* (2009). https://doi.org/10.1016/j.ejpb.2008.09.026.

[235] Wang Y.; Deng Y.; Luo H.; Zhu A.; Ke H.; Yang H.; Chen H. Light-Responsive Nanoparticles for Highly Efficient Cytoplasmic Delivery of Anticancer Agents. *ACS Nano.* (2017). https://doi.org/10.1021/acsnano.7b05214.

[236] Jain T.K.; Richey J.; Strand M.; Leslie-Pelecky D.L.; Flask C.; Labhasetwar V. Magnetic Nanoparticles with Dual Functional Properties: Drug Delivery and Magnetic Resonance Imaging. *Biomaterials* (2008). https://doi.org/10.1016%2Fj.biomaterials.2008.07.004.

[237] Maeda H.; Wu J.; Sawa T.; Matsumura Y.; Hori K. Tumor vascular permeability and the EPR effect in macromolecular therapeutics: a review. *J Control Release* (2000). https://doi.org/10.1016/s0168-3659(99)00248-5.

[238] Peer D.; Karp J.M.; Hong S.; Farokhzad O.C.; Margalit R.; Langer R. Nanocarriers as an emerging platform for cancer therapy. *Nature Nanotech.* (2007). https://doi.org/10.1038/nnano.2007.387.

[239] Dreaden E.C.; Alkilany A.M.; Huang X.; Murphy C.J.; El-Sayed M.A. The golden age: gold nanoparticles for biomedicine. *Chemical Society Reviews* (2012). https://doi.org/10.1039/C1CS15237H.

[240] Albanese A.; Tang P.S.; Chan W.C. The effect of nanoparticle size, shape, and surface chemistry on biological systems. *Annual Review of Biomedical Engineering* (2012). https://doi.org/10.1146/annurev-bioeng-071811-150124.

[241] Zhang L.; Gu F.; Chan J.; Wang A.; Langer R.; Farokhzad O. Nanoparticles in medicine: Therapeutic applications and developments. *Clinical Pharmacology & Therapeutics* (2008). https://doi.org/10.1038/sj.clpt.6100400.

[242] Torchilin V.P. Multifunctional, stimuli-sensitive nanoparticulate systems for drug delivery. *Nature Reviews Drug Discovery* (2014). https://doi.org/10.1038/nrd4333.

[243] Allen T.M.; Cullis P.R. Liposomal drug delivery systems: from concept to clinical applications. *Adv Drug Deliv Rev.* (2013).

https://doi.org/10.1016/j.addr.2012.09.037.
[244] Danhier F.; Ansorena E.; Silva J.M.; Coco R.; Le Breton A.; Préat V. PLGA-based nanoparticles: an overview of biomedical applications. *J Control Release*. (2012). https://doi.org/10.1016/j.jconrel.2012.01.043.
[245] Yang K.; Zhang S.; Zhang G.; Sun X.; Lee S-T.; Liu Z. Graphene in Mice: Ultrahigh In Vivo Tumor Uptake and Efficient Photothermal Therapy. *Nano Lett.* (2010). https://doi.org/10.1021/nl100996u.
[246] Kalluri R.; LeBleu V.S. The biology, function, and biomedical applications of exosomes. *Science*. (2020). https://doi.org/10.1126/science.aau6977.
[247] Elsabahy M.; Wooley K.L. Design of polymeric nanoparticles for biomedical delivery applications. *Chemical Society Reviews* (2012). https://doi.org/10.1039/c2cs15327k.
[248] Farokhzad O.C.; Langer R. Impact of nanotechnology on drug delivery. *ACS Nano* (2009). https://doi.org/10.1021/nn900002m.
[249] Kesselheim A.S.; Avorn J.; Sarpatwari A. The High Cost of Prescription Drugs in the United States: Origins and Prospects for Reform. *JAMA* (2016). https://doi.org/10.1001/jama.2016.11237.
[250] Woodcock J.; Woosley R. The FDA critical path initiative and its influence on new drug development. *Annual Review of Medicine* (2008). https://doi.org/10.1146/annurev.med.59.090506.155819.
[251] Perrault S.D.; Walkey C.; Jennings T.; Fischer H.C.; Chan W.C. Mediating tumor targeting efficiency of nanoparticles through design. *Nano Letters* (2009). https://doi.org/10.1021/nl900031y.
[252] Shi J.; Kantoff P.W.; Wooster R.; Farokhzad O.C. Cancer nanomedicine: Progress, challenges, and opportunities. *Nature Reviews Cancer* (2017). https://doi.org/10.1038/nrc.2016.108.
[253] Peer D.; Karp J.M.; Hong S.; Farokhzad O.C.; Margalit R.; Langer R. Nanocarriers as an emerging platform for cancer therapy. *Nature Nanotechnology* (2007). https://doi.org/10.1038/nnano.2007.387.

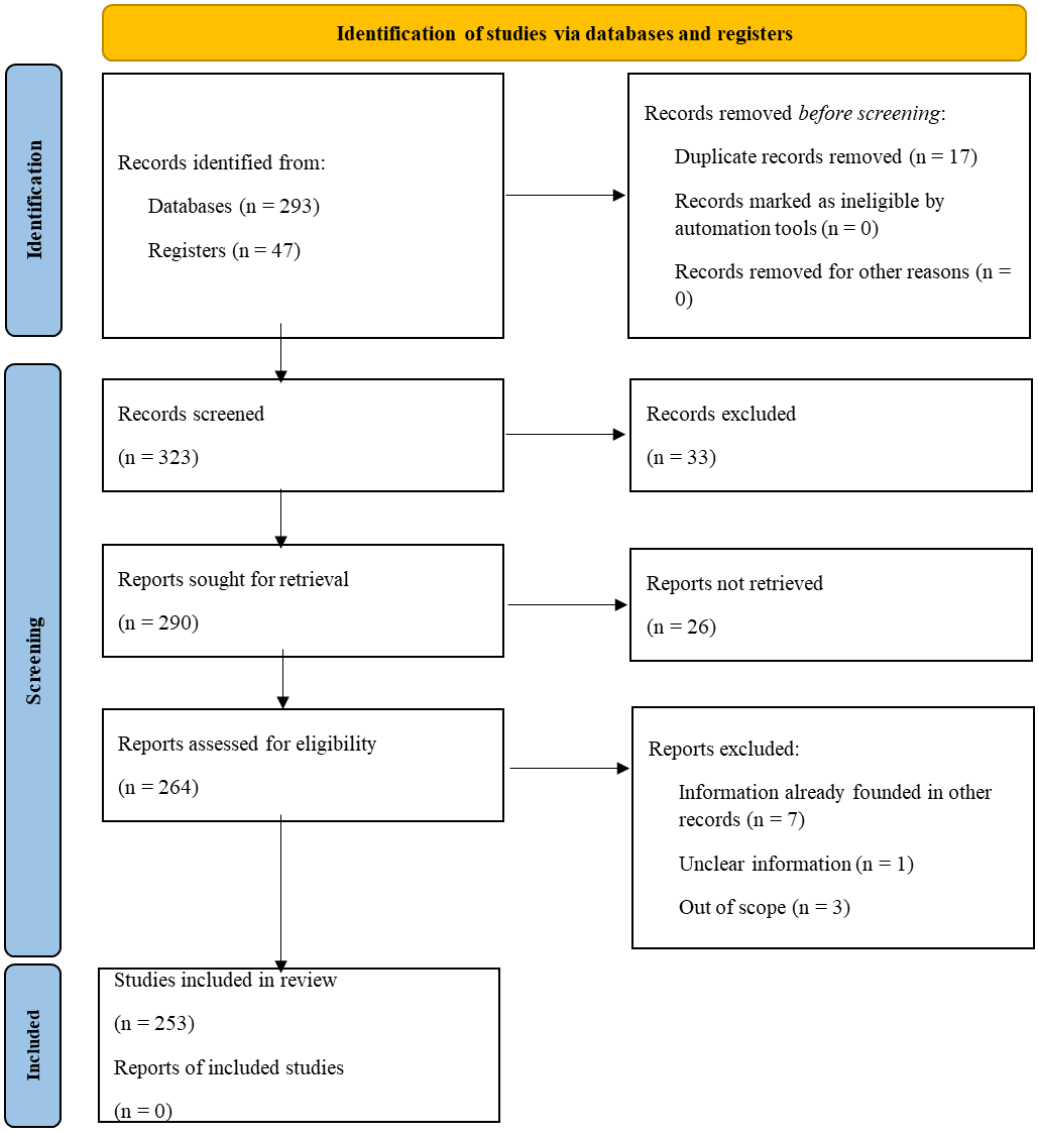

Fig. S1: PRISMA flow diagram showing the selection process of records.

3.2 Capítulo 2: Development and characterization of a temozolomide-loaded nanoemulsion and the effect of ferrocene pre and co-treatments in glioblastoma cell models

Artigo científico publicado na revista *Pharmacological Reports* (fator de impacto 4.4).

Pharmacological Reports
https://doi.org/10.1007/s43440-023-00537-6

ARTICLE

Development and characterization of a temozolomide-loaded nanoemulsion and the effect of ferrocene pre and co-treatments in glioblastoma cell models

Jeferson Gustavo Henn[1,2] · Matheus Bernardes Ferro[1] · Gabriel Antonio Lopes Alves[3] · Flávia Pires Peña[3] · João Vitor Raupp de Oliveira[3] · Bárbara Müller de Souza[4] · Leonardo Fonseca da Silva[4] · Victória Rapack Jacinto Silva[1] · Ana Carolina Silva Pinheiro[1] · Luiza Steffens Reinhardt[1] · Ana Moira Morás[1] · Michael Nugent[2] · Ricardo Gomes da Rosa[4] · Tanira Alessandra Silveira Aguirre[3] · Dinara Jaqueline Moura[1]

Received: 3 August 2023 / Revised: 25 September 2023 / Accepted: 26 September 2023

Abstract

Background Glioblastoma is a severe brain tumor that requires aggressive treatment involving surgery, radiotherapy, and chemotherapy, offering a survival rate of only 15 months. Fortunately, recent nanotechnology progress has enabled novel approaches and, alongside ferrocenes' unique properties of cytotoxicity, sensitization, and interaction with reactive oxygen species, have brought new possibilities to complement chemotherapy in nanocarrier systems, enhancing treatment results.

Methods In this work, we developed and characterized a temozolomide-loaded nanoemulsion and evaluated its cytotoxic potential in combination with ferrocene in the temozolomide-resistant T98G and temozolomide-sensitive U87 cell lines. The effects of the treatments were assessed through acute assays of cell viability, cell death, mitochondrial alterations, and a treatment protocol simulation based on different two-cycle regimens.

Results Temozolomide nanoemulsion showed a z-average diameter of 173.37 ± 0.86 nm and a zeta potential of − 6.53 ± 1.13 mV. Physicochemical characterization revealed that temozolomide is probably associated with nanoemulsion droplets instead of being entrapped within the nanostructure, allowing a rapid drug release. In combination with ferrocene, temozolomide nanoemulsion reduced glioblastoma cell viability in both acute and two-cycle regimen assays. The combined treatment approach also reversed T98G's temozolomide-resistant profile by altering the mitochondrial membrane potential of the cells, thus increasing reactive oxygen species generation, and ultimately inducing cell death.

Conclusions Altogether, our results indicate that using nanoemulsion containing temozolomide and combination with ferrocene is an effective approach to improve glioblastoma therapy outcomes.

Graphical abstract

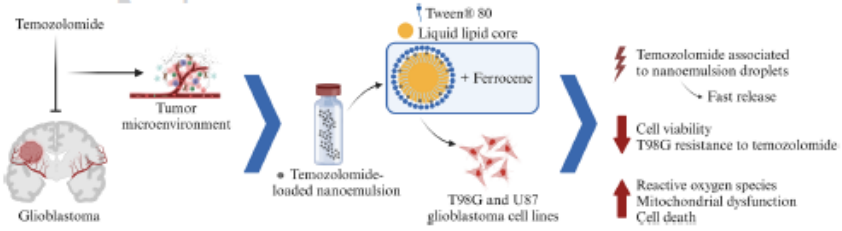

Keywords Glioblastoma · Temozolomide · Ferrocene · Nanoemulsion · Drug delivery system

Extended author information available on the last page of the article

Journal : Large 43440 | Article No : 537 | Pages : 13 | MS Code : 537 | Dispatch : 10-10-2023

Abbreviations

BBB	Blood–brain barrier
DMEM	Dulbecco's Modified Eagle Medium
DDS	Drug delivery system
EE%	Encapsulation efficiency
FBS	Fetal bovine serum
Fc	Ferrocene
FITC	Fluorescein isothiocyanate
GB	Glioblastoma
LOD	Limit of detection
LOQ	Limit of quantification
MCT	Medium chain triglycerides
NE	Nanoemulsion
NRU	Neutral red uptake
PBS	Phosphate-buffered saline
PDI	Polydispersity index
PI	Propidium iodide
ROS	Reactive oxygen species
TEM	Transmission electron microscopy
TMRE	Tetramethylrhodamine ethyl ester
TMZ	Temozolomide

Introduction

Glioma is a common type of brain tumor that comprises four different grades of malignancy, with glioblastoma (GB) being the most common brain tumor in adults, accounting for 15% of all central nervous system tumors and 45% of primary malignant brain tumors. GB has an extremely poor prognosis, with a median overall survival of 15 months and progression-free survival of merely 6 months, therefore generating a negative impact on patients' life quality [1–5].

Its current standard of care consists of maximally safe surgical resection followed by radiation with concurrent and adjuvant chemotherapy with temozolomide (TMZ). However, despite the recent improvements in cancer therapy, GB treatment has proved to be a challenge since most tumors are surgically unresectable due to the brain complexity, and TMZ, although well-tolerated, usually presents both low bioavailability and efficacy [6–8]. Its mechanism of action consists of transferring an electrophilic alkyl group to nucleophilic DNA atoms. However, these lesions can be easily repaired by different DNA repair mechanisms, which are commonly overexpressed in GB patients, consequently contributing to TMZ resistance [9, 10].

As an alternative, a special look has been given to the ferrocenes (Fc), a group of metal–organic compounds with AQ3 electrochemical properties that allow them to interact with biological molecules; therefore, they have already shown antifungal, antimicrobial, anticancer, and HIV-suppressing properties [11, 12]. Cancer cells typically present high levels of reactive oxygen species (ROS), especially hydrogen peroxide (H_2O_2), which may generate hydroxyl radical (OH^-) via the Fenton reaction, where Fe^{2+} plays a key role. Fc can be used as an exogenous source of Fe^{2+}, increasing H_2O_2 catalysis to generate OH^-, which has a short lifetime and consequently damages the tumor cells without reaching adjacent cells [13, 14]. Additionally, modifications on Fc structures, such as their pegylation, may increase their blood circulation time, preventing early opsonization and subsequently increasing their concentration at the tumor site [15].

Additional aspects involved in GB therapy, such as its high infiltrative capacity into normal tissue and the lack of drug effectiveness caused by the blood–brain barrier (BBB) impermeability, have been key barrier to treatment success [16–21]. Therefore, developing drug delivery systems (DDS) to deliver molecules straight to the tumor site at therapeutic concentrations may constitute an important alternative to improve therapeutic outcomes and reduce side effects and systemic toxicity.

Although many of these systems are costly, some options are easier to produce and versatile, allowing the insertion of several molecules into the carrier. For instance, oil-in-water nanoemulsions (NE) comprise heterogeneous systems formed by an oily phase dispersed as droplets in an aqueous phase. These systems have advantages such as kinetic stability and reproducible properties, making them more stable to aggregation and gravitational separation than other macroemulsions [22]. Moreover, NE surface-adsorbed drugs can offer rapid onset of action, enhancing cytotoxic effects, as well as they can be combined with other molecules with low release profile for synergistic purposes [23, 24]. Finally, the encapsulation of unstable drugs may increase their half-time in plasma [25–27], allowing them to infiltrate inaccessible areas, a key event in TMZ's success in treating GB. Therefore, in this study, we present the development, characterization, and in vitro efficacy evaluation of nanocarrier systems containing TMZ. Furthermore, we explore novel combinations of TMZ-loaded nanocarriers (TMZ-NE) with Fc as a potential therapeutic approach for treating GB.

Materials and methods

Materials

Ferrocene (087202.A1) (Fig. S1A) was acquired from Thermo Fisher Scientific (Waltham, USA), and their modified monopegylated (Fig. S1B) and dipegylated (Fig. S1C) versions using triethylene glycol were synthesized by R.G.R.'s Laboratory (unpublished results). T98G and U87 human GB cells were acquired from the American Type Culture Collection (Manassas, USA). Acetic acid (V800018), acetone (270,725), acetonitrile (34,851), caprylic/capric triglyceride, medium chain triglycerides (MCT, W367000),

Journal : Large 43440 | Article No : 537 | Pages : 13 | MS Code : 537 | Dispatch : 10-10-2023

ethanol (09–0851), methanol (34,860), neutral red (N4638), Span®-60 (840,121), Tween®-80 (P1754), and temozolomide (T2577) were purchased from Merck (Darmstadt, Germany). Dulbecco's Modified Eagle Medium (DMEM, 12,100,046), fetal bovine serum (FBS, 16,000,044), L-glutamine (25,030,081), MitoSOX kit (M36008), penicillin/streptomycin (15,140,122), phosphate-buffered saline (PBS, 21,600,010), and trypsin–EDTA (25,200,056) were obtained from Thermo Fisher Scientific (Waltham, USA). Dead Cell Apoptosis Kit with annexin-V FITC and propidium iodide (PI) (V13242) was obtained from Invitrogen (Carlsbad, USA), and the Mitostatus TMRE kit (564,696) was purchased from BD Biosciences (San Diego, USA).

Preparation of NE containing TMZ

TMZ-NE were prepared using the solvent displacement method as shown elsewhere but omitting the presence of the polymer in the organic phase [28], with an aqueous phase composed of 53 mL ultrapure water (Milli-Q®, Merck, Darmstadt, Germany) and 70 µL Tween®-80, and the organic phase being a mixture of 27 mL acetone, 38 mg Span®-60, 160 µL MCT, and TMZ (2 mg). Both phases were stirred and heated to 40 °C. After pouring the organic phase into the aqueous phase through a specific funnel, the formulations formed were left under stirring and heating at 40 °C for 10 min. Finally, they were taken to a rotary evaporator to reduce their volume to 10 mL. After volume reduction, the theoretical concentration of TMZ was 0.2 mg/mL, and this concentration was used as the starting point for all experiments. A blank NE without TMZ was also prepared as described for comparison purposes.

TMZ quantification

TMZ quantification method was developed and performed by HPLC–DAD in a Shimadzu Prominence (Kyoto, Japan) chromatograph equipped with a quaternary, low-pressure mixing pump, and inline vacuum degassing, controlled by a CBM-20A interface module, an automatic injector (SIL-20A) and diode array detector (SPD-M20A). The separation was carried out by an isocratic system, using a reverse-phase Phenomenex Luna 3 µm C18(2) 100 (Å) (250 × 4.0 mm) column, kept at 35 °C. TMZ was identified by comparing the retention times of samples with its authentic standard. The mobile phase consisted of 0.5% (v/v) acetic acid in ultrapure water (solvent A) and acetonitrile (solvent B) (1:1), the injection volume was 20 µL, the flow rate was 0.7 mL/min, and the samples were monitored at 330 nm.

The HPLC–DAD methodology was validated for specificity, linearity, intraday and interday precisions, and accuracy. Briefly, 2 mg TMZ were weighed in triplicate and dissolved in 80 mL acetonitrile:ultrapure water (v/v, 1:1, 25 µg/mL), each generating a calibration curve with the concentrations of 0.5, 1, 2.5, 5, 7.5 and 10 µg/mL. Three other calibration curves were prepared at the same concentrations using phosphate buffer at pH 6.8 as diluent. After the intraday and interday precisions assay, six 5 µg TMZ/mL samples were prepared and were analyzed twice, at the time of dilution and 24 h later. Finally, in the accuracy assay, each 25 µg/mL solution was diluted in triplicate to generate solutions of 1, 5, and 10 µg/mL, followed by the addition of corresponding amounts of blank NE to simulate the formulation matrix. All solutions were sonicated and filtered before assays. Limit of detection (LOD) and limit of quantification (LOQ) were calculated using the following formulas:

$$LOD = \frac{3.3x\sigma}{IC} \; and \; LOQ = \frac{10x\sigma}{IC},$$

where IC is the calibration curve inclination, and σ is the standard deviation obtained from the standard deviation of the intercept with the Y axis of at least three calibration curves containing analyte concentrations close to the supposed LOD.

The quantification of TMZ was performed and expressed in concentration (m/v), interpolating the area of the analyte in the sample with a linear equation obtained for each correspondent media.

TMZ-NE characterization

Physicochemical characterization

Volume-weighted mean diameters ($D_{4,3}$) and polydispersity (Span) were evaluated by dynamic light scattering laser diffraction (Mastersizer® 2000, Malvern Panalytical, UK). Briefly, the samples were mixed with ultrapure water in the dispersion unit of the equipment to achieve the minimal obscuration index of 2%. Span values, which denote the polydispersity of the system, were calculated as follows:

$$Span = \frac{d(0.9) - d(0.1)}{d(0.5)},$$

where d(0.9), d(0.1), and d(0.5) are the diameters at 90%, 10%, and 50% of the cumulative distribution of the diameter curve, respectively.

Nanodroplet morphology was analyzed by transmission electron microscopy (TEM) operating at 100 kV (JEOL 1400 Exll, Akishima, Japan). The aqueous formulations were diluted in ultrapure water (1/10, v/v), deposited on a 400-mesh Formvar carbon film-coated copper grid, and negatively stained with 2% (w/v) uranyl acetate aqueous solution.

The polydispersity index (PDI) and particle size (z-average hydrodynamic diameter) were evaluated by photon

Journal : Large 43440 | Article No : 537 | Pages : 13 | MS Code : 537 | Dispatch : 18-10-2023

correlation spectroscopy (Zetasizer Nanoseries, Malvern Panalytical, UK). An aliquot of each formulation was diluted in ultrapure water (500x). Zeta potential was determined based on electrophoretic mobility after formulations were diluted 500× in a 10 mM NaCl aqueous solution.

Formulation drug content was determined by diluting 250 µL of the samples in 10 mL of acetonitrile:ultrapure water (v/v, 1:1), followed by 15 min sonication. Samples were filtered in a 0.45-µm membrane, and their contents were analyzed by the validated HPLC–DAD method.

Drug concentration in the ultrafiltrate (non-encapsulated drug) was separated by ultrafiltration/centrifugation (Microcon®; MC Millipore 10 kDa, 10,000 rpm for 5 min) from each formulation, and analyzed by HPLC–DAD method. Encapsulation efficiency (EE%) was assessed by the difference between the total drug content and the drug concentration in the ultrafiltrate divided by the drug content and multiplied by 100.

Drug release studies

In vitro release profiles of TMZ-NE and the drug dissolved in ultrapure water (control) were studied under sink conditions using cellulose dialysis bags (25 × 16 mm, cut-off of 12–14 kDa, Merck, Darmstadt, Germany). Samples (2 mL containing 200 µg/mL TMZ) were transferred to the dialysis bags and placed in closed glass flasks containing 50 mL of the release medium (phosphate buffer at pH 6.8) and kept under magnetic stirring at 37 ± 0.5 °C. Aliquots of 1 mL were collected at predetermined time intervals (0.08, 0.17, 0.25, 0.33, 0.42, 0.5, 0.75, 1, 1.25, and 1.5 h) and replaced with an equal volume of fresh medium. The samples were analyzed by HPLC–DAD.

Cell viability evaluation

T98G and U87 cells were maintained in DMEM supplemented with FBS (10%) and L-glutamine at 37 °C in a humidified 5% CO_2 incubator. Neutral red uptake (NRU) assay was performed in T98G and U87 cells using only the three synthesized Fc, TMZ, TMZ-NE, or co-treatments of Fc and TMZ-NE. Cells were seeded in a 96-well tissue culture microplate at 1.3×10^5 cells/mL in complete media and grown for 24 h before treatment. Cells were treated with Fc, TMZ, TMZ-NE or a combination of Fc and TMZ-NE in concentrations ranging from 0.5 to 100 µM, as well as with blank NE or vehicle (negative control; DMEM supplemented with FBS 5%). The assay was carried out according to Borenfreund & Puerner (1985) [29], with some modifications. In brief, after being treated, cells were washed with 250 µL of PBS before the addition of 250 µL neutral red dye (25 µg/mL) dissolved in serum-free media and incubated for 3 h at 37 °C in a humidified 5% CO_2 incubator. Cells were washed with PBS, and 125 µL of a desorb solution (ethanol:acetic acid:water, 50:1:49) was added, followed by gentle shaking for 30 min for complete dissolution. Absorbance was measured at 540 nm using a microtiter plate reader. Cell viability was calculated as a percentage of the negative control, and according to these results, one of the cell lines was selected for the following assays.

Cell death evaluation

After 24-h treatments with Fc, TMZ, TMZ-NE, or a combination of Fc and TMZ-NE in concentrations ranging from 0.5 to 100 µM, T98G-cell pellets were incubated with 100 µL of binding buffer 1× added by 3 µL Annexin-V FITC and 1 µL of PI (100 µg/mL) at room temperature for 15 min. After this period, 400 µL of binding buffer was added. Data collection and analysis were performed by using a FACS Calibur flow cytometer (Becton Dickinson, San Diego, USA) combined with CellQuest software. 10,000 events per sample were collected at least, and the percentage of dead cells was determined and compared to the negative control. Blank NE-treated cells were also used for matrix effect evaluation purposes.

Cell oxidative stress evaluation

Mitochondrial membrane potential changes were evaluated by MitoStatus TMRE assay, following manufacturer recommendations. Briefly, MitoStatus is a cationic and lipophilic fluorescent dye that is promptly sequestered by active mitochondria. When the membrane is hyperpolarized, the fluorescence shows higher levels, while when the mitochondrial membrane depolarizes, the fluorescence diminishes its levels. After 24-h treatments with Fc, TMZ, TMZ-NE, or a combination of Fc and TMZ-NE in concentrations ranging from 0.5 to 100 µM, an aliquot of T98G-suspension cell was incubated with MitoStatus TMRE (50 nM) for 30 min at 37 °C, protected from light, followed by centrifugation and resuspension in PBS. The samples were afterwards analyzed in a FACS Calibur flow cytometer, in the order of 10,000 events per sample, and the percentage of mitochondrial depolarization and hyperpolarization were determined and compared to the negative control. Blank NE-treated cells were also used for matrix effect evaluation purposes.

To assess mitochondrial oxidative stress levels, cells were incubated after the same previous treatments with 5 µM MitoSOX, which is a superoxide-reacting dye, at 37 °C for 10 min. The samples were then analyzed in a FACS Calibur flow cytometer. At least 10,000 events were collected per sample, and the results are presented as the mean percentage normalized to the negative control.

Journal : Large 43440 | Article No : 537 | Pages : 13 | MS Code : 537 | Dispatch : 18-10-2023

Treatment protocol simulation based on two-cycle regimens

To better evaluate the formulation when in contact with T98G cells, a treatment protocol simulation based on different two-cycle regimens has been established. Cells were seeded in a 96-well tissue culture microtiter plate at 1.3×10^4 cells/mL) in complete media and grown for 24 h before different treatment schemes, according to Han et al. (2014) [30] and Wick et al. (2009) [31], with some modifications. Briefly, cells were treated for two cycles with Fc or TMZ on their own and their combination, TMZ-NE on its own and in combination with Fc, or Fc in a 2-day pretreatment followed by TMZ or TMZ-NE treatments. Each cycle was carried out for 5, 7, or 9 days (according to the combinations), and cells were kept under a 2-day recovery period (in complete media) between the cycles and before cell viability evaluation by NRU assay (Fig. S2).

Statistical analysis

NE characterization and quantification were analyzed in triplicate of batches and expressed as mean ± SD. All in vitro assays were independently repeated at least three times, and results are expressed as mean ± SEM (Figs. 4, 5, and 6) or SD (Fig. 7). Statistical significance was determined by unpaired *t* test (zeta potential, Span, droplets size, hydrodynamic diameter, and PDI), two-way ANOVA followed by Sidak's (Fig. 3), Tukey's (Figs. 5, 6A, C, and 7 – when compared between groups), or Bonferroni's (Fig. 7 – when compared to the negative control) multiple comparison tests, and one-way ANOVA followed by Tukey's (Figs. 4 and 6B) multiple comparison test. Data were checked for normal distribution whenever possible, and a p value < 0.05 was considered statistically significant.

Results

TMZ-NE physicochemical characterization

In our experiments, laser diffraction analysis revealed mean droplet sizes of 163 ± 7 and 195 ± 20 nm for blank and TMZ-NE formulations, respectively ($t = 2.69$, no statistical difference) (Fig. 1A), and the hydrodynamic mean diameters (z-average diameter, calculated using the method of cumulants) for blank and TMZ-NE were 165.07 ± 2.79 and 173.37 ± 0.86 nm, respectively ($t = 4.917$, $p = 0.0079$) (Fig. 1B).

TEM analysis showed spherical droplets in our TMZ-NE, with the surfactant covering its entire surface (Fig. 2). Span values for blank and TMZ-NE were 1.42 ± 0.05 and 1.66 ± 0.14, respectively ($t = 2.756$, no statistical difference). PDI measured the formulation's heterogeneity, and the results corroborated with the laser diffraction technique, showing values of 0.09 ± 0.01 and 0.10 ± 0.02 for blank and TMZ-NE, respectively ($t = 1.158$, no statistical difference).

Zeta potential values of our formulations were found to be – 6.53 ± 1.13 and – 7.28 ± 0.84 mV for blank and TMZ-NE, respectively ($t = 0.929$, no statistical difference), leading to the possibility of incipient stability considering electrostatic stabilization. Even though TMZ loading in NE was close to the expected value of 0.2 mg/mL (92.62% ± 5.93 or 0.19 mg/mL ± 0.01), the quantification of the ultrafiltrate for EE%

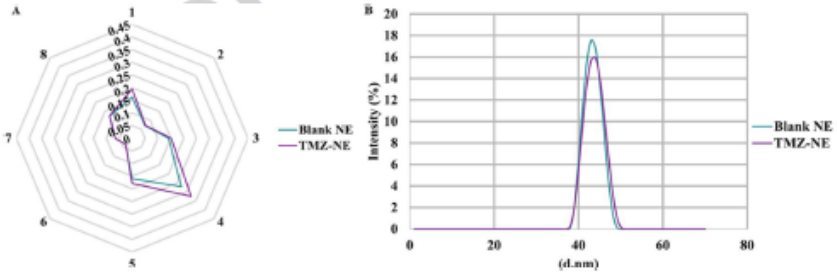

Fig. 1 Blank NE and TMZ-NE characterization. Data were statistically analyzed by unpaired *t* test. **A** Laser diffraction radar chart plot for blank and TMZ-NE (in μm). [Axes: 1 – volume-weighted mean diameter by volume of particles, d[4,3]v; 2 – diameter by volume at percentile 10 under the distribution curve, d(0.1)v; 3 – diameter by volume at percentile 50 under the distribution curve, d(0.5)v; 4 – diameter by volume at percentile 90 under the distribution curve, d(0.9)v; 5 – volume-weighted mean diameter by number of particles, d[4,3]n; 6 – diameter by number at percentile 10 under the distribution curve, d(0.1)n; 7 – diameter by number at percentile 50 under the distribution curve, d(0.5)n; 8 – diameter by number at percentile 90 under the distribution curve, d(0.9)n]. **B** Dynamic light scattering for blank and TMZ-NE (in diameter values in nanometers, d.nm). Experiments were performed in triplicate ($p = 0.0079$). *NE* nanoemulsion. *TMZ* temozolomide

Journal : Large 43440 | Article No : 537 | Pages : 13 | MS Code : 537 | Dispatch : 18-10-2023

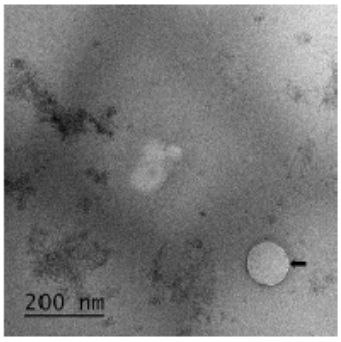

Fig. 2 Morphological characterization of developed nanoemulsion: TEM image of TMZ-NE at 60.000× (at the arrow), scale bar 200 nm. *TEM* transmission electron microscopy, *TMZ* temozolomide, *NE* nanoemulsion

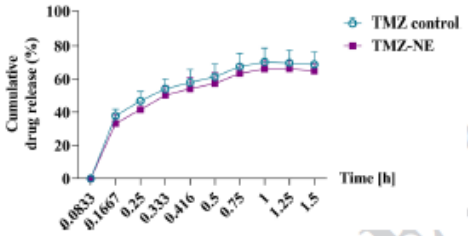

Fig. 3 Drug release profiles for TMZ control and TMZ-NE. The study was carried out under sink conditions using 25×16 mm cellulose dialysis bags (cut-off of 12–14 kDa). Samples (2 mL containing 8 µg/mL TMZ-NE or 200 µg/mL TMZ control) were transferred to the dialysis bags and placed in closed glass flasks containing 50 mL of the release medium (phosphate buffer at pH 6.8) and maintained under magnetic stirring at 37.0 ± 0.5 °C. Results are shown as mean ± SD, followed by two-way ANOVA and Sidak's multiple comparisons test. Experiments were performed in triplicate. *TMZ* temozolomide, *NE* nanoemulsion

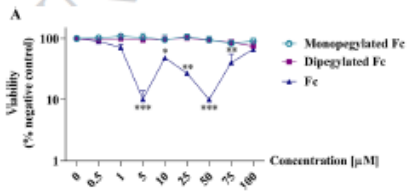

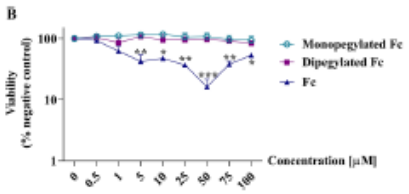

Fig. 4 Fc reduces GB cell viability. In vitro cell viability evaluation. **A** U87 cells. **B** T98 cells. Both cells were treated for 24 h with 0.5 to 100 µM of monopegylated Fc, dipegylated Fc or Fc, followed by the NRU assay. Results are shown as the mean ± SEM of three biological replicates. Statistical analysis was carried out using one-way ANOVA and Tukey's multiple comparisons test. A p value < 0.05 was considered statistically significant. *$p = 0.0332$, **$p = 0.0021$ and ***$p = 0.0002$ when compared to the negative control. *Fc* ferrocene, *GB* glioblastoma, *NRU* neutral red uptake

calculation showed a mean result close to the initial amount of drug used, suggesting that the drug is not entrapped in the droplet.

TMZ-NE drug release profile

It is well known that the GB site presents a pH beyond physiological values, typically around 6.8 [32], mainly because these cells usually release high amounts of lactate and H^+ as part of their metabolic route change from oxidative phosphorylation to glycolysis, and this feature is highly associated with tumor progression and resistance behaviors [33]. Taking this into account, we investigated TMZ release from our formulations using a phosphate buffer solution simulating this tumor site environment. Our results showed that TMZ-NE has a similar release profile when compared to its control ($F_{9,39} = 0.078$, no statistical difference), with a fast release within the first hour, reaching its maximum values between 1 and 1.25 h (70,32 ± 8.40 and 69.72 ± 7.71% for TMZ control, and 66.16 ± 5.47 and 66.24 ± 4.84% for TMZ-NE, respectively), then decreasing to initial values in 24 h (Fig. 3).

TMZ quantification

HPLC–DAD quantification method was validated for specificity, linearity, intraday and interday precision, and accuracy, following ICH Harmonised Tripartite Guideline (2005) [34] and Resolution 166/2017 (Brasil, 2017) [35]. LOD and LOQ were calculated as per Resolution 166/2017 (Brasil, 2017) [35].

Linearity was evaluated on a calibration curve obtained from TMZ standard solutions ranging from 0.5 to 10 µg/mL. A linear model was adjusted according to the peak area and concentration by applying the linear regression technique with 95% confidence, and the model was found to be appropriate to establish a relationship between area and concentration in all concentrations tested ($r^2 = 0{,}9994$). The

Journal : Large 43440 | Article No : 537 | Pages : 13 | MS Code : 537 | Dispatch : 10-10-2023

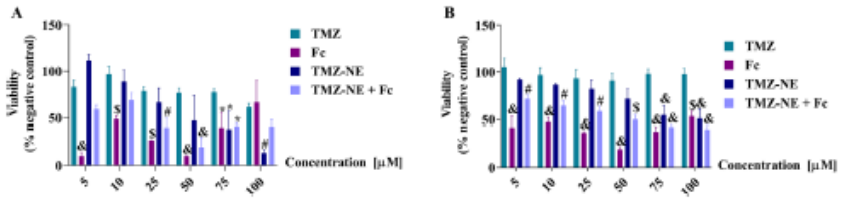

Fig. 5 The combined treatment of TMZ-NE and Fc is effective in reducing GB cell viability. In vitro cell viability evaluation. **A** U87 cells. **B** T98G cells. Both cells were treated for 24 h with 5 to 100 µM of TMZ, Fc, TMZ-NE, and TMZ-NE + Fc (same concentration for both), followed by the NRU assay. Results are shown as the mean ± SEM of three biological replicates. Statistical analysis was carried out using two-way ANOVA and Tukey's multiple comparisons test. A p value < 0.05 ($F_{18,47} = 5.896$ for **A**; $F_{18,49} = 4.232$ for **B**) was considered statistically significant. $^{*}p = 0.0332$, $^{\#}p = 0.0021$, $^{\$}p = 0.0002$ and $^{\&}p = 0.0001$, when compared to TMZ treatment. Blank NE did not reduce cell viability (data not shown). *TMZ* temozolomide, *NE* nanoemulsion, *Fc* ferrocene, *NRU* neutral red uptake

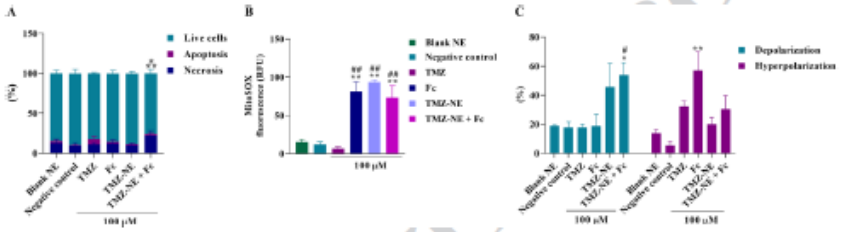

Fig. 6 Fc and TMZ-NE treatments alter mitochondrial polarization status, leading to high ROS generation and cell death via necrosis **A** cell death profile in T98G cells under annexin-V FITC and PI labeling. **B** superoxide anion generation in T98G cells under MitoSOX labeling. **C** mitochondrial membrane depolarization in T98G cells under Mitostatus labeling. In **A**, results are shown as the mean ± SEM of three biological replicates. Statistical analysis was carried out using two-way ANOVA and Tukey's multiple comparisons test. A p value < 0.05 was considered statistically significant. $^{*}p = 0.0032$ for TMZ-NE + Fc necrosis when compared to TMZ, Fc and TMZ-NE, and $^{**}p = 0.0021$ for TMZ-NE + Fc necrosis when compared to the negative control. For **B** and **C**, results are shown as the mean ± SEM of three biological replicates. Cells were treated with 100 µM of both compounds for 24 h. Statistical analysis was carried out using one-way (**B**) and two-way (**A**, **C**) ANOVA, respectively, and Tukey's multiple comparisons test. p value < 0.05 ($F_{8,29} = 3.878$ for (**A**); $F_{4,8} = 1.001$ for (**B**); $F_{4,18} = 4.841$ for (C)) was considered statistically significant. $^{*}p = 0.0332$ and $^{**}p = 0.0021$ when compared to the negative control; $^{\#}p = 0.0332$, and $^{\#\#}p = 0.0021$ when compared to TMZ. *Fc* ferrocene, *TMZ* temozolomide, *NE* nanoemulsion, *ROS* reactive oxygen species, *PI* propidium iodide

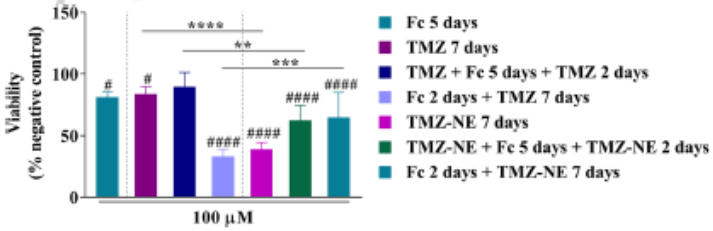

Fig. 7 Fc acts as a sensitizer for further treatment with TMZ. In vitro clinical protocol simulations. T98G cells were treated for different days with different combinations of Fc, TMZ, and TMZ-NE in 2 cycles separated by a 2-day recovery period under fully supplemented culture media. After the second recovery period, the NRU assay was performed. Results are shown as the mean ± SD of three biological replicates. Cells were treated with 100 µM of both compounds. Statistical analysis was carried out using two-way ANOVA and Bonferroni's multiple comparisons test when compared to the negative control ($^{\#}$) and Tukey's multiple comparisons test when compared between groups (*). A p value < 0.05 ($F_{6,25} = 15.40$) was considered statistically significant. $^{\#}p = 0.0032$, $^{\#\#\#\#}p = 0.0001$, $^{**}p = 0.0021$, $^{***}p = 0.0002$, and $^{****}p = 0.0001$. *Fc* ferrocene, *TMZ* temozolomide, *NE* nanoemulsion, *NRU* neutral red uptake

Journal : Large 43440 | Article No : 537 | Pages : 13 | MS Code : 537 | Dispatch : 10-10-2023

precision of the method was performed at two levels using a 5 µg/mL TMZ solution: firstly, intraday repeatability was carried out to evaluate the concordance between results on day 0 with the same analyst and instrumentation. Secondly, inter-day repeatability analyzed the correlation between results obtained after 24 h of the first analysis. Mean values showed appropriate repeatability, with a low relative standard deviation value (4.77%). Accuracy was carried out by using three TMZ solutions of 1, 5, and 10 µg/mL, with the addition of corresponding amounts of blank NE for matrix simulation purposes. The LOD and LOQ concentrations were 0.09 and 0.29 µg/mL, respectively. Recovery values (measured concentration/nominal concentration × 100) were 107%, 108.8%, and 102.4%, respectively. It is important to mention that this method is specific for TMZ as no other substance in formulations absorbs at the same retention time at the same wavelength.

Cell viability screening for Fc, monopegylated Fc, and dipegylated Fc

The effects of the Fc products or Fc on cell viability were evaluated using U87 (Fig. 4A) and T98G (Fig. 4B) cell lines. The results revealed that a 24-h treatment with monopegylated Fc and dipegylated Fc concentrations ranging from 0.5 to 100 µM did not induce significant cytotoxicity in both cell lines. On the other hand, Fc significantly reduced cell viability ($F_{8,14} = 10.36$, $p < 0.05$) (Fig. 4A, B).

Cell viability assays

To evaluate the influence of Fc and the formulation on decreasing GB cell viability, different combinations of treatments were performed using two GB cell lines: T98G, which has a resistant profile to TMZ, and U87, which is sensitive to TMZ (Lee, 2016). Cells were tested for 24 h with TMZ, Fc, TMZ-NE, and TMZ-NE + Fc in concentrations ranging from 5 to 100 µM, followed by the NRU assay (Fig. 5).

When compared to the negative control, the U87 cell line revealed a slight decrease in cell viability at the highest TMZ concentration, with better results when the drug was adsorbed on the NE, and significant results in all treatments with Fc and TMZ-NE + Fc. T98G also exhibited a decrease in cell viability in all treatments with Fc and TMZ-NE + Fc, as well as at the highest concentrations of TMZ-NE.

We also compared the treatment schemes with a standard TMZ treatment. In the U87 cell line, Fc on its own showed the highest decrease in cell viability, with better results at the lowest treatment concentrations. TMZ-NE had significant results only at the highest concentrations, and the combination TMZ-NE + Fc significantly reduced cell viability at the concentrations of 25, 50, and 75 µM (Fig. 5A). Surprisingly, in the T98G cell line, the combination of TMZ-NE and Fc significantly reduced cell viability in a concentration-dependent manner, reaching about 40% at 100 µM (Fig. 5B).

Cell death and mitochondrial status assays

As our previous results showed a decrease in T98G cell viability under our proposed treatments, we decided to investigate the possible mechanisms behind these findings. Thus, we performed three assays to evaluate how cells respond to our treatments regarding their death mechanisms and mitochondrial functioning status. T98G cells were tested for 24 h with 100 µM of TMZ, Fc, TMZ-NE, and TMZ-NE + Fc, followed by incubation with annexin-V FITC + PI for cell death studies, MitoSOX for mitochondrial superoxide anion generation purposes, and Mitosatus TMRE for mitochondrial membrane potential studies. Cells treated with TMZ-NE + Fc showed significantly higher necrotic levels when compared to the negative control, TMZ, and TMZ-NE (Fig. 6A).

Although no remarkable levels of cell death were observed for the other treatments, mitochondrial status assays exhibited interesting outcomes. Apart from the TMZ group, all other treatments revealed high values of superoxide anion generation when compared to the negative control and TMZ (Fig. 6B). The mitochondrial membrane potential significantly changed to a depolarized status when cells were treated with TMZ-NE + Fc, in comparison to the negative control and TMZ groups. On the other hand, Fc treatments statistically hyperpolarized mitochondrial membranes when compared to the negative control group (Fig. 6C).

Fc pre and co-treatments with TMZ-NE under a protocol simulation based on two-cycle regimens

To better understand the performance of T98G cells under our treatments and to get closer to clinical reality, we proposed the establishment of a clinical protocol simulation based on preceding studies [30, 31], with some modifications regarding experimental procedures, cell line behavior, and the use of a molecule not yet described for this purpose (Fig. S2). Cells were treated for two cycles of five, seven, or nine days, depending on the molecules' combination, and between each cycle, cells were kept in fully supplemented culture media to simulate a recovery period. In the end, the NRU assay was performed to evaluate cell viability.

Comparisons in-between treatments performed for the same number of days showed a significant reduction in cell viability in groups TMZ-NE 7 days, TMZ-NE + Fc 5 days + TMZ-NE 2 days, and Fc 2 days + TMZ-NE 7 days. When compared to the negative control, all treatments except TMZ + Fc 5 days + TMZ 2 days significantly decreased cell viability, especially in those where TMZ-NE treatments

Journal : Large 43440 | Article No : 537 | Pages : 13 | MS Code : 537 | Dispatch : 18-10-2023

were involved. Moreover, the Fc 2 days+TMZ 7 days group showed the highest cell viability reduction (Fig. 7), and this finding is very interesting since it involved a pretreatment with Fc for 2 days before a 7-day treatment with TMZ.

Discussion

In this study, we developed, characterized, and investigated the in vitro efficacy of a TMZ-NE in different combinations with Fc for treating GB. Firstly, formulation analysis must be carried out after each new batch of production to ensure a satisfactory DDS. Particle size analysis of both blank and TMZ-NE by laser diffraction demonstrated that they have a monomodal and narrow size distribution. The Span values corroborated these results since, generally, the smaller the value, the narrower the distribution of particles/droplets, with values near 1 being adequate for pharmaceutical applications [36]. Also, TEM analysis confirmed the spheric shape and that the surfactant well covers the NE. Additionally, PDI measured the formulations' heterogeneity, and the results corroborated with the laser diffraction technique, showing that all NE presented narrow particle sizes and unimodal distributions, as their PDI values were < 0.2 [37]. Overall, our results indicated that we obtained a uniform TMZ-NE formulation with a suitable mean droplet size.

To some extent, zeta potential also provides an idea about whether charged molecules are adsorbed onto the nanostructure surface rather than encapsulated, with values narrowing to zero related to surface adsorption [38, 39]. Moreover, the particle surface charge is a determining factor for biological interactions between different compounds and environments, and system stability is generally optimized the more negative or positive the zeta potential value is [40, 41]. As the surfactant surrounds NE droplets adsorbed at the surface, the relatively low zeta potential values may also be related to the amount of Tween®-80—a non-ionic surfactant, used in TMZ-NE. On the other hand, steric repulsion caused by the hydrophilic head groups of Tween®-80 molecules acts by stabilizing droplets, allowing TMZ to also be located on this interface [42, 43]. This prospect corroborates the absence of encapsulation of our TMZ-NE observed by ultrafiltration/centrifugation analysis. Furthermore, the TMZ in *vitro* release profile showed no statistical difference from the control, likely due to a lack of encapsulation. The change in zeta potential for TMZ-NE compared to blank NE may reinforce the idea that the drug could be adsorbed onto the droplet surface. The nature of the colloidal system of TMZ-NE reduces the probability of the drug being dispersed into the continuous phase. Altogether, our data suggest that the formulation is suitable for pharmaceutical purposes and that TMZ is associated with the droplet's surface due to interfacial phenomena, leading to a fast release due to the lack of encapsulation.

TMZ is a well-known hydrophilic molecule extensively used for GB treatment. However, this characteristic acts as a restriction factor for clinical application due to its fast clearance and unfavorable distribution across different tissues, therefore requiring a multiple-dose regimen, which increases the risk of side effects [44, 45]. Besides, its low molecular weight and log *P* value of – 1.1 turn it into a compound with weak interactions with numerous conventional nanocarriers [46]. Therefore, the system organization obtained here is not surprising due to the hydrophilicity of TMZ and the hydrophobicity of the NE core. Overall, NE are formulations that are easy to prepare, reproducible, and possible to scale up to an industrial batch, and therefore were chosen for this study as a carrier for TMZ.

Some studies have already shown the role of molecules adsorbed on the surface of nanoparticles in cancer cell models. Maiti et al. (2016) [47] developed $ZnFe_2O_4$ nanoparticles for daunorubicin delivery, and their results revealed that the adsorbed molecule was able to induce significant death in HeLa carcinoma cells. According to Chenthamara et al. (2019) [48], this surface interaction is mainly possible because of peculiar electrostatic interactions between the drug and the surface composition. Similar outcomes were found by Singh et al. (2012) [49], where a surface-adsorbed NE of olmesartan medoxomil successfully delivered the drug in a capsular dosage form. Regarding TMZ, a previous study using the drug and its (*N*)3-propargyl analog, both partially encapsulated and partially adsorbed on the nanoliposomes surface, revealed that the non-encapsulated portion played an important role in the rapid onset of action of the molecules, enhancing cytotoxic effects against tumor cells [23].

GB treatment remains a challenge, mainly because of biological barriers such as the BBB and its tight cell junctions and complex angiogenesis [50, 51]. Several drugs have been tested against this cancer; however, most of them failed to achieve reasonable concentrations at the tumor site, leaving TMZ as one of the few standard therapeutic approaches [7]. Notwithstanding, methylations caused by TMZ are easily repaired by different DNA repair pathways, which are commonly upregulated in patients, allowing the tumor to survive and progress to an untreatable stage [52].

Taking this into account, the discovery of new molecules that can add some effect to TMZ treatment is a promising path to improve therapy outcomes and patients' life quality. For this purpose, three different Fc compounds were screened in this study: Fc on its own, and its monopegylated and dipegylated synthesized versions. The 24-h treatments followed by cell viability assays revealed that only Fc on its reduced cell viability in both U87 and T98G cell lines. It is important to mention that iron is stored in the body both as

Journal : Large 43440 | Article No : 537 | Pages : 13 | MS Code : 537 | Dispatch : 10-10-2023

ferritin and hemosiderin. This prevents it from being found in its free form, which in contact with oxygen could promote abnormal synthesis of toxic ROS, which can damage macromolecules [53]. On the other hand, tumor cells normally have high levels of ROS due to the hypermetabolism necessary for its growth and proliferation [54]. Within cells, Fe^{2+} and Fe^{3+} tend to be found in constant equilibrium; however, this balance can be exogenously influenced by Fc through a fast and reversible electronic transfer, generating more ROS [54, 55]. This behavior can be used as an enhancer for cancer treatments, and therefore Fc on its own was selected for further experiments.

Next, we performed 24-h treatments with different combinations and concentrations of TMZ, Fc, and/or TMZ-NE. NRU assays revealed that TMZ-NE + Fc decreased cell viability in both GB cell lines. T98G cell line, which so far has a TMZ-resistant profile, exhibited a significant dose-dependent decrease in cell viability when treated with TMZ-NE, especially when combined with Fc at its highest concentration. This could be interpreted as a possible reversion of this profile, which led us to choose the T98G cell line and the concentration of 100 µM for both compounds for further mechanistic investigation.

To better explore T98G internal behavior under 24-h treatment schemes, we analyzed the cell death profile via annexin-V FITC + PI labeling, and the results indicated that the combination of TMZ-NE + Fc significantly increased cell necrotic levels. Furthermore, we used MitoSOX and Mitostatus assays to respectively measure the amount of mitochondrial superoxide anion generated and eventual changes in mitochondrial polarization status. All treatments showed increased levels of ROS generation, whereas treatments with Fc and TMZ-NE + Fc also changed mitochondrial polarization status. Mitochondria are one of the major sources of ROS, and despite the large ROS generation outside the mitochondrial environment, the correct use of the MitoSOX protocol allows the selective detection of superoxide anions inside the organelle [56]. Also, mitochondrial membrane potential maintenance is essential for cell metabolism, ROS production, intracellular ion homeostasis, and cell death mechanisms regulation [57]. Our findings are in accordance with the cell viability ones, especially for the Fc and TMZ-NE + Fc groups, as the observed cytotoxicity may be related to increased cell death, ROS generation, and membrane destabilization. Likewise, MitoSOX and Mitostatus outcomes reinforce previous studies regarding the influence of Fc on ROS generation [13, 14], again highlighting its use as a chemotherapy adjuvant.

Although the TMZ-NE group has also shown high levels of ROS generation, this result did not reflect on either apoptotic or necrotic levels. This may be related to T98G's intrinsic resistance mechanism to TMZ [58], and because part of the superoxide anions detected could have been generated from a source outside the mitochondrial environment [56], which justifies the low changes in mitochondrial polarization status. Altogether, our results revealed that the apparent reversal of the T98G's resistance profile to TMZ occurs as a result of changes in mitochondrial polarization status, leading to high ROS generation and cell death via necrosis.

Finally, to better understand the performance of T98G cells under our treatments and to get closer to clinical reality, we proposed the establishment of a clinical protocol simulation (Fig. S2). Overall, pre-treatments with Fc followed by treatments with TMZ-NE showed a significant reduction in cell viability, and these results are in accordance with previous works describing Fc as a tumor cell sensitizer, particularly by increasing ROS generation and inhibiting pathways related to tumorigenesis progression in breast cancer cell lines pretreated with Fc before radiation and chemotherapy [59, 60]. Similarly, studies with ferroquine, a Fc analogue, showed increased metabolic stress in prostate cancer cell models via mitochondrial function impairment [61], while ferrocene-cinchona hybrids presented selective activity towards multidrug-resistant cancer cells, as well as the potential to overcome paclitaxel resistance in non-small cell lung, colorectal, and GB models [62]. To the best of our knowledge, our results are the first to describe a similar effect on a GB TMZ-resistant cell line, offering new perspectives for the design of antitumor drugs for GB treatment.

Conclusions

Our study successfully developed and characterized nanocarriers (NE) containing temozolomide (TMZ), resulting in rapid drug release and remarkable outcomes. Combining these nanocarriers with ferrocenes (Fc), both individually and as a pretreatment, significantly reduced the viability of glioblastoma (GB) cell lines in acute and clinical protocol simulations. Notably, our research is the first to investigate the correlation between TMZ organization at the NE interface and its enhanced effectiveness, both in isolation and when combined with Fc. Furthermore, our findings revealed that these improvements in efficacy were attributed to alterations in mitochondrial membrane potential, leading to increased generation of reactive oxygen species (ROS) and subsequent cell death. The introduction of Fc in our experiments played a crucial role as an exogenous source of Fe^{2+}, thereby promoting enhanced ROS catalysis and the generation of more toxic byproducts, effectively damaging the tumor site. The developed NE formulation and its combination with Fc hold promising potential as pioneering therapeutic approaches for GB. However, it is imperative to conduct further studies to extend the drug release profile and evaluate their application in in vivo models. These AQ4

Journal : Large 43440 | Article No : 537 | Pages : 13 | MS Code : 537 | Dispatch : 10-10-2023

investigations will provide valuable insights for advancing these strategies toward clinical implementation.

Supplementary Information The online version contains supplementary material available at https://doi.org/10.1007/s43440-023-00537-6.

Acknowledgements This study was supported in parts by grants and/or scholarships from FAPERGS (Fundação de Apoio à Pesquisa do Rio Grande do Sul, Brazil, Grant nº 21/2551-0001965-4), CAPES (Coordenação de Aperfeiçoamento de Pessoal de Nível Superior, Brazil) and CNPq (Conselho Nacional de Desenvolvimento Científico e Tecnológico, Brazil). The graphical abstract was created with BioRender.com.

Author contributions JGH: conceptualization, data curation, formal analysis, investigation, methodology, project administration, validation, visualization, writing – original draft, and writing – review & editing. MBF, JVRO, BMS, LFS, VRJS, and ACSP: data curation, and investigation. GALA and FPP: data curation, investigation, methodology, and validation. LSR, AMM, and RGR: investigation, methodology, resources, and writing – review & editing. MN: resources, and writing – review & editing. TASA: conceptualization, funding acquisition, methodology, project administration, resources, validation, and writing – review & editing. DJM: conceptualization, funding acquisition, methodology, project administration, resources, supervision, validation, and writing – review & editing. All authors reviewed the final manuscript.

Funding This study was supported in parts by grants and/or scholarships from FAPERGS (Fundação de Apoio à Pesquisa do Rio Grande do Sul, Brazil, Grant nº 21/2551-0001965-4), CAPES (Coordenação de Aperfeiçoamento de Pessoal de Nível Superior, Brazil) and CNPq (Conselho Nacional de Desenvolvimento Científico e Tecnológico, Brazil). The graphical abstract was created with BioRender.com.

Data availability The datasets generated during and/or analyzed during the current study are available from the corresponding author upon reasonable request.

Declarations

Conflict of interest There is no conflict of interest.

Declaration of generative AI and AI-assisted technologies in the writing process The authors declare that no Generative AI and AI-assisted technologies were used in the writing process.

References

1. Brodbelt A, Greenberg D, Winters T, Williams M, Vernon S, Collins VP. Glioblastoma in England: 2007–2011. Eur J Cancer. 2015;51(4):533–42.
2. Bray F, Ferlay J, Soerjomataram I, Siegel RL, Torre LA, Jemal A. Global cancer statistics 2018: GLOBOCAN estimates of incidence and mortality worldwide for 36 cancers in 185 countries. CA Cancer J Clin. 2018;68(6):394–424.
3. Guntuku L, Naidu VGM, Ganesh YV. Mitochondrial dysfunction in gliomas: pharmacotherapeutic potential of natural compounds. Curr Neuropharmacol. 2016;14(6):567–83.
4. Norouzi M, Nazari B, Miller DW. Injectable hydrogel-based drug delivery systems for local cancer therapy. Drug Discov Today. 2016;21:1835–49.
5. Tseng YY, Su CH, Yang ST, Huang YC, Lee WH, Wang YC, et al. Advanced interstitial chemotherapy combined with targeted treatment of malignant glioma in rats by using drug-loaded nanofibrous membranes [Internet]. Vol. 7. Available from: www.impactjournals.com/oncotarget
6. Akbar U, Jones T, Winestone J, Michael M, Shukla A, Sun Y, et al. Delivery of temozolomide to the tumor bed via biodegradable gel matrices in a novel model of intracranial glioma with resection. J Neurooncol. 2009;94(2):203–12.
7. Denny BJ, Wheelhouse RT, Stevens MFG, Tsang LLH, Slack JA. NMR and molecular modeling investigation of the mechanism of activation of the antitumor drug temozolomide and its interaction with DNA. Biochemistry. 1994;33(31):9045–51.
8. Ohka F, Natsume A, Wakabayashi T. Current trends in targeted therapies for glioblastoma multiforme. Neurol Res Int. 2012;2012:1–13.
9. Drabløs F, Feyzi E, Aas PA, Vaagbø CB, Kavli B, Bratlie MS, et al. Alkylation damage in DNA and RNA—repair mechanisms and medical significance. DNA Repair (Amst). 2004;3(11):1389–407.
10. Strobel H, Baisch T, Fitzel R, Schilberg K, Siegelin MD, Karpel-Massler G, et al. Temozolomide and other alkylating agents in glioblastoma therapy. Biomedicines. 2019;7(3):69.
11. Braga SS, Silva AMS. A new age for iron: antitumoral ferrocenes. Organometallics. 2013;32(20):5626–39.
12. Ornelas C. Application of ferrocene and its derivatives in cancer research. New J Chem. 2011;35(10):1973.
13. Na Y, Woo J, Choi WI, Sung D. Novel carboxylated ferrocene polymer nanocapsule with high reactive oxygen species sensitivity and on-demand drug release for effective cancer therapy. Colloids Surf B Biointerfaces. 2021;200: 111566.
14. Qian Y, Zhang J, Xu R, Li Q, Shen Q, Zhu G. Nanoparticles based on polymers modified with pH-sensitive molecular switch and low molecular weight heparin carrying celastrol and ferrocene for breast cancer treatment. Int J Biol Macromol. 2021;183:2215–26.
15. Idlas P, Lepeltier E, Jaouen G, Passirani C. Ferrocifen loaded lipid nanocapsules: a promising anticancer medication against multidrug resistant tumors. Cancers. 2021;13(10):2291.
16. Fan CH, Ting CY, Chang YC, Wei KC, Liu HL, Yeh CK. Drug-loaded bubbles with matched focused ultrasound excitation for concurrent blood-brain barrier opening and brain-tumor drug delivery. Acta Biomater. 2015;15(15):89–101.
17. Housman G, Byler S, Heerboth S, Lapinska K, Longacre M, Snyder N, et al. Drug resistance in cancer: an overview. Cancers. 2014;6:1769–92.
18. Huang D, Lin C, Wen X, Gu S, Zhao P. A potential nanofiber membrane device for filling surgical residual cavity to prevent glioma recurrence and improve local neural tissue reconstruction. PLoS ONE. 2016;11(8): e0161435.
19. Sawyer AJ, Piepmeier JM, Saltzman WM. New methods for direct delivery of chemotherapy for treating brain tumors. Yale J Biol Med. 2006;79(3–4):141.
20. Wei X, Chen X, Ying M, Lu W. Brain tumor-targeted drug delivery strategies. Acta Pharm Sin B. 2014;4(3):193–201.
21. Weller M, Cloughesy T, Perry JR, Wick W. Standards of care for treatment of recurrent glioblastoma-are we there yet? Neuro Oncol. 2013;15:4–27.
22. Borthakur P, Boruah PK, Sharma B, Das MR. Nanoemulsion: preparation and its application in food industry. In: Emulsions. Elsevier; 2016. p. 153–91.
23. Heravi Shargh V, Luckett J, Bouzinab K, Paisey S, Turyanska L, Singleton WGB, et al. Chemosensitization of temozolomide-resistant pediatric diffuse midline glioma using potent nanoencapsulated forms of a N(3)-propargyl analogue. ACS Appl Mater Interfaces. 2021;13(30):35266–80.
24. Chen D, Liu X, Lu X, Tian J. Nanoparticle drug delivery systems for synergistic delivery of tumor therapy. Front Pharmacol. 2023;16:14.

25. Ganta S, Talekar M, Singh A, Coleman TP, Amiji MM. Nanoemulsions in translational research—opportunities and challenges in targeted cancer therapy. AAPS PharmSciTech. 2014;15(3):694–708.
26. Jiang Y, Liu C, Zhai W, Zhuang N, Han T, Ding Z. The optimization design of lactoferrin loaded hupa nanoemulsion for targeted drug transport via intranasal route. Int J Nanomed. 2019;14:9217–34.
27. Sánchez-López E, Guerra M, Dias-Ferreira J, Lopez-Machado A, Ettcheto M, Cano A, et al. Current applications of nanoemulsions in cancer therapeutics. Nanomaterials. 2019;9(6):821.
28. Venturini CG, Jäger E, Oliveira CP, Bernardi A, Battastini AMO, Guterres SS, et al. Formulation of lipid core nanocapsules. Colloids Surf A Physicochem Eng Asp. 2011;375(1–3):200–8.
29. Borenfreund E, Puerner JA. toxicity determined in vitro by morphological alterations and neutral red absorption (Surfactants; highest tolerated dose; in vitro alternative; spectrophotometric analysis). Toxicol Lett. 1985;24(2–3):119–24.
30. Han SJ, Rolston JD, Molinaro AM, Clarke JL, Prados MD, Chang SM, et al. Phase II trial of 7 days on/7 days off temozolmide for recurrent high-grade glioma. Neuro Oncol. 2014;16(9):1255–62.
31. Wick W, Platten M, Weller M. New (alternative) temozolomide regimens for the treatment of glioma. Neuro Oncol. 2009;11(1):69–79.
32. Honasoge A, Sontheimer H. Involvement of tumor acidification in brain cancer pathophysiology. Front Physiol. 2013;4:316.
33. Gatenby RA, Gillies RJ. Why do cancers have high aerobic glycolysis? Nat Rev Cancer. 2004;4:891–9.
34. ICH Harmonised Tripartite Guideline (2005) Validation of Analytical Procedures: Text and Methodology Q2 (R1). International Conference on Harmonisation of Technical Requirements for Registration of Pharmaceuticals for Human Use, Geneva, 1–17. https://database.ich.org/sites/default/files/Q2%28R1%29%20Guideline.pdf.
35. Brasil MS (2017) Resolução da Diretoria Colegiada - RDC no 166. Diário Oficial da República Federativa do Brasil, 2017, 1–22. http://antigo.anvisa.gov.br/documents/10181/2721567/RDC_166_2017_COMP.pdf/d5fb92b3-6c6b-4130-8670-4e3263763401.
36. Bianchin MD, Kulkamp-Guerreiro IC, De Oliveira CP, Contri RV, Guterres SS, Pohlmann AR. Radar charts based on particle sizing as an approach to establish the fingerprints of polymeric nanoparticles in aqueous formulations. J Drug Deliv Sci Technol. 2015;1(30):180–9.
37. Cardoso AM, de Oliveira EG, Coradini K, Bruinsmann FA, Aguirre T, Lorenzoni R, et al. Chitosan hydrogels containing nanoencapsulated phenytoin for cutaneous use: skin permeation/penetration and efficacy in wound healing. Mater Sci Eng, C. 2019;1(96):205–17.
38. Metin CO, Lake LW, Miranda CR, Nguyen QP. Stability of aqueous silica nanoparticle dispersions. J Nanopart Res. 2011;13(2):839–50.
39. Raval N, Maheshwari R, Kalyane D, Youngren-Ortiz SR, Chougule MB, Tekade RK. Importance of physicochemical characterization of nanoparticles in pharmaceutical product development. In: Basic fundamentals of drug delivery. Elsevier; 2018. p. 369–400.
40. Giri K, Shameer K, Zimmermann MT, Saha S, Chakraborty PK, Sharma A, et al. Understanding protein-nanoparticle interaction: a new gateway to disease therapeutics. Bioconjug Chem. 2014;25(6):1078–90.
41. Krai J, Beckenkamp A, Gaelzer MM, Pohlmann AR, Guterres SS, Filippi-Chiela EC, et al. Doxazosin nanoencapsulation improves its in vitro antiproliferative and anticlonogenic effects on breast cancer cells. Biomed Pharmacother. 2017;1(94):10–20.
42. Sari TP, Mann B, Kumar R, Singh RRB, Sharma R, Bhardwaj M, et al. Preparation and characterization of nanoemulsion encapsulating curcumin. Food Hydrocoll. 2015;1(43):540–6.
43. Walia N, Zhang S, Wismer W, Chen L. A low energy approach to develop nanoemulsion by combining pea protein and Tween 80 and its application for vitamin D delivery. Food Hydrocoll Health. 2022;1:2.
44. Ananta JS, Paulmurugan R, Massoud TF. Temozolomide-loaded PLGA nanoparticles to treat glioblastoma cells: a biophysical and cell culture evaluation. Neurol Res. 2016;38(1):51–9.
45. Ramazani F, Chen W, van Nostrum CF, Storm G, Kiessling F, Lammers T, et al. Strategies for encapsulation of small hydrophilic and amphiphilic drugs in PLGA microspheres: state-of-the-art and challenges. Int J Pharm. 2016;499(1–2):358–67.
46. Li Q, Li X, Zhao C. Strategies to obtain encapsulation and controlled release of small hydrophilic molecules. Front Bioeng Biotechnol. 2020;8:437.
47. Maiti D, Saha A, Devi PS. Surface modified multifunctional $ZnFe_2O_4$ nanoparticles for hydrophobic and hydrophilic anti-cancer drug molecule loading. Phys Chem Chem Phys. 2016;18(3):1439–50.
48. Chenthamara D, Subramaniam S, Ramakrishnan SG, Krishnaswamy S, Essa MM, Lin FH, et al. Therapeutic efficacy of nanoparticles and routes of administration. Biomater Res. 2019;23(1):1–29.
49. Singh S, Pathak K, Bali V. Product development studies on surface-adsorbed nanoemulsion of olmesartan medoxomil as a capsular dosage form. AAPS PharmSciTech. 2012;13(4):1212–21.
50. Irani M, Sadeghi GMM, Haririan I. The sustained delivery of temozolomide from electrospun PCL-Diol-b-PU/gold nanocomposite nanofibers to treat glioblastoma tumors. Mater Sci Eng, C. 2017;75:165–74.
51. Reinhardt LS, Morás AM, Henn JG, Arantes PR, Ferro MB, Braganhol E, et al. Nek1-inhibitor and temozolomide-loaded microfibers as a co-therapy strategy for glioblastoma treatment. Int J Pharm. 2022;617: 121584.
52. Morás AM, Henn JG, Steffens Reinhardt L, Lenz G, Moura DJ. Recent developments in drug delivery strategies for targeting DNA damage response in glioblastoma. Life Sci. 2021;287: 120128.
53. Grotto HZW. Metabolismo do ferro: uma revisão sobre os principais mecanismos envolvidos em sua homeostase. Rev Bras Hematol Hemoter. 2008;30(5):390–7.
54. Murillo MI, Gaiddon C, Le Lagadec R. Targeting of the intracellular redox balance by metal complexes towards anticancer therapy. Front Chem. 2022;11:10.
55. Köpf-Maier P, Köpf H, Neuse EW. Ferricenium complexes: a new type of water-soluble antitumor agent. J Cancer Res Clin Oncol. 1984;108(3):336–40.
56. Kauffman M, Kauffman M, Traore K, Zhu H, Trush M, Jia Z, et al. MitoSOX-based flow cytometry for detecting mitochondrial ROS. React Oxyg Species. 2016;2(5):361.
57. Perry SW, Norman JP, Barbieri J, Brown EB, Gelbard HA. Mitochondrial membrane potential probes and the proton gradient: a practical usage guide. Biotechniques. 2011;50:98–115.
58. Lee SY. Temozolomide resistance in glioblastoma multiforme. Genes Dis. 2016;3(3):198–210.
59. Atmaca H, Özkan AN, Zora M. Novel ferrocenyl pyrazoles inhibit breast cancer cell viability via induction of apoptosis and inhibition of PI3K/Akt and ERK1/2 signaling. Chem Biol Interact. 2017;263:28–35.
60. Tian J, Chen J, Ge C, Liu X, He J, Ni P, et al. Synthesis of PEGylated ferrocene nanoconjugates as the radiosensitizer of cancer cells. Bioconjug Chem. 2016;27(6):1518–24.
61. Kondratskyi A, Kondratska K, Vanden Abeele F, Gordienko D, Dubois C, Toillon RA, et al. Ferroquine, the next

Journal : Large 43440 | Article No : 537 | Pages : 13 | MS Code : 537 | Dispatch : 10-10-2023

generation antimalarial drug, has antitumor activity. Sci Rep. 2017;7(1):15896.
62. Podolski-Renić A, Bősze S, Dinić J, Kocsis L, Hudecz F, Csámpai A, et al. Ferrocene–cinchona hybrids with triazolyl-chalcone linkers act as pro-oxidants and sensitize human cancer cell lines to paclitaxel. Metallomics. 2017;9(8):1132–41.

Authors and Affiliations

Jeferson Gustavo Henn[1,2] · Matheus Bernardes Ferro[1] · Gabriel Antonio Lopes Alves[3] · Flávia Pires Peña[3] · João Vitor Raupp de Oliveira[3] · Bárbara Müller de Souza[4] · Leonardo Fonseca da Silva[4] · Victória Rapack Jacinto Silva[1] · Ana Carolina Silva Pinheiro[1] · Luiza Steffens Reinhardt[1] · Ana Moira Morás[1] · Michael Nugent[2] · Ricardo Gomes da Rosa[4] · Tanira Alessandra Silveira Aguirre[3] · Dinara Jaqueline Moura[1]

✉ Dinara Jaqueline Moura
dinaram@ufcspa.edu.br

[1] Laboratório de Genética Toxicológica, Universidade Federal de Ciências da Saúde de Porto Alegre, 245 Sarmento Leite Street, Lab. 714, Porto Alegre, Rio Grande do Sul 90050-170, Brazil

[2] Materials Research Institute, Technological University of the Shannon: Midlands Midwest, Athlone, Co. Westmeath N37HD68, Ireland

[3] Laboratório de Farmacociências, Universidade Federal de Ciências da Saúde de Porto Alegre, Porto Alegre, Rio Grande do Sul 90050-170, Brazil

[4] Departamento de Química Inorgânica, Universidade Federal do Rio Grande do Sul, Porto Alegre, Rio Grande do Sul 91501-970, Brazil

Journal : Large 43440	Article No : 537	Pages : 13	MS Code : 537	Dispatch : 18-10-2023

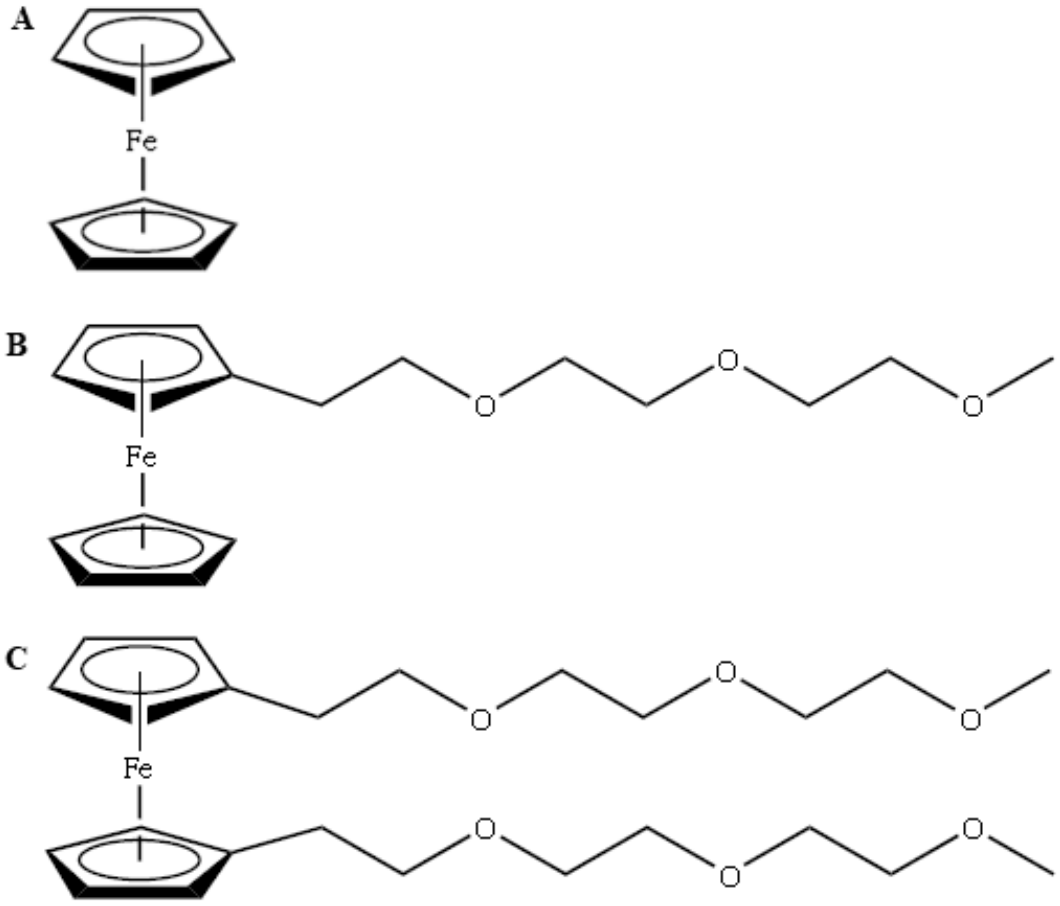

Fig. S1. Schematic representation of ferrocene (**1A**), monopegylated ferrocene (**1B**) and dipegylated ferrocene (**1C**).

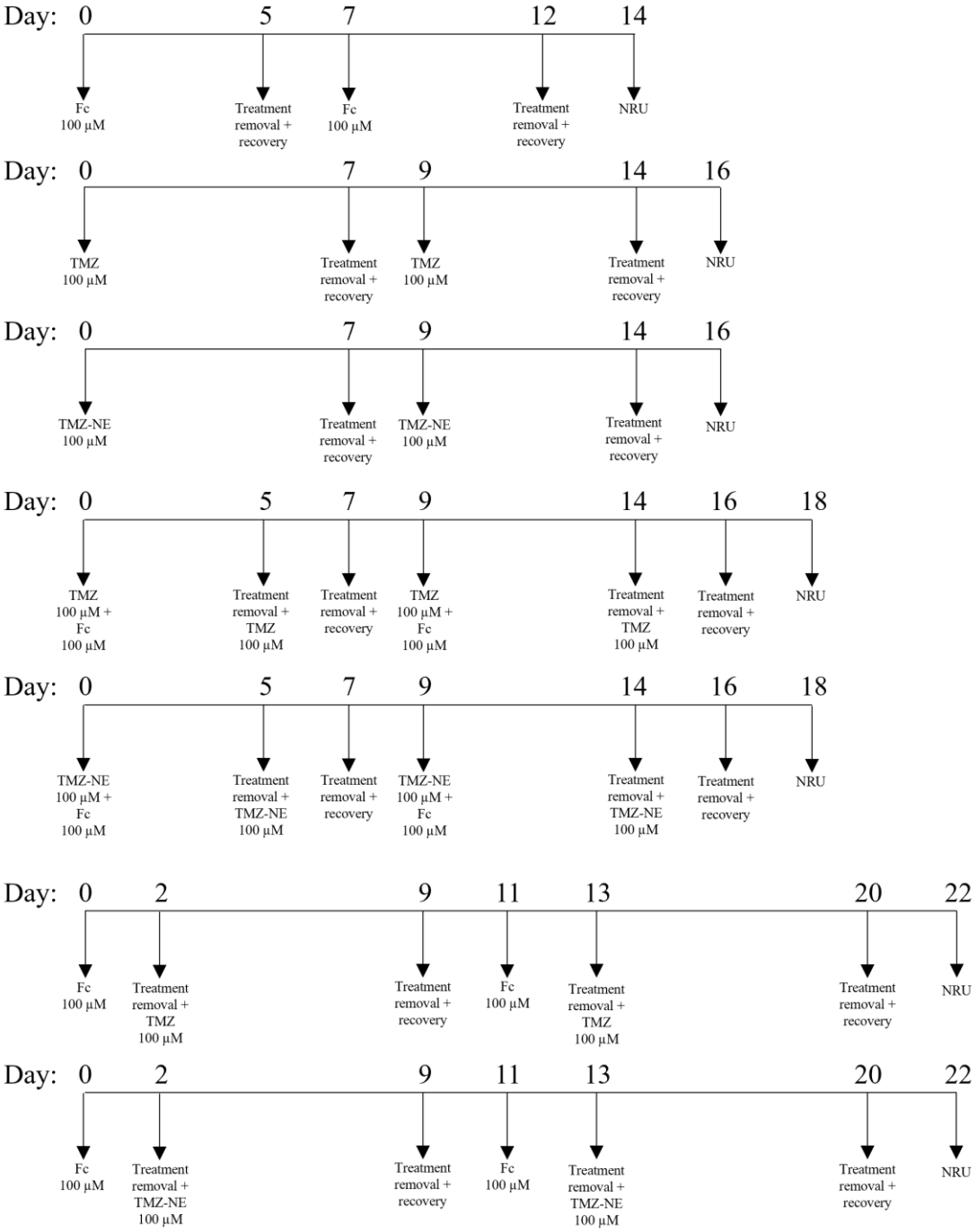

Fig. S2. Schematic representation of different treatment protocol simulation based on two-cycle regimens: T98G cells were treated for different days either with 100 µM of Fc and/or TMZ on their own, or TMZ-NE on its own or in combination with Fc, dissolved in DMEM + FBS (5%). In all recovery periods cells were kept in culture media with DMEM + FBS (10 %). All regimens comprised two treatment cycles and in the end cell viability was carried out by NRU assay. Fc: ferrocene. TMZ: temozolomide. NE: nanoemulsion. FBS: fetal bovine serum. NRU: neutral red uptake.

4 DISCUSSÃO

O tratamento do glioblastoma continua sendo um desafio significativo na medicina contemporânea, com a terapia padrão mais amplamente aceita consistindo na combinação de ressecção cirúrgica, radioterapia e quimioterapia com temozolomida (TMZ). No entanto, é importante notar que essa abordagem terapêutica não experimentou avanços substanciais ao longo das últimas décadas. Isso resultou em taxas de insucesso no tratamento da doença que permanecem elevadas, principalmente devido à baixa biodisponibilidade da TMZ, à presença da barreira hematoencefálica (BHE) e aos mecanismos de resistência tumoral. Tais fatores são os principais contribuintes para o aumento da reincidência do tumor e a consequente baixa expectativa de vida dos pacientes acometidos (Bush et al., 2017), e reiteram a necessidade da exploração de novas moléculas e modelos terapêuticos mais eficazes e capazes de burlar estas barreiras e aumentar a eficácia do tratamento.

Neste contexto, os compostos de Fc têm chamado atenção em razão de suas propriedades físico-químicas que favorecem sua interação com estruturas biológicas, tendo já reportado atividade antitumoral via mecanismos de sensibilização celular (Atmaca et al., 2017; Ornelas, 2011). A citotoxicidade e atividade antitumoral destes compostos são influenciadas por mecanismos de ação intrínsecos que envolvem, principalmente, a geração de ROS. Os Fc têm potencial redox de +0,40 V, o que é compatível com o potencial redox intracelular, que varia entre -0,44 e +0,40 V. Desta forma, estes compostos tornam-se suscetíveis a reações de transferência de elétrons e ciclos redox no meio intracelular, fazendo com que o Fe^{2+} sofra oxidação reversível a Fe^{3+} via reação de Fenton, gerando o radical ·OH, que por sua vez gera danos ao DNA com potencial morte celular. Por outro lado, a atividade antitumoral dos Fc por si só é mínima, especialmente em razão da sua baixa translocação celular e baixa solubilidade (Ludwig et al., 2021), o que justifica seu uso concomitante a outras moléculas e métodos de administração.

Conforme abordado no Capítulo 1 desta tese, o advento de DDS como alternativas para resolver total ou parcialmente alguns desafios, tais como o

direcionamento de fármacos ao sítio específico e sua passagem por barreiras biológicas, tem representado um importante avanço no tratamento de diversos tumores, minimizando o acúmulo de fármacos fora do tecido-alvo e consequentemente reduzindo os efeitos colaterais e aumentando a adesão dos pacientes (Vargason et al., 2021b). Estes sistemas podem ser classificados, quanto à sua composição, em NP inorgânicas e poliméricas, conjugados poliméricos, micelas, lipossomas e exossomas, e sua escolha depende de fatores como as interações físico-químicas entre a moléculas de interesse e o material, a via de administração, o alvo terapêutico e o mecanismo de direcionamento ao tecido-alvo (Arranja et al., 2017; Chaturvedi et al., 2018).

Além destes DDS já mencionados, outro sistema nanoestruturado, as NE de núcleo lipídico, pode ser considerado um dos mais promissores sistemas de nanocarreamento de fármacos devido à sua versatilidade, estabilidade termodinâmica e cinética, e preparação relativamente fácil (Pavoni et al., 2020; Rai et al., 2018), e já têm demonstrado efetividade contra os mais variados tipos tumorais em ensaios pré-clínicos e clínicos (Graván et al., 2023; Sánchez-López et al., 2019).

Nos dados apresentados no Capítulo 2 desta tese, foi abordado o desenvolvimento, a caracterização e a avaliação *in vitro* de uma NE de núcleo lipídico contento TMZ (TMZ-NE) adsorvida em sua interface, em diferentes combinações com Fc, no tratamento de linhagens celulares de GB humano. Análises comparativas entre a formulação desenvolvida e sua versão branca demonstraram que ambas possuem tamanho e distribuição de partículas unimodais, e um baixo valor de Span. Estes dados foram corroborados pelas análises de índice de polidispersão e por difração a *laser*, e o caráter esférico das gotículas foi confirmado pela microscopia eletrônica. Conforme Bianchin et al. (2015) e Cardoso et al. (2019), os valores de Span e de índice de polidispersão encontrados em nosso estudo são perfeitamente adequados a aplicações farmacêuticas.

Diferentemente do comum, quando as moléculas carreadas por uma NE ficam internalizadas na porção lipídica da nanoestrutura, a análise do potencial zeta da TMZ-NE desenvolvida indicou que o fármaco está adsorvido na interface do

sistema. Tal efeito já foi descrito por Metin et al. (2011) e Raval et al. (2018), que associaram esta condição a valores de potencial zeta próximos a zero. Além disso, a utilização do surfactante Tween®-80 na formulação também desempenhou um papel importante na alocação do fármaco no sistema. Sabe-se que em condições de pH entre 5 e 7, como simulado no estudo aqui apresentado, este surfactante apresenta caráter não-iônico que, associado à sua baixa concentração na formulação (aproximadamente 0,14%), permite a ação de forças de repulsão restritas à porção hidrofílica do surfactante, estabilizando as gotículas nesta interface, e consequentemente permitindo a adsorção da TMZ nesta região (Sari et al., 2015; Walia et al., 2022). Na sequência, esta hipótese foi confirmada pela quase ausência de encapsulação observada no ensaio de perfil de liberação do fármaco.

Com o intuito de analisar a performance da TMZ-NE em linhagens celulares de GB humano, e ao mesmo tempo propor a inserção de uma molécula sensibilizante tumoral, optou-se por realizar tratamentos agudos de 24 h com diferentes combinações de TMZ, Fc e/ou TMZ-NE. Ensaios de viabilidade celular nas linhagens U87 e T98G revelaram que a combinação entre TMZ-NE e Fc aumentou significativamente a citotoxicidade em ambas as linhagens, com um interessante efeito dose-dependente na linhagem T98G, a única das duas com conhecido perfil de resistência à TMZ. Este achado nos levou a optar por esta linhagem celular para estudos posteriores, a fim de se compreender melhor o mecanismo envolvido nesta aparente sensibilização do perfil de resistência à TMZ.

Análises do perfil de morte celular e do estresse mitocondrial após tratamentos de 24 h demonstraram elevados níveis de necrose celular, provavelmente associados à alta geração de ânion superóxido. Os grupos tratados com Fc e TMZ-NE + Fc também apresentaram alteração do status de polarização da membrana mitocondrial. Sabe-se que a manutenção do potencial de membrana mitocondrial é essencial para o seu funcionamento, o equilíbrio do metabolismo celular, o controle da geração de ROS e dos mecanismos de regulação de morte celular (Perry et al., 2011). Portanto, estes resultados compilados não somente reforçaram o aumento da sensibilidade em uma linhagem com perfil de resistência, como a T98G, como também confirmaram a ação do Fc neste evento via geração

de ROS, desestabilização mitocondrial e morte celular, corroborando achados já descritos por Na et al. (2021) e Qian et al. (2021).

Atmaca et al. (2017) e Tian et al. (2016) já haviam demonstrado as propriedades sensibilizantes dos compostos de Fc em linhagens tumorais posteriormente submetidas a radioterapia e outros agentes quimioterápicos. De posse desta informação, optou-se por estabelecer um protocolo clínico adaptado e constituído de dois ciclos de tratamento, onde a linhagem celular T98G foi tratada por cinco, sete ou nove dias conforme as combinações de Fc, TMZ e/ou TMZ-NE utilizadas, com um período de recuperação de dois dias entre os ciclos. O principal objetivo desta etapa foi observar se o Fc exerce alguma ação sensibilizante nas linhagens ao ser incorporado por dias anteriormente à adição de TMZ ou TMZ-NE, e avaliação se deu por ensaio de viabilidade celular. De um modo geral, observou-se significativa redução da viabilidade celular nos grupos pré-tratados com Fc seguidos da adição de TMZ e TMZ-NE. Estudos utilizando análogos de Fc em modelos de câncer de próstata, pulmão, colorretal e glioma já haviam relatados efeitos similares, reforçando o uso destes compostos como adjuvantes a tratamentos convencionais (Kondratskyi et al., 2017; Podolski-Renić et al., 2017).

5 CONCLUSÕES

O desenvolvimento de DDS para a entrega de fármacos ao cérebro representa um avanço importante à terapia convencional do GB. A versatilidade destes sistemas permite a incorporação das mais variadas moléculas, ampliando assim o rol de aplicação destas estruturas, bem como a melhora na entrega de fármacos, o potencial de atravessar a BHE, a redução de efeitos colaterais, a habilidade em combinar múltiplas moléculas, a capacidade de direcionamento a tecidos-alvo, e a possibilidade de se criar abordagens terapêuticas personalizadas.

Neste trabalho foi apresentado o desenvolvimento e caracterização com êxito uma NE contendo TMZ, em combinação com um composto de Fc, um composto organometálico com atividade sensibilizante tumoral e capaz de aumentar a geração de ROS no meio intracelular. Os dados produzidos por esta tese revelaram que esta abordagem combinada não só reduziu a viabilidade celular em linhagens celulares de GB humano, como também reverteu o perfil de resistência à TMZ da linhagem T98G em tratamentos agudos. Estudos de mecanística associaram este fato a alterações no potencial da membrana mitocondrial mediado pela geração de ROS, com consequente morte celular. Não obstante, o Fc demonstrou considerável atividade sensibilizante tumoral em ciclos de pré-tratamento seguidos da adição TMZ-NE, reforçando seu papel crucial como fonte exógena de Fe^{2+}, promovendo uma maior catálise de ROS e a geração de subprodutos tóxicos ao ambiente tumoral.

De um modo geral, a combinação entre TMZ-NE e Fc mostrou-se uma abordagem terapêutica promissora ao tratamento do GB, embora estudos *in vivo* devam ser conduzidos para o melhor entendimento da mecanística envolvida neste processo. À medida que o campo da nanomedicina avança, haverá dispositivos e terapias ainda mais sofisticados e eficazes para o tratamento do câncer e, apesar de seus potenciais benefícios, há também desafios a serem enfrentados, como a toxicidade, questões regulatórias e a necessidade de ensaios clínicos mais robustos para demonstrar a eficácia. No entanto, com investigação e desenvolvimento contínuos, a nanomedicina tem enorme potencial de revolucionar o tratamento do câncer e aumentar a sobrevida dos pacientes.

6 PERSPECTIVAS

Os dados apresentados no Capítulo 2 desta tese geraram novos questionamentos para os quais serão necessários novos experimentos a fim de se avaliar a potencial ação antitumoral da combinação proposta em esquemas de tratamento envolvendo sistemas mais complexos. Para isso, será crucial responder às seguintes perguntas:

- O Fc e/ou sua combinação com TMZ têm algum efeito sobre via de sinalização e progressão tumorais?
- Qual a melhor via de administração da NE desenvolvida, a fim de que a entrega de TMZ ao ambiente tumoral atinja doses terapêuticas?
- Qual a melhor via de administração para o Fc, a fim de que sua entrega ao ambiente tumoral atinja doses terapêuticas?
- Quais os parâmetros de toxicidade do Fc?
- É possível combinar o Fc com a TMZ na mesma NE?
- Quais modificações poderiam ser feitas na NE a fim de se modular seu perfil de liberação?
- O efeito sensibilizante do Fc e a reversão do perfil de resistência à TMZ observados nos ensaios *in vitro* serão igualmente reproduzidos em ensaios *in vivo*?
- Seria possível o desenvolvimento de um DDS de aplicação local contendo TMZ e Fc para o tratamento do GB?

7 REFERÊNCIAS BIBLIOGRÁFICAS

Ahmand, G., El Sadda, R., Botchkina, G., Ojima, I., Egan, J., Amiji, M. (2017). Nanoemulsion formulation of a novel taxoid DHA-SBT-1214 inhibits prostate cancer stem cell-induced tumor growth. *Cancer Letters, 406*, 71-80. https://doi.org/10.1016/j.canlet.2017.08.004

Allen, T. M., & Cullis, P. R. (2004). Drug Delivery Systems: Entering the Mainstream. In *Science* (Vol. 303, Issue 5665, pp. 1818–1822). https://doi.org/10.1126/science.1095833

Alzial, G., Renoult, O., Paris, F., Gratas, C., Clavreul, A., & Pecqueur, C. (2022). Wild-type isocitrate dehydrogenase under the spotlight in glioblastoma. *Oncogene*, *41*(5), 613–621. https://doi.org/10.1038/s41388-021-02056-1

Anselmo, A. C., & Mitragotri, S. (2019). Nanoparticles in the clinic: An update. *Bioengineering & Translational Medicine*, *4*(3). https://doi.org/10.1002/btm2.10143

Arranja, A. G., Pathak, V., Lammers, T., & Shi, Y. (2017). Tumor-targeted nanomedicines for cancer theranostics. *Pharmacological Research*, *115*, 87–95. https://doi.org/10.1016/j.phrs.2016.11.014

Atmaca, H., Özkan, A. N., & Zora, M. (2017). Novel ferrocenyl pyrazoles inhibit breast cancer cell viability via induction of apoptosis and inhibition of PI3K/Akt and ERK1/2 signaling. *Chemico-Biological Interactions*, *263*, 28–35. https://doi.org/10.1016/j.cbi.2016.12.010

Banerjee, S. S., Aher, N., Patil, R., & Khandare, J. (2012). Poly(ethylene glycol)-Prodrug Conjugates: Concept, Design, and Applications. *Journal of Drug Delivery*, *2012*, 1–17. https://doi.org/10.1155/2012/103973

Banik, B. L., Fattahi, P., & Brown, J. L. (2016). Polymeric nanoparticles: The future of nanomedicine. In *Wiley Interdisciplinary Reviews: Nanomedicine and Nanobiotechnology* (Vol. 8, Issue 2, pp. 271–299). Wiley-Blackwell. https://doi.org/10.1002/wnan.1364

Batash, R., Asna, N., Schaffer, P., Francis, N., & Schaffer, M. (2017). Glioblastoma Multiforme, Diagnosis and Treatment; Recent Literature Review. *Current Medicinal Chemistry*, *24*(27). https://doi.org/10.2174/0929867324666170516123206

Beck-Broichsitter, M., Rytting, E., Lebhardt, T., Wang, X., & Kissel, T. (2010). Preparation of nanoparticles by solvent displacement for drug delivery: A shift in the “ ouzo region” upon drug loading. *European Journal of Pharmaceutical Sciences*, *41*(2), 244–253. https://doi.org/10.1016/j.ejps.2010.06.007

Berkland, C., King, M., Cox, A., Kim, K., & Pack, D. W. (2002). P recise control of PLG microsphere size provides enhanced control of drug release rate a a a b. In *Journal of Controlled Release* (Vol. 82). www.elsevier.com/locate/jconrel

Bertrand, N., Wu, J., Xu, X., Kamaly, N., & Farokhzad, O. C. (2014). Cancer nanotechnology: The impact of passive and active targeting in the era of modern cancer biology. In *Advanced Drug Delivery Reviews* (Vol. 66, pp. 2–25). Elsevier B.V. https://doi.org/10.1016/j.addr.2013.11.009

Bianchin, M. D., Külkamp-Guerreiro, I. C., De Oliveira, C. P., Contri, R. V., Guterres, S. S., & Pohlmann, A. R. (2015). Radar charts based on particle sizing as an approach to establish the fingerprints of polymeric nanoparticles

in aqueous formulations. *Journal of Drug Delivery Science and Technology*, *30*, 180–189. https://doi.org/10.1016/j.jddst.2015.10.015

Botchkina, G. I., Zuniga, E. S., Das, M., Wang, Y., Wang, H., Zhu, S., Savitt, A. G., Rowehl, R. A., Leyfman, Y., Ju, J., Shroyer, K., Ojima, I. (2010). New-generation taxoid SB-T-1214 inhibits stem cell-related gene expression in 3D cancer spheroids induced by purified colon tumor-initiating cells. *Molecular Cancer, 9*. https://doi.org/10.1186/1476-4598-9-192

Bray, F., Ferlay, J., Soerjomataram, I., Siegel, R. L., Torre, L. A., & Jemal, A. (2018). Global cancer statistics 2018: GLOBOCAN estimates of incidence and mortality worldwide for 36 cancers in 185 countries. *CA: A Cancer Journal for Clinicians*, *68*(6), 394–424. https://doi.org/10.3322/caac.21492

Bregoli, L., Movia, D., Gavigan-Imedio, J. D., Lysaght, J., Reynolds, J., & Prina-Mello, A. (2016). Nanomedicine applied to translational oncology: A future perspective on cancer treatment. In *Nanomedicine: Nanotechnology, Biology, and Medicine* (Vol. 12, Issue 1, pp. 81–103). Elsevier Inc. https://doi.org/10.1016/j.nano.2015.08.006

Bush, N. A. O., Chang, S. M., & Berger, M. S. (2017). Current and future strategies for treatment of glioma. In *Neurosurgical Review* (Vol. 40, Issue 1). Springer Verlag. https://doi.org/10.1007/s10143-016-0709-8

Calvert, A. E., Chalastanis, A., Wu, Y., Hurley, L. A., Kouri, F. M., Bi, Y., Kachman, M., May, J. L., Bartom, E., Hua, Y., Mishra, R. K., Schiltz, G. E., Dubrovskyi, O., Mazar, A. P., Peter, M. E., Zheng, H., James, C. D., Burant, C. F., Chandel, N. S., … Stegh, A. H. (2017). Cancer-Associated IDH1 Promotes Growth and Resistance to Targeted Therapies in the Absence of Mutation. *Cell Reports*, *19*(9), 1858–1873. https://doi.org/10.1016/j.celrep.2017.05.014

Cardoso, A. M., de Oliveira, E. G., Coradini, K., Bruinsmann, F. A., Aguirre, T., Lorenzoni, R., Barcelos, R. C. S., Roversi, K., Rossato, D. R., Pohlmann, A. R., Guterres, S. S., Burger, M. E., & Beck, R. C. R. (2019). Chitosan hydrogels containing nanoencapsulated phenytoin for cutaneous use: Skin permeation/penetration and efficacy in wound healing. *Materials Science and Engineering C*, *96*, 205–217. https://doi.org/10.1016/j.msec.2018.11.013

Chang, M., Zhang, F., Wei, T., Zuo, T., Guan, Y., Lin, G., & Shao, W. (2016). Smart linkers in polymer-drug conjugates for tumor-targeted delivery. In *Journal of Drug Targeting* (Vol. 24, Issue 6, pp. 475–491). Taylor and Francis Ltd. https://doi.org/10.3109/1061186X.2015.1108324

Chaturvedi, V. K., Singh, A., Singh, V. K., & Singh, M. P. (2018). Cancer Nanotechnology: A New Revolution for Cancer Diagnosis and Therapy. *Current Drug Metabolism*, *20*(6), 416–429. https://doi.org/10.2174/1389200219666180918111528

Chen, D., Liu, X., Lu, X., & Tian, J. (2023). Nanoparticle drug delivery systems for synergistic delivery of tumor therapy. *Frontiers in Pharmacology*, *14*. https://doi.org/10.3389/fphar.2023.1111991

Chen, R., Smith-Cohn, M., Cohen, A. L., & Colman, H. (2017). Glioma Subclassifications and Their Clinical Significance. *Neurotherapeutics*, *14*(2), 284–297. https://doi.org/10.1007/s13311-017-0519-x

Colombo, M., Figueiró, F., Dias, A. de F., Teixeira, H. F., Battastini A. M. O., Koester, L. S. (2018). Kaempferol-loaded mucoadhesive nanoemulsion for intranasal administration reduces glioma growth *in vitro*. *International Journal*

of Pharmaceutics, 543(1-2), 214-223. https://doi.org/10.1016/j.ijpharm.2018.03.055

Couto, N., Caja, S., Maia, J., Strano Moraes, M. C., & Costa-Silva, B. (2018). Exosomes as emerging players in cancer biology. In *Biochimie* (Vol. 155, pp. 2–10). Elsevier B.V. https://doi.org/10.1016/j.biochi.2018.03.006

Cronin, M. T. D., Dearden, J. C., Duffy, J. C., Edwards, R., Manga, N., Worth, A. P., Worgan, A. D. P. (2010). The importance of hydrophobicity and electrophilicity descriptors in mechanistically-based QSARs for toxicological endpoints. *SAR and QSAR in Environmental Research, 13*(1), 167-176. https://doi.org/10.1080/10629360290002316

Ekladious, I., Colson, Y. L., & Grinstaff, M. W. (2019). Polymer–drug conjugate therapeutics: advances, insights and prospects. In *Nature Reviews Drug Discovery* (Vol. 18, Issue 4, pp. 273–294). Nature Publishing Group. https://doi.org/10.1038/s41573-018-0005-0

Elkhodiry, M. A., Momah, C. C., Suwaidi, S. R., Gadalla, D., Martins, A. M., Vitor, R. F., & Husseini, G. A. (2016). Synergistic nanomedicine: Passive, active, and ultrasound-triggered drug delivery in cancer treatment. In *Journal of Nanoscience and Nanotechnology* (Vol. 16, Issue 1, pp. 1–18). American Scientific Publishers. https://doi.org/10.1166/jnn.2016.11124

El-Say, K. M., & El-Sawy, H. S. (2017). Polymeric nanoparticles: Promising platform for drug delivery. In *International Journal of Pharmaceutics* (Vol. 528, Issues 1–2, pp. 675–691). Elsevier B.V. https://doi.org/10.1016/j.ijpharm.2017.06.052

Endo, K., Ueno, T., Kondo, S., Wakisaka, N., Murono, S., Ito, M., Kataoka, K., Kato, Y., & Yoshizaki, T. (2013). Tumor-targeted chemotherapy with the nanopolymer-based drug NC-6004 for oral squamous cell carcinoma. *Cancer Science*, *104*(3), 369–374. https://doi.org/10.1111/cas.12079

Erasimus, H., Gobin, M., Niclou, S., & Van Dyck, E. (2016). DNA repair mechanisms and their clinical impact in glioblastoma. *Mutation Research/Reviews in Mutation Research*, *769*, 19–35. https://doi.org/10.1016/j.mrrev.2016.05.005

Fathi, M., Mozafari, M. R., & Mohebbi, M. (2012). Nanoencapsulation of food ingredients using lipid based delivery systems. In *Trends in Food Science and Technology* (Vol. 23, Issue 1, pp. 13–27). https://doi.org/10.1016/j.tifs.2011.08.003

Graván, P., Aguilera-Garrido, A., Marchal, J. A., Navarro-Marchal, S. A., & Galisteo-González, F. (2023). Lipid-core nanoparticles: Classification, preparation methods, routes of administration and recent advances in cancer treatment. In *Advances in Colloid and Interface Science* (Vol. 314). Elsevier B.V. https://doi.org/10.1016/j.cis.2023.102871

Greening, D. W., Gopal, S. K., Xu, R., Simpson, R. J., & Chen, W. (2015). Exosomes and their roles in immune regulation and cancer. In *Seminars in Cell and Developmental Biology* (Vol. 40, pp. 72–81). Academic Press. https://doi.org/10.1016/j.semcdb.2015.02.009

Greulich, C., Diendorf, J., Simon, T., Eggeler, G., Epple, M., & Köller, M. (2011). Uptake and intracellular distribution of silver nanoparticles in human mesenchymal stem cells. *Acta Biomaterialia*, *7*(1), 347–354. https://doi.org/10.1016/j.actbio.2010.08.003

Grotto, H. Z. W. (2008). Metabolismo do ferro: uma revisão sobre os principais mecanismos envolvidos em sua homeostase. *Revista Brasileira de Hematologia e Hemoterapia*, *30*(5). https://doi.org/10.1590/S1516-84842008000500012

Guan, Y-b., Zhou, S-y., Zhang, Y-q., Wang, J-l., Tian Y-d., Jia, Y-y., Sun, Y-j. (2017). Therapeutic effects of curcumin nanoemulsions on prostate cancer. *Journal of Huazhong University of Science and Technology [Medical Sciences], 37*, 371-378. https://doi.org/10.1007/s11596-017-1742-8

Guntuku, L., Naidu, V. G. M., & Ganesh Yerra, V. (2016). Mitochondrial Dysfunction in Gliomas: Pharmacotherapeutic Potential of Natural Compounds. *Current Neuropharmacology*, *14*(6), 567–583. https://doi.org/10.2174/1570159X14666160121115641

Harwansh, R. K., Deshmukh, R., & Rahman, M. A. (2019). Nanoemulsion: Promising nanocarrier system for delivery of herbal bioactives. In *Journal of Drug Delivery Science and Technology* (Vol. 51, pp. 224–233). Editions de Sante. https://doi.org/10.1016/j.jddst.2019.03.006

Heravi Shargh, V., Luckett, J., Bouzinab, K., Paisey, S., Turyanska, L., Singleton, W. G. B., Lowis, S., Gershkovich, P., Bradshaw, T. D., Stevens, M. F. G., Bienemann, A., & Coyle, B. (2021). Chemosensitization of Temozolomide-Resistant Pediatric Diffuse Midline Glioma Using Potent Nanoencapsulated Forms of a N(3)-Propargyl Analogue. *ACS Applied Materials and Interfaces*, *13*(30), 35266–35280. https://doi.org/10.1021/acsami.1c04164

Hicks, H. R., Carreras, B. A., Holmes, J. A., & Langer, R. (1985). New Methods of Drug Delivery. In *23. R. J. Goldston, Plasma Phys. Controlled Fusion* (Vol. 28). Office of Technology Assessment. http://science.sciencemag.org/

Jeyaraj, M., Sathishkumar, G., Sivanandhan, G., MubarakAli, D., Rajesh, M., Arun, R., Kapildev, G., Manickavasagam, M., Thajuddin, N., Premkumar, K., & Ganapathi, A. (2013). Biogenic silver nanoparticles for cancer treatment: An experimental report. *Colloids and Surfaces B: Biointerfaces*, *106*, 86–92. https://doi.org/10.1016/j.colsurfb.2013.01.027

Kalluri, R. (2016). The biology and function of exosomes in cancer. In *Journal of Clinical Investigation* (Vol. 126, Issue 4, pp. 1208–1215). American Society for Clinical Investigation. https://doi.org/10.1172/JCI81135

Kondratskyi, A., Kondratska, K., Vanden Abeele, F., Gordienko, D., Dubois, C., Toillon, R.-A., Slomianny, C., Lemière, S., Delcourt, P., Dewailly, E., Skryma, R., Biot, C., & Prevarskaya, N. (2017). Ferroquine, the next generation antimalarial drug, has antitumor activity. *Scientific Reports*, *7*(1), 15896. https://doi.org/10.1038/s41598-017-16154-2

Köpf-Maier, P., Köpf, H., & Neuse, E. W. (1984). Ferricenium complexes: A new type of water-soluble antitumor agent. *Journal of Cancer Research and Clinical Oncology*, *108*(3), 336–340. https://doi.org/10.1007/BF00390468

Lasic, D. D., & Needhamt, D. (1995). *The “Stealth” Liposome: A Prototypical Biomaterial* (Vol. 95).

Le Rhun, E., Preusser, M., Roth, P., Reardon, D. A., van den Bent, M., Wen, P., Reifenberger, G., & Weller, M. (2019). Molecular targeted therapy of glioblastoma. In *Cancer Treatment Reviews* (Vol. 80). W.B. Saunders Ltd. https://doi.org/10.1016/j.ctrv.2019.101896

Lee, S. Y. (2016). Temozolomide resistance in glioblastoma multiforme. *Genes & Diseases*, *3*(3), 198–210. https://doi.org/10.1016/j.gendis.2016.04.007

Lee Ventola, C. (2017). *Progress in Nanomedicine: Approved and Investigational Nanodrugs* (Vol. 42, Issue 12).

Letchford, K., & Burt, H. (2007). A review of the formation and classification of amphiphilic block copolymer nanoparticulate structures: micelles, nanospheres, nanocapsules and polymersomes. In *European Journal of Pharmaceutics and Biopharmaceutics* (Vol. 65, Issue 3, pp. 259–269). https://doi.org/10.1016/j.ejpb.2006.11.009

Li, Z., Tan, S., Li, S., Shen, Q., & Wang, K. (2017). Cancer drug delivery in the nano era: An overview and perspectives (Review). In *Oncology Reports* (Vol. 38, Issue 2, pp. 611–624). Spandidos Publications. https://doi.org/10.3892/or.2017.5718

Lim, W., & Kim, H. S. (2019). Exosomes as Therapeutic Vehicles for Cancer. In *Tissue Engineering and Regenerative Medicine* (Vol. 16, Issue 3, pp. 213–223). Korean Tissue Engineering and Regenerative Medicine Society. https://doi.org/10.1007/s13770-019-00190-2

Lomkova, E. A., Chytil, P., Janoušková, O., Mueller, T., Lucas, H., Filippov, S. K., Trhlíková, O., Aleshunin, P. A., Skorik, Y. A., Ulbrich, K., & Etrych, T. (2016). Biodegradable Micellar HPMA-Based Polymer-Drug Conjugates with Betulinic Acid for Passive Tumor Targeting. *Biomacromolecules*, *17*(11), 3493–3507. https://doi.org/10.1021/acs.biomac.6b00947

Louis, D. N., Perry, A., Wesseling, P., Brat, D. J., Cree, I. A., Figarella-Branger, D., Hawkins, C., Ng, H. K., Pfister, S. M., Reifenberger, G., Soffietti, R., von Deimling, A., & Ellison, D. W. (2021). The 2021 WHO Classification of Tumors of the Central Nervous System: a summary. *Neuro-Oncology*, *23*(8), 1231–1251. https://doi.org/10.1093/neuonc/noab106

Ludwig, B. S., Tomassi, S., Di Maro, S., Di Leva, F. S., Benge, A., Reichart, F., Nieberler, M., Kühn, F. E., Kessler, H., Marinelli, L., Reuning, U., & Kossatz, S. (2021). The organometallic ferrocene exhibits amplified anti-tumor activity by targeted delivery via highly selective ligands to αvβ3, αvβ6, or α5β1 integrins. *Biomaterials*, *271*, 120754. https://doi.org/10.1016/j.biomaterials.2021.120754

Markman, J. L., Rekechenetskiy, A., Holler, E., & Ljubimova, J. Y. (2013). Nanomedicine therapeutic approaches to overcome cancer drug resistance. *Advanced Drug Delivery Reviews*, *65*(13–14), 1866–1879. https://doi.org/10.1016/j.addr.2013.09.019

Metin, C. O., Lake, L. W., Miranda, C. R., & Nguyen, Q. P. (2011). Stability of aqueous silica nanoparticle dispersions. *Journal of Nanoparticle Research*, *13*(2), 839–850. https://doi.org/10.1007/s11051-010-0085-1

Miranda, A., Blanco-Prieto, M., Sousa, J., Pais, A., & Vitorino, C. (2017). Breaching barriers in glioblastoma. Part I: Molecular pathways and novel treatment approaches. *International Journal of Pharmaceutics*, *531*(1), 372–388. https://doi.org/10.1016/j.ijpharm.2017.07.056

Morás, A. M., Henn, J. G., Steffens Reinhardt, L., Lenz, G., & Moura, D. J. (2021). Recent developments in drug delivery strategies for targeting DNA damage response in glioblastoma. *Life Sciences*, *287*, 120128. https://doi.org/10.1016/j.lfs.2021.120128

Mukerjee, A., P. Ranjan, A., & K. Vishwanatha, J. (2012). Combinatorial Nanoparticles for Cancer Diagnosis and Therapy. *Current Medicinal Chemistry*, *19*(22), 3714–3721. https://doi.org/10.2174/092986712801661176

Murillo, M. I., Gaiddon, C., & Le Lagadec, R. (2022). Targeting of the intracellular redox balance by metal complexes towards anticancer therapy. *Frontiers in Chemistry*, *10*. https://doi.org/10.3389/fchem.2022.967337

Na, Y., Woo, J., Choi, W. Il, & Sung, D. (2021). Novel carboxylated ferrocene polymer nanocapsule with high reactive oxygen species sensitivity and on-demand drug release for effective cancer therapy. *Colloids and Surfaces B: Biointerfaces*, *200*, 111566. https://doi.org/10.1016/j.colsurfb.2021.111566

Nastiti, C. M. R. R., Ponto, T., Abd, E., Grice, J. E., Benson, H. A. E., & Roberts, M. S. (2017). Topical nano and microemulsions for skin delivery. In *Pharmaceutics* (Vol. 9, Issue 4). MDPI AG. https://doi.org/10.3390/pharmaceutics9040037

Natesan, S., Sugumaran, A., Ponnusamy, C., Thiagarajan, V., Palanichamy, R., Kandasamy, R. (2017). Chitosan stabilized camptothecin nanoemulsions: Development, evaluation and biodistribution in preclinical breast cancer animal mode. *Int J Bio Macromol., 104*(Pt B), 1846-1852. https://doi.org/10.1016/j.ijbiomac.2017.05.127

Negrini, S., Gorgoulis, V. G., & Halazonetis, T. D. (2010). Genomic instability an evolving hallmark of cancer. In *Nature Reviews Molecular Cell Biology* (Vol. 11, Issue 3, pp. 220–228). https://doi.org/10.1038/nrm2858

Neuse, E. W. (2008). Synthetic Polymers as Drug-Delivery Vehicles in Medicine. *Metal-Based Drugs*, *2008*, 1–19. https://doi.org/10.1155/2008/469531

Ornelas, C. (2011). Application of ferrocene and its derivatives in cancer research. *New Journal of Chemistry*, *35*(10), 1973. https://doi.org/10.1039/c1nj20172g

Ortiz, R., Perazzoli, G., Cabeza, L., Jiménez-Luna, C., Luque, R., Prados, J., & Melguizo, C. (2021). Temozolomide: An Updated Overview of Resistance Mechanisms, Nanotechnology Advances and Clinical Applications. *Current Neuropharmacology*, *19*(4), 513–537. https://doi.org/10.2174/1570159X18666200626204005

Ostrom, Q. T., Gittleman, H., Stetson, L., Virk, S. M., & Barnholtz-Sloan, J. S. (2015). *Epidemiology of Gliomas* (pp. 1–14). https://doi.org/10.1007/978-3-319-12048-5_1

Pang, X., Yang, X., & Zhai, G. (2014). Polymer-drug conjugates: Recent progress on administration routes. In *Expert Opinion on Drug Delivery* (Vol. 11, Issue 7, pp. 1075–1086). Informa Healthcare. https://doi.org/10.1517/17425247.2014.912779

Parveen, S., & Sahoo, S. K. (2008). Polymeric nanoparticles for cancer therapy. In *Journal of Drug Targeting* (Vol. 16, Issue 2, pp. 108–123). https://doi.org/10.1080/10611860701794353

Pavoni, L., Perinelli, D. R., Ciacciarelli, A., Quassinti, L., Bramucci, M., Miano, A., Casettari, L., Cespi, M., Bonacucina, G., & Palmieri, G. F. (2020). Properties and stability of nanoemulsions: How relevant is the type of surfactant? *Journal of Drug Delivery Science and Technology*, *58*. https://doi.org/10.1016/j.jddst.2020.101772

Pérez-Herrero, E., & Fernández-Medarde, A. (2015). Advanced targeted therapies in cancer: Drug nanocarriers, the future of chemotherapy. In *European Journal of Pharmaceutics and Biopharmaceutics* (Vol. 93, pp. 52–79). Elsevier B.V. https://doi.org/10.1016/j.ejpb.2015.03.018

Perry, S. W., Norman, J. P., Barbieri, J., Brown, E. B., & Gelbard, H. A. (2011). Mitochondrial membrane potential probes and the proton gradient: A practical usage guide. In *BioTechniques* (Vol. 50, Issue 2, pp. 98–115). https://doi.org/10.2144/000113610

Peter, S., & Aderibigbe, B. A. (2019). Ferrocene-Based Compounds with Antimalaria/Anticancer Activity. *Molecules*, *24*(19), 3604. https://doi.org/10.3390/molecules24193604

Podolski-Renić, A., Bősze, S., Dinić, J., Kocsis, L., Hudecz, F., Csámpai, A., & Pešić, M. (2017). Ferrocene–cinchona hybrids with triazolyl-chalcone linkers act as pro-oxidants and sensitize human cancer cell lines to paclitaxel. *Metallomics*, *9*(8), 1132–1141. https://doi.org/10.1039/C7MT00183E

Prabhu, R. H., Patravale, V. B., & Joshi, M. D. (2015). Polymeric nanoparticles for targeted treatment in oncology: Current insights. In *International Journal of Nanomedicine* (Vol. 10, pp. 1001–1018). Dove Medical Press Ltd. https://doi.org/10.2147/IJN.S56932

Probst, C. E., Zrazhevskiy, P., Bagalkot, V., & Gao, X. (2013). Quantum dots as a platform for nanoparticle drug delivery vehicle design. *Advanced Drug Delivery Reviews*, *65*(5), 703–718. https://doi.org/10.1016/j.addr.2012.09.036

Qian, Y., Zhang, J., Xu, R., Li, Q., Shen, Q., & Zhu, G. (2021). Nanoparticles based on polymers modified with pH-sensitive molecular switch and low molecular weight heparin carrying Celastrol and ferrocene for breast cancer treatment. *International Journal of Biological Macromolecules*, *183*, 2215–2226. https://doi.org/10.1016/j.ijbiomac.2021.05.204

Qiu, H., Min, Y., Rodgers, Z., Zhang, L., & Wang, A. Z. (2017). Nanomedicine approaches to improve cancer immunotherapy. In *Wiley Interdisciplinary Reviews: Nanomedicine and Nanobiotechnology* (Vol. 9, Issue 5). Wiley-Blackwell. https://doi.org/10.1002/wnan.1456

Rai, V. K., Mishra, N., Yadav, K. S., & Yadav, N. P. (2018). Nanoemulsion as pharmaceutical carrier for dermal and transdermal drug delivery: Formulation development, stability issues, basic considerations and applications. In *Journal of Controlled Release* (Vol. 270, pp. 203–225). Elsevier B.V. https://doi.org/10.1016/j.jconrel.2017.11.049

Raval, N., Maheshwari, R., Kalyane, D., Youngren-Ortiz, S. R., Chougule, M. B., & Tekade, R. K. (2018). Importance of physicochemical characterization of nanoparticles in pharmaceutical product development. In *Basic Fundamentals of Drug Delivery* (pp. 369–400). Elsevier. https://doi.org/10.1016/B978-0-12-817909-3.00010-8

Rezende, L. F. M. de, Lee, D. H., Louzada, M. L. da C., Song, M., Giovannucci, E., & Eluf-Neto, J. (2019). Proportion of cancer cases and deaths attributable to lifestyle risk factors in Brazil. *Cancer Epidemiology*, *59*, 148–157. https://doi.org/10.1016/j.canep.2019.01.021

Rizwanullah, M., Amin, S., Mir, S. R., Fakhri, K. U., & Rizvi, M. M. A. (2018). Phytochemical based nanomedicines against cancer: current status and future prospects. In *Journal of Drug Targeting* (Vol. 26, Issue 9, pp. 731–

752). Taylor and Francis Ltd. https://doi.org/10.1080/1061186X.2017.1408115

Saiyin, W., Wang, D., Li, L., Zhu, L., Liu, B., Sheng, L., Li, Y., Zhu, B., Mao, L., Li, G., & Zhu, X. (2014). Sequential release of autophagy inhibitor and chemotherapeutic drug with polymeric delivery system for oral squamous cell carcinoma therapy. *Molecular Pharmaceutics*, *11*(5), 1662–1675. https://doi.org/10.1021/mp5000423

Sánchez-López, E., Guerra, M., Dias-Ferreira, J., Lopez-Machado, A., Ettcheto, M., Cano, A., Espina, M., Camins, A., Garcia, M. L., & Souto, E. B. (2019). Current applications of nanoemulsions in cancer therapeutics. In *Nanomaterials* (Vol. 9, Issue 6). MDPI AG. https://doi.org/10.3390/nano9060821

Sari, T. P., Mann, B., Kumar, R., Singh, R. R. B., Sharma, R., Bhardwaj, M., & Athira, S. (2015). Preparation and characterization of nanoemulsion encapsulating curcumin. *Food Hydrocolloids*, *43*, 540–546. https://doi.org/10.1016/j.foodhyd.2014.07.011

Seymour, L. W., Ferry, D. R., Kerr, D. J., Rea, D., Whitlock, M., Poyner, R., Boivin, C., Hesselewood, S., Twelves, C., Blackie, R., Schatzlein, A., Jodrell, D., Bissett, D., Calvert, H., Lind, M., Robbins, A., Burtles, S., Duncan, R., & Cassidy, J. (2009). Phase II studies of polymer-doxorubicin (PK1, FCE28068) in the treatment of breast, lung and colorectal cancer. *International Journal of Oncology*, *34*(6), 1629–1636. https://doi.org/10.3892/ijo_00000293

Shaker, D. S., Ishak, R. A. H., Ghoneim, A., & Elhuoni, M. A. (2019). Nanoemulsion: A review on mechanisms for the transdermal delivery of hydrophobic and hydrophilic drugs. In *Scientia Pharmaceutica* (Vol. 87, Issue 3). MDPI AG. https://doi.org/10.3390/scipharm87030017

Singh, Y., Meher, J. G., Raval, K., Khan, F. A., Chaurasia, M., Jain, N. K., & Chourasia, M. K. (2017). Nanoemulsion: Concepts, development and applications in drug delivery. In *Journal of Controlled Release* (Vol. 252, pp. 28–49). Elsevier B.V. https://doi.org/10.1016/j.jconrel.2017.03.008

Stevens, M. F., Hickman, J. A., Langdon, S. P., Chubb, D., Vickers, L., Stone, R., Baig, G., Goddard, C., Gibson, N. W., & Slack, J. A. (1987). Antitumor activity and pharmacokinetics in mice of 8-carbamoyl-3-methyl-imidazo[5,1-d]-1,2,3,5-tetrazin-4(3H)-one (CCRG 81045; M & B 39831), a novel drug with potential as an alternative to dacarbazine. *Cancer Research*, *47*(22), 5846–5852.

Strobel, H., Baisch, T., Fitzel, R., Schilberg, K., Siegelin, M. D., Karpel-Massler, G., Debatin, K.-M., & Westhoff, M.-A. (2019). Temozolomide and Other Alkylating Agents in Glioblastoma Therapy. *Biomedicines*, *7*(3), 69. https://doi.org/10.3390/biomedicines7030069.

Stupp, R., Mason, W. P., van den Bent, M. J. et al. (2005). Radiotherapy plus Concomitant and Adjuvant Temozolomide for Glioblastoma. *New England Journal of Medicine, 352*(10), 987-996. https://doi.org/10.1056/nejmoa043330.

Tian, J., Chen, J., Ge, C., Liu, X., He, J., Ni, P., & Pan, Y. (2016). Synthesis of PEGylated Ferrocene Nanoconjugates as the Radiosensitizer of Cancer

Cells. *Bioconjugate Chemistry*, *27*(6), 1518–1524. https://doi.org/10.1021/acs.bioconjchem.6b00168

Torchilin, V. P. (2005). Recent advances with liposomes as pharmaceutical carriers. In *Nature Reviews Drug Discovery* (Vol. 4, Issue 2, pp. 145–160). https://doi.org/10.1038/nrd1632

Tran, S., DeGiovanni, P., Piel, B., & Rai, P. (2017). Cancer nanomedicine: a review of recent success in drug delivery. *Clinical and Translational Medicine*, *6*(1). https://doi.org/10.1186/s40169-017-0175-0

Vallet-Regi, M., Rámila, A., del Real, R. P., & Pérez-Pariente, J. (2001). A New Property of MCM-41: Drug Delivery System. *Chemistry of Materials*, *13*(2), 308–311. https://doi.org/10.1021/cm0011559

Vargason, A. M., Anselmo, A. C., & Mitragotri, S. (2021a). The evolution of commercial drug delivery technologies. In *Nature Biomedical Engineering* (Vol. 5, Issue 9, pp. 951–967). Nature Research. https://doi.org/10.1038/s41551-021-00698-w

Vargason, A. M., Anselmo, A. C., & Mitragotri, S. (2021b). The evolution of commercial drug delivery technologies. *Nature Biomedical Engineering*, *5*(9), 951–967. https://doi.org/10.1038/s41551-021-00698-w

Wakaskar, R. R. (2018). Promising effects of nanomedicine in cancer drug delivery. *Journal of Drug Targeting*, *26*(4), 319–324. https://doi.org/10.1080/1061186X.2017.1377207

Walia, N., Zhang, S., Wismer, W., & Chen, L. (2022). A low energy approach to develop nanoemulsion by combining pea protein and Tween 80 and its application for vitamin D delivery. *Food Hydrocolloids for Health*, *2*. https://doi.org/10.1016/j.fhfh.2022.100078

Wang, F., Li, C., Cheng, J., & Yuan, Z. (2016). Recent advances on inorganic nanoparticle-based cancer therapeutic agents. In *International Journal of Environmental Research and Public Health* (Vol. 13, Issue 12). MDPI. https://doi.org/10.3390/ijerph13121182

Wang, J., Wang, H., & Qian, H. (2018). Biological effects of radiation on cancer cells. *Military Medical Research*, *5*(1), 20. https://doi.org/10.1186/s40779-018-0167-4

Wesolowski, J. R., Rajdev, P., & Mukherji, S. K. (2010). Temozolomide (Temodar). *American Journal of Neuroradiology*, *31*(8), 1383–1384. https://doi.org/10.3174/ajnr.A2170

Whittlesey, K. J., & Shea, L. D. (2004). Delivery systems for small molecule drugs, proteins, and DNA: The neuroscience/biomaterial interface. In *Experimental Neurology* (Vol. 190, Issue 1, pp. 1–16). https://doi.org/10.1016/j.expneurol.2004.06.020

Xu, J., Liao, K., Jiang, H., & Zhou, W. (2018). Research progress of novel inorganic nanometre materials carriers in nanomedicine for cancer diagnosis and treatment. *Artificial Cells, Nanomedicine, and Biotechnology*, *46*(sup3), 492–502. https://doi.org/10.1080/21691401.2018.1499665

Yang, F., Jin, C., Subedi, S., Lee, C. L., Wang, Q., Jiang, Y., Li, J., Di, Y., & Fu, D. (2012). Emerging inorganic nanomaterials for pancreatic cancer diagnosis and treatment. In *Cancer Treatment Reviews* (Vol. 38, Issue 6, pp. 566–579). https://doi.org/10.1016/j.ctrv.2012.02.003

Yang, Y., & Yu, C. (2016). Advances in silica based nanoparticles for targeted cancer therapy. *Nanomedicine: Nanotechnology, Biology and Medicine*, *12*(2), 317–332. https://doi.org/10.1016/j.nano.2015.10.018

Yeon Nam, J., & de Groot, J. F. (2017). *ASSOCIATED CONTENT Treatment of Glioblastoma*. https://doi.org/10.1200/JOP

Yezhelyev, M., Yacoub, R., & O'Regan, R. (2009). Inorganic nanoparticles for predictive oncology of breast cancer. In *Nanomedicine* (Vol. 4, Issue 1, pp. 83–103). https://doi.org/10.2217/17435889.4.1.83

ANEXO A

Nek1-inhibitor and temozolomide-loaded microfibers as a co-therapy strategy for glioblastoma treatment

Artigo científico publicado em coautoria na revista *International Journal of Pharmaceutics* (fator de impacto 5.8).

International Journal of Pharmaceutics 617 (2022) 121584

Contents lists available at ScienceDirect

International Journal of Pharmaceutics

journal homepage: www.elsevier.com/locate/ijpharm

Nek1-inhibitor and temozolomide-loaded microfibers as a co-therapy strategy for glioblastoma treatment

Luiza Steffens Reinhardt [a,b,1], Ana Moira Morás [a,b,1], Jeferson Gustavo Henn [a,b,1], Pablo Ricardo Arantes [c], Matheus Bernardes Ferro [a], Elizandra Braganhol [b], Priscila Oliveira de Souza [b], Josias de Oliveira Merib [d], Gabriela Ramos Borges [d], Carolina Silveira Dalanhol [d], Mabilly Cox Holanda de Barros Dias [e], Michael Nugent [f], Dinara Jaqueline Moura [a,*]

[a] Laboratory of Genetic Toxicology, Federal University of Health Sciences of Porto Alegre (UFCSPA), Porto Alegre, Rio Grande do Sul, Brazil
[b] Biosciences Graduation Course, UFCSPA, Porto Alegre, Rio Grande do Sul, Brazil
[c] Department of Bioengineering, University of California, Riverside, USA
[d] Analytical Center, UFCSPA, Porto Alegre, Rio Grande do Sul, Brazil
[e] Bioscience Research Institute, Technological University of the Shannon, Midlands Midwest (TUS), Athlone, Co. Westmeath, Ireland
[f] Materials Research Institute, TUS, Athlone, Co. Westmeath, Ireland

ARTICLE INFO

Keywords:
Glioblastoma
Temozolomide
NIMA-related kinase 1
Polyvinyl alcohol
Microfibers
Drug delivery systems
Electrospinning

ABSTRACT

Malignant glioblastoma (GB) is the predominant primary brain tumour in adults, but despite the efforts towards novel therapies, the median survival of GB patients has not significantly improved in the last decades. Therefore, localised approaches that treat GB straight into the tumour site provide an alternative to enhance chemotherapy bioavailability and efficacy, reducing systemic toxicity. Likewise, the discovery of protein targets, such as the NIMA-related kinase 1 (Nek1), which was previously shown to be associated with temozolomide (TMZ) resistance in GB, has stimulated the clinical development of target therapy approaches to treat GB patients. In this study, we report an electrospun polyvinyl alcohol (PVA) microfiber (MF) brain-implant prepared for the controlled release of Nek1 protein inhibitor (iNek1) and TMZ or TMZ-loaded nanoparticles. The formulations revealed adequate stability and drug loading, which prolonged the drugs' release allowing a sustained exposure of the GB cells to the treatment and enhancing the drugs' therapeutic effects. TMZ-loaded MF provided the highest concentration of TMZ within the brain of tumour-bearing rats, and it was statistically significant when compared to TMZ via intraperitoneal (IP). All animals treated with either co-therapy formulation (TMZ + iNek1 MF or TMZ nanoparticles + iNek1 MF) survived until the endpoint (60 days), whereas the Blank MF (drug-unloaded), TMZ MF and TMZ IP-treated rats' median survival was found to be 16, 31 and 25 days, respectively. The tumour/brain area ratio of the rats implanted with either MF co-therapy was found to be reduced by 5-fold when compared to Blank MF-implanted rats. Taken together, our results strongly suggest that Nek1 is an

Abbreviations: ALT, alanine aminotransferase; ALP, alkaline phosphatase; ATM, ataxia telangiectasia mutated; ATR, ataxia telangiectasia and Rad3-related protein; AST, aspartate aminotransferase; BBB, blood-brain barrier; CK, creatine kinase; CN, coordination number; DMEM, Dulbecco's Modified Eagle Medium; DDR, DNA damage response; DDS, drug delivery systems; DSB, double-strand breaks; EE%, percentage of entrapment efficiency; FBS, foetal bovine serum; GB, malignant glioblastoma; GGT, gamma-glutamyl transferase; H2AX, histone 2AX; iNek1, Nek1 inhibitor; JNK2, c-Jun NH (2)-terminal kinase 2; MGMT, O^6-methylguanine-DNA methyltransferase; MF, microfiber; Mre11, double strand break repair nuclease; MTT, methylthiazolyldiphenyl-tetrazolium bromide; Nek1, NIMA-related kinase 1; NMR, nuclear magnetic resonance; NP, nanoparticles; PBS, phosphate-buffered saline; PVA, polyvinyl alcohol; SASA, solvent-accessible surface area; SD, standard deviation; TMZ, temozolomide; UV, ultraviolet; VDAC1, mitochondrial voltage-dependent anion channel.

* Corresponding author at: Federal University of Health Sciences of Porto Alegre – UFCSPA, Sarmento Leite Street, 245, Lab. 714, Porto Alegre, Rio Grande do Sul, Brazil.

E mail addresses: luizasteffens@live.com, luizast@ufcspa.edu.br (L.S. Reinhardt), anamoiramoras@gmail.com, anamoira@ufcspa.edu.br (A.M. Morás), jefersonghenn@gmail.com, jefersonh@ufcspa.edu.br (J.G. Henn), pabloa@ucr.edu (P.R. Arantes), matheusbf@ufcspa.edu.br (M.B. Ferro), ebraganhol@ufcspa.edu.br (E. Braganhol), priscilaoliveira2@hotmail.com, priscilasouza@ufcspa.edu.br (P.O. de Souza), josias@ufcspa.edu.br (J. de Oliveira Merib), gabriela@ufcspa.edu.br (G.R. Borges), mdbdias@research.ait.ie (C.S. Dalanhol), cdalanhol@gmail.com, carolinasd@ufcspa.edu.br (M.C.H. de Barros Dias), michael.nugent@tus.ie (M. Nugent), dinaram@ufcspa.edu.br (D.J. Moura).

[1] The authors contributed equally.

https://doi.org/10.1016/j.ijpharm.2022.121584
Received 4 November 2021; Received in revised form 29 January 2022; Accepted 11 February 2022
Available online 22 February 2022

important GB oncotarget and the inhibition of Nek1's activity significantly decreases GB cells' viability and tumour size when combined with TMZ treatment.

1. Introduction

Malignant glioblastoma (GB) is the predominant primary brain tumour in adults, with a median survival of < 2 years (Norouzi et al., 2016; Tseng et al., 2016; Brodbelt et al., 2015; Rape et al., 2014; Tan et al., 2020). Currently, surgical resection followed by radiotherapy and adjuvant chemotherapy is considered the standard therapy for GB patients (Tseng et al., 2015; Huang et al., 2016). However, GB exhibits a high capacity of infiltrating normal tissue, which makes it practically impossible the complete tumour resection through surgery, and even after resection, the recurrent GB invasive cells can form tumours within few centimetres of the original site (Tseng et al., 2015; Huang et al., 2016; Weller et al., 2013; Sawyer et al., 2006).

Amid the obstacles of GB therapy, the blood–brain barrier (BBB) and its tortuous angiogenesis restrict effective drug delivery to the brain, contributing to chemotherapy inefficacy (Sun et al., 2017; Irani et al., 2017; Wei et al., 2014; Fan et al., 2015; Park et al., 2017). Several drugs fail to achieve therapeutic concentrations at the tumour site, even at toxic systemic level concentrations (Tseng et al., 2015; Tseng et al., 2013). Therefore, temozolomide (TMZ) is still being used as the standard chemotherapeutical drug by oral administration (Denny et al., 1994), since the use of this alkylating agent as adjuvant therapy after surgery has been widely accepted as the most effective and well-tolerated option (Akbar et al., 2009).

The discovery of potent genetic and protein targets has stimulated the clinical development of novel therapeutic approaches to treat patients with GB (Zhu et al., 2016). However, several of these approaches, including O^6-benzylguanine (Quinn et al., 20092009) and AZD0156 (Abida et al., 2018), which inhibit O^6-methylguanine-DNA methyltransferase (MGMT) and ataxia telangiectasia mutated (ATM) respectively, fail in offering improvements in patients' prognostics. One of the reasons that justify the clinic failure of these approaches may be the incapacity of conventional treatment modalities to reach the tumour site using tolerable doses of chemotherapeutical agents throughout highly disseminated tumours and to target oncotargets that are contributing to tumour resistance (Westphal and Lamszus, 2011). Nek1 (NIMA-related Kinase 1) is a member of the Nek family kinases (Patil et al., 2013; White and Quarmby, 2008), acting in mitosis (Patil et al., 2013; White and Quarmby, 2008) and DNA damage repair (Liu et al., 2013; Spies et al., 2016). Nek1 is required for activating DNA damage response (DDR) pathways through ATR (Liu et al., 2013); moreover, its upregulation has an anti-apoptotic effect through phosphorylation and deactivation of the mitochondrial voltage-dependent anion channel (VDAC1) (Chen et al., 2009; Chen et al., 2010; Chen et al., 2014). In addition, other DNA damage-related proteins including Rad54 and Mre11, are associated with Nek1 (Spies et al., 2016), and recently, Higelin et al. demonstrated that compromised DDR machinery caused by *NEK1* mutation in motoneurons of amyotrophic lateral sclerosis patients lead to accumulation of DNA damage and increased cell death (Higelin et al., 2018), highlighting the role of this protein in DDR. In a cancer context, Nek1 has been associated with prostate cancer progression (Singh et al., 2019; Singh et al., 2019; Singh et al., 2020), decreased sensitivity to DNA-damaging therapy in renal cell carcinoma (Chen et al., 2014), reduced disease-free survival in cervical cancer (Freund et al., 2020), malignancy and aggressiveness of thyroid cancers (Melo-Hanchuk et al., 2020), and TMZ-resistance in GB cells (Zhu et al., 2016). In glioma cells, Zhu et al. suggested that Nek1 may be a novel and important oncotarget since its role in GB malignancy is related to cell growth promotion and chemoresistance (Zhu et al., 2016). Our unpublished data suggest that Nek1 knockout in U87MG GB cells increases the cells sensitivity to DNA-damaging agents such as TMZ and a radiomimetic drug, and modulates the DDR. Taken together, these studies imply the importance of inhibiting the activity of Nek1 during therapies that activate the DDR.

To improve the therapeutic effectiveness of TMZ and decrease its side effects such as hematologic toxicity (Stupp et al., 2005; Corsa et al., 2006; Mutter and Stupp, 2006; Vera et al., 2004); *in situ* drug delivery systems (DDS) can be administered to prevent tumour recurrence. Localised and controlled approaches that treat GB directly into the tumour site provide an alternative to enhance chemotherapy efficacy and reduce systemic toxicity (Ranganath and Wang, 2008; Han et al., 2017; Kuramitsu et al., 2014; Hirschberg et al., 2013). Due to their biocompatibility, polymers are one of the most promising resources for DDS development (Bei et al., 2009). Several DDS, such as micro- and nanosystems, and wafers have been developed to provide adequate drug release into the GB site (Irani et al., 2017; Ranganath and Wang, 2008; Ahmed et al., 2006; Kumarnaraharisetti et al., 2007; Hernán Pérez de la Ossa et al., 2013; Scott et al., 2011; Kim et al., 2007; Hua et al., 2011; Ramachandran et al., 2017; Ramachandran et al., 2014; Játiva and Ceña, 2017; Cheng et al., 2014; Mangraviti et al., 2016). Nevertheless, given the high interstitial pressure in the brain, micro- and nanoparticles (NP) can be easily expelled from the target site, and these formulations frequently present burst release of loaded drugs causing neurotoxicity (Irani et al., 2017, Fernandes et al). Additionally, hydrogels and wafers have low surface areas resulting in inappropriate and inconsistent drug dissolution (Norouzi et al., 2016, Ranganath and Wang, 2008).

Our research group has been working with polyvinyl alcohol (PVA), which is a noteworthy choice for designing DDS since it is biodegradable and presents very low toxicity (Ranganath and Wang, 2008, Ahmed et al., 2006, Pourgholi et al., 2016, Steffens et al, 2020, Reinhardt et al, 2021, Seba et al., 2021). Recently, we produced dacarbazine-PVA nanofibers to treat GB and this formulation showed great mechanical and delivery properties improving the *in vitro* efficacy of dacarbazine (Steffens et al., 2020). Hence, in this study, we aimed the development of electrospun PVA microfibers (MF) to be used as brain implants for the controlled release of a co-therapy of TMZ and Nek1 inhibitor (iNek1). Moreover, this study aimed the evaluation of Nek1 as a GB oncotarget. Our results strongly indicate that Nek1 inhibition could improve therapy outcome *in vivo* when combined with TMZ treatment, and the use of implantable DDS could enhance therapy efficacy and facilitate the delivery of compounds to the brain.

2. Material and methods

2.1. In silico evaluations

2.1.1. Molecular modelling

Nek1 complex was obtained through molecular modelling of missing loops of PDB ID 4APC model. The process was performed on Modeller v.9.19 (Webb and Sali, 2016). For each model was build 1000 models and selected the one with the best stereo chemical quality with DOPE assessment method evaluation. The quality of the model was checked with Procheck (Laskowski, 2001), Verify 3D (Bowie et al., 1991; Lüthy et al., 1992) and MolProbity (Chen et al., 2010) software.

2.1.2. Molecular docking protocol and validation

Molecular docking assays were performed using AutoDock Vina (Trott and Olson, 2010). AutoDock Vina employs a gradient-based conformational search method and outlines the search space by a grid box defined by the box centre coordinates and its dimensions of x, y and z in grid resolution internally assigned to 1 Ã… (Trott and Olson, 2010). The number of binding modes was set to 1000 and exhaustiveness set to 200 to control how many times the calculations are repeated. The grid

dimensions were 40 × 40 × 40 (x, y, z) points centre on the binding site −26.22 × 11.13 × 16.78 (x, y, z). The scoring of the generated docking poses and ranking of the ligands were based on the Vina empirical scoring function. All rotatable dihedral angles of iNek1 were considered as flexible. The orientations of the iNek1 molecule at the binding sites on Nek1 and JNK2 (PDB ID 3NPC) proteins were chosen from docked conformations as representative of the lower energy clusters generated by Autodock Vina.

2.1.3. Nomenclature and software

For nomenclature and symbols, the IUPAC recommendations were applied in the present work. Concerning MD simulations, the GROMACS 2019 simulation suite (Pronk et al., 2013) was used; along with the GROMOS 53A6 force field (Oostenbrink et al., 2004) and the GROMOS 53A6GLYC force field (Pol-Fachin et al., 2012; Pol-Fachin et al., 2014). For iNek1 and TMZ molecules; the parameters of previous work were selected (Polêto et al., 2018). For the manipulation and generation of the entire PVA molecule; the Assemble! (Degiacomi et al., 2016) tool was used. This tool makes easier the simulation of polymeric systems. Assemble! permits the creation of polymers from monomer building blocks with a user-defined force field. For the manipulation and visualisation of structures; the software VMD (Humphrey et al, 1996) and PyMOL (Delano) were used.

2.1.4. Molecular dynamics simulations

For the construction of the system, the same approach of our previous paper has been utilised (Steffens et al., 2020). The system was generated by applying the Assemble! tool (Degiacomi et al., 2016) under the following experimental data: 1 molecule of PVA (1765 units) was set as 5%, the iNek1 as 0.05% and the TMZ as 0.05%, resulting on 8 molecules of the drugs (4 iNek1 and 4 TMZ) for 1 PVA molecule. Two systems were constructed, PVA with four molecules of iNek1 and four molecules of TMZ and eight drugs (iNek1 and TMZ) molecules in water. To randomise the structure and relax local stresses, PVA chain was exposed to the steepest descent energy minimisation and 1 ns of molecular dynamics pre-equilibration of the polymer around the drug, as previously described (Steffens et al., 2020; Kyrychenko et al., 2017; Tallury and Pasquinelli, 2010). Subsequent to the pre-equilibration steps, the dodecahedron box was solvated with SPC water model (Berendsen et al., 1987) and periodic boundary conditions. Prior to this process, to retain the physiological ionic strength 0.15 M NaCl was added to the aqueous solution. The LINCS algorithm (Hess et al., 1997) was selected to constrain covalent bond lengths. This way, an integration step of 2 fs was applied. As for the electrostatic interactions, calculations were performed by the particle mesh Ewald (PME) method (Darden et al., 1993). The pressure barostat chosen was Parrinello–Rahman (Parrinello and Rahman, 1981; Nosé and Klein, 1983), with a 2.0 ps coupling constant, while the temperature thermostats chosen were V-rescale (NVT step) (Bussi et al., 2007) and Nosé–Hoover (NPT equilibration and production MD) (Nosé, 1984; Hoover, 1985), with a coupling constant of $\tau = 0.5$. Constant temperature of 298 K and constant pressure of 1 atm were also applied. Steepest Descent algorithm was used in the energy minimisations performed. First, two simulations of equilibration were carried out with position restraints: an NVT and an NPT of 2 ns and 5 ns, respectively. Not only that, 500 ns of unrestrained NPT MD simulations were carried out for each system (iNek1-TMZ and PVA-iNek1-TMZ), creating the production run from which data were collected. Each system was simulated in three independent runs, with distinct starting velocities, to filter conformational events of low probability (Nemec and Hoffmann, 2017; Perez et al., 2016). For analysis, coordination number is the total number of neighbours of a nitrogen atom on the imidazole rings, obtained from optimal binding distance calculated by radial distribution function.

2.2. Preparation of temozolomide-loaded nanocarriers

Temozolomide (TMZ; Merck, Darmstadt, Germany)-loaded stearic acid (Merck) nanocarriers (TMZ NP) were produced by solvent diffusion method according to Hafeez et al. (Hafeez and Kazmi, 2017) with minor modifications. TMZ (10% w/w) and stearic acid were suspended in an organic phase prepared using acetone:ethanol (Merck) mixture (1:1). Then, the aqueous phase was prepared by heating up to 70 °C distilled water (dH_2O) on a continuous stirring. Finally, the organic phase was poured and mixed into the aqueous phase during 30 min. After cooling at room temperature, the mixture was sonicated for 5 min and frozen overnight. Later, the mixture was lyophilised in a freeze dryer (Heto, LyoLab 3000, Thermo Fisher Scientific, MA, United States). For comparison purposes, blank nanocarriers (Blank NP) were prepared by using stearic acid only.

2.3. Particle size and zeta potential

Particle size and zeta potential analyses were carried out on the Beckman Coulter Delsa Nano C (Beckman Coulter, CA, United States). For particle sizing, the sample was run 9 times to ensure that results were statistically relevant. Analysis was carried out on the measured autocorrelation functions using the non-negative least square algorithm. Very large aggregate results (>5 μm) were removed from the analysis as the fitting and algorithm cannot provide accurate results at this size. For zeta potential, the sample was run 3 times (as each run is repeated 10 times and averaged to provide the result). The applied voltage on the electrodes of the cell was 60 mV.

2.4. Preparation of microfibers

Polyvinyl alcohol (PVA; Merck) hydrogel solutions were produced by dissolving PVA at 10% (w/v) in dH_2O at 90 °C, under continuous stirring until its whole solubilisation. After the solutions were colder, ethanol (10% v/v) was added. Then, different solutions were prepared by adding known amounts of TMZ (0.01% w/w) or TMZ and Nek1 inhibitor (0.01% w/w; iNek1; JNK inhibitor II; Merck) solutions prepared in DMSO or TMZ NP (10% w/w; TMZ final concentration in nanocarriers: 0.1% w/w) or TMZ NP and iNek1 solution into the PVA solution. The formulations were electrospun (Spraybase, Co. Kildare, Ireland) through a blunt-end 20-gauge needle, with a flow rate of 0.5 mL/h, a conductivity of 9 kV, and a distance of 5 cm between the needle tip and the collector plate. For comparison purposes, Blank MF were prepared by using only PVA or by adding Blank NP into a PVA solution prior electrospinning. For visualisation of fluorescent fibers, curcumin (Merck) MF were prepared by adding Blank NP into a curcumin (0.01% w/w)-PVA solution prior electrospinning.

2.5. Microfiber sterilisation and sterility validation

Isolated colonies of *Escherichia coli* (*E. coli*) (NC 12241) and *Staphylococcus aureus* (*S. aureus*) (NC 12981) from stock strains cryogenised at −80 °C were obtained through isolation seeding and grown overnight. Each colony of each bacterium was separately suspended in 5 mL of sterile PBS (Thermo Fisher Scientific) and standardised with spectrophotometer by 0.5 McFarland scale (1.5×10^8 CFU/mL in 600 nm wavelength). Subsequently, 50 μL of standardised bacterial suspension were added into each polymer sample (1 cm^2 each sample) on 3 cm^2 diameter sterile plates. Contaminated samples were sterilised by total immersion in 500 μL of isopropanol (IPA; Merck) for ten seconds, and subsequently drained. Serial dilution of samples was conducted in a 96-well sterile microplate previously filled with 270 μL of sterile PBS until the fifth well. Each sample was dispersed into 1 mL of sterile PBS and briefly mixed. From this dilution, 30 μL were taken out and transferred to the first well in the microplate, briefly mixed, being now the 10^{-1} dilution, and this went through until the 10^{-5} dilution. This procedure

was repeated for each sample separately. From each dilution 100 μL were taken and inoculated through spread plate method in agar plate with 20 mL of solid nutrient agar (NA; Merck) with a bent rod at once. Other three replicates were made with micro drop technique (10 μL) in NA plates. Plates were then incubated at 37 °C for 24 h. After the first reading, the plates were left on incubator for 2 weeks to analyse the growth possibility and no bacterial growth was observed on sterilised plates.

2.6. Microfiber size and morphology analysis

The fibers' and particles' morphologies were observed via scanning electron microscope (SEM; Tescan Mira XMU SEM, TESCAN, Brno, Czech Republic). Back-scattered electron mode was used with magnifications ranging from 10 kX to 30 kX after the fibers were sputtered with gold. For fiber size analysis, ImageJ software (ImageJ 1.53v, National Institute of Health, Bethesda, MD, United States) was used and the mean diameter was extracted by analysing >300 fibers. Fluorescence images of the fibers were acquired using a Leica DM 2000 confocal microscope with an x40 oil lens (Leica Microsystems, Ashbourne, Ireland). Image acquisition was achieved by using the LAS V3.8 software (Leica Microsystems, Ashbourne, Ireland).

2.7. Solid-state NMR

The stability of the drugs and the polymer after formulation preparation was evaluated by nuclear magnetic resonance (NMR) spectroscopy. The analysis was executed using a Bruker 400 MHz Avance III HD (Bruker, MA, United States) equipped with a 3.2 mm H/X CPMAS probe.

2.8. Determination of the encapsulation efficiency of TMZ and iNek1

To measure the percent encapsulation efficiency (EE%) and the total amount of loaded TMZ and iNek1, MF or NP were entirely dissolved in DMSO (Merck) and the amount of released drug was measured by ultraviolet (UV) light on a Shimadzu UV 1280 spectrometer (Shimadzu, Kyoto, Japan) at 328 and 407 nm, respectively. Loaded formulations were used to generate standard curves for each drug. Empty (blank) formulations were also dissolved in DMSO and used as the blank for the spectrometer reading. The EE% was determined as follows:

$$EE\% = \frac{actualamountofdrugrelease}{theoreticalamountofloadeddrug} X100$$

2.9. In vitro drug release studies

Drug dissolution studies were performed using a Distek Model 2500 Dissolution System (Distek Inc., NJ, United States). The samples were tested in PBS (Thermo Fisher Scientific) buffers (pH 7.4 or 6.8) at 37 °C. Each vessel contained 300 mL of dissolution media and a stir rate of 50 rpm was used. Samples were taken at set intervals and measured by UV light on a Shimadzu UV 1280 spectrometer (Shimadzu). Loaded formulations were used to generate standard curves for each drug. Empty (blank) formulations were used as the blank for the spectrometer reading.

2.10. Nek1 protein expression

U87MG GB cells were maintained in Dulbeco's Modified Eagle Medium (DMEM), supplemented with 10% foetal bovine serum (FBS), penicillin, streptomycin and L-glutamine (Thermo Fisher Scientific) at 37 °C in a 5% CO_2 humidified atmosphere. Cells were treated with TMZ (75 μM) for 24 h. After treatment, the cells were trypsinised (Thermo Fisher Scientific), 15 min fixed with 3.7% paraformaldehyde (v/v) (Merck), permeabilised with 0.5% Triton X-100 (v/v) (Merck) in PBS (Thermo Fisher Scientific) buffer for 15 min and blocked with 10% FBS in PBS buffer (v/v) for 1 h. In the next step, the samples were incubated overnight at 4 °C with the following diluted antibodies: 1:100 Alexa Fluor 488 Mouse anti- γH2AX (pS-139) (BD Biosciences, CA, United States), 1:50 anti-vinculin-FITC (Merck) or 1:100 anti-Nek1 (Merck). Anti-rabbit Alexa Fluor 594 (Life Technologies) at a dilution of 1:500 was used as the secondary antibody for Nek1 staining. The samples were placed in a glass slide and each slide was dropwise stained with Hoechst 33,258 (Thermo Fisher Scientific) for cells' nuclei visualisation. The slides were observed in a cell imaging system (IN Cell Analyser 2200, GE Healthcare Life Sciences, NJ, United States). Nek1 protein expression was also evaluated by western blot. Briefly, U87MG, A172, M059J, T98G and U138MG cells were treated with TMZ (75 μM) for 24 h and protein extracts were prepared by using lysis buffer and separated by sodium dodecyl sulphate–polyacrylamide gel electrophoresis. The membranes were blocked with 5% skim milk in tris-buffered saline with 0.05% of Tween 20 (Merck) (v/v) for 1 h and incubated overnight at 4 °C with following antibodies at a dilution of 1:500 anti-Nek1 (Merck) or 1:500 anti-β-actin (Santa Cruz Biotechnology, CA, United States). The secondary antibodies used were 1:3000 mouse-anti-rabbit or 1:3000 goat-anti-mouse (Santa Cruz Biotechnology). The membranes were incubated with Luminol-based Enhanced Chemiluminescent mix and exposed to films to develop.

2.11. Cell viability evaluation

Two different media (pH 6.8 or 7.4) were used to perform this evaluation. The drugs screening and the formulations cytotoxicity potential were determined by using methylthiazolyldiphenyl-tetrazolium bromide (MTT; Merck) colorimetric assay. Firstly, TMZ and iNek1 stock solutions prepared in DMSO (stock solution TMZ: 21 mM and iNek1: 13.6 mM) were further diluted in 10% FBS DMEM and tested aiming to select the IC_{50} used in the following experiments. Briefly, U87MG cells were seeded in 96-well plates at $1x10^5$ cells/well, following 24 h, cells were treated with increasing concentrations of TMZ (25–200 μM) or iNek1 (15–240 μM) for 48 h. Following treatment, cells were incubated with MTT for 3 h at 37 °C. Then, formazan crystals were dissolved in DMSO, and the absorbance was recorded at 540 nm in a microplate reader (BioTek Synergy HT, Swindon, United Kingdom). The cell viability was assessed by using the negative control (cells treated with vehicle: 0.1% DMSO) as 100%. After this screening, U87MG cells were treated with several formulations at the IC_{50} previously determined or with the neat drugs during 2, 5 or 5 (+2 days of recovery = media replenish) days. C6 cells were also treated with TMZ (75 μM) or the co-treatment (TMZ 75 μM + iNek1 50 μM) during 5 days. For the 3D cell culture assessment, cells were incubated with magnetic NP (NanoShuttle™-PL, Greiner Bio-One, Frickenhausen, Germany) for 24 h at 37 °C, thereafter disposed into a cell-repellent 96-well plate at $1x10^5$ cells/well and incubated for 24 h over a magnetic drive. Then, cells were exposed to complete media (negative control), neat drugs or the formulations for 5 (+2 day of recovery) days. Spheroid size was analysed by using an EVOS FL Auto 2, Imaging System microscope (Thermo Fisher Scientific) and calculated by using ImageJ software.

2.12. Animals

All experimental procedures were reviewed, approved, and performed in accordance with the Federal University of Health Sciences from Porto Alegre's Ethics Committee guidelines (approval number: 603/18). Sixty days-old and around 300 g male Wistar rats were obtained from animal housing facility of UFCSPA and were maintained in the laboratory at 22 ± 2 °C, with water and food *ad libitum*, and under a 12:12 h light and dark photoperiod.

2.13. In vivo evaluation

C6 glioma cells were cultured in DMEM supplied with 10% FBS,

penicillin, streptomycin and L-glutamine at 37 °C in a 5% CO_2-humidified atmosphere incubator to approximately 70% confluence. Then, cells were trypsinised, counted with trypan blue staining and a total of $1x10^6$ cells were suspended in 3 μL of free-FBS DMEM. The animals were anesthetised using ketamine/xylazine (Agener Uniao, SP, Brazil), and the cell suspension was implanted by stereotaxic surgery into the right striatum of the brain of the rats at a depth of 6.0 mm (coordinates with regard from bregma: 0.5 mm posterior and 3.0 mm lateral) with injection flow of 1 μL/min (Braganhol et al., 2009). On the tenth day from tumour inoculation, the animals were sedated using ketamine/xylazine and a circular incision (around 5 mm of diameter) was made in the brain cap using stereotaxic equipment (following the same coordinates as previously mentioned) to implant the MF (15 mg/MF) (Fig. 5A). The animals were randomly divided into six groups with three to eight animals each: Blank MF (control formulation), TMZ MF, TMZ + iNek1 MF, TMZ NP + Blank MF, TMZ NP + iNek1 MF or intraperitoneal (IP) TMZ (5 mg/kg; once a day for five days). Post-operative pain was evaluated for the first five hours, and then daily using the grimace scale (Sotocina et al., 2011). Three animals/group of Blank MF, TMZ MF or TMZ NP + Blank MF were followed up for two days (for TMZ quantification within the brain). The other animals were followed up until they reached endpoint criteria (moribund animal and/or loss of > 15% of initial body weight) up to sixty days. Clinical and behavioural changes were monitored daily, and signs of pain were treated by IP opioid administration (tramadol 12.5 mg/kg; every eight hours up to five days). Body weight was recorded biweekly with a digital weighing balance for body weight change evaluation and at the end of treatment. All animals were euthanised by overdose of ketamine and xylazine. After euthanasia, the brain tissue was rapidly removed. The brains were excised and preserved in 3.7% formaldehyde solution (v/v; pH 7.4) or were washed in PBS (Thermo Fisher Scientific) and kept in −80 °C. The samples processing and hematoxylin and eosin slides preparation were performed by UFCSPA's Pathology Laboratory according to established protocols. The slides were scanned by using an EVOS FL Auto 2, Imaging System microscope (Thermo Fisher Scientific) and measured by using ImageJ software. The brain and the tumour areas were measured and the tumour/brain area ratio was calculated. Kidney and lung tissues were collected for histological evaluation and preserved in formaldehyde solution. Blood samples were collected from the abdominal aorta artery by puncture in a test tube without anticoagulant substances to obtain serum samples, followed by immediate centrifugation at 3000 rpm for 15 min. The collected serum was preserved at −70 °C for biochemical analysis.

2.14. Biochemical analysis

Urea, creatinine, amylase, aspartate aminotransferase (AST), alanine aminotransferase (ALT), alkaline phosphatase (ALP), gamma-glutamyl transferase (GGT), total protein, lactate, and creatine kinase (CK) (Bioclin, MG, Brazil) analyses were performed by the chemistry analyser BS-120 (Mindray, SP, Brazil) at UFCSPA's Clinical Analysis Laboratory.

2.15. TMZ extraction and quantification from the brain tissue

The samples' preparation was based on previous studies with minor modifications (Khosa et al., 2018). Briefly, 100 mg of brain tissue were used to extract TMZ. The samples were acidified by using 200 μL of acetic acid (0.1% v/v; Merck) and homogenized. The protein amount was precipitated by adding 200 μL of cold acetonitrile (Merck), the samples were vortexed and centrifuged for 10 min at 10,000 rpm. The supernatants were collected and filtered by using a 0.45 μm filter. For the TMZ standard curve, brain tissue from control rats were used and spiked with a range of TMZ solutions (0.05 – 5 μg/mL) in acetic acid. Control samples (without TMZ) were also evaluated to assess possible interferences in the composition. The HPLC-DAD method was based on previous studies (Gilant et al., 2012; Michels et al., 2019) and was carried out in a Shimadzu Prominence (Shimadzu, Tokyo, Japan) chromatograph equipped with a quaternary, low-pressure mixing pump and inline vacuum degassing, controlled by a CBM-20^A interface module, an automatic injector (SIL-20A) and Diode Array Detector (SPD-M20A). The separation was performed using a reverse-phase Phenomenex – Luna C18 (5 μm × 150 mm × 4.6 mm) column. The mobile phases consisted of acetic acid (2% v/v) – phase A and acetonitrile – phase B. The injection volume was set at 20 μL with a flow rate of 1.1 mL/min and the samples were monitored at 330 nm. The running time was set at 10 min and the retention time of TMZ was found to be 1.6 min (Supplementary Fig. 1).

2.16. Statistical analysis

Quantitative data were expressed as the mean ± standard deviation (SD) and statistical analysis was achieved by unpaired *t*-test or one-way ANOVA followed by Tukey post-test. Kaplan–Meier survival curves were generated to compare the different mice treatment groups (GraphPad Prism 8.0, La Jolla, CA, USA). P value < 0.05 was assumed as statistically significant.

3. Results and discussion

3.1. Nek1 expression in GB cells

It is known that Nek1 plays a vital role in DNA damage signalling and that the genetic inhibition of this protein increases apoptosis in glioma cells followed by TMZ treatment (Zhu et al., 2016; Liu et al., 2013; Spies et al., 2016). Thus, aiming to verify if Nek1 responds to stress induced by TMZ we analysed the expression of Nek1 in different GB cell lines after treatment with TMZ. Firstly, a screening of TMZ concentrations was performed to find the IC_{50}, which was used for the *in vitro* experiments (a dose–response curve of TMZ is shown in Supplementary Fig. 2A; the IC_{50} was found to be 76.3 μM, thus, 75 μM was chosen for the further experiments). Among the different cell lines (U87MG, A172, M059J, T98G and U138MG), the highest expression of Nek1 was observed in the U87MG cell line (Supplementary Fig. 3A), thus, we selected this cell line to perform the following *in vitro* experiments. U87MG cells were treated with TMZ, then fixed and co-stained with vinculin and Nek1 antibodies and the localisation and expression of Nek1 was evaluated. Results showed a significant increase ($p < 0.05$) of Nek1 expression in the nucleus (Supplementary Fig. 3B, C) following treatment when compared to non-treated cells, suggesting that Nek1 translocated to the nucleus to act during the DDR signalling (Liu et al., 2013).

During the DNA damage repair triggered by TMZ-induced lesions, there is a formation of double-strand breaks (DSB) and when DSB establish in DNA, the histone 2AX (H2AX) flanks the damage site and it is phosphorylated (γ). Owing to the fact that γH2AX foci usually increases after DSB formation (Nakamura et al., 2006), its expression was also verified after TMZ treatment. The intensity of fluorescence of γH2AX and Nek1 increased and they were correlated ($p < 0.05$) (Supplementary Fig. 3B-E).

3.2. JNK2 inhibitor in silico interaction with Nek1

Given Nek1′s role in the DDR and its increased expression after TMZ exposure, we hypothesised that by inhibiting Nek1 and combining it with TMZ treatment, the GB therapy efficacy would improve. Aiming to inhibit Nek1 activity, an ATP-mimetic inhibitor was used, which has been previously found to inhibit Nek1′s activity in almost 30% (to 71.5% ± 0.1%) at a 50 μM concentration (Moraes et al., 2015). Since the inhibitor was produced as a c-Jun NH (2)-terminal kinase 2 (JNK2) inhibitor, its *in silico* interaction with Nek1 and JNK2 was evaluated (Fig. 1).

Although Nek1 has two structures deposited in the Protein Data Bank (PDB ID 4APC and PDB ID 4B9D), it was necessary to carry out the

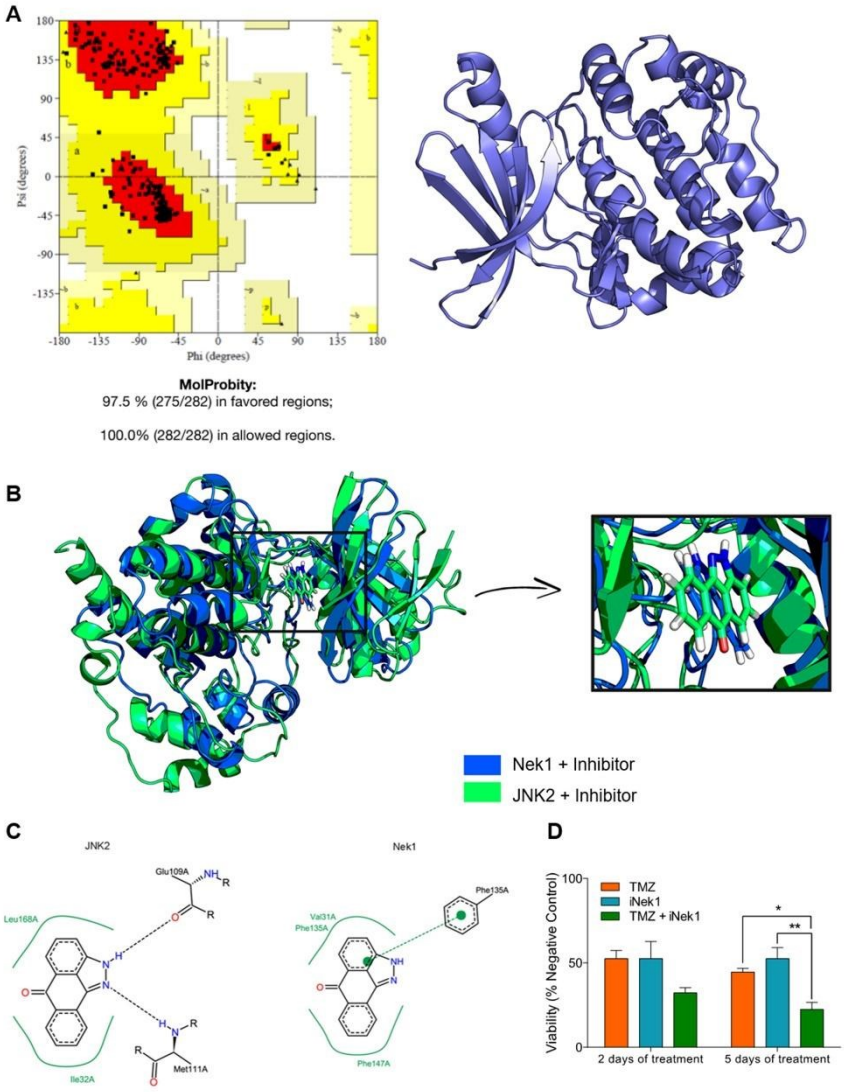

Fig. 1. JNK2 inhibitor II (referred to as iNek1) interacts with Nek1 and decreases cells viability. (A) Ramachandran plot for the new Nek1 model. In blue, the complete structure of Nek1 built in the present study. (B) Results of molecular docking calculations between Nek1 (blue) and JNK2 (green) proteins with iNek1 inhibitor. The iNek1 orientations on both structures are similar and binding energy values are practically the same for both proteins: JNK2-iNek1 = − 9.5 kcal/mol and Nek1-iNek1 = − 9.9 kcal/mol. (C) Main interactions between iNek1 and JNK2 or Nek1 proteins. Both systems have shown hydrophobic interactions (green lines). Hydrogen bonds between the inhibitor and JNK2 are shown as dashed lines, and Nek1-iNek1 pi-pi (π - π) stacking interactions is shown as a dashed green line. (D) Cell viability analysis of TMZ, iNek1 or the co-treatment of TMZ + iNek1. Statistical analysis was performed using one-way ANOVA and Tukey post-test. Data were considered significant different at $p < 0.05$ (*) and $p < 0.01$ (**). (For interpretation of the references to colour in this figure legend, the reader is referred to the web version of this article.)

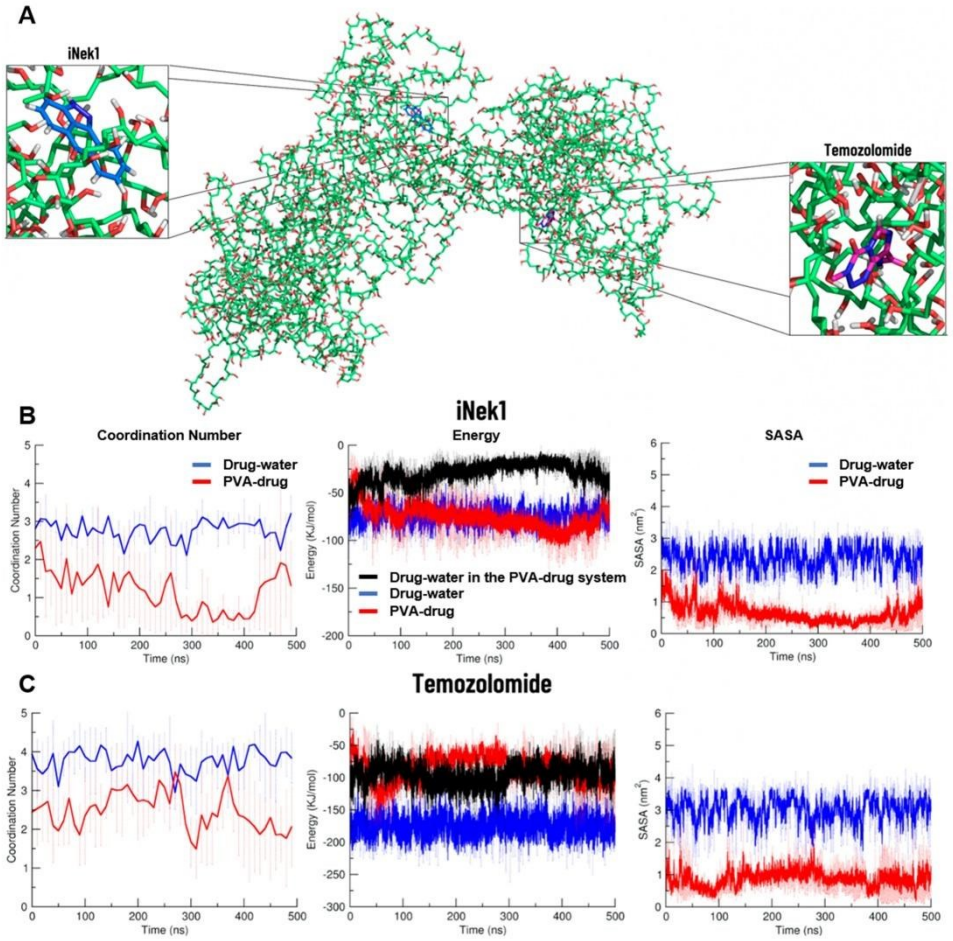

Fig. 2. Interaction between the polymer, iNek1 and TMZ. (A) PVA, iNek1 and TMZ are presented as sticks highlighted in green, blue and pink, respectively. The frame was retrieved at 400 ns of MD simulations. (B, C) Coordination number (CN) of water molecules on nitrogen atom of imidazole rings, total interaction energy between PVA-drugs and water-drugs and average of solvent accessible surface area (SASA) on drugs during the molecular dynamics simulations. (B) Left: CN calculation of the system of PVA-iNek1 (red) and iNek1-water (blue). Middle: the total interaction energy between PVA-iNek1 (red), and the total interaction energy between water-iNek1 in each system, PVA-iNek1 (black) and iNek1-water (blue). Right: SASA of the system of PVA-iNek1 (red) and iNek1-water (blue). (C) Left: CN calculation of the system PVA-TMZ (red) and TMZ-water (blue). Middle: the total interaction energy between PVA-TMZ (red), and the total interaction energy between water-TMZ in each system, PVA-TMZ (black) and TMZ-water (blue). Right: SASA of the system PVA-TMZ (red) and TMZ-water (blue). Each point in the graphs represents the average of three simulations for each system. (For interpretation of the references to colour in this figure legend, the reader is referred to the web version of this article.)

construction of a model by comparative modelling. The Nek1 structures available in the database presented problems, probably due to the resolution of the crystal, where parts of the sequence were not elucidated. These gaps in the structure were solved with the construction of a new model. The protein was modelled using the structure found under the PDB ID 4B9D. MODELLER9v17 (Webb and Sali, 2016) software was used, using as input an alignment of the two amino acid sequences carried out by the Clustal Omega (Sievers et al., 2011) software. The sequences were: complete Nek1 to be modelled, the crystal sequence of PDB ID 4B9D. The routine used in the production of the models was *model* and 1000 models were built. Thus, among these built structures, the selected model was the one that had the best score in the evaluation of stereochemistry (analysed with the PDB sum server and the PROCHECK (Laskowski, 2001) program). The quality of the Nek1 model was checked with Procheck, Verify 3D and MolProbity. MolProbity revealed through the Ramachandran plot that 97.5% (275/282) of all residues were in favoured (98%) regions and 100.0% (282/282) of all residues were in allowed (>99.8%) regions. The results of the Ramachandran plot (Fig. 1A), and analysis of the dihedral angles ϕ and ψ for the protein amino acids showed that the model presents acceptable results. It is clear

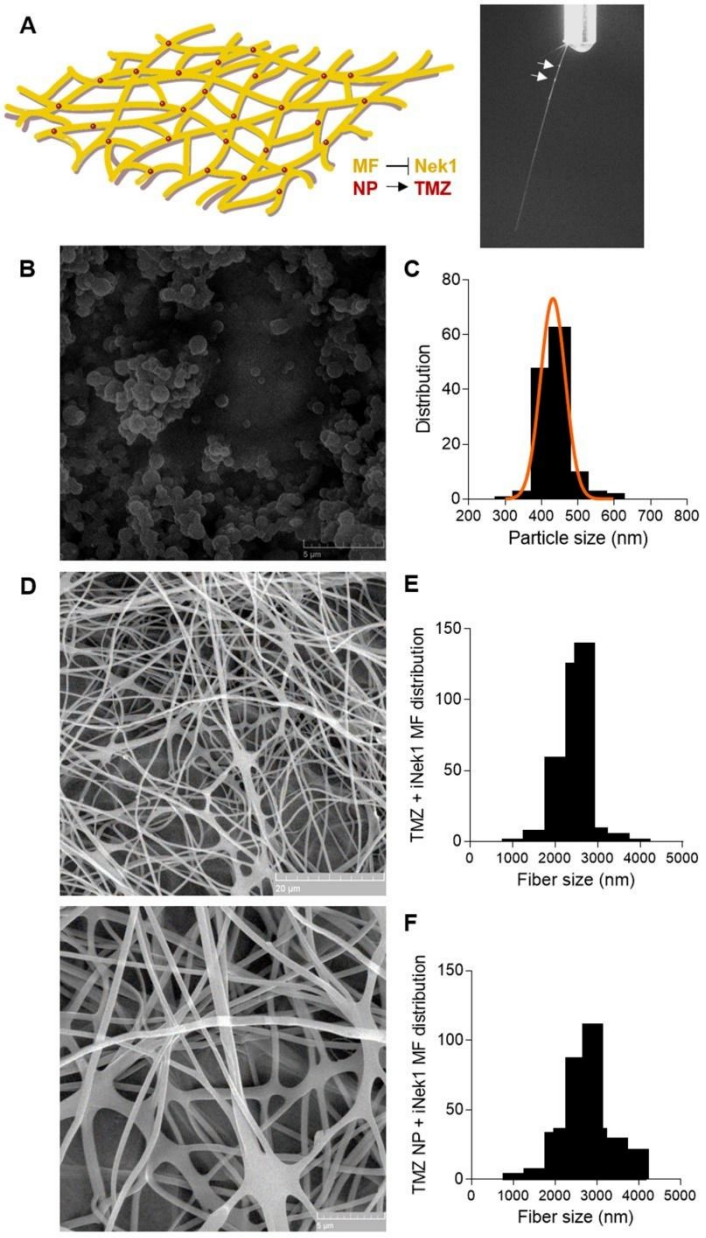

Fig. 3. Characterisation of the formulations. (A) Left: schematic representation of TMZ NP inside electrospun iNek1 MF. Right: representative image of the PVA solution with NP during electrospinning (white arrows demonstrate the NP inside of the MF). (B) TMZ NP SEM characterisation and (C) particle size distribution (the experiment was repeated 9 times). (D) TMZ + iNek1 MF morphology by SEM and (E) TMZ + iNek1 MF fiber size distribution. (F) TMZ NP + iNek1 MF fiber size distribution.

that there is a high number of residues in favourable regions in the model, and waste in unfavourable regions has an extremely low value in the model obtained, confirming a robust model. With these results, it is possible to infer that the model obtained has a suitable resolution compared to the Nek1 crystal, allowing us to obtain the complete three-dimensional structure of Nek1, which was used in the following steps of the work for molecular docking calculations.

It was possible to observe that iNek1 orientations on both structures are similar and binding energy values are practically the same for both proteins: JNK2-iNek1 = -9.5 kcal/mol and Nek1-iNek1 = -9.9 kcal/mol (Fig. 1B). Both systems have shown hydrophobic interactions (green lines), however, when compared both proteins, clearly, the JNK2 protein presents hydrogen bonds and Nek1 pi-pi (π - π) stacking interactions (Fig. 1C), suggesting that the inhibitor not only is capable of inhibiting Nek1, supporting previous studies (Moraes et al., 2015), but possibly the interaction of Nek1-iNek1 is stronger than iNek1-JNK2. It is important to state that since this inhibitor is an ATP-mimetic, it is capable of inhibiting other mitotic kinases not tested in this work, including other Neks (Moraes et al., 2015). Nevertheless, this extensive inhibition capacity could contribute to the results found here.

3.3. Nek1 inhibitor treatment decreases GB cells viability

Aiming to evaluate the efficacy of iNek1 in decreasing the viability of GB cells, a screening of iNek1 concentrations was performed (Supplementary Fig. 1B). The IC_{50} was found to be 54.4 μM, thus, 50 μM was chosen for the further experiments. Subsequently, U87MG and C6 cells were treated with the combination treatment (TMZ + iNek1) (Fig. 1D, Supplementary Fig. 4). It was observed that the co-therapy significantly decreased U87MG cells' viability after 5 days of treatment when compared to TMZ ($p < 0.05$) or iNek1 ($p < 0.01$) (Fig. 1D). Similarly, C6 cells' viability decreased following TMZ + iNek1 treatment when compared to TMZ ($p < 0.05$) (Supplementary Fig. 4), indicating that inhibiting Nek1's activity enhances TMZ efficacy in killing GB cells.

3.4. In silico interaction between PVA and iNek1 or TMZ

TMZ presents poor solubility in water and a short half-life in blood circulation along with severe side effects (Stupp et al., 2005; Corsa et al., 2006; Mutter and Stupp, 2006; Vera et al., 2004), considering these features, the current study aimed at the controlled release of TMZ. Moreover, given the difficulties of delivering drugs to the brain, a polymeric DDS for local application was developed. Prior to the production of the DDS, in order to assess the main interactions between PVA and iNek1 or TMZ, two systems were constructed: (1) iNek1 and TMZ in water and (2) PVA-iNek1 and TMZ in water. Each system was simulated in three independent runs to filter low probability conformational events (Nemec and Hoffmann, 2017; Perez et al., 2016) and the obtained data are shown as an average of these three simulations. With regards to the possibility of PVA interaction with the iNek1 and TMZ, the exposition of all molecules to solvent was investigated using different approaches as demonstrated in our previous study (Steffens et al., 2020). The analyses include the coordination number (CN) of water molecules, the total energetic contribution for the interaction between PVA-iNek1-TMZ and solvent-accessible surface area (SASA) surrounding the drugs (Fig. 2B, C), as well as the visual examination of drugs during the simulations (Fig. 2A). Accordingly, when complexed to the polymer, both drugs do not expose to solvent (Fig. 2A-C, Supplementary Fig. 5, 6). The CN of water molecules agreed with the interaction energy and SASA results, reinforcing the drugs' complexation with PVA. However, when comparing iNek1 and TMZ molecules, clearly iNek1 has more interaction with PVA than TMZ. The interaction energy data (Fig. 2B, C) have shown a higher interaction between iNek1 and PVA. In fact, the interaction of these molecules is in the same range of interaction energy of iNek1 with water. On the other hand, the interaction energy between the PVA and TMZ is lower when compared to the interaction of TMZ and water. The CN of waters is higher on TMZ than iNek1, reinforcing this data.

The visual examination (Fig. 2A) confirmed the interaction of the polymer with the drugs, probably through electrostatic interactions. It was possible to observe during the simulations that not all drugs'

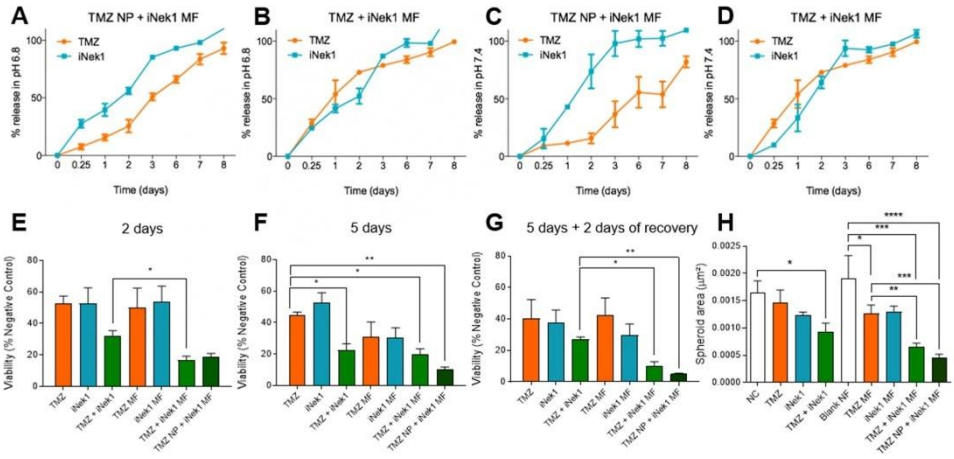

Fig. 4. Drug release studies and *in vitro* efficacy analysis of the formulations. (A) TMZ NP + iNek1 MF and (B) TMZ + iNek1 MF using pH 6.8 buffer. (C) TMZ NP + iNek1 MF (D) TMZ + iNek1 MF using pH 7.4 buffer. (E) Cell viability analysis using the U87MG cell line of all formulations after 2 days of treatment, (F) 5 days of treatment or (G) 5 days of treatment + 2 days of recovery (media replenish). Results are expressed as mean in treated cells compared to vehicle-treated cells (negative control) ± SD. (H) Cell spheroids size after 5 days of treatment + 2 days of recovery with or without the formulations. Data shown represent three independent experiments. Statistical analysis was performed using one-way ANOVA and Tukey post-test. Data were considered significant different at $p < 0.05$ (*), $p < 0.01$ (**), $p < 0.001$ (***) and $p < 0.0001$ (****).

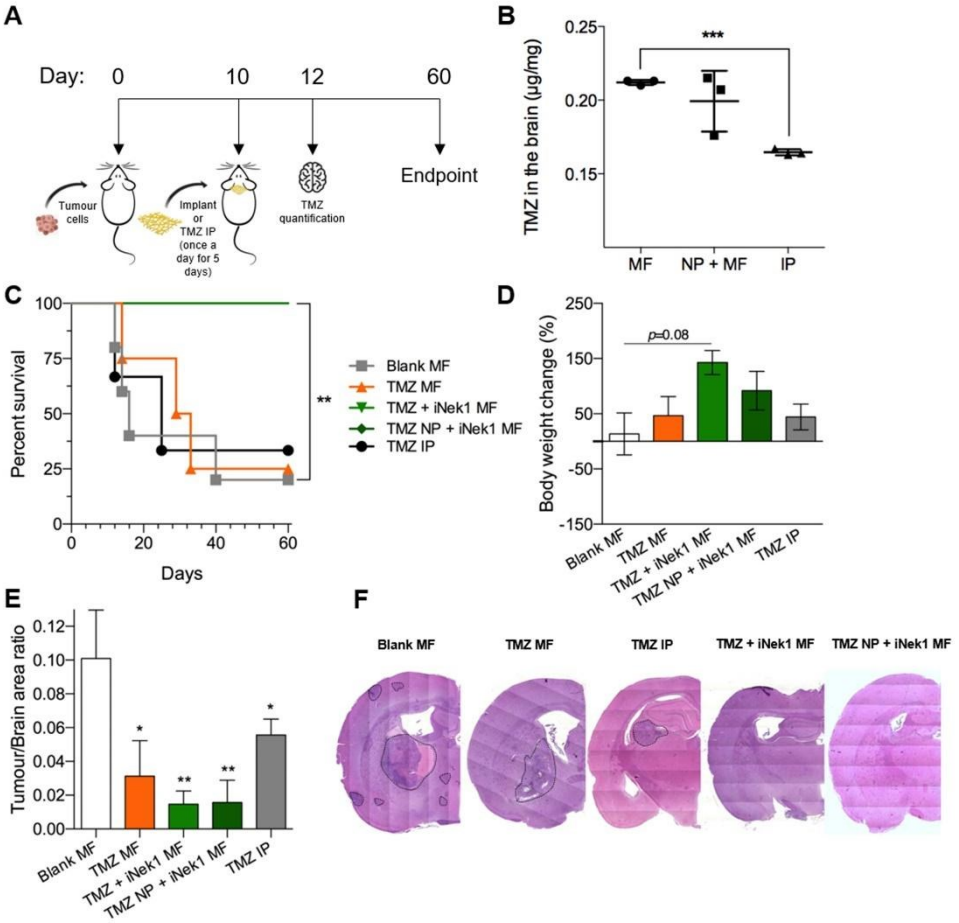

Fig. 5. *In vivo* efficacy analysis of the formulations. (A) Schematic representation of the *in vivo* treatment: on day 0, the animals were orthotopic injected with C6 cells, following ten days, the animals were implanted with Blank MF, TMZ MF, TMZ + iNek1 MF, or TMZ NP + iNek1 MF, or treated with TMZ IP once a day for five days. The animals were monitored until end-point criteria or until the sixth day. In a separated experiment, three animals/group were implanted with TMZ MF or TMZ NP + blank MF or treated with TMZ IP, and on the twelfth day, the animals were euthanised for drug quantification within the brain. (B) TMZ quantification in the brain of treated rats. (C) Kaplan-Meier curve of the survival of the treated groups. (D) Body weight was measured weekly and the body weight change (%) was calculated at the end of the experiment. (E) Tumour/brain area ratio was measured by using ImageJ software. (F) Histological representation of the brains of the animals (tumour location is shown in dashed lines). Statistical analysis was performed using one-way ANOVA and Tukey post-test. Data were considered significant different at $p < 0.05$ (*), $p < 0.01$ (**), $p < 0.001$ (***) and $p < 0.0001$ (****).

molecules interact with PVA (Supplementary Fig. 5, 6). This result is in agreement with our previous work (Steffens et al., 2020), where we have been shown the controlled release of a TMZ analogue, dacarbazine, in PVA systems. Furthermore, the higher interaction of PVA with iNek1 when compared to TMZ helped to design the next steps of the work. The molecular dynamics simulations data were an important step in the present study to decide to produce TMZ-loaded NP to protect the drug from the solvent (Fig. 3A). As previously demonstrated, the TMZ has less affinity for PVA resulting in higher interaction with the solvent.

3.5. Formulations preparation and sterility validation

PVA electrospun MF were produced loaded with TMZ and iNek1 (TMZ + iNek1 MF), or MF loaded with iNek1 and TMZ NP (TMZ NP + iNek1 MF) (Fig. 3A – white arrows point to NP inside the MF during the electrospinning), which aimed the release of iNek1 prior to TMZ targeting Nek1's activity and then releasing TMZ. MF loaded with only TMZ or iNek1 were also produced for comparison reasons. To generate TMZ NP, TMZ was incorporated in nanostructured lipid NP by using an emulsion method. Prior to characterisation and efficacy testing, it was necessary to ensure that the implant samples are absolutely sterilised due to the further *in vitro* and *in vivo* analyses. In order to evaluate the

efficiency of the sterilisation process used for the MF, the samples were contaminated with *E. coli* and *S. aureus* and IPA was used for decontamination. There was no observable growth in any of the plates of the sterilisation groups, including those containing the MF. These results show that the IPA sterilisation method was suitable for eradicating bacterial contaminants from PVA MF (Supplementary Fig. 7). Even though this method has proven efficient, for future applications of PVA MF, sterilisation methods more related with pharmaceutical industry reality and clinical application must be established.

3.6. Formulations characterisation

Morphology, size and distribution of NP are essential in the evaluation of nanocarrier formulations (Zeng et al., 2016), with particle size showing a significant effect on drug release rates. In our experiments, TMZ NP presented a circular shape analysed by SEM (Fig. 3B) and a mean size of 419.5 ± 52 nm and (Fig. 3C). Additionally, the particle surface charge determines its interaction with biological environments and its interaction with biologically active compounds (Giri et al., 2014). In general, optimum colloidal stability, where there is no particle aggregation, is improved when zeta potential is more positive or negative, around ± 45 mV (Krai et al., 2017). The zeta potential of the TMZ NP was found to be −31.6 ± 0.7 mV, therefore, we anticipated high stability and efficacy of the produced nanocarriers.

The MF were produced by electrospinning and were characterised according to their morphology and size using SEM (Fig. 3D-F). MF loaded with TMZ and iNek1 mixture presented a distribution size of 2723 ± 684 nm (Fig. 3D, E, Supplementary Fig. 8), while TMZ NP + iNek1 MF showed a distribution size of 2900 ± 1142 nm (Fig. 3F, Supplementary Fig. 8). Supplementary Fig. 8 shows TMZ + iNek1 MF after 2 h of incubation in PBS where the MF size increased only 2-fold indicating no significant water uptake, which would avoid possible side effects associated with sample swelling during the application *in situ*. Supplementary Fig. 8 shows curcumin MF with Blank NP inside, which could be used in future localised cell uptake *in vivo* studies.

The stability of the samples after drug encapsulation was examined by using NMR. In the ^{13}C analysis (Supplementary Fig. 9A), stearic acid Blank NP presented peaks in 14.7 ppm (C11), 32.5 ppm (C3) and 182.1 ppm (C1), the other carbon peaks were not obtained. TMZ NP presented these three peaks corresponding to the stearic acid and peaks related to TMZ: 36.8, 128.1, 137.1, 140.3 and 164.9 ppm (Łaszcz et al., 2013). PVA presents four NMR fingerprints peaks: a sharp peak related to CH_2 (around 45 ppm) and three CH-OH typical peaks (between 60 and 80 ppm). It was possible to observe these peaks in all MF samples (Supplementary Fig. 9B). No significant peaks related to the drugs are visible given that the drug concentrations are very low in the formulations when compared to the polymeric concentration, however, the TMZ NP + iNek1 MF sample presented peaks related to stearic acid. No shifting peaks were observed; therefore, these results suggested that the formulations were stable and because of that, TMZ and iNek1 bioactivities were preserved in the formulations (Vashisth et al., 2015).

To investigate the total percentage of encapsulated drugs into the formulations, the samples were totally dissolved in DMSO and the EE% was measured by using the absorbance values. The EE% of TMZ from the TMZ NP formulation was found to be 79.8 ± 6.8, whereas the EE% of TMZ from the MF formulation presented an EE% of 75.2 ± 5.9. The EE% of iNek1 from the MF formulation was 79.2 ± 7.3. Finally, TMZ + iNek1 MF were incubated in PBS buffer and the sample's weight was recorded daily to assess the MF weight loss. The results showed that the MF lost 50% of their initial weight after 30 days and 80% after 40 days (Supplementary Fig. 10).

3.7. MF drug release studies

Given that the GB site presents an acidic extracellular pH around 6.8 (Honasoge and Sontheimer, 2013), we decided to investigate the drug release using two different pH: 6.8 and 7.4. GB cells usually change their metabolic route from oxidative phosphorylation to glycolysis and when this happens the cells release lactate and H + generating an acid microenvironment, which has been associated with tumour progression and resistance (Honasoge and Sontheimer, 2013; Estrella et al., 2013).

The resulting drug release from the formulations provided a continuous release profile of TMZ and iNek1 over 8 days (Fig. 4A-D). The TMZ NP + iNek1 MF samples presented 50% release of TMZ after 3 days in pH 6.8 (Fig. 4A) and 6 days in pH 7.4 (Fig. 4C), whereas, in the TMZ + iNek1 MF formulation, TMZ was 50% released after 1 day in both pH: 6.8 (Fig. 4B) and 7.4 (Fig. 4D). This observation indicates the interesting approach of nanocarriers inside fibers to slow the release of drugs such as TMZ. iNek1 was 50% released after ~ 2 days in pH 6.8 (Fig. 4A, B) and pH 7.4 (Fig. 4B, D).

3.8. In vitro efficacy of formulations

To evaluate the efficacy of the formulations in decreasing GB cells viability, U87MG cells were used and tested in pH 6.8 media at three different treatment points: 2 days, 5 days or 5 (+2 days of recovery = media replenish) days and compared to the previously found IC_{50} of the drugs. For the control samples, the results (Supplementary Fig. 11) visibly shown a lack of cytotoxicity of the unloaded formulations, since the percentage of viable cells was >90% after all treatments (Blank MF, Blank NP, or Blank NP-loaded Blank MF). However, the MF might not facilitate cell attachment, and this can explain the slight decrease in cell viability.

All treatment strategies (with and without formulations) significantly decreased cell viability when compared to the non-treated cells at all treatment points ($p < 0.01$) (data not shown). After 2 days of treatment, the TMZ + iNek1 MF was more efficient in decreasing cell viability than the co-therapy without formulation (Fig. 4E), however, after 5 days of treatment no differences were found between the co-therapies (MF versus no formulation), nevertheless, the three co-therapy treatment groups (TMZ + iNek1, TMZ + iNek1 MF and TMZ NP + iNek1 MF) were more effective reducing cell viability when compared to TMZ alone (Fig. 4F). Interestingly, after 5 (+2 days of recovery) days, both TMZ + iNek1 MF and TMZ NP + iNek1 MF were more effective than the co-therapy without formulation (Fig. 4G). To confirm these results, the formulations were tested in 3D cell spheroids for 5 (+2 days of recovery) days (Fig. 4H). It was possible to observe that the co-therapy of TMZ + iNek1 significantly decreased spheroid size when compared to the vehicle-treated spheroids (Fig. 4H), however, no differences were found when compared to the drugs alone. Contrasting, both formulations, TMZ + iNek1 MF and TMZ NP + iNek1 MF, were able to significantly reduce spheroid size when compared to Blank MF, TMZ MF and iNek1 MF (Fig. 4H). This result suggests the importance of inhibiting Nek1 in GB to improve the response to TMZ, moreover, the prolonged and sustained treatment provided by the MF could significantly maintain the therapeutical effect of TMZ and iNek1.

3.9. In vivo efficacy in glioblastoma therapy

Next, it was evaluated if the formulations could provide higher concentrations of TMZ within the brain when compared to TMZ delivered via IP (Fig. 5A, B). Three animals/group were euthanised after 2 days of TMZ MF or TMZ NP + Blank MF implantation or TMZ IP treatment and their brains were collected for TMZ quantification. MF provided the highest concentration of TMZ in the brain, and it was statistically significant when compared to TMZ IP ($p < 0.001$) (Fig. 5B). Moreover, it was possible to observe a higher variation among the animals treated with TMZ NP + Blank MF, suggesting that this formulation provides less TMZ release uniformity, but still, the mean concentration was higher than for the TMZ IP-treated animals.

For the *in vivo* efficacy evaluation of the formulations, the tumour-bearing animals were implanted with Blank MF, TMZ MF, TMZ +

iNek1 MF, TMZ NP + iNek1 MF or treated with TMZ IP (once a day for five days; (Cancer), and were followed up for 60 days or until they reached end-point criteria (Fig. 5A). The survival analysis (Fig. 5C) demonstrated no statistical differences for the Blank MF when compared to TMZ MF or IP, where the Blank MF-treated rats' median survival was found to be 16 days, and 25 and 31 days for the TMZ IP and TMZ MF-treated groups, respectively. However, all animals treated with either co-therapy formulation (TMZ + iNek1 MF or TMZ NP + iNek1 MF) survived until the 60th day (Fig. 5C). With exception of the Blank MF-treated rats, all animals presented a positive body weight change after treatment (Fig. 5D), demonstrating that the treated rats were able to maintain or increase their weights. The lack of side effects observed was supported by the biochemical analysis (Supplementary Fig. 12), as we did not detect any significant sign of renal and pancreatic toxicity. Moreover, macroscopic analysis of kidneys and lungs revealed no signs of organ-specific toxicity (data not shown). Regarding liver function, ALT, which is a specific marker of liver damage, showed a significant decrease in all treatment groups, even so remaining within the reference values (21–52 IU/L). Similar results were observed in AST, which can also be found in muscles (reference values: 96–200 IU/L) (Palmeiro et al., 2003). Blank MF-treated rats showed increased values for both ALT and AST, however, due to the high SD of these groups, and the absence of significant differences in other markers, such as GGT and ALP, this set of results may be of no clinical relevance, suggesting that there was no collateral toxicity associated with the implants.

The tumour/brain area ratio of the rats implanted with either co-therapy MF was found to be reduced by 5-fold when compared to Blank MF-implanted rats ($p < 0.001$) (Fig. 5E, F), furthermore, both delivery strategies for TMZ (MF or IP) were able to significantly ($p < 0.05$) reduce tumour size when compared to the control (Fig. 5E, F). Other studies have shown promising results associated with the local implantation of fibers and wafers (Reviewed by (Norouzi, 2018), nevertheless, only a few studies have compared the formulations with the standard treatment using TMZ and/or other antitumour drugs, therefore, it is a challenge to predict the real efficacy associated with the implant formulations and if the risks associated with the implantation are worthwhile. Even though our study demonstrates great potential, TMZ and iNek1 release rates must be improved to decrease the probability of tumour recurrence.

Despite the fact that brain implants and wafers are effective in controlling tumour growth locally, several side effects have been previously reported, hence, this management strategy might be a double-edged sword because of the chance of severe symptomatic oedema within the brain (Kuramitsu et al., 2014), nonetheless, these side effects are strongly related to high concentrations of cytotoxic drugs. The results shown in this manuscript revealed that it is possible to achieve a successful treatment outcome with reduced drug concentration combined with a DDR-related kinase inhibitor by using a versatile and straightforward technique. Finally, the NP inside MF strategy could be used for a plethora of protein inhibitors, including DDR-related targets, and/or gene therapy such as RNA interference technologies that might need extra protection during delivery.

4. Conclusion

GB presents a high capacity of tumour recurrence, consequently, localised and controlled therapy approaches could provide an alternative to enhance chemotherapy efficacy and reduce systemic toxicity. In addition, GB resistance is related to oncotargets upregulation, and the impairment of their cellular activities could improve treatment efficacy. Nek1, one of these possible oncotargets, was previously related to cell proliferation and TMZ-resistance. Our results support previous findings (Zhu et al., 2016) and strongly suggest that Nek1 is an important target in GB cells and its inhibition significantly decreases cell viability when combined with TMZ. Furthermore, in this study, polymeric brain-implants prepared using TMZ and iNek1 were effectively produced, characterised and their anticancer efficacy was determined. The formulations revealed a high drug loading, which prolonged the drug's release improving the antitumor effects of iNek1 and TMZ. The produced brain-implants may be promising approaches for innovative *in situ* therapies, however, further research aiming to improve and prolong the drug release rate must be engaged.

Declaration of Competing Interest

The authors declare that they have no known competing financial interests or personal relationships that could have appeared to influence the work reported in this paper.

Acknowledgments

This study was supported in parts by grants from CAPES (Coordenação de Aperfeiçoamento de Pessoal de Nível Superior, Brazil, code 001) and FAPERGS (Fundação de Apoio à Pesquisa do Rio Grande do Sul, Grant n° 17/2551-0001388-3 and Grant n° 21/2551-0001965-4).

Statement of authors' contributions to manuscript

L.S.R. conceived and planned the experiments, produced and characterised the formulations. L.S.R. and A.M.M. carried out cell experiments and statistical analysis. L.S.R., A.M.M., J.G.H., M.B.F, E.B. and P. O.S performed the *in vivo* experiments. P.R.A developed the *in silico* simulations and analysis. J.O.M, G.R.B. and C.S.D. contributed to sample preparation and drug quantification. M.C.H.B. conducted the sterilisation of the formulations. L.S.R. wrote the original draft. L.S.R. wrote the manuscript in consultation with A.M.M., J.G.H., M.N. and D.J.M. D. J.M. and M.N. acquired the funding used in this project. All authors reviewed the final manuscript.

Appendix A. Supplementary data

Supplementary data to this article can be found online at https://doi.org/10.1016/j.ijpharm.2022.121584.

References

Abida, W., Bang, Y. J., Carter, L., Azaro, A., Krebs, M., Im, S.-A., Chen, Y., Buil-Bruna, N., Li, Y., Eaton, D., Stephens, C., Ross, G., Pass, M., Rodon, J., Dean, E., Abstract A094: Phase I modular study of AZD0156, a first-in-class oral selective inhibitor of ataxia telangiectasia mutated protein kinase (ATM), in combination with olaparib (ATOM Study, Module 1). Molecular Cancer Therapeutics 2018, 17 (1 Supplement), A094.

Ahmed, F., Pakunlu, R.I., Brannan, A., Bates, F., Minko, T., Discher, D.E., 2006. Biodegradable polymersomes loaded with both paclitaxel and doxorubicin permeate and shrink tumors, inducing apoptosis in proportion to accumulated drug. J. Control. Release 116 (2), 150–158.

Akbar, U., Jones, T., Winestone, J., Michael, M., Shukla, A., Sun, Y., Duntsch, C., 2009. Delivery of temozolomide to the tumor bed via biodegradable gel matrices in a novel model of intracranial glioma with resection. J. Neurooncol. 94 (2), 203–212.

Bei, D., Marszalek, J., Youan, B.B., 2009. Formulation of dacarbazine-loaded cubosomes-part I: influence of formulation variables. AAPS PharmSciTech 10 (3), 1032–1039.

Berendsen, H.J.C., Grigera, J.R., Straatsma, T.P., 1987. The missing term in effective pair potentials. J. Phys. Chem. 91 (24), 6269–6271.

Bowie, J.U., Lüthy, R., Eisenberg, D., 1991. A method to identify protein sequences that fold into a known three-dimensional structure. Science 253 (5016), 164–170.

Bragaunol, E., Morrone, F.B., Bernardi, A., Huppes, D., Meurer, L., Edelweiss, M.I.A., Lenz, G., Wink, M.R., Robson, S.C., Battastini, A.M.O., 2009. Selective NTPDase2 expression modulates in vivo rat glioma growth. Cancer Sci. 100 (8), 1434–1442.

Brodbelt, A., Greenberg, D., Winters, T., Williams, M., Vernon, S., Collins, V.P., 2015. Glioblastoma in England: 2007–2011. Eur. J. Cancer 51 (4), 533–542.

Bussi, G., Donadio, D., Parrinello, M., 2007. Canonical sampling through velocity rescaling. J. Chem. Phys. 126 (1), 014101. https://doi.org/10.1063/1.2408420.

Cancer, B. BC Cancer Protocol Summary for Therapy for Malignant Brain Tumours using Temozolomide. http://www.bccancer.bc.ca/chemotherapy-protocols-site/Documents/Neuro-Oncology/CNTEMOZ_Protocol.pdf.

Chen, V.B., Arendall, W.B., Headd, J.J., Keedy, D.A., Immormino, R.M., Kapral, G.J., Murray, L.W., Richardson, J.S., Richardson, D.C., 2010. MolProbity: all-atom structure validation for macromolecular crystallography. Acta Crystallogr. D Biol. Crystallogr. 66 (1), 12–21.

Chen, Y., Craigen, W.J., Riley, D.J., 2009. Nek1 regulates cell death and mitochondrial membrane permeability through phosphorylation of VDAC1. Cell Cycle 8 (2), 257–267.

Chen, Y., Gaczynska, M., Osmulski, P., Polci, R., Riley, D.J., 2010. Phosphorylation by Nek1 regulates opening and closing of voltage dependent anion channel 1. Biochem. Biophys. Res. Commun. 394 (3), 798–803.

Chen, Y., Chen, C.-F., Polci, R., Wei, R., Riley, D.J., Chen, P.-L., 2014. Increased Nek1 expression in renal cell carcinoma cells is associated with decreased sensitivity to DNA-damaging treatment. Oncotarget 5 (12), 4283–4294.

Cheng, Y., Morshed, R.A., Auffinger, B., Tobias, A.L., Lesniak, M.S., 2014. Multifunctional nanoparticles for brain tumor imaging and therapy. Adv. Drug Deliv. Rev. 66, 42–57.

Corsa, P., Parisi, S., Raguso, A., Troiano, M., Perrone, A., Cossa, S., Munafò, T., Piombino, M., Spagnoletti, G., Borgia, F., 2006. Temozolomide and radiotherapy as first line treatment of high grade gliomas. Tumori 92 (4), 299–305.

Darden, T., York, D., Pedersen, L., 1993. Particle mesh Ewald: An N·log(N) method for Ewald sums in large systems. J. Chem. Phys. 98 (12), 10089–10092.

Degiacomi, M.T., Erastova, V., Wilson, M.R., 2016. Easy creation of polymeric systems for molecular dynamics with Assemble! Comput. Phys. Commun. 202, 304–309.

Delano, W.L. PyMOL: An Open-Source Molecular Graphics Tool.. http://www.ccp4.ac.uk/newsletters/newsletter40/11_pymol.pdf.

Denny, B.J., Wheelhouse, R.T., Stevens, M.F.G., Tsang, L.L.H., Slack, J.A., 1994. NMR and molecular modeling investigation of the mechanism of activation of the antitumor drug temozolomide and its interaction with DNA. Biochemistry 33 (31), 9045–9051.

Estrella, V., Chen, T., Lloyd, M., Wojtkowiak, J., Cornnell, H.H., Ibrahim-Hashim, A., Bailey, K., Balagurunathan, Y., Rothberg, J.M., Sloane, B.F., Johnson, J., Gatenby, R. A., Gillies, R.J., 2013. Acidity generated by the tumor microenvironment drives local invasion. Cancer Res. 73 (5), 1524–1535.

Fan, C.H., Ting, C.Y., Chang, Y.C., Wei, K.C., Liu, H.L., Yeh, C.K., 2015. Drug-loaded bubbles with matched focused ultrasound excitation for concurrent blood-brain barrier opening and brain-tumor drug delivery. Acta Biomater. 15, 89–101.

Fernandes, C., Suares, D., Yergeri, M. C., 2 18. Tumor microenvironment targeted nanotherapy. Frontiers in Pharmacology 9 (1230).

Freund, I., Helılgans, S., Martin, D., Ensminger, M., Fokas, E., Rödel, C., Löbrich, M., Rödel, F., 2020. Fractionation-dependent radiosensitization by molecular targeting of Nek1. Cells 9 (5), 1235. https://doi.org/10.3390/cells9051235.

Gilant, E., Kaza, M., Szlagowska, A., Serafin Byczak, K., Rudzki, P.J., 2012. Validated HPLC method for determination of temozolomide in human plasma. Acta Pol. Pharm. 69 (6), 1347–1355.

Giri, K., Shameer, K., Zimmermann, M.T., Saha, S., Chakraborty, P.K., Sharma, A., Arvizo, R.R., Madden, B.J., Mccormick, D.J., Kocher, J.-P., Bhattacharya, R., Mukherjee, P., 2014. Understanding protein-nanoparticle interaction: a new gateway to disease therapeutics. Bioconjug. Chem. 25 (6), 1078–1090.

Hafeez, A., Kazmi, I., 2017. Dacarbazine nanoparticle topical delivery system for the treatment of melanoma. Sci. Rep. 7 (1), 16517.

Han, D., Sasaki, M., Yoshino, H., Kofuji, S., Sasaki, A.T., Steckl, A.J., 2017. In-vitro evaluation of MPA-loaded electrospun coaxial fiber membranes for local treatment of glioblastoma tumor cells. J. Drug Delivery Sci. Technol. 40, 45–50.

Hernán Pérez de la Ossa, D., Lorente, M., Gil-Alegre, M.E., Torres, S., García-Taboada, E., Aberturas, M.D.R., Molpeceres, J., Velasco, G., Torres-Suárez, A.I., Aravindan, N., 2013. I., Local delivery of cannabinoid-loaded microparticles inhibits tumor growth in a murine xenograft model of glioblastoma multiforme. PLoS ONE 8 (1), e54795.

Hess, B., Bekker, H., Berendsen, H.J.C., Fraaije, J.G.E.M., 1997. LINCS: A linear constraint solver for molecular simulations. J. Comput. Chem. 18 (12), 1463–1472.

Higelin, J., Catanese, A., Semelink Sedlacek, L.L., Oeztuerk, S., Lutz, A.-K., Bausinger, J., Barbi, G., Speit, G., Andersen, P.M., Ludolph, A.C., Demestre, M., Boeckers, T.M., 2018. NEK1 loss-of-function mutation induces DNA damage accumulation in ALS patient-derived motoneurons. Stem Cell Res. 30, 150–162.

Hirschberg, H., Photo activated Cancer Therapy: Potential for Treatment of Brain Tumors. In *Optical Methods and Instrumentation in Brain Imaging and Therapy. Bioanalysis (Advanced Materials, Methods, and Devices)*, S., M., Ed. Springer: New York, 2013; Vol. 3.

Honasoge, A., Sontheimer, H., 2013. Involvement of tumor acidification in brain cancer pathophysiology. Front. Physiol. 4, 316.

Hoover, W.G., 1985. Canonical dynamics: Equilibrium phase-space distributions. Phys. Rev. A 31 (3), 1695–1697.

Hua, M.-Y., Liu, H.-L., Yang, H.-W., Chen, P.-Y., Tsai, R.-Y., Huang, C.-Y., Tseng, I.-C., Lyu, L.-A., Ma, C.-C., Tang, H.-J., Yen, T.-C., Wei, K.-C., 2011. The effectiveness of a magnetic nanoparticle-based delivery system for BCNU in the treatment of gliomas. Biomaterials 32 (2), 516–527.

Huang, D., Lin, C., Wen, X., Gu, S., Zhao, P., Pisignano, D., 2016. A potential nanofiber membrane device for filling surgical residual cavity to prevent glioma recurrence and improve local neural tissue reconstruction. PLoS ONE 11 (8), e0161435.

Humphrey, W., Dalke, A., Schulten, K., 1996. VMD: visual molecular dynamics. J. Mol. Graph. 14 (1), 33–38.

Irani, M., Sadeghi, G.M.M., Haririan, I., 2017. The sustained delivery of temozolomide from electrospun PCL-Diol-b-PU/gold nanocompsite nanofibers to treat glioblastoma tumors. Mater. Sci. Eng. C Mater. Biol. Appl. 75, 165–174.

Játiva, P., Ceña, V., 2017. Use of nanoparticles for glioblastoma treatment: a new approach. Nanomedicine (Lond) 12 (20), 2533–2554.

Khosa, A., Krishna, K.V., Saha, R.N., Dubey, S.K., Reddi, S., 2018. A simplified and sensitive validated RP-HPLC method for determination of temozolomide in rat plasma and its application to a pharmacokinetic study. J. Liq. Chromatogr. Relat. Technol. 41 (10), 692–697.

Kim, G.Y., Tyler, B.M., Tupper, M.M., Karp, J.M., Langer, R.S., Brem, H., Cima, M.J., 2007. Resorbable polymer microchips releasing BCNU inhibit tumor growth in the rat 9L flank model. J. Controlled Release : Official J. Controlled Release Soc. 123 (2), 172–178.

Krai, J., Beckenkamp, A., Gaelzer, M.M., Pohlmann, A.R., Guterres, S.S., Filippi-Chiela, E. C., Salbego, C., Buffon, A., Beck, R.C.R., 2017. Doxazosin nanoencapsulation improves its in vitro antiproliferative and anticlonogenic effects on breast cancer cells. Biomed. Pharmacother. 94, 10–20.

Kumarnaharisetti, P., Yungshengong, B., Weixie, J., Kamyiulee, T., Wang, C., Sahinidis, N., 2007. V., In vivo performance of implantable biodegradable preparations delivering Paclitaxel and Etanidazole for the treatment of glioma. Biomaterials 28 (5), 886–894.

Kuramitsu, S., Motomura, K., Natsume, A., Wakabayashi, T., 2014. Double-edged sword in the placement of carmustine (BCNU) wafers along the eloquent area: A case report. NMC Case Rep. J. 2 (1), 40–45.

Kyrychenko, A., Pasko, D.A., Kalugin, O.N., 2017. Poly(vinyl alcohol) as a water protecting agent for silver nanoparticles: the role of polymer size and structure. PCCP 19 (13), 8742–8756.

Laskowski, R.A., 2001. PDBsum: summaries and analyses of PDB structures. Nucleic Acids Res. 29 (1), 221–222.

Łaszcz, M., Kubiszewski, M., Jedynak, L., Kaczmarska, M., Kaczmarek, Ł., Łuniewski, W., Gabarski, K., Witkowska, A., Kuziak, K., Maliñska, M., 2013. Identification and physicochemical characteristics of temozolomide process-related impurities. Molecules 18 (12), 15344–15356.

Liu, S., Ho, C.K., Ouyang, J., Zou, L., 2013. Nek1 kinase associates with ATR-ATRIP and primes ATR for efficient DNA damage signaling. Proc. Natl. Acad. Sci. U. S. A. 110 (6), 2175–2180.

Lüthy, R., Bowie, J.U., Eisenberg, D., 1992. Assessment of protein models with three-dimensional profiles. Nature 356 (6364), 83–85.

Mangraviti, A., Gullotti, D., Tyler, B., Brem, H., 2016. Nanobiotechnology-based delivery strategies: New frontiers in brain tumor targeted therapies. J. Control. Release 240, 443–453.

Melo-Hanchuk, T.D., Martins, M.B., Cunha, I.L., Soares, F.A., Ward, L.S., Vassallo, J., Kobarg, J., 2020. Expression of the NEK family in normal and cancer tissue: an immunohistochemical study. BMC Cancer 20 (1), 23.

Michels, L.R., Fachel, F.N.S., Azambuja, J.H., Gelsleichter, N.E., Braganhol, E., Teixeira, H.F., 2019. HPLC UV method for temozolomide determination in complex biological matrices: Application for in vitro, ex vivo and in vivo studies. Biomed. Chromatogr. 33 (10) https://doi.org/10.1002/bmc.v33.1010.1002/bmc.4615.

Moraes, E.C., Meirelles, G.V., Honorato, R.V., de Souza Tde, A., de Souza, E.E., Murakami, M.T., de Oliveira, P.S., Kobarg, J., 2015. Kinase inhibitor profile for human nek1, nek6, and nek7 and analysis of the structural basis for inhibitor specificity. Molecules 20 (1), 1176–1191.

Mutter, N., Stupp, R., 2006. Temozolomide: a milestone in neuro-oncology and beyond? Expert Rev. Anticancer Ther. 6 (8), 1187–1204.

Nakamura, A., Sedelnikova, O.A., Redon, C., Pilch, D.R., Sinogeeva, N.I., Shroff, R., Lichten, M., Bonner, W.M., 2006. Techniques for gamma-H2AX detection. Methods Enzymol. 409, 236–250.

Nemec, M., Hoffmann, D., 2017. Quantitative assessment of molecular dynamics sampling for flexible systems. J. Chem. Theory Comput. 13 (2), 400–414.

Norouzi, M., 2018. Recent advances in brain tumor therapy: application of electrospun nanofibers. Drug Discovery Today 23 (4), 912–919.

Norouzi, M., Nazari, B., Miller, D.W., 2016. Injectable hydrogel based drug delivery systems for local cancer therapy. Drug Discov. Today 21 (11), 1835–1849.

Nosé, S., 1984. A molecular dynamics method for simulations in the canonical ensemble. Mol. Phys. 52 (2), 255–268.

Nosé, S., Klein, M.L., 1983. Constant pressure molecular dynamics for molecular systems. Mol. Phys. 50 (5), 1055–1076.

Oostenbrink, C., Villa, A., Mark, A.E., Van Gunsteren, W.F., 2004. A biomolecular force field based on the free enthalpy of hydration and solvation: the GROMOS force field parameter sets 53A5 and 53A6. J. Comput. Chem. 25 (13), 1656–1676.

Palmeiro, N.M.S., Almeida, C.E., Ghedini, P.C., Goulart, L.S., Pereira, M.C.F., Huber, S., da Silva, J.E.P., Lopes, S., 2003. Oral subchronic toxicity of aqueous crude extract of Plantago australis leaves. J. Ethnopharmacol. 88 (1), 15–18.

Park, J., Aryal, M., Vykhodtseva, N., Zhang, Y.Z., McDannold, N., 2017. Evaluation of permeability, doxorubicin delivery, and drug retention in a rat brain tumor model after ultrasound induced blood tumor barrier disruption. J. Control. Release 250, 77–85.

Parrinello, M., Rahman, A., 1981. Polymorphic transitions in single crystals: A new molecular dynamics method. J. Appl. Phys. 52 (12), 7182–7190.

Patil, M., Pabla, N., Ding, H.-F., Dong, Z., 2013. Nek1 interacts with Ku80 to assist chromatin loading of replication factors and S-phase progression. Cell Cycle 12 (16), 2608–2616.

Perez, J.J., Tomas, M.S., Rubio-Martinez, J., 2016. Assessment of the sampling performance of multiple-copy dynamics versus a unique trajectory. J. Chem. Inf. Model. 56 (10), 1950–1962.

Polèto, M.D., Rusu, V.H., Grisci, B.I., Dorn, M., Lins, R.D., Verli, H., 2018. Aromatic rings commonly used in medicinal chemistry: force fields comparison and interactions with water toward the design of new chemical entities. Front. Pharmacol. 9, 395.

Pol Fachin, L., Rusu, V.H., Verli, H., Lins, R.D., 2012. GROMOS 53A6GLYC, an improved GROMOS force field for hexopyranose-based carbohydrates. J. Chem. Theory Comput. 8 (11), 4681–4690.

Pol Fachin, L., Verli, H., Lins, R.D., 2014. Extension and validation of the GROMOS 53A6 (GLYC) parameter set for glycoproteins. J. Comput. Chem. 35 (29), 2087–2095.

Pourgholi, F., Hajivalili, M., Farhad, J.N., Kafil, H.S., Yousefi, M., 2016. Nanoparticles: Novel vehicles in treatment of Glioblastoma. Biomed. Pharmacother. 77, 98–107.

Pronk, S., Páll, S., Schulz, R., Larsson, P., Bjelkmar, P., Apostolov, R., Shirts, M.R., Smith, J.C., Kasson, P.M., van der Spoel, D., Hess, B., Lindahl, E., Gromacs,, 2013. 4.5: a high-throughput and highly parallel open source molecular simulation toolkit. Bioinformatics 29 (7), 845–854.

Quinn, J.A., Jiang, S.X., Reardon, D.A., Desjardins, A., Vredenburgh, J.J., Rich, J.N., Gururangan, S., Friedman, A.H., Bigner, D.D., Sampson, J.H., McLendon, R.E., Herndon, J.E., Jr., Walker, A., Friedman, H.S., 2009. Phase I trial of temozolomide plus O6-benzylguanine 5-day regimen with recurrent malignant glioma. Neuro-oncology 11 (5), 556-561.

Ramachandran, R., Malarvizhi, G. L., Chandran, P., Gupta, N., Menon, D., Panikar, D., Nair, S., Koyakutty, M., A Polymer Protein Core-Shell Nanomedicine for Inhibiting Cancer Migration Followed by Photo-Triggered Killing (Journal of Biomedical Nanotechnology, Vol. 10(8), pp. 1401-1415 (2014)). J Biomed Nanotechnol 2020, 16 (2), 259.

Ramachandran, R., Junnuthula, V.R., Gowd, G.S., Ashokan, A., Thomas, J., Peethambaran, R., Thomas, A., Unni, A.K.K., Panikar, D., Nair, S.V., Koyakutty, M., 2017. Theranostic 3-Dimensional nano brain-implant for prolonged and localized treatment of recurrent glioma. Sci. Rep. 7 (1), 43271.

Ranganath, S.H., Wang, C.-H., 2008. Biodegradable microfiber implants delivering paclitaxel for post-surgical chemotherapy against malignant glioma. Biomaterials 29 (20), 2996–3003.

Rape, A., Ananthanarayanan, B., Kumar, S., 2014. Engineering strategies to mimic the glioblastoma microenvironment. Adv. Drug Deliv. Rev. 79-80, 172–183.

Reinhardt, L.S., Henn, J.G., Morás, A.M., de Moura Sperotto, N.D., Ferro, M.B., Cao, Z., Roehe, A.V., Petry, A.U.S., Nugent, M., Moura, D.J., 2021. Plantago australis hydroethanolic extract-loaded formulations: promising dressings for wound healing. Revista Brasileira de Farmacognosia 31 (1), 91–101.

Sawyer, A.J., Piepmeier, J.M., Saltzman, W.M., 2006. New methods for direct delivery of chemotherapy for treating brain tumors. Yale J. Biol. Med. 79 (3–4), 141–152.

Scott, A.W., Tyler, B.M., Masi, B.C., Upadhyay, U.M., Patta, Y.R., Grossman, R., Basaldella, L., Langer, R.S., Brem, H., Cima, M.J., 2011. Intracranial microcapsule drug delivery device for the treatment of an experimental gliosarcoma model. Biomaterials 32 (10), 2532–2539.

Seba, V., de Lima, G.G., Pereira, B.L., Silva, G., Reinhardt, L.S., Arantes, P.R., Chee, B.S., dos Santos, M.B., França, S.C., Regasini, L.O., Fachin, A.L., Cao, Z., Nugent, M.J.D., Marins, M., 2021. Development, characterization and cell viability inhibition of PVA spheres loaded with doxorubicin and 4′ amino 1 naphthyl chalcone (D14) for osteosarcoma. Polymers 13 (16), 2611.

Sievers, F., Wilm, A., Dineen, D., Gibson, T.J., Karplus, K., Li, W., Lopez, R., McWilliam, H., Remmert, M., Söding, J., Thompson, J.D., Higgins, D.G., 2011. Fast, scalable generation of high quality protein multiple sequence alignments using Clustal Omega. Mol. Syst. Biol. 7, 539–539.

Singh, V., Jaiswal, P.K., Ghosh, I., Koul, H.K., Yu, X., De Benedetti, A., 2019. Targeting the TLK1/NEK1 DDR axis with Thioridazine suppresses outgrowth of androgen independent prostate tumors. Int. J. Cancer 145 (4), 1055–1067.

Singh, V., Jaiswal, P.K., Ghosh, I., Koul, H.K., Yu, X., De Benedetti, A., 2019. The TLK1-Nek1 axis promotes prostate cancer progression. Cancer Lett. 453, 131–141.

Singh, V., Khalil, M.I., De Benedetti, A., 2020. The TLK1/Nek1 axis contributes to mitochondrial integrity and apoptosis prevention via phosphorylation of VDAC1. Cell Cycle 19 (3), 363–375.

Sotocinal, S.G., Sorge, R.E., Zaloum, A., Tuttle, A.H., Martin, L.J., Wieskopf, J.S., Mapplebeck, J.C., Wei, P., Zhan, S., Zhang, S., McDougall, J.J., King, O.D., Mogil, J. S., 2011. The Rat Grimace Scale: a partially automated method for quantifying pain in the laboratory rat via facial expressions. Mol. Pain 7, 55.

Spies, J., Waizenegger, A., Barton, O., Sürder, M., Wright, W., Heyer, W.-D., Löbrich, M., 2016. Nek1 regulates Rad54 to orchestrate homologous recombination and replication fork stability. Mol. Cell 62 (6), 903–917.

Steffens, L., Morás, A.M., Arantes, P.R., Masterson, K., Cao, Z., Nugent, M., Moura, D.J., 2020. Electrospun PVA-Dacarbazine nanofibers as a novel nano brain-implant for treatment of glioblastoma: in silico and in vitro characterization. Eur. J. Pharm. Sci. 143, 105183. https://doi.org/10.1016/j.ejps.2019.105183.

Stupp, R., Mason, W.P., van den Bent, M.J., Weller, M., Fisher, B., Taphoorn, M.J.B., Belanger, K., Brandes, A.A., Marosi, C., Bogdahn, U., Curschmann, J., Janzer, R.C., Ludwin, S.K., Gorlia, T., Allgeier, A., Lacombe, D., Cairncross, J.G., Eisenhauer, E., Mirimanoff, R.O., 2005. Radiotherapy plus concomitant and adjuvant temozolomide for glioblastoma. N. Engl. J. Med. 352 (10), 987–996.

Sun, C., Ding, Y., Zhou, L.i., Shi, D.i., Sun, L., Webster, T.J., Shen, Y., 2017. Noninvasive nanoparticle strategies for brain tumor targeting. Nanomedicine 13 (8), 2605–2621.

Tallury, S.S., Pasquinelli, M.A., 2010. Molecular dynamics simulations of polymers with stiff backbones interacting with single-walled carbon nanotubes. J. Phys. Chem. B 114 (29), 9349–9355.

Tan, A.C., Ashley, D.M., López, G.Y., Malinzak, M., Friedman, H.S., Khasraw, M., 2020. Management of glioblastoma: State of the art and future directions. CA Cancer J. Clin. 70 (4), 299–312.

Trott, O., Olson, A.J., 2010. AutoDock Vina: improving the speed and accuracy of docking with a new scoring function, efficient optimization, and multithreading. J. Comput. Chem. 31 (2), 455–461.

Tseng, Y.Y., Liao, J.Y., Chen, W.A., Kao, Y.C., Liu, S.J., 2013. Sustainable release of carmustine from biodegradable poly[(D, L)-lactide-co-glycolide] nanofibrous membranes in the cerebral cavity: in vitro and in vivo studies. Expert Opin. Drug Deliv. 10 (7), 879–888.

Tseng, Y.-Y., Su, C.-H., Yang, S.-T., Huang, Y.-C., Lee, W.-H., Wang, Y.-C., Liu, S.-C., Liu, S.-J., 2016. Advanced interstitial chemotherapy combined with targeted treatment of malignant glioma in rats by using drug-loaded nanofibrous membranes. Oncotarget 7 (37), 59902–59916.

Tseng, Y.Y., Wang, Y.C., Su, C.H., Yang, T.C., Chang, T.M., Kau, Y.C., Liu, S.J., 2015. Concurrent delivery of carmustine, irinotecan, and cisplatin to the cerebral cavity using biodegradable nanofibers: In vitro and in vivo studies. Colloids Surf. B Biointerfaces 134, 254–261.

Vashisth, P., Kumar, N., Sharma, M., Pruthi, V., 2015. Biomedical applications of ferulic acid encapsulated electrospun nanofibers. Biotechnol Rep (Amst) 8, 36–44.

Vera, K., Djafari, L., Faivre, S., Guillamo, J.-S., Djazouli, K., Osorio, M., Parker, F., Cioloca, C., Abdulkarim, B., Armand, J.-P., Raymond, E., 2004. Dose-dense regimen of temozolomide given every other week in patients with primary central nervous system tumors. Ann. Oncol. 15 (1), 161–171.

Webb, B., Sali, A., 2016. Comparative protein structure modeling using MODELLER. Curr. Protoc. Bioinformatics 54 (1). https://doi.org/10.1002/0471250953.2016.54.issue-110.1002/cpbi.3.

Wei, X., Chen, X., Ying, M., Lu, W., 2014. Brain tumor-targeted drug delivery strategies. Acta Pharm. Sin. B 4 (3), 193–201.

Weller, M., Cloughesy, T., Perry, J.R., Wick, W., 2013. Standards of care for treatment of recurrent glioblastoma–are we there yet? Neuro Oncol. 15 (1), 4–27.

Westphal, M., Lamszus, K., 2011. The neurobiology of gliomas: from cell biology to the development of therapeutic approaches. Nat. Rev. Neurosci. 12 (9), 495–508.

White, M.C., Quarmby, L.M., 2008. The NIMA-family kinase, Nek1 affects the stability of centrosomes and ciliogenesis. BMC Cell Biol. 9, 29.

Zeng, Z., Yu, D., He, Z., Liu, J., Xiao, F.-X., Zhang, Y., Wang, R., Bhattacharyya, D., Tan, T.T.Y., 2016. Graphene oxide quantum dots covalently functionalized PVDF membrane with significantly-enhanced bactericidal and antibiofouling performances. Sci. Rep. 6 (1), 20142.

Zhu, J., Cai, Y.u., Liu, P., Zhao, W., 2016. Frequent Nek1 overexpression in human gliomas. Biochem. Biophys. Res. Commun. 476 (4), 522–527.

Supplementary

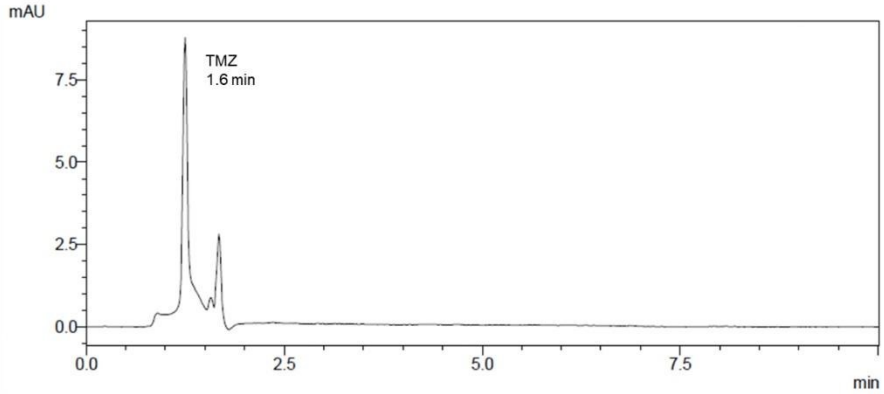

Supplementary Figure 1: TMZ chromatogram. The running time was set at 10 min and the retention time of TMZ was found to be 1.6 min. mAU: milli-Absorbance Units.

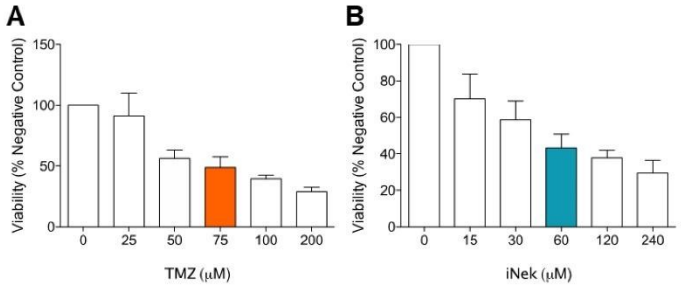

Supplementary Figure 2: A range of concentrations of TMZ or iNek1 was used to select the IC_{50} of the drugs. (A) TMZ and (B) iNek1 viability analysis in U87MG cells. Data shown represent three independent experiments.

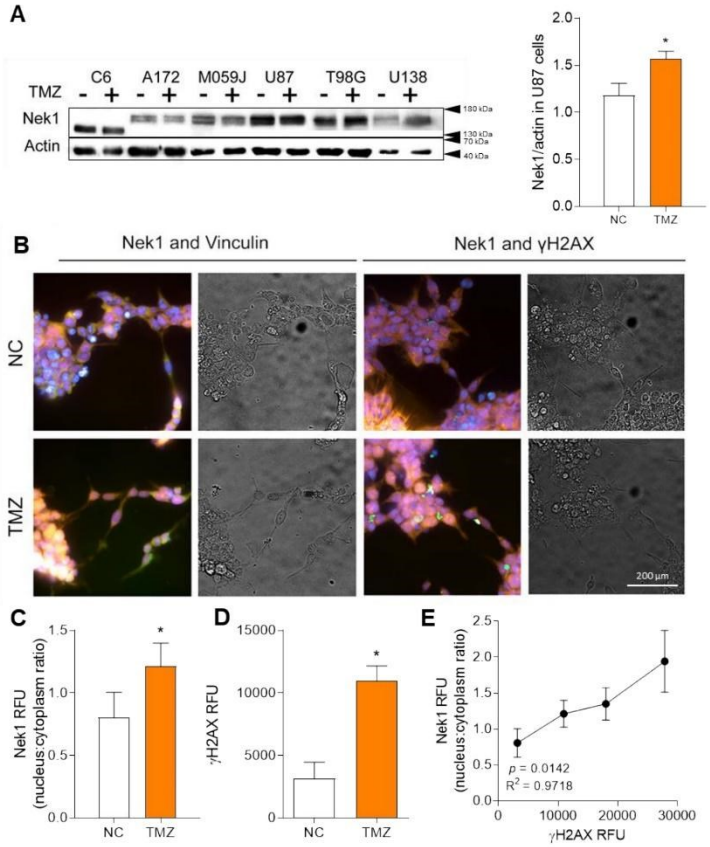

Supplementary Figure 3: Nek1 expression analysis in GB cells. (A) Left: several GB cell lines were treated with TMZ or vehicle for 24 h and the expression of Nek1 was assessed by western blotting. β-actin was used as loading control. Right: quantification of Nek1/actin expression ratio in U87MG cells. (B) Immunofluorescence evaluation of Nek1 and vinculin (left) and Nek1 and γH2AX (right). Merge and bright field images are shown of cells treated with TMZ or vehicle (negative control: NC). (C) The ratio of Nek1 fluorescence intensity in the nucleus:cytoplasm. (D) γH2AX fluorescence intensity quantification. (E) Nek1 fluorescence intensity and γH2AX fluorescence intensity correlation. Results are expressed as mean in treated cells compared to NC ± SD. Data shown represent three independent experiments. Statistical analysis was performed using unpaired t-test or Pearson's correlation coefficient. Data were considered significant different when compared to NC at $p < 0.05$ (*).

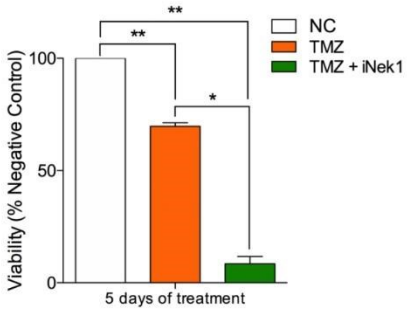

Supplementary Figure 4: C6 cells' viability analysis of TMZ or the co-treatment of TMZ + iNek1. Statistical analysis was performed using one-way ANOVA and Tukey post-test. Data were considered significant different at $p < 0.05$ (*) and $p < 0.01$ (**).

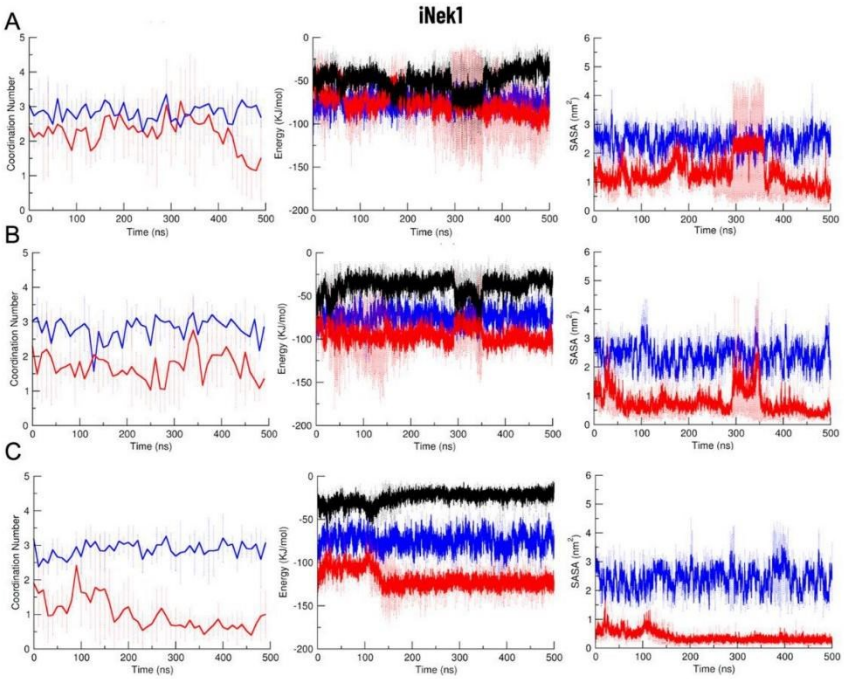

Supplementary Figure 5: The three simulations for each system with iNek1. Coordination number of water molecules (CN) on nitrogen atom of iNek1 imidazole ring, total interaction energy between PVA-iNek1 and Water-iNek1 and average of solvent accessible surface area (SASA) on drug during the molecular dynamics simulations. Left: CN calculation of the system of PVA-iNek1 (red) and iNek1-water (blue). Middle: the total interaction energy between PVA-iNek1 (red), and the total interaction energy between water-iNek1 in each system, PVA-iNek1 (black) and iNek1-water (blue). Right: SASA of the system of PVA-iNek1 (red) and iNek1-water (blue).

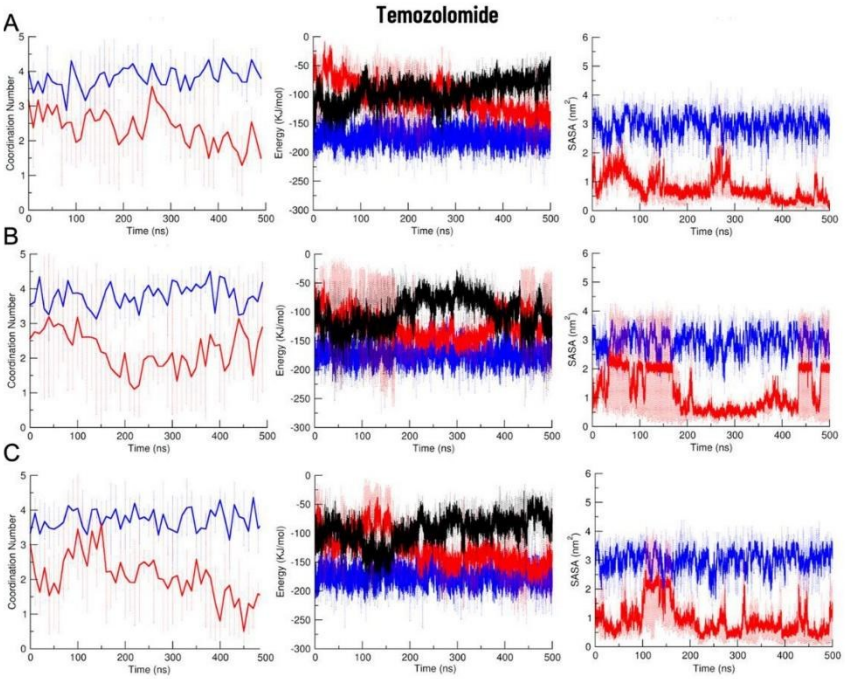

Supplementary Figure 6: The three simulations for each system with TMZ. Coordination number of water molecules (CN) on nitrogen atom of TMZ imidazole ring, total interaction energy between PVA-TMZ and water-TMZ and average of solvent accessible surface area (SASA) on drug during the molecular dynamics simulations. Left: CN calculation of the system PVA-TMZ (red) and TMZ-water (blue). Middle: the total interaction energy between PVA-TMZ (red), and the total interaction energy between water-TMZ in each system, PVA-TMZ (black) and TMZ-water (blue). Right: SASA of the system PVA-TMZ (red) and TMZ-water (blue).

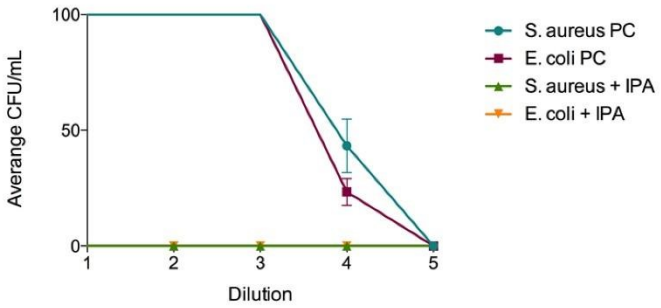

Supplementary Figure 7: Serial dilutions of MF suspension contaminated with bacteria after and without (positive control: PC) sterilisation by using IPA. Results are expressed as average colony-forming unit (CFU)/mL. Data shown represent three independent experiments.

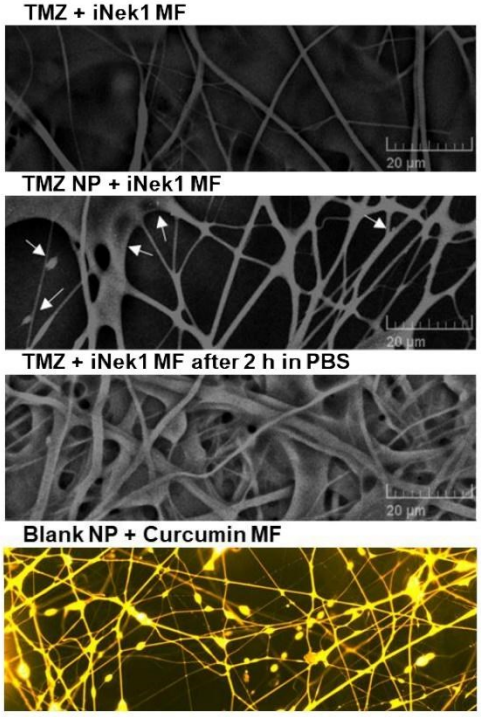

Supplementary Figure 8: Representative pictures of the MF formulations. From top to bottom: TMZ + iNek1 MF, TMZ + iNek1 MF and TMZ + iNek1 MF after 2 hours immerse in saline solution observed by SEM, and curcumin MF loaded with Blank NP observed by fluorescence microscopy.

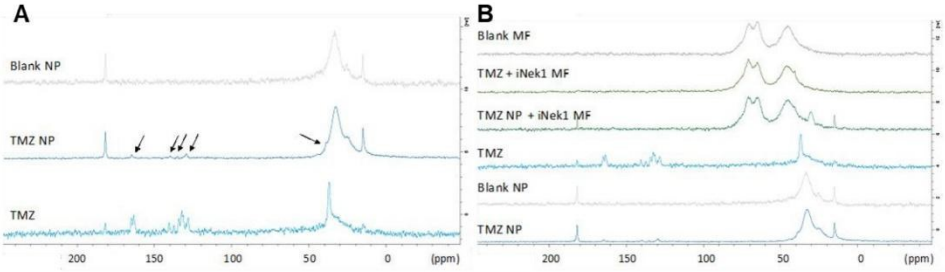

Supplementary Figure 9: NMR evaluation. (A) ^{13}C NMR of the NP formulations and TMZ. (A) ^{13}C NMR of the NP and MF formulations and TMZ.

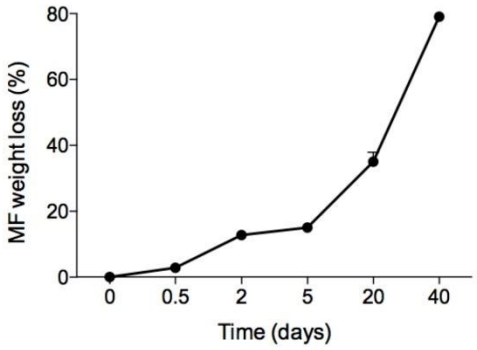

Supplementary Figure 10: MF weight loss (%). MF were incubated with saline solution and the sample's weight was recorded daily. Results are expressed as mean ± SD. Data shown represent three independent experiments.

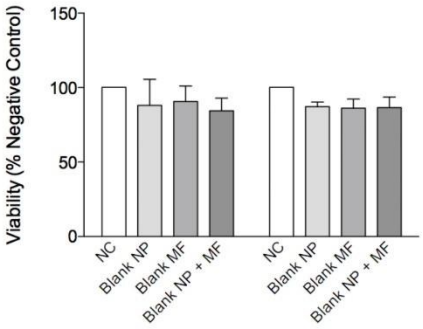

Supplementary Figure 11: Cell viability evaluation of the blank formulations. Results are expressed as mean in treated cells compared to NC ± SD. Data shown represent three independent experiments.

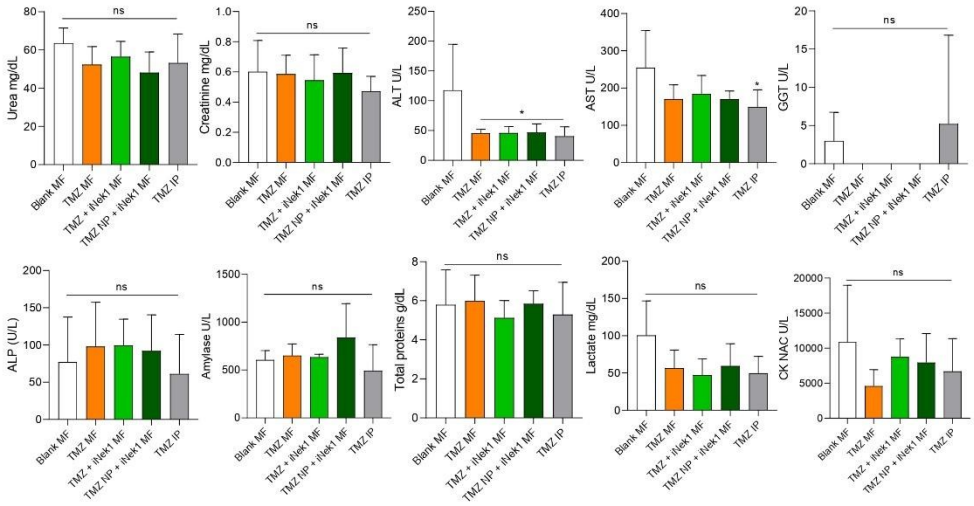

Supplementary Figure 12: Biochemical evaluation of urea, creatinine, amylase, aspartate aminotransferase (AST), alanine aminotransferase (ALT), alkaline phosphatase (ALP), gamma-glutamyl transferase (GGT), total protein, lactate, and creatine kinase (CK) in the serum. Statistical analysis was performed using one-way ANOVA and Tukey post-test. Data were considered significant different at $p < 0.05$ (*).

ANEXO B

Recent developments in drug delivery strategies for targeting DNA damage response in glioblastoma

Artigo científico publicado em coautoria na revista *Life Sciences* (fator de impacto 6.1).

Life Sciences 287 (2021) 120128

Contents lists available at ScienceDirect

Life Sciences

journal homepage: www.elsevier.com/locate/lifescie

Review article

Recent developments in drug delivery strategies for targeting DNA damage response in glioblastoma

A.M. Morás [a,1], J.G. Henn [a,1], L. Steffens Reinhardt [a,1], G. Lenz [b], D.J. Moura [a,*]

[a] Laboratory of Genetic Toxicology, Federal University of Health Sciences of Porto Alegre, (UFCSPA), Porto Alegre, Brazil
[b] Department of Biophysics and Center of Biotechnology, Federal University of Rio Grande do Sul (UFRGS), Porto Alegre, Brazil

ARTICLE INFO

Keywords:
Glioblastoma
DNA repair
Drug resistance
Local delivery
Ionizing radiation
Temozolomide

ABSTRACT

Glioblastoma is the most frequent and malignant brain tumor. The median survival for this disease is approximately 15 months, and despite all the available treatment strategies employed, it remains an incurable disease. Preclinical and clinical research have shown that the resistance process related to DNA damage repair pathways, glioma stem cells, blood-brain barrier selectivity, and dose-limiting toxicity of systemic treatment leads to poor clinical outcomes. In this context, the advent of drug delivery systems associated with localized treatment seems to be a promising and versatile alternative to overcome the failure of the current treatment approaches. In order to bypass therapeutic tumor resistance mechanisms, more effective combinatorial therapies should be identified, such as the use of cytotoxic drugs combined with the inhibition of DNA damage response (DDR)-related targets. Additionally, critical reasoning about the delivery approach and administration route in brain tumors treatment innovation is essential. The outcomes of future experimental studies regarding the association of delivery systems, alternative treatment routes, and DDR targets are expected to lead to the development of refined therapeutic interventions. Novel therapeutic approaches could improve the life's quality of glioblastoma patients and increase their survival rate.

1. Introduction

Glioblastoma (GBM) is the most malignant and frequent primary central nervous system (CNS) tumor, representing 30% of all CNS tumors and 80% of CNS primary malignant tumors [1]. Despite all recent progress in treatment strategies, there are no current curative therapeutic options for GBM, and its median survival is approximately 15 months from the time of diagnosis [2]. GBM is histologically defined as astrocytoma and molecularly classified according to the isocitrate dehydrogenase (IDH) status and O^6-methylguanine-DNA methyltransferase (MGMT) promoter methylation [3,4]. GBM exhibits a diffuse nature, and its complete etiology and pathophysiology are not yet known. Although GBM can occur at any age, it should be noted that the incidence increases with age, with the average diagnosis age being around 65 years [5].

The standard therapy of newly diagnosed GBM consists of maximal safe resection, followed by radiotherapy (RT) plus concomitant and adjuvant temozolomide (TMZ)-based chemotherapy (CT). However, there are several challenges. The highly infiltrative nature of GBM makes complete surgical resection nearly impossible, and the recurrence is inevitable [6,7]. RT and CT directly or indirectly induce cell death through DNA damage [8,9], and several biochemistry pathways influence the therapy success. Also, the genetic background significantly affects the treatment outcome. The cellular response comprises a complex signaling cascade named the DNA damage response (DDR), which is responsible for recognizing, signaling, and correcting DNA damage (Fig. 1).

Different kinds of lesion formed in the DNA require specific DNA repair pathways which allow damage resolution and might contribute to radio and chemoresistance [10]. In this regard, a plethora of treatment approaches aiming at novel molecular targets have been developed, which could be used as therapeutic alternatives. Nevertheless, most of them fail during clinical trials, suggesting that a single targeting strategy does not improve therapeutic outcomes [5,11]. The failure related to

* Correspondence to: D.J. Moura, Laboratory of Genetic Toxicology, Federal University of Health Sciences of Porto Alegre, (UFCSPA), Porto Alegre, Brazil, UFCSPA: Universidade Federal de Ciencias da Saude de Porto Alegre, Brazil.
E-mail addresses: anamoiramoras@gmail.com (A.M. Morás), jefersonghenn@gmail.com (J.G. Henn), luizasteffens@live.com (L. Steffens Reinhardt), lenz@ufrgs.br (G. Lenz), dinaram@ufcspa.edu.br (D.J. Moura).
[1] These authors equally contributed to this work.

https://doi.org/10.1016/j.lfs.2021.120128
Received 9 June 2021; Received in revised form 29 October 2021; Accepted 5 November 2021
Available online 11 November 2021

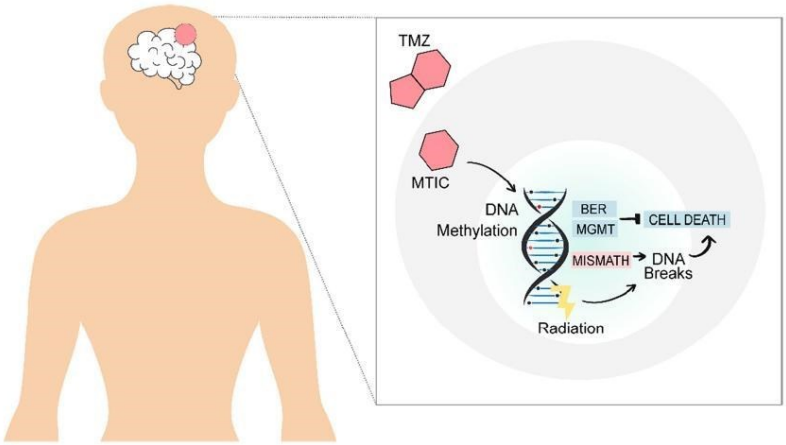

Fig. 1. Direct and indirect DNA damage induced by chemo- and radiotherapy. The mechanism of action of chemotherapy based on temozolomide administration as well as radiotherapy is associated with the modulation of DDR pathways, which can promote cell survival through DNA repair or lead cells to cell death.
Abbreviations: Base excision Repair (BER), O-6-methylguanine-DNA methyltransferase (MGMT), 5-(3-methyl triazen-1-yl)imidazole-4-carbozamide (MTIC). Temozolomide (TMZ).

these approaches might be associated with the compensatory DDR mechanisms, high systemic toxicity, lack of drugs' stability, and insufficiency of *in vitro* and *in vivo* studies demonstrating the efficacy of novel drugs [12].

To bypass GBM resistance mechanisms and decrease treatment side effects, well-designed drug delivery systems (DDS) associated with alternative exposure pathways have become crucial for GBM therapy. Hence, the purpose of this review is to explore how DDR mechanisms contribute to GBM treatment resistance and to present how drug delivery strategies could be used to fine-tune the therapy targeting DNA repair and revert the unhappy out in GBM treatment.

2. The current clinical treatment protocol of glioblastoma (GBM)

GBM is known for its diffusely infiltrative profile that invades multiple lobes and both hemispheres of the brain. Hence, establishing the extent of resection and defining how to balance the benefits and risks of surgery prove to be extremely complicated [13]. Even though high resection rates are usually predictive of survival, it is necessary to thoroughly evaluate the improvement in survival with postoperative neurological deficits as neurological morbidity [14]. Despite being beneficial, surgery has limited efficacy, thus indicating that a combined treatment modality is required.

After surgery, GBM treatment involves a partial-brain fractionated RT of 30 fractions of 2-Gy over six weeks with concomitant daily TMZ (75 mg/m^2 P.O.) 1 h prior. This multimodal treatment is followed by six to twelve cycles of adjuvant TMZ at 150 mg/m^2/day (days 1–5 of a 28-day cycle). The dose can be increased if it is well tolerated by the patient. Wang et al. [15] showed that oral CT plus RT contributed significantly to the improvement in the overall survival (OS) and progression-free survival (PFS) in patients with newly diagnosed GBM when compared to RT alone [16,17]. Still, establishing the ideal therapy in the management of GBM is challenging due to the complexity of this disease and response variability among the general population.

There are several other drugs considered for recurrent gliomas (to review treatment and resistance mechanisms of recurrent GBM, read Campos et al. [18], Díaz et al. [19] and Nam and de Groot [4]). A second alkylating agent, namely lomustine, is frequently used and applied in association with a monoclonal antibody, bevacizumab, in some cases [20]. Recently, Herrlinger et al. [21] demonstrated the effectiveness of the association between lomustine and TMZ *versus* TMZ in a phase III study (ClinicalTrials.gov number NCT01149109). The average OS rate was increased from 31.4 to 48.1 months [21], suggesting a significant improvement in treatment outcome.

RT is a treatment approach that uses ionizing radiation (IR) (*e.g.*, X-ray) to eliminate tumors or prevent malignant cells from growing and metastasizing [22]. Although the cellular death mechanism associated with RT exposure is not completely understood, cellular death is known to be caused by two main reasons, namely cellular stress and DNA damage [9,22]. The DNA damage is caused by the direct interaction of X-ray with several small and macromolecules, inducing DNA single- and double-strand breaks (SSB and DSB respectively), DNA crosslinks, and DNA-protein crosslinks, and by an indirect mechanism caused by reactive oxygen species (ROS) and reactive nitrogen species (RNS). The cellular water radiolysis induced by IR can produce superoxide anion ($O2^{-}$•), hydroxyl radicals (OH•), and hydrogen peroxide (H2O2), which cause organelles and macromolecules damage, including oxidation of DNA bases, SSB, abasic sites, and DSB [23].

Despite the several different types of damage triggered by IR, the most harmful effect of radiation is a clustered DNA damage, defined as two or more lesions formed by the passage of one radiation track, which could be bistrand or in tandem to the DNA strand localization [24]. DSB clusters can lead to chromosome aberrations and cell death, and non-DSB clusters can induce mutations and chromosomal abnormalities that increase the genomic instability of cancer cells [25]. However, tumor cells can adapt their responses to radiation by increasing cellular defenses to neutralize cellular stress activating hypoxia in order to decrease the oxygen supply and limit the production of ROS [26,27]. Furthermore, tumor cells can augment their antioxidant defenses to neutralize oxidative molecules before promoting any cell damage [23].

CT is generally used in combination with RT to treat gliomas, and the most frequently used drug is TMZ, which is rapidly absorbed intact and can cross the blood-brain barrier (BBB). After being absorbed, TMZ undergoes a spontaneous hydrolysis process in pH > 7 and is converted to its active metabolite 5-(3-methyl triazen-1-yl) imidazole-4-

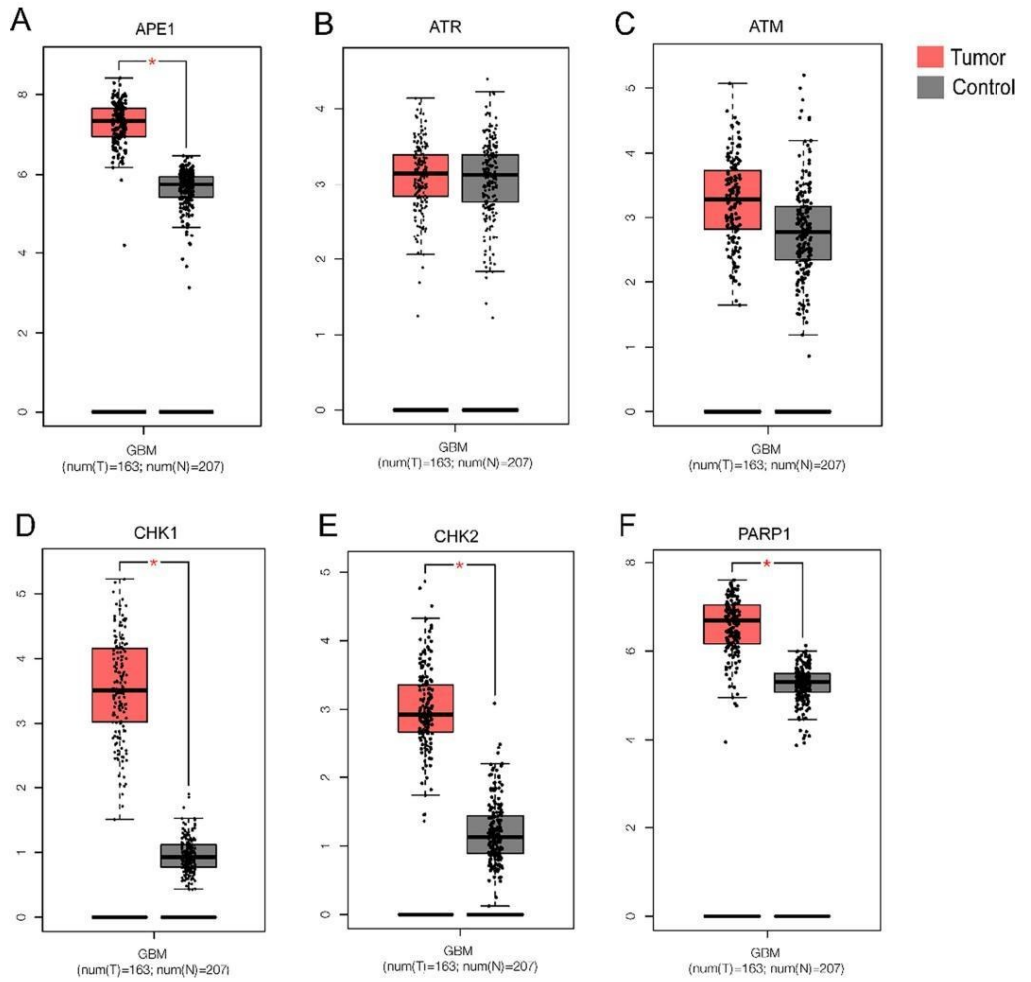

Fig. 2. Expression of DNA repair genes. The expression of the main repair genes involved in the resistance process was evaluated by comparing 163 patients with GBM to 207 controls derived from the GEPIA dataset (http://gepia.cancer-pku.cn/index.html) [34]. The analysis was performed by ANOVA, the $|Log_2FC|$ Cutoff was 0.01 (q-value 0.01) with the match between TCGA and GTEx data.
Abbreviations: DNA-(apurinic or apyrimidinic site) endonuclease (APE1), Ataxia telangiectasia and Rad3 related (ATR), Ataxia telangiectasia mutated (ATM), Checkpoint kinase 1 (CHK1), Checkpoint kinase 2 (CHK2), poly(ADP-ribose) polymerase 1 (PARP-1), Glioblastoma (GBM).

carbozamide (MTIC) [28]. MTIC is further hydrolyzed to methyldiazonium cation and 5 aminoimidazole-4-carboxamide (AIC) [29].

TMZ belongs to the class of alkylating agents, and its mechanism of action consists of the transference of its electrophilic alkyl group to the most nucleophilic atom within the DNA [29]. The methyldiazonium cation preferentially methylates DNA at the N3 position of adenine and N7 position of guanine (90%) but also methylates O^6-guanine (5–10%). Despite being the least frequent lesion, O^6-methylguanine (O^6-MG) is the most cytotoxic and mutagenic lesion leading to the insertion of thymine during the subsequent DNA replication phase [29]. TMZ also induces methylation of macromolecules, such as proteins and lipids. Unfortunately, even though the TMZ-induced methylation of macromolecules has been of great biological importance, it is poorly understood and little is known about its therapeutic contribution [30].

Certainly, the inclusion of TMZ in the newly diagnosed glioma treatment regimen represented an increase in the patient's survival. However, there are several critical consequences associated with the systemic administration of TMZ, such as gastrointestinal or hematological effects [31]. In addition, its clinical use is limited by the need for higher systemic doses for achieving therapeutic effects in the brain [12].

3. Therapeutic resistance process in GBM

Improvements in the GBM treatment have contributed to

ameliorating patients' quality of life and survival outcomes. Nevertheless, the improvements do not translate the considerable technological advances that have occurred in the biomedical areas in the past years. Several resistance mechanisms are related to the failure of current treatments against GBM, including the DNA repair mechanisms, the BBB and blood-brain tumor barrier (BBTB), and the glioma stem cells [10,12], which can be addressed to improve therapy outcomes.

3.1. Lesions induced by chemotherapy (CT) and radiotherapy (RT) can be restored by DNA repair mechanisms

The role of DDR in carcinogenesis and tumor resistance is closely dependent on the timing of evaluation and DNA damage type. The DDR-related proteins have been associated with the two following important aspects: at the beginning of gliomagenesis, DDR breaks the expansion of malignant cells. However, when the cancer cells and tumor niche are installed, DDR contributes to enduring the genomic instability and correcting damages caused by external agents such as CT drugs or radiation [8]. Both CT and RT aim to generate direct DNA damage triggering cell death. A complex protein network is activated in response to different DNA lesions to mediate cellular changes (*e.g.*, cell-cycle arrest) and to directly repair the lesion. Cells activate different repair mechanisms depending on the cellular context and the type of substrate or lesion to be corrected. The repair mechanisms are pro-survival and are related to the resistance process and tumor recurrence [32,33].

In order to evaluate the expression of the members of DNA repair systems, the gene expression of therapeutic targets in human samples was investigated (Fig. 2). The specific role of each of these genes will be discussed in sequence, however, it can be observed in Fig. 2 that the DDR markers are upregulated in tumor samples compared to control samples, contributing to the resistance process in the GBM cells.

There are three main DNA repair pathways that process TMZ alkylation lesions: direct repair by MGMT, base excision repair (BER), and mismatch repair (MMR) [32,33]. O^6-MG lesions are directly repaired by the one-step enzyme MGMT. The expression of *MGMT* is correlated with the resistance to TMZ, mainly because MGMT removes the methyl group from O^6-MG, restoring the integrity of guanine bases in the DNA. The benefits of alkylating agents are largely restricted to patients whose tumors show methylation of *MGMT* promoter [35,36]. If not repaired by MGMT, the thymine misincorporation that occurred during the replication of O^6-MG activates the MMR pathway. This process enters in a futile cycle which replaces the misincorporated thymine with another thymine, leading to energy-consuming cycles, replication fork arrest, and DNA breaks. The conversion of misincorporation errors to a DSB activates DSB repair pathways, and, if the repair fails, apoptosis is triggered [8].

Most of the TMZ-induced lesions, such as N3-methyladenine and N7-methylguanine, are primarily repaired by the BER pathway. Consequently, a functional BER pathway contributes to TMZ resistance and is associated with a worse prognosis in GBM [29]. Additionally to alkylation lesions, the oxidative lesions in DNA bases are usually repaired by BER. In this pathway, a glycosylase initiates the repair process by breaking the glycosidic bond and forming an abasic site. Endonucleases are responsible for cleaving the phosphodiester bond, and finally, the gap is further repaired by DNA polymerases, DNA ligases, and XRCC1 ([23,37]; to review this repair pathway in detail, read [38]).

APE1 is a multifunctional enzyme involved in different activities depending on the protein domain [29]. The main function of APE1 in BER is to create a nick in the phosphodiester backbone of the AP site that has been established when the DNA glycosylase removed the damaged base. When the repair process is concluded, the damage is restored, which contributes to the survival of tumor cells [39]. *APE1* expression is shown in Fig. 2A as being overexpressed in tumor samples. Hudson et al. [40] investigated pre-treatment and posttreatment GBM to identify molecular changes following treatment and recurrence of disease and also demonstrated that specimens had molecular changes that correlated with known resistance mechanisms, including increased expression of APE1. Moreover, APE1 contributes to chemoresistance, facilitating the BRCA1-mediated Homologous recombination (HR) repair in response to DSB [41]. Thus, inhibiting APE1 is an interesting strategy to induce toxicity and decrease the resistance of GBM to TMZ [42].

As previously mentioned, DSBs are highly toxic radiation-induced DNA lesions, and their repair can trigger genomic rearrangements and mutation or apoptosis. The response to DSB starts with the MRN complex (MRE11, RAD53, and NBS1 proteins) sensing the lesion. This complex activates the damage signaling mediated by two proteins related to cell cycle checkpoint mechanisms, namely Rad3-related protein (ATR) and ataxia telangiectasia mutated (ATM), whose action will culminate in DNA damage repair. These proteins phosphorylate downstream targets to coordinate several processes. ATM activates Chk1 and Chk2 to control cell cycle, allowing cell cycle arrest, and 53BP1 and H2AX to model chromatin [43]. ATM phosphorylates p53, inducing G1-arrest by p53-p21 pathway and preventing cells with damaged DNA from entering S-phase [5,44]. As shown in Fig. 2, ATR and ATM are not differently expressed in the evaluated samples, however, Chk1 and Chk2 are highly expressed in GBM patients' samples (Fig. 2B–E).

The repair of DSB can be mediated by HR, an error-free pathway that is dependent on DNA ends resection and template availability, or by Non-homologous end joining (NHEJ) which repairs the damage without the necessity of a template and is hence error-prone [8,45]. Defining which pathway the cells will activate depends on several regulation steps, including DSB extension and availability of DNA repair proteins ([5]; to review these pathways, consult Kakarougkas and Jeggo [43] and Ranjha et al. [46]).

The repair of SSB involves the participation of a protein named poly (ADP-ribose) polymerase 1 (PARP-1). PARP1 bound to DNA strand breaks and assists the repair signaling of this type of lesion by producing a poly (ADP-ribose) chain from the substrate NAD+ [47]. Furthermore, its expression is higher in GBM than non-tumoral tissue (Fig. 2F). In accordance, Galia et al. [48] demonstrated that *PARP-1* is expressed in 27 GBM samples, and Murnyák et al. [47] showed that *PARP-1* upregulation is a characteristic of high-grade astrocytomas and that high *PARP-1* levels are negatively associated with patient survival. Since PARP1 is overexpressed in GBM and its function corresponds to an anti-apoptotic factor that generates cell death resistance, it has been studied as a promising therapeutic target [49].

Contrary to TMZ-related lesions, RT induces damage in clusters whose repair involves a more complex mechanism than individual damage sites. The efficiency of DNA repair proteins can be inhibited by the difficult access to the DNA damage site, thus increasing the repair process time. These unrepaired clusters may generate additional DSB, which increases the genomic instability [25]. DSB in clusters can also induce a shift between DSB repair pathways, which increases genomic instability and cell death even more [50]. In consequence, the cells' ability to repair DNA lesions is compromised by increasing the complexity of the damage, which indicates the importance of RT-induced lesions in therapy and presents possibilities of radioresistance modulation.

3.2. Selective permeability of blood-brain barrier (BBB) and blood-brain tumor barrier (BBTB) can cause treatment resistance

The brain is a complex and delicate organ that involves a vast mechanism of defense formed by a huge vascular network of over 100 billion capillaries tightly joined to the endothelial cells, pericytes, astrocytes, and microglia of the CNS [51,52]. As a result, it causes several challenges to therapeutic approaches, including chemotherapeutic interventions, which are often unable to cross the BBB, rendering the therapy ineffective in many cases of brain cancer [53].

The transport across the BBB may occur by two different pathways: (i) the paracellular transport where substances pass between the

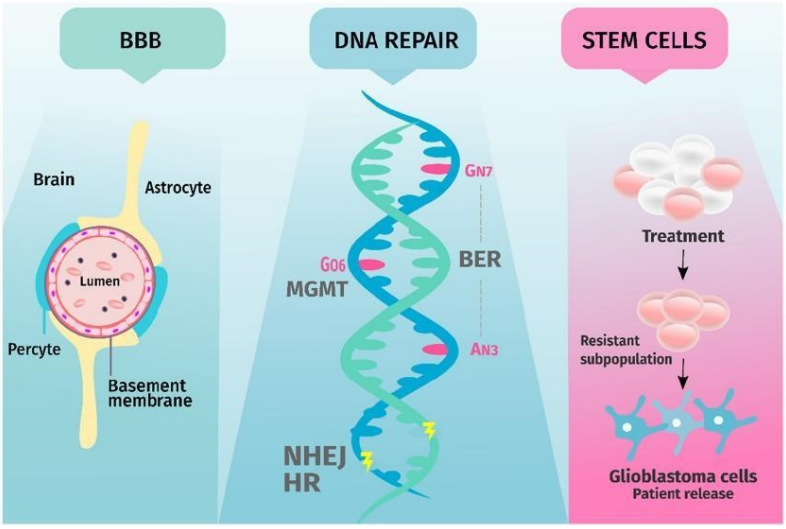

Fig. 3. Cellular mechanisms contributing to GBM resistance. Several resistance mechanisms are related to the failure of current treatments against GBM including Blood-brain barrier, DNA repair mechanisms, and the glioma stem cells. The restricted permeability of the blood-brain interface decreases drug levels in the brain, while the DNA repair pathways act on DNA methylations caused by TMZ and the breaks caused by radiation inducing tumor cell survival, and finally, the resistance of tumor stem cells to treatment and later differentiation in GBM cells contribute to GBM recurrence.
Abbreviations: Blood-brain barrier (BBB); Base excision Repair (BER), O-6-methylguanine-DNA methyltransferase (MGMT); Non-homologous End Join (NHEJ); Homologous Recombination (HR).

endothelial cells and (ii) the transcellular transport where substances pass across the luminal side of the endothelial cells. Similarly, some substances may require other transport mechanisms such as the carrier and receptor-mediated transport. Molecular size and weight, surface charge and lipophilicity of molecules, and integrity of the BBB are common characteristics that regulate these pathways [54]. Besides, the intravascularly administered drug is known to be distributed asymmetrically in smaller amounts to the brain but in larger amounts to other tissues [55,56].

The specialized brain endothelium cells exert barrier properties and are essential to protect the brain from potentially neurotoxic compounds. The normal BBB is vital not only to protect the brain but to also supply it with nutrients and oxygen. The functioning and organization of BBB can be altered in pathological conditions like high-grade gliomas [57]. Thus, in gliomas, their rapid growth and migration are maintained by a structure that resembles the BBB [58]. In this structure, tumor vasculature is in most cases different from the normal vasculature, with branching pattern and cellular and molecular components considerably different from a normal vasculature. The tumor cells damage the BBB and as an effort to grow even more, they create new vascular networks and form a BBTB, which is distinct from the BBB, allowing greater permeability in bulk tumor areas and the opposite in the peripheral ones [59]. Moreover, the capillaries from this vascular system are distended and formed by leaky walls, presenting a sluggish flow and a high interstitial pressure due to the internal accumulation of fluid, which makes this set of factors responsible for variability in drug delivery [60].

Although BBB plays a crucial role in maintaining the local homeostasis in healthy brains by hindering the entrance of substances from the blood, it has been a significant obstacle for brain drug delivery [61,62].

3.3. Glioma stem cells as key drivers of tumor resistance

Glioma stem cells (GSCs) are a small subpopulation of cells within tumors with capabilities of unlimited self-renew and are different to all cell populations present in original tumors [63]. After the first line of chemoradiotherapy, a restricted cell population of stem cells activates DDR, inducing a resistant profile. This cell population might be responsible for the inevitable recurrence of GBM ([64,65,175]).

One explanation for resistance mediated by GSCs is the high levels of DNA replication stress caused by radiation exposure that activates DDR. GSCs constitutively exhibit stress replication caused by replication/transcription collisions and consequent upregulation of DDR, which triggers radioresistance [66]. Previous studies found an association between radioresistance and CD133 status, where the results demonstrated that CD133+ cell populations increase the basal response to DSB, exhibiting active phosphorylation of proteins related to cell cycle checkpoints, such as Rad17, Chk1, and Chk2. Besides, the activation of ATM after radiation exposure is exacerbated in CD133+ cell populations [8,67,68]. The properties of GSCs allow these cell populations to be exposed to CT and later differentiated into highly proliferative tumor cells that might be more resistant than non-stem tumor cells. Consequently, as the local concentration of TMZ cannot eliminate the differentiated cells, tumor recurrence might occur [69].

Fig. 3 summarizes the three main GBM resistance mechanisms. The restricted permeability of the blood-brain interface decreases drug levels in the brain, while the DNA repair pathways act on DNA methylations caused by TMZ and the breaks caused by radiation inducing tumor cell survival. Finally, the resistance of tumor stem cells to treatment and later differentiation in GBM cells contribute to GBM recurrence.

Table 1
Clinical studies (clinical trials database - NIH) carried out with inhibitors of DNA damage response-related targets.

Author or clinical trial ID	Year	Study type	Target	Repair pathway	Drug	Outcome
Quinn et al.	2009a	Phase I	MGMT	Direct repair	O^6-BG	Schedule dose definition. Tolerance limited by myelosuppression
Quinn et al.	2009b	Phase I	MGMT	Direct repair	O^6-BG	1 of 34 patients responded to the treatment. Hematological effects in 48% of the patients.
Adair et al. (NCT00669669)	2014	Phase I/II	MGMT	Direct repair	O^6-BG	increase tolerated cycles of 1.7 to 4.4 PFS = 9 months OS = 20 months
NCT01587144	2012	Phase II	APEI	BER	Lucanthone	Trial in progress
Grupta et al.	2016	GBM PDX lines grown as orthotopic xenografts	PARP1	BER	Veliparib	Increase the TMZ efficiency in MGMT-hypermethylated lines
NCT02152982	2014	Phase II/III	PARP1	BER	Veliparib	Trial in progress
NCT01514201	2012	Phase I/II	PARP1	BER	Veliparib	OS 3 years = 5.3%; PFS 3 years = 2,9%
Abida et al. (NCT02588105)	2018	Phase I	ATM PARP1	DDR DDR	AZD0156 Olaparib	Tolerance limited by hematological toxicity
NCT03423628	2018	Phase I	ATR	DDR	AZD1390	Trial in progress

Abbreviations: ataxia-telangiectasia mutated (ATM); Poly [ADP-ribose] polymerase 1 (PARP1); DNA-(apurinic or apyrimidinic site) endonuclease (APE1); O^6-benzylguanine (O^6-BG); O^6-methylguanine-DNA methyltransferase (MGMT); DNA damage response (DDR); Base Excision Repair (BER).

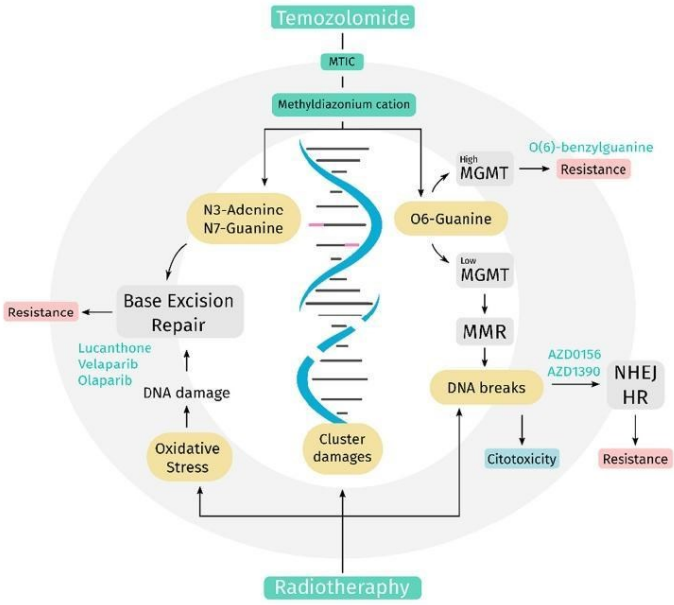

Fig. 4. Repair pathways activated in each damage caused by classical therapies. TMZ is a prodrug that is spontaneously converted to its active metabolite MTIC in a spontaneous hydrolysis process in pH > 7. MTIC is further hydrolyzed to methyldiazonium cation and 5 aminoimidazole-4-carboxamide (AIC). The cation is the active compound responsible for the delivery of methyl groups to DNA, mostly at guanine residues. Approximately 90% of lesions are N3-methyladenine and N7-methylguanine, however, just 5–10% are O^6-MG. Radiotherapy can cause direct damages as DNA breaks or indirect by reactive species generation. However, the most harmful effect of radiation is a clustered DNA damage, defined as two or more lesions formed by the passage of one radiation track. Each of these damages is repaired by specific pathways, which increase the resistance. Several inhibitor molecules have been tested in clinical trials as adjuvants drugs (green). (For interpretation of the references to colour in this figure legend, the reader is referred to the web version of this article.)
Abbreviations: O^6-methylguanine-DNA methyltransferase (MGMT); Mismatch Repair (MMR); Non-homologous End Join (NHEJ); Homologous Recombination (HR); 5-(3-methyl triazen-1-yl)imidazole-4-carbozamide (MTIC).

4. Therapies for glioblastoma targeting DNA damage response

One of the disadvantages of traditional cancer therapy is its absence of specificity. This is easily observed by the fact that the current chemotherapeutic protocols do not only affect the cancerous cells but also damage healthy cells and tissues surrounding the tumor or, in some cases, compromise the entire system, making the risk-benefit ratio even more doubtful [70,71]. Inhibitors of DDR could be a strategy to overcome the resistance, which may provide a therapeutic advantage to reduce tumor recurrence [72]. In this sense, many efforts have been expended to improve the effectiveness of RT and CT. Clinical results of drugs that are emerging as options for modulating the response to DNA damage in GBM (Table 1 and Fig. 4) will be discussed below [73,74].

O^6-benzylguanine (O^6-BG), a synthetic derivative of guanine and competitor of O^6-MG, acts as an inhibitor of MGMT. There are 18 clinical trials registered with O^6-BG. Quinn et al. [75] published studies of phase I and phase II that evaluate the treatment of TMZ plus O^6-BG. The phase I trial established the best schedule of treatment and found that myelosuppression was the limiting effect. The phase II trial demonstrated that only one of 34 patients with GBM responded to the addition of O^6-BG in the treatment schedule and the main signal of toxicity was hematological side effects [76]. This compound, when combined with TMZ or BCNU, was able to bypass tumor resistance when tested in clinical trials (phase I and II) [75–79,176]. Adair et al. [80] reported an interesting strategy to increase the tolerance and efficacy of the combination of O^6-BG with other alkylating agents (NCT00669669). Patients received

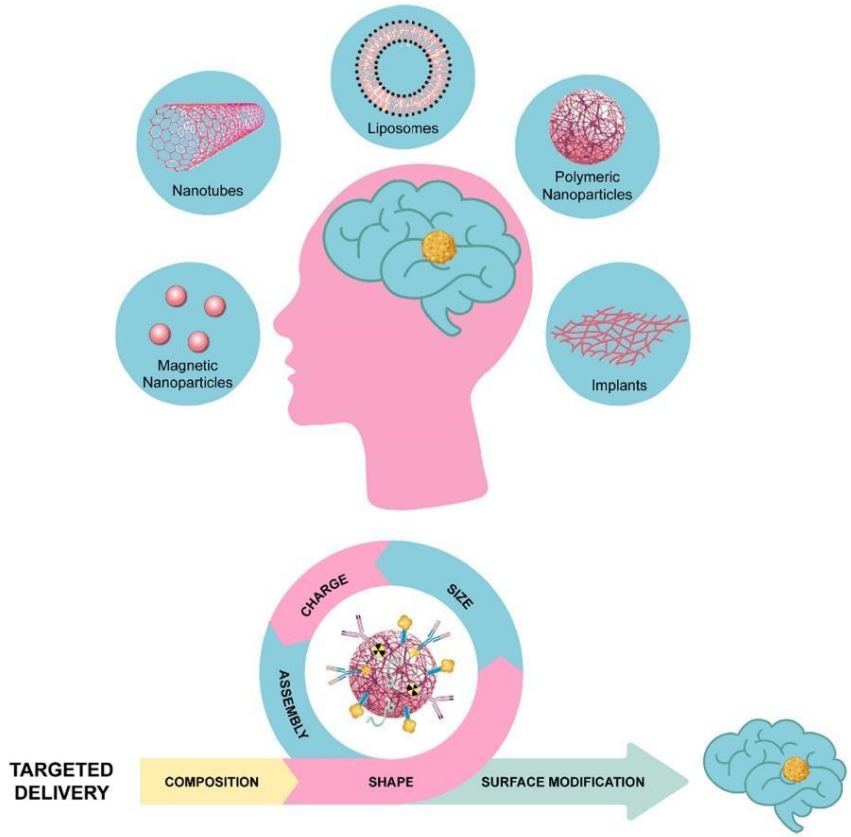

Fig. 5. Drug delivery strategies to target GBM. DDS including magnetic nanoparticles, nanotubes, liposomes, polymeric nanoparticles, and implants can be developed to deliver CT drugs and gene-based therapies to the brain. These strategies can be modified among their physical and chemical properties to generate nanosystems able to recognize and target cancerous cells.

MGMT mutant *P140K* gene-modified autologous hematopoietic $CD34^{+}$ cells which provide chemoprotection against hematopoietic toxicity. The gene therapy increases the mean number of tolerated cycles from 1.7 to 4.4, and the main outcomes were PFS from a diagnosis of nine months and median OS of 20 months. This strategy implies that an increase in the TMZ dose leads to better tolerance of patients to TMZ and survival outcomes. Nevertheless, the study was carried out with only a few patients, and a larger scale study is certainly needed to determine the real impact of this therapy. However, the strategy indicates that adverse effects can be reduced and patients' tolerance to TMZ can be increased.

Lucanthone is a thioxanthone-based DNA intercalator and inhibitor of DNA repair proteins like topoisomerases and APE1 [81]. A phase II study (NCT01587144) evaluates the safety and efficacy of lucanthone as an adjunct with TMZ and RT, however, the results were not available at the time of the manuscript's submission.

Five registered clinical trials can be found with the terms GBM and PARP1. Gupta et al. [82] demonstrated that veliparib increases TMZ efficiency in *MGMT*-hypermethylated GBM cell lines evaluated in orthotopic xenografts, and this was established as an eligibility criterion for the Clinical Trial NCT02152982, a phase II/III study that investigates the combination of TMZ and veliparib compared to only TMZ (there were no results reported at the time of the manuscript's submission). However, a phase I/II study (NCT01514201) that evaluated veliparib, RT, and TMZ in the treatment of younger patients with newly diagnosed diffuse pontine gliomas showed that hematological and gastrointestinal adverse effects can limit veliparib tolerance and that the OS and PFS do not demonstrate a major impact of adding PARP1 inhibitor to the treatment (OS 3 years = 5.3%; PFS 3 years = 2.9%). These unsatisfactory observations could be due to the employment of a systemic treatment approach (oral administration).

As previously discussed, radioresistance is responsible for the treatment failure and relapse in GBM [44], and ATM/Chk2 certainly represents one of the factors that contribute to radioresistance owing to its role as a DSB sensor [83]. Previous studies indicated that ATM is a prognosis factor related to longer survival in GBM [8,84–87]. Romano et al. [44] evaluated ATM protein expression in 21 GBM patients, and a high p-ATM score (++/+++) strongly correlated to shorter survival ($p = 0.022$). In accordance, Squatrito et al. [83] showed in pre-clinical models that the loss of a single copy or both copies of ATM

significantly accelerates glioma formation in mice. Based on these reports, researchers have been testing the clinical application of ATM inhibitors. Due to ATM's prosurvival role in DDR, its inhibition induces DNA damage accumulation, which improves the RT response. AZS1390 and AZD0456 are oral drugs available in GBM tests that have been included in clinical evaluations [88]. Even though ATM has been described as a promising target, there is no clinical data to support the application of ATM inhibitors. In the clinical trials database, there is one study with AZD0156 (NCT02588105) that aims to assess the safety of ATR inhibition in combination with other anticancer drugs in patients with advanced solid tumors. A summary published by the authors' reports that hematologic toxicity decreases the tolerance of AZD0156 with PARP inhibitors [88,89]. Moreover, a phase I study is currently evaluating the safety of AZD1390 in GBM and other brain tumors (NCT03423628) but is still at the recruitment step.

The clinical data shows that although there are many targets considered as promising in the DDR context (Fig. 4), the results are not highly promising in the GBM therapy. It is important to understand that in the context of DNA repair, the inhibition of an overexpressed target associated with the resistance process, for example, is only suitable if it happens at the tumor tissue. Otherwise, it can trigger side effects in normal cells, changing the normal DDR of healthy cells, and this can explain the hematological toxicity caused by the combination of olaparib and AZT0156 for instance [89]. Therefore, the pursuit for alternative therapeutic methods is a necessity for GBM therapy and could be achieved by using DDS that can deliver drugs into the brain and maintain the drugs stable.

5. Overview of drug delivery systems (DDS) for cancer therapy

In a way to overcome the lack of success of the systemic administration of drugs, the advent of DDS seems to be a promising and versatile perspective once this field of research has a range of materials that can be used to increase the cellular uptake of several chemotherapeutic agents [70]. Since this approach allows the mixture of diverse materials by several techniques, it facilitates the combination of different molecules (even the poorly soluble ones), increases their protection from earlier degradation, modifies their targets, modulates membrane interactions, and decreases side effects [90].

Those formulations can be administered by using different routes, which facilitates the delivery to several tissues, especially in brain tumors such as GBM, since this organ is constantly surrounded and shielded by the BBB, not to mention the BBTB that provides extra protection for the tumor microenvironment. Even in cases where those strategies might not be available, the use of localized treatment approaches to bypass some DDS drawbacks is still possible [91,92].

5.1. Use of nanotechnological structures as delivery systems to decrease toxicity and increase efficiency

The conception of complex nanocarriers (Fig. 5) allows the internalization and protection of drugs improving aspects related to the therapy outcome, including the efficiency of drug delivery in a specific target, the physicochemical stability, the surpassing of biological barriers and pharmacological properties, and the administration of different structures, such as proteins and RNAs; besides, multiple agents conjugate in a single nanosystem [93]. Since their surfaces can be modified with targeting molecules, nanocarriers acquire functions that not only deliver molecules to a specific location but also hold a more ample functionality since they may avoid bioactive compounds' early degradation and the consequent loss of effectiveness [94]. Also, the drug targeting concentrates the molecules in the aimed location, avoiding several effects and sometimes allowing the use of lower concentrations and spacing treatment schemes [95], not to mention that these nanocarriers may be able to accumulate inside tumors due to their reduced lymphatic drainage, which is one of the main characteristics of the enhanced permeability and retention (EPR) effect which will be discussed below.

With regard to their main advantages, nanotechnological structures can be designed by several approaches using lipidic and/or polymeric materials, which will generate structures such as liposomes, micelles, exosomes, polymeric and inorganic nanoparticles, and polymer conjugates. The selection of the most suitable material depends on the physicochemical characteristics and interactions between the system and the molecule to be integrated, the route of administration, and the target [96,97].

Liposomes are the most common form of lipid nanosystems and are based on phospholipidic vesicles that allow the loading of hydrophilic agents inside them and hydrophobic molecules at their lipid bilayer [97]. Their composition assembles to the cell membrane, increasing their biocompatibility compared to other nanomaterials, and their structure acts as a shell that protects the drug from early degradation. Even so, disadvantages such as poor solubility and oxidation of their phospholipids could appear. Nevertheless, these disadvantages may be solved by physicochemical and structural adjustments [98,99].

Micelles are colloidal nanostructures with the amphiphilic feature, formed by an external shell with sufficient polarity grade to dissolute in aqueous solutions and an internal hydrophobic core. They are a good approach to increasing the bioavailability of low-solubility drugs [100,101]. Contrary to liposomes and micelles, the exosomes are extracellular vesicles secreted by almost all cell types, and these multiple origins summed to their bilipid layer allow them to interact with different tissues and carry different molecules [102–104].

Polymeric nanoparticles are biodegradable and biocompatible solid colloidal structures that enable therapeutic agents with different characteristics to be entrapped, encapsulated, or absorbed onto the polymeric matrix. They encompass numerous types of natural or synthetic polymers, such as chitosan, albumin, poly(lactide-co-glycolide) (PLGA), poly(acrylic acid) (PAA), polylactide (PLA), and polyvinyl alcohol (PVA), all of them being capable to result in nanocapsules or nanospheres, depending on the process of formation. For differentiation purposes, when compared to natural polymers, the synthetic ones are feasible for better controlled or sustained drug release systems, whereas the difference between nanocapsules and nanospheres is based on the drug allocation (confined to the first one and dispersed all over the second one) [105–107]. Finally, polymers can also be covalently bonded to proteins, drugs, and other molecules as a way of avoiding a possible lack of interaction that may be present by polymeric nanoparticles. Once formed, these polymer conjugates can extend drug circulation time in the blood and improve their bioavailability and local burst release, which reduces adverse effects [108–110].

Inorganic nanoparticles are a wide group that consists of silica, magnetic, silver, and gold structures, which have a relatively easy development process in common, showing a surface engineering and physicochemical properties that provide them with special biocompatibility features [111,112]. Among these different types of nanoparticles, the gold ones have shown interesting results owing to their surface plasmon resonance which turns light into heat and kills local cells by the hypothermia caused [113,114]. Similarly, silver nanoparticles have remarkable conductivity properties that allow them to internalize into cells by endocytosis and release their content to the cytoplasm [115].

5.2. Administration routes to overcome blood-brain barrier (BBB) selectivity

The GBM resistance process is partially imposed by the BBB, which acts as a filter for several molecules, and is not a task to be easily overcome. Other consequences of GBM occurrence may constitute obstacles for brain drug delivery, such as the aggressive infiltration of the tumor, which releases cancer cells into neighboring areas, leading to a recurrent glioma, and the low level of drug diffusion that may cause unexpected local toxicity, reinforcing the requirement of DDS with

Table 2
Strategies and routes for the delivery of nano carriers on the brain.[a]

Strategies	Route	Advantages	Limitations	Reference
Intravascular delivery	Cross[a]	Selective drug delivery High-dose chemotherapy	Lack of treatment to the contralateral hemisphere	[60]
Intracerebral delivery	Bypass[a]	Targeting	Slow diffusion within the brain	[60,116]
Intrathecal and intraventricular infusion	Bypass	High concentrations in cerebrospinal fluid	Invasive Limited concentrations	[51,173]
Intranasal deliver	Bypass	Non-invasive	Local irritation Low efficiency	[51,116]
Intracarotid infusion	Bypass	Free drug diffusion	Passage of pathogens	[61]
Interstitial delivery	Bypass	Sustained and/or controlled release	Invasive Limited distribution through extracellular space	[51]
Transmucosal drug delivery	Bypass	High concentrations delivery	Cost	[61]
Implantable DDS	Bypass	DDS depot directly placed into the extracellular space	Cost	[118]
CED	Bypass	Minimally invasive	Cost	[119]
Direct intratumoral drug administration	Bypass	Fewer side effects	Not feasible depending on the tumor location	[118]
Targeted delivery	Cross	Selective drug delivery High-dose chemotherapy	BBB	[120]
BBB disruption	Bypass	Momentary and localized effects	Non-selective for specific drug/purpose	[118,120]

Abbreviations: blood-brain barrier (BBB); convection-enhanced delivery (CED).
[a] Strategies that cross the BBB are considered to be those that are systematically distributed and can cross the barrier, reaching the brain tissue. On the other hand, strategies that bypass the BBB are locally distributed, not needing to cross the BBB.

reasonable diffusion levels [91,92].

To date, several strategies have been explored to overcome BBB and therefore enhance local drug delivery [116]. These approaches can be divided into physiological, pharmacological, and invasive models [117], encompassing conventional strategies, such as the barrier disruption and transport systems modifications, and alternative methods involving DDS into the brain that can cross or bypass the BBB completely, such as nanoparticle carriers, focused ultrasound, and intrathecal, intraventricular, intranasal and interstitial routes (Table 2).

Once these DDS find a gateway for drug delivery to the brain, they can take advantage of the permeable tumor site vasculature, poor local lymphatic drainage, and compression of lymphatic vessels to reach tumoral environment and accumulate *in situ*, thus reducing systemic cytotoxic effects [121]. This peculiarity, referred to as the EPR effect, can be manipulated by modifications in the nanoparticles' structures, such as their size, shape, physicochemical properties, and porosity [93].

Although the EPR effect diverges between both patients and tumor characteristics, considering its relevance has become the center of several cancer treatments [90], especially when this effect can be used as an enhancer in the treatment of tumors placed beyond physiological barriers that make the therapeutic target almost unreachable, such as brain tumors.

5.2.1. Localized treatment of glioblastoma (GBM) can overcome chemotherapy drawbacks

Localized treatment involves the direct administration of drugs, such as gene delivery, chemotherapeutics, and immunotherapeutics, to the tumor site. This approach has been considerably studied in view of decreasing the adverse effects related to systemic CT. Among the benefits of local administration, the increased amount of drug at the tumor site and the decreased side effects on healthy cells significantly improve the efficacy of treatment. Thus, combining localized treatment with DDS nanocarriers can significantly increase drug stability by targeting the drug release directly into the tumor without the need to bypass biological barriers. Moreover, when these systems are directly delivered to the tumor site, formulations can be generated with diminished drug load. Owing to these advantages, the local treatment modality has been widely studied in the literature [118,122,123] and will only be briefly discussed here. The concept of localized treatment is known to be an easy solution for bypassing BBB, and the DDS used locally can be delivered in different ways as follows:

(i) local implant: depot of DDS directly placed into the extracellular space;
(ii) convection-enhanced delivery (CED): using a pressure head to drive a drug or DDS through the extracellular space. The CED is a method that delivers therapeutics directly through the interstitial spaces of the CNS by an infusion catheter. Results demonstrated prolonged survival of mice treated with CED etoposide compared to control mice [119];
(iii) direct intratumoral drug administration;
(iv) target delivery: cellular receptors-mediated delivery;
(v) BBB disruption: opening the tight junctions in the BBB for a short period and in a specific site.

In GBM, the localized approach is being used mainly to avoid the recurrence by targeting vascular endothelial growth factor (VEGF) overexpressing cells with monoclonal antibodies and the drug bevacizumab since the recurrent tumor is highly vascular [18,120]. Until now, the results indicated that the localized application significantly improves the efficacy of these drugs [124].

Regarding the implantable DDS, several attempts have been made to produce functional brain implants [125–130]. However, the only implant that has been approved by the Food and Drug Administration (FDA) is the Gliadel®. This wafer aims the sustained release of 1,3-bis(2-chloroethyl)-1-nitrosourea (BCNU or carmustine), but its use has only produced modest improvement in patients' survival [131,132]. The implantable therapy approach, combined with controlled-release polymer-based DDS, could allow the use of drugs that were previously not utilized for GBM treatment due to their systemic toxicity, poor availability, and BBB bypassing. Thus, it opens a possibility to target new cellular pathways to treat GBM.

6. Drug delivery strategies applied in the DNA damage context for glioblastoma (GBM)

Despite the treatment management used against GBM, this disease is still an important challenge for the current medicine although several drugs and DDS have been tested. In several cases, the *in vitro* results are very promising but without success in *in vivo* GBM models.

Many reasons can explain this discordant result, including the low selectivity of the treatment and the incapacity of crossing the BBB. For instance, the application of Topoisomerases II poisons against GBM reflects one of these problems. These drugs impair the action of Topoisomerase II, an enzyme that removes the supercoiled DNA events by creating DSB, passing a separate DNA duplex through the breaks generated and rejoining the DNA ends [133]. While the preclinical data are promising, the low levels of intratumoral drug concentrations limit

Table 3
Drug delivery strategies applied in the DNA damage context for GBM tested *in vitro* and/or *in vivo*.

Delivery system	Conventional treatment	DDR target	Delivery approach	Outcome	Reference
Targeting direct repair					
Cationic liposome (LipoTrust™ EX Oligo)	–	MGMT siRNA	Intratumoral injection	The liposome efficiently delivered MGMT-siRNA *in vivo* and enhanced TMZ cytotoxicity.	[137]
Cationic liposome (LipoTrust™ EX Oligo)	–	MGMT siRNA	Intratumoral injection and CED infusions	The DDS did not achieve enough distribution.	[138]
Electrospun PLGA nanofiber	TMZ and BCNU	O^6-BG	Surgically implanted onto the surface of the brain parenchyma	Controlled and sustained release; The treatment efficiency was improved *in vivo*.	[139]
Apoferritin nanocage	TMZ	N3-propargyl imidazotetrazine analog (N3P)	*In vitro*	Greater cells uptake; Increased O^6-MG formation.	[140]
Targeting BER					
Superparamagnetic iron oxide nanoparticles coated with chitosan, PEG, and PEI	RT	APE1 siRNA	Intravenous injection	Mice treated with the combination (nanoparticle + RT) exhibited double extension in survival.	[141]
Oxidized graphene nanoribbons coated with DSPE-PEG	–	Lucanthone	*In vitro*	Enhanced cytotoxicity against GBM cells.	[142]
A fluorescent virus-like particle with a modified surface (cell-penetrating peptide and apolipoprotein E peptide)	TMZ	c-MET siRNA and RNAi	Intravenous injection	It significantly bypassed TMZ-resistance promoting cell death in time and dose-dependent manners, but no improvement was found in animal survival.	[143]
Targeting RT-related DDR					
MDH-DSPE-PEG-2000- cholesterol liposome	RT	DNA repair inhibitor Dbait	Intravenous injection	The treatment was able to effectively sensitize GBM cells to RT inhibiting tumor growth and augmenting the survival of mice.	[144]
PLA-PEG nanoparticle	Fractionated RT	Inhibitors for DNA-PK, ATM, ATR, and Chk1 proteins	Delivered locally *via* CED	The use of the ATR inhibitor impaired HR with insignificant influence on NHEJ and increased animals' survival.	[145]

Abbreviations: convection-enhanced delivery (CED); DNA strand break bait (Dbait); 1,2-distearoyl-sn-glycero- 3-phosphoethanolamine-N–amino (DSPE); O′1,O′1-(3-(dimethylamino) pro-pane-1, 2-diyl) 16-bis (2-(2-methyl-5-nitro1-1H-imidazol-1-yl)ethyl) di (hexadecanedioate) (MDH); polyethylene glycol (PEG); polyethyleneimine (PEI); polylactic acid (PLA); poly(lactic-co-glycolic acid) (PLGA); radiotherapy (RT); temozolomide (TMZ).

the efficacy of clinical applications [134]. In order to overcome this issue, a few delivery strategies were developed. Bruce et al. [135] demonstrated the safety of CED in the treatment of recurrent malignant gliomas treated with the topoisomerase poison Topotecan. Topotecan has an interesting antitumor activity with minimal drug-associated toxicity [135]. In this sense, clinical trials for GBM treatment with doxorubicin have been conducted using delivery strategies, including the Laser Interstitial Thermal Therapy (LITT) to modulate the BBB (NCT01851733) and a nanoparticle delivery targeting cells using bispecific antibodies (NCT02766699) [136].

Table 3 shows studies that developed DDS for targeting DNA repair in a GBM context.

6.1. Drug delivery strategies targeting direct repair

Owing to the importance of MGMT for the effectiveness of GBM CT, since this protein reverses the DNA damage effect of TMZ, several strategies have been developed to improve the efficacy of alkylating agents by inhibiting MGMT activity and diminishing CT resistance (reviewed by [146,147]). Among these strategies is the LipoTrust™ EX Oligo liposome DDS that delivers siRNA downregulating MGMT [137], which suggests that even TMZ-resistant cells could be sensitized to TMZ in both *in vitro* and *in vivo* tumor models after transduction. Similarly, Tsujiuchi et al. [138] used the same DDS for MGMT siRNA delivery. However, even by using CED in the application, the liposomes did not achieve enough distribution in the brain of rats and pigs.

As previously discussed, several studies have revealed that O^6-BG can improve the therapeutic efficacy of alkylating drugs by modulating MGMT activity [148,149]. However, the systemic administration of O^6-BG includes the inability to cross membranes and toxic side effects that can be overcome by an *in situ* approach. Therefore, Liu et al. [139] developed an electrospun poly(lactic-co-glycolic acid) (PLGA) nanofiber loaded with O^6-BG, TMZ, and BCNU. This system presented a controlled and sustained release of O^6-BG for two weeks followed by TMZ and BCNU for >14 weeks, and the *in vivo* results performed in F98 tumor-bearing rats suggested that the treatment efficiency was improved compared to a combined treatment of O^6-BG intraperitoneally, Gliadel® wafer implantation, or oral TMZ. Finally, the authors concluded that the O^6-BG-loaded nanofibers could be potentially used in therapy owing to their release properties that enhance the treatment and decrease systemic toxic effects [139]. This study shows the importance of targeting DNA repair while treating cancer cells with DNA-damaging agents.

An interesting study was designed by Bouzinab et al. [140] where TMZ was loaded into a nanocage made of apoferritin, which can be internalized by the transferrin receptor-1 and can facilitate cell uptake. Following GBM cell exposure to these nanosystems, an increased O^6-MG formation and consequent DNA damage burden were observed. Moreover, the N3-propargyl imidazotetrazine analog (N3P) was used with the apoferritin-nanosystem to overcome TMZ-resistant cells, which suggests that this approach could be further evaluated *in vivo* to confirm its enhanced therapy efficacy.

6.2. Drug delivery strategies targeting BER

A promising approach was established by Kievit et al. [141] in which nanoparticles comprising superparamagnetic iron oxide cores coated with chitosan, PEG, and polyethyleneimine (PEI), transporting anti-APE1 siRNA, were produced and injected intravenously through the tail vein of genetically modified mouse models, and finally, after 24 h, the animals were exposed to RT. The results showed that a reduction of 40% in APE1 activity was achieved only in the tumor tissue and that mice treated with the combination (nanoparticle + RT) exhibited double extension in survival compared to RT alone, which indicates that APE1 inhibition could improve RT outcomes. Another study targeting APE1

was developed by Chowdhury et al. [142] in which nanoribbons of oxidized graphene coated with amphiphilic polymer 1,2-distearoyl-*sn*-glycero-3-phosphoethanolamine-N -amino (DSPE)-PEG were prepared and loaded with lucanthone, an endonuclease inhibitor of APE1. Certain cancer-specificities were observed since this system enhanced cytotoxicity against GBM cells, but there was no toxicity when exposed to other cells such as breast cancer and rat glial progenitor cells [142].

As discussed before, PARP1 is another interesting target for GBM therapy [68] since this protein is considered as a cell-survival factor that acts during the repair of SSB, maintaining the genomic integrity. Several PARP1 inhibition attempts have been performed [68] by using siRNA or commonly known drugs like olaparib. Nevertheless, the results *in vitro* present great potential, while the outcomes *in vivo* do not seem to improve the treatment. It was shown that the inhibition of PARP1 with siRNA or the drug 3-aminobenzamide combined with silencing of MGMT followed by TMZ exposure significantly increased GBM cell death, which suggests that targeting BER and MGMT could be a promising strategy to solve TMZ-resistance [150].

Recently, Pang et al. [143] developed an elegant strategy to improve GBM therapy that aims to target DNA repair synergistically with TMZ exposure and enhances cell uptake by adding a surface modification in the nanosystem. Fluorescent virus-like particle/RNAi nano complexes modified with cell-penetrating peptide and apolipoprotein E peptide (dP@VLP/RNAi) were produced, targeting the tyrosine-protein kinase Met (c-MET), and evaluated *in vivo*. It is classically known that c-MET is a growth factor receptor but is also associated with the maintenance of genomic stability and DDR signaling (reviewed by [151]). c-MET siRNA and the entire complex, dP@VLP/c-MET RNAi, significantly revert TMZ-resistance, promoting cell death in time and dose-dependent manners. Importantly, the stability of the siRNA in the complex was greater than the naked siRNA. The complex was able to cross the BBB and, together with oral TMZ, significantly improved the animals' median survival from 25 days in the oral TMZ group to 42 days in the combination, indicating that the downregulation of c-MET can decrease the repair efficiency and revert CT resistance.

6.3. Drug delivery strategies targeting the radiotherapy-related DNA damage response (DDR)

A promising approach for maximizing GBM therapy is the combination of DNA repair inhibitors and RT. Recently, Liu et al. [144] produced a radiosensitizer-prodrug liposome for the delivery of the DNA repair inhibitor Dbait (DNA strand break bait), which mimics DSB by trapping DNA repair proteins, thus inhibiting the repair of DNA damage associated with RT. Due to the synergistic effects of this combination, the treatment was able to effectively sensitize GBM cells to RT inhibiting tumor growth and augment the survival time of mice [144]. Following the same line, King et al. [145] developed polylactic acid (PLA)-polyethylene glycol (PEG) nanoparticles loaded with DNA repair protein inhibitors, including DNA-PK, ATM, ATR, and Chk1, to be delivered *via* CED, aiming to radiosensitize the gliomas. The authors showed that nanoparticles containing VE822 (ATR inhibitor) could impair HR with insignificant influence on NHEJ, which increases the survival of *in vivo* models when in combination with fractionated RT. The study demonstrated the applicability of combinations of standard therapy and inhibitors for the local treatment of gliomas with the possibility of using this approach in different types of cancers [145].

7. Nanoparticles in cancer research

The most used strategies to drug deliver in the brain have been the pharmacological, neurosurgical-based approaches and destabilization of BBB [119,152]. Regardless of the delivery method, all drugs trigger tumor resistance and tolerance mechanisms that might limit the doses. Nevertheless, understanding the molecular basis of GBM can assist in novel combinatorial therapies such as the use of cytotoxic drugs and DDR-related proteins or synthetic lethality strategies. All approaches have advantages and disadvantages, and hence, understanding the characteristics of each tumor is important in this choice [152]. Many treatment strategies are based on the development of nanoparticles. The following topic will discuss relevant aspects in this context and the importance of evaluating the interaction between biological systems and nanocarriers.

Table 4
NanoEL effect observed in nanoparticles evaluations.

NP	Features	Outcome	Ref
TiO_2	Size: 23.5 and 680 nm Concentration: 5–1.250 μM	NP migrated into the inter-endothelial adherens junction niche, bounded directly to VE-cadherin and disrupted cell-cell interactions causing cell leakiness. This disruption resulted in the loss of interaction between VE-cad with β-catenin and with p120, triggering actin-rearrangement.	[158]
Silica	Size: 48 nm Charge: −18 mV Density: 1.45 g/cm^3 Concentration: 2.0 × 10^{11} NP/ml	NP disrupted the VE-cad-VE-cad interaction at the cell-cell junction of the endothelial cells. The overall gap formation process initiated by interactions of heavy NP. Underflow conditions the chance of NanoEL occurring increases.	[160]
Au	Size: 10 to 30 nm Charge: −16 mV Concentration: 25 μM	NP-induced micrometers sized gaps between endothelial cells within 30 min of exposure. The NanoEL occurred *via* disruption of VE-cad-VE-cad triggering actin remodeling.	[159]
PEI	Size: 25 kD	NP had the potential to activate the immune response *in vivo*. The ROS generation and inflammation activation contributed to immune system dysfunction and cancer metastasis.	[174]
Iron oxide	Size: 16 and 33 nm *application of an external magnetic field	The external magnetic field temporarily disrupted endothelial adherens junctions through internalized iron oxide NP, activating the paracellular transport pathway and facilitating local extravasation of circulating substances.	[157]
Au	Size from 37.66 to 68.43 nm Charge: −40, −20, +15 and +40 mV Concentration: 10 μM	The negative charge on Au NP induced more NanoEL. This NP could be repelled by the negatively charged glycocalyx in a bouncing manner toward the cell-cell junctions.	[161]
Titanium dioxide, silica, Au	Size: around 18 to 23 nm Charge: −20 mV Concentration: 10–40 μg/ml	Intravenously injected NP accelerated both extravasation and intravasation of breast cancer cells *in vivo*, inducing metastasis.	[166]

Abbreviations: nanoparticles (NP); titanium dioxide (TiO2); vascular endothelial (VE); gold (Au); Polyetherimide (PEI).

7.1. Nanoparticles: the cell leakiness drawback

DDS offers several prospects in treating and diagnosing tumors thanks to their many promising and attractive approaches [153–156]. Given the fact that some nanoparticles can provoke endothelial leakiness (NanoEL) [157–161], DDS aiming cancer therapy [162–164] can also accidentally induce NanoEL of the tumor vasculature, thus decreasing the impediment for intravasation entrance of persisting tumor cells into the circulation.

The term NanoEL is related to the cell-cell interaction disruption

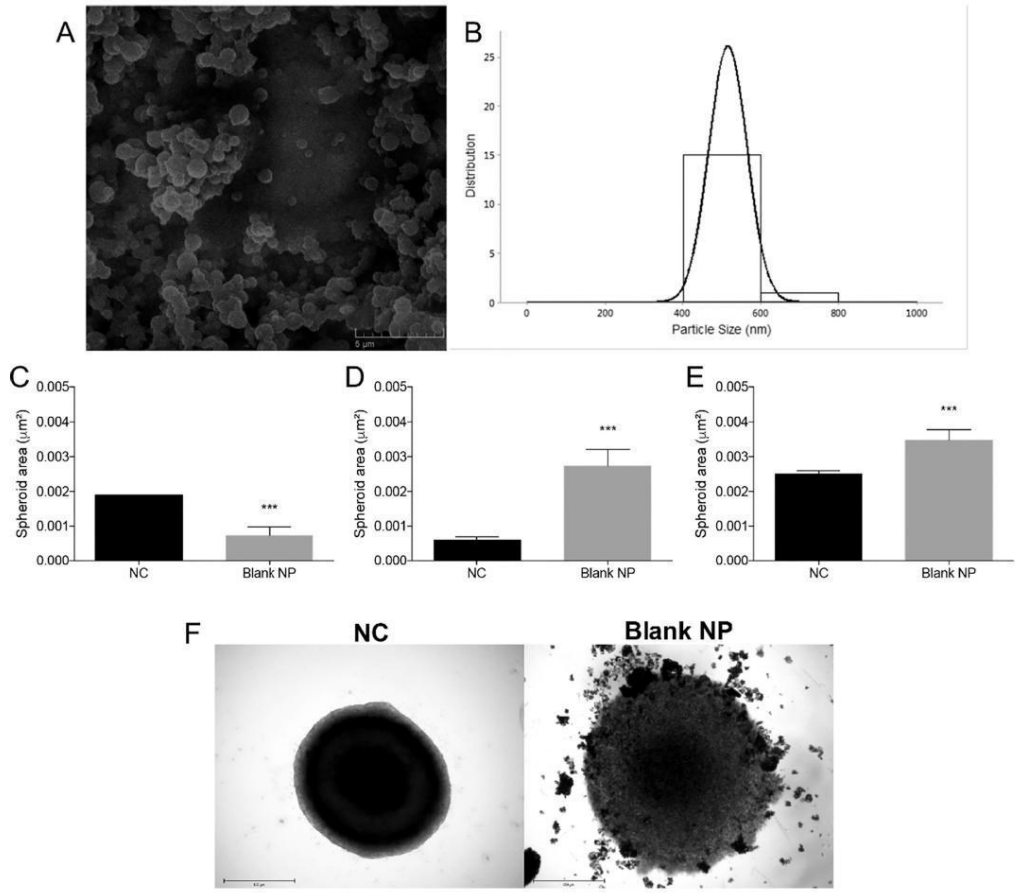

Fig. 6. Characterization of stearic acid nanoparticles. (A) SEM analysis of the nanoparticles. (B) Particle size distribution. (C) Spheroid size. (D) Expansion spheroid area (halo of live cells), (E) total spheroid size (spheroid area plus halo area), and (F) images of spheroids after 5 days of exposure. Results are expressed as mean spheroid area ± SD. Statistical analysis was achieved using one-way ANOVA. Data was considered significant at $^{***}p < 0.005$. NC: negative control.

caused by nanocarriers when it binds to adherent junction proteins, including vascular endothelial-cadherin (VE-cadherin) [158]. After the nanoparticle binds, there is an establishment of a force that disrupts the VE-cadherin interface [160]. The subsequent micrometer-sized gaps formed between the neighboring cells are caused by the intracellular signaling and the endothelial cell tension [158]. These cell junctions' disruptions were discovered to be linked with nanoparticles' size [159], the charge of the surface [161], and intrinsic mass density [160]. Given the importance that this drawback of nanocarriers could imply in nanotechnological approaches for cancer therapy, there is rising evidence of nanoproducts that can trigger endothelial gaps (Table 4) [158,159,165]. Exploring nanoparticles' effects on metastasis can increase the side effects knowledge of nanocarriers and stimulate more examinations on how to reduce the side effects and improve the proposed antitumor effect.

An impressive study developed by Peng et al. [166] systematically analyzed the effects of NanoEF induced by TiO_2 nanoparticles through the investigation of the multiphasic process of metastasis and its various cellular steps. The authors reported that these nanoparticles can promote the adhesion and migration of breast cancer cells to vascular endothelial cells and the permeability induced by the nanoparticle triggered extravasation and intravasation of breast cancer cells *in vivo* by interacting with the capillary endothelium and accelerating the extravasation of circulating cancer cells.

Our research group has prepared and characterized stearic acid nanoparticles (Fig. 6). These nanoparticles were produced by the emulsion method according to Hafeez and Kazmi [167] with minor modifications and characterized according to their size and zeta potential. These carriers presented a mean size of 519.5 ± 52 nm, and the zeta potential was found to be −31.6 ± 0.7 mV (Fig. 6A–B). Its efficacy *in vitro* was evaluated by using 3D cell culture of the U87 cell line. It was observed that after treatment with the nanoparticles, the total spheroid size (Fig. 6E) - spheroid area (Supplementary Fig. 1D) plus the halo formed by the expansion of live cells (Fig. 6C) - was bigger than the control spheroids (negative control). Moreover, the cells were slowly released from the spheroid and the spheroid exhibited a loose

morphology (Fig. 6F), suggesting a decreased tightness of cell contact which could provoke cell extravasation.

As suggested by our data, during the DDS development for cancer treatment, it is necessary to evaluate the interaction between biological systems and nanocarriers. Since nanoproducts can be related to new metastatic sites, an in-depth investigation of NanoEL during the DDS efficacy evaluation must be conducted, mainly in nanocarriers that can accumulate in human tissues and degrade slowly. Therefore, more studies are needed to better understand and regulate the NanoEL effect [168].

8. Conclusions

To date, the most acceptable therapy for newly diagnosed GBM is the combination of surgical resection, chemoradiotherapy with TMZ as adjuvant therapy. GBM remains incurable, and therefore, several new targets have been proposed to increase the patient's responsiveness to the treatment. Some of these targets include DDR proteins with the strategy of decreasing the DNA damage reparation capacity and inducing cell death. However, the low tolerability of these therapies impairs the efficacy and the improvement of survival outcomes [177]. In order to overcome these negative features, extensive attention has been drawn to the field of DDS and several new technologies have been developed to combat GBM [119,152].

The pharmacological approaches based on liposomes, polymeric nanoparticles, and wafers have been used in the context of DNA damage response inhibition [137–139,144,145,169]. These approaches allow the incorporation of several effective antitumor agents in the GBM treatment protocol, whose application was impaired by low BBB permeability such as doxorubicin [152]. Overcoming BBB selectivity with DDS unlocks a range of possibilities with known drugs whose tolerance and toxicity are already known. Nevertheless, the main challenge of using nanoparticles and liposomes is the short half-life in a systemic application [170,171].

In light of this, neurosurgical-based approaches allow the delivery at specific regions, which increases the bioavailability and efficiency of drugs [152]. The CED approach allows a continuous drug delivery *via* a catheter using positive pressure to increase the circulation throughout the brain tissue [119]. The invasiveness of this technology and the infection risk are some of the disadvantages. However, the local administration enables high drug concentrations, decreasing resistance mechanisms and avoiding systemic toxicity [119,135,152]. Furthermore, the delivery systems could assist in drug repositioning for GBM, which is a promising option as it aims to expand the possibilities of drugs whose pharmacokinetics and toxicity are already known [128,172].

Lastly, as described by this review, recent progress in DDS to the brain demonstrates the potential of new delivery strategies to permit novel and commonly used CT drugs and gene-based therapies to target brain cancer cells. These strategies can be modified among their physical and chemical properties to generate nanosystems that can recognize and target cancerous cells. It is expected that the ideas resulting from future experimental studies with the association of delivery systems and DDR targets will lead to the development of improved therapeutic interventions, which could bring hope to the incurable scenario of GBM patients.

Declaration of competing interest

The authors declare that they have no known competing financial interests or personal relationships that could have influenced the work reported in this paper.

Acknowledgments

The research was supported by grants from the Brazilian Agencies "Coordenação de Aperfeiçoamento de Pessoal de Nível Superior (CAPES)" and "Fundação de Amparo à Pesquisa do Rio Grande do Sul (FAPERGS)."

References

[1] N.A. Bush, S.M. Chang, M.S. Berger, Current and future strategies for treatment of glioma, Neurosurg. Rev. 40 (1) (2017) 1–14, https://doi.org/10.1007/s10143-016-0709-8.
[2] M.T.C. Poon, C.L.M. Sudlow, J.D. Figueroa, P.M. Brennan, Sci. Rep. 10 (1) (2020), https://doi.org/10.1038/s41598-020-68011-4.
[3] D.N. Louis, A. Perry, G. Reifenberger, et al., The 2016 World Health Organization classification of tumors of the central nervous system: a summary, Acta Neuropathol. 131 (6) (2016) 803–820, https://doi.org/10.1007/s00401-016-1545-1.
[4] J.Y. Nam, J.F. de Groot, Treatment of glioblastoma, J. Oncol. Pract. 13 (10) (2017) 629–638, https://doi.org/10.1200/JOP.2017.025536.
[5] E. Le Rhun, M. Preusser, P. Roth, D.A. Reardon, M. van den Bent, P. Wen, G. Reifenberger, M. Weller, Molecular targeted therapy of glioblastoma, Cancer Treat. Rev. 80 (2019), 101896, https://doi.org/10.1016/j.ctrv.2019.101896.
[6] J. Bartek, K. Ng, J. Bartek, W. Fischer, B. Carter, C.C. Chen, Key concepts in glioblastoma therapy, J. Neurol. Neurosurg. Psychiatry 83 (7) (2012) 753–760, https://doi.org/10.1136/jnnp-2011-300709.
[7] A. Hatoum, R. Mohammed, O. Zakieh, The unique invasiveness of glioblastoma and possible drug targets on extracellular matrix, Cancer Manag. Res. 11 (2019) 1843–1855, https://doi.org/10.2147/cmar.s186142.
[8] L. Annovazzi, M. Mellai, D. Schiffer, Chemotherapeutic drugs: DNA damage and repair in glioblastoma, Cancers (Basel) (2017) 57, https://doi.org/10.3390/cancers9060057. Published 2017 May 26.
[9] M. Lomax, L. Folkes, P. O'Neill, Biological consequences of radiation-induced DNA damage: relevance to radiotherapy, Clin. Oncol. 25 (10) (2013) 578–585.
[10] C.P. Haar, P. Hebbar, G.C. Wallace, A. Das, W.A. Vandergrift, J.A. Smith, P. Giglio, S.J. Patel, K.R. Swapan, N.L. Banik, Drug resistance in glioblastoma: a mini review, Neurochem. Res. 37 (6) (2012) 1192–1200.
[11] R. Batash, N. Asna, P. Schaffer, N. Francis, M. Schaffer, Glioblastoma multiforme, diagnosis and treatment; recent literature review 24 (27) (2017) 3002–3009, https://doi.org/10.2174/0929867324666170516123206.
[12] A. Miranda, M. Blanco-Prieto, J. Sousa, A. Pais, C. Vitorino, Breaching barriers in glioblastoma. Part I: molecular pathways and novel treatment approaches, Int. J. Pharm. 531 (1) (2017) 372–388, https://doi.org/10.1016/j.ijpharm.2017.07.056.
[13] R.L. Yong, R.R. Lonser, Surgery for glioblastoma multiforme: striking a balance, World Neurosurg. 76 (6) (2011) 528–530, https://doi.org/10.1016/j.wneu.2011.06.053.
[14] M.E. Oppenlander, A.B. Wolf, L.A. Snyder, et al., An extent of resection threshold for recurrent glioblastoma and its risk for neurological morbidity, J. Neurosurg. 120 (4) (2014) 846–853, https://doi.org/10.3171/2013.12.JNS13184.
[15] Z. Wang, G. Yang, Y.Y. Zhang, Y. Yao, L.H. Dong, A comparison between oral chemotherapy combined with radiotherapy and radiotherapy for newly diagnosed glioblastoma: a systematic review and meta-analysis, Medicine (Baltimore) (2017), e8444, https://doi.org/10.1097/MD.0000000000008444.
[16] R. Stupp, W.P. Mason, M.J. van den Bent, et al., Radiotherapy plus concomitant and adjuvant temozolomide for glioblastoma, N. Engl. J. Med. 352 (10) (2005) 987–996.
[17] R. Stupp, Changing paradigms - an update on the multidisciplinary management of malignant glioma, Oncologist 11 (2) (2006) 165–180, https://doi.org/10.1634/theoncologist.11-2-165.
[18] B. Campos, L.R. Olsen, T. Urup, H.S. Poulsen, A comprehensive profile of recurrent glioblastoma, Oncogene 35 (45) (2016) 5819–5825, https://doi.org/10.1038/onc.2016.85.
[19] R.J. Díaz, S. Ali, M.G. Qadir, M.I. de la Fuente, M.E. Ivan, R.J. Komotar, The role of bevacizumab in the treatment of glioblastoma, J. Neuro-Oncol. 133 (3) (2017) 455–467, https://doi.org/10.1007/s11060-017-2477-x.
[20] W. Wick, T. Gorlia, M. Bendszus, M. Taphoorn, F. Sahm, I. Harting, A.A. Brandes, W. Taal, J. Domont, A. Ibdaih, M. Campone, P.M. Clement, R. Stupp, M. Fabbro, E. Le Rhun, F. Dubois, M. Weller, A. von Deimling, V. Golfinopoulos, J. C. Bromber, M. Platten, M. Klein, M.J. van den Bent, Lomustine and bevacizumab in progressive glioblastoma, N. Engl. J. Med. 377 (20) (2017) 1954–1963.
[21] U. Herrlinger, T. Tzaridis, F. Mack, et al., Lomustine-temozolomide combination therapy versus standard temozolomide therapy in patients with newly diagnosed glioblastoma with methylated MGMT promoter (CeTeG/NOA-09): a randomised, open-label, phase 3 trial, Lancet 393 (10172) (2019) 678–688, https://doi.org/10.1016/S0140-6736(18)31791-4.
[22] J.-S. Wang, H.-J. Wang, H.-L. Qian, Biological effects of radiation on cancer cells, Mil. Med. Res. 5 (20) (2018) 1–10, https://doi.org/10.1186/s40779-018-0167-4.
[23] W. Kim, S. Lee, D. Seo, D. Kim, K. Kim, E. Kim, J. Kang, K.M. Seong, H. Youn, B. Youn, Cellular stress responses in radiotherapy, Cells 9 (8) (2019) 1105, https://doi.org/10.3390/cells8091105.
[24] L.J. Eccles, P. O'Neill, M.E. Lomax, Delayed repair of radiation induced clustered DNA damage: friend or foe? Mutat. Res. 711 (1–2) (2011) 134–141, https://doi.org/10.1016/j.mrfmmm.2010.11.003.
[25] A. Asaithamby, D.J. Chen, Mechanism of cluster DNA damage repair in response to high-atomic number and energy particles radiation, Mutat. Res. 711 (1–2) (2011) 87–99, https://doi.org/10.1016/j.mrfmmm.2010.11.002.
[26] S. Rey, L. Schito, M. Koritzinsky, B.G. Wouters, Molecular targeting of hypoxia in radiotherapy, Adv. Drug Deliv. Rev. 109 (2017) 45–62.

[27] A. Salazar-Ramiro, D. Ramírez-Ortega, V.P. de la Cruz, N.Y. Hérnandez-Pedro, D. F. González-Esquivel, J. Sotelo, B. Pineda, Role of redox status in development of glioblastoma, Front. Immunol. 7 (2016) 1–15.
[28] J. Zhang, M.F. Stevens, T.D. Bradshaw, Temozolomide: mechanisms of action, repair and resistance, Curr. Mol. Pharmacol. 5 (1) (2012) 102–114, https://doi.org/10.2174/1874467211205010102.
[29] H. Strobel, T. Baisch, R. Fitzel, et al., Temozolomide and other alkylating agents in glioblastoma therapy 7 (3) (2019) 69, https://doi.org/10.3390/biomedicines7030069.
[30] F. Drabløs, E. Feyzi, P.A. Aas, C.B. Vaagbø, B. Kavli, M.S. Bratlie, J. Peña-Diaz, M. Otterlei, G. Slupphaug, Z.E. Krokan, Alkylation damage in DNA and RNA–repair mechanisms and medical significance, DNA Repair 3 (11) (2004) 1389–1407, https://doi.org/10.1016/j.dnarep.2004.05.004.
[31] S.H. Bae, M.J. Park, M.M. Lee, T.M. Kim, S.H. Lee, S.Y. Cho, Y.H. Kim, Y.J. Kim, C.K. Park, C.Y. Kim, Toxicity profile of temozolomide in the treatment of 300 malignant glioma patients in Korea, J. Korean Med. Sci. 29 (7) (2014) 980–984, https://doi.org/10.3346/jkms.2014.29.7.980.
[32] H. Erasimus, M. Gobin, S. Niclou, E. van Dyck, DNA repair mechanisms and their clinical impact in glioblastoma 769 (2016) 19–35, https://doi.org/10.1016/j.mrrev.2016.05.005.
[33] R.J. Head, M.F. Fay, L. Cosgrove, K.Y.C. Fung, D. Rundle-Thiele, J.H. Martin, Persistence of DNA adducts, hypermutation and acquisition of cellular resistance to alkylating agents in glioblastoma 18 (12) (2017) 917–926, https://doi.org/10.1080/15384047.2017.1385680.
[34] Z. Tang, et al., GEPIA: a web server for cancer and normal gene expression profiling and interactive analyses, Nucleic Acids Res. (2017), https://doi.org/10.1093/nar/gkx247.
[35] M. Christmann, B. Kaina, Epigenetic regulation of DNA repair genes and implications for tumor therapy 780 (2017) 15–28, https://doi.org/10.1016/j.mrrev.2017.10.001.
[36] M.E. Hegi, E. Genbrugge, T. Gorlia, et al., MGMT promoter methylation cutoff with safety margin for selecting glioblastoma patients into trials omitting temozolomide: a pooled analysis of four clinical trials, Clin. Cancer Res. 25 (6) (2019) 1809–1816, https://doi.org/10.1158/1078-0432.CCR-18-3181.
[37] D. Svilar, E.M. Goellner, K.H. Almeida, R.W. Sobol, Base excision repair and lesion-dependent subpathways for repair of oxidative DNA damage, Antioxid. Redox Signal. 14 (12) (2011) 2491–2507, https://doi.org/10.1089/ars.2010.3466.
[38] T. Visnes, M. Grube, B.M.F. Hanna, C. Benitez-Buelga, A. Cázares-Körner, T. Helleday, Targeting BER enzymes in cancer therapy, DNA Repair (Amst) 71 (2018) 118–126, https://doi.org/10.1016/j.dnarep.2018.08.015.
[39] G. Tell, F. Quadrifoglio, C. Tiribelli, M.R. Kelley, The many functions of APE1/Ref-1: not only a DNA repair enzyme, Antioxid. Redox. Signal. 11 (3) (2009) 601–620, https://doi.org/10.1089/ars.2008.2194.
[40] A.L. Hudson, N.R. Parker, P. Khong, Glioblastoma recurrence correlates with increased APE1 and polarization toward an immuno-suppressive microenvironment, Front Oncol. 8 (2018) 314, https://doi.org/10.3389/fonc.2018.00314. Published 2018 Aug 13.
[41] T. Ströbel, S. Madlener, S. Tuna, et al., Ape1 guides DNA repair pathway choice that is associated with drug tolerance in glioblastoma, Sci. Rep. 7 (1) (2017) 9674, https://doi.org/10.1038/s41598-017-10013-w.
[42] T. Izumi, B. Brown, C.V. Naidu, K.K. Bhakat, M. Macinnes, H. Saito, D.J. Chen, S. Mitra, Two essential but distinct functions of the mammalian abasic endonuclease, Proc. Natl. Acad. Sci. U. S. A. 102 (16) (2005) 5739–5743.
[43] A. Kakarougkas, P.A. Jeggo, DNA DSB repair pathway choice: an orchestrated handover mechanism, Br. J. Radiol. (2014), 20130685, https://doi.org/10.1259/bjr.20130685.
[44] F.J. Romano, E. Guadagno, D. Solari, G. Borrelli, S. Pignatiello, P. Cappabianca, M.D.B. de Caro, ATM and p53 combined analysis predicts survival in glioblastoma multiforme patients: a clinicopathologic study, J. Cell. Biochem. 119 (6) (2018) 4867–4877, https://doi.org/10.1002/jcb.26699.
[45] G. Iliakis, H. Wang, A.R. Perrault, W. Boecker, B. Rosidi, F. Windhofer, W. Wu, J. Guan, G. Terzoudi, G. Pantelias, Mechanisms of DNA double strand break repair and chromosome aberration formation 104 (1–4) (2004) 14–20, https://doi.org/10.1159/00007746.
[46] L. Ranjha, S.M. Howard, P. Cejka, Main steps in DNA double-strand break repair: an introduction to homologous recombination and related processes, Chromosoma 127 (2) (2018) 187–214, https://doi.org/10.1007/s00412-017-0.
[47] B. Murnyák, M.C. Kouhsari, R. Hershkovitch, B. Kálmán, G. Marko-Varga, Á. Klekner, T. Hortobágyi, PARP1 expression and its correlation with survival is tumour molecular subtype dependent in glioblastoma, Oncotarget 8 (28) (2017) 46348–46362. 10.18632/oncotarget.18013.
[48] A. Galin, A.E. Calogero, R. Condorelli, et al., PARP-1 protein expression in glioblastoma multiforme, Eur. J. Histochem. 56 (1) (2012), e9.
[49] S.A. Jannetti, G. Carlucci, B. Carney, S. Kossatz, L. Shenker, L.M. Carter, B. Salinas, C. Brand, A. Sadique, P.L. Donabedian, K.M. Cunanan, M. Gönen, V. Ponomarev, B.M. Zeglis, M.M. Souweidane, J.S. Lewis, W.A. Weber, J. L. Humm, T. Reiner, PARP-1-targeted radiotherapy in mouse models of glioblastoma, J. Nucl. Med. 59 (8) (2018) 1225–1233.
[50] J.A. Nickoloff, N. Sharma, L. Taylor, Clustered DNA double-strand breaks: biological effects and relevance to cancer radiotherapy, Genes (Basel) 11 (1) (2020) 99.
[51] D.S. Hersh, A.S. Wadajkar, N.B. Roberts, J.G. Perez, N.P. Connolly, V. Frenkel, J. A. Winkles, G.F. Woodworth, A.J. Kim, Evolving drug delivery strategies to overcome the blood brain barrier, Curr. Pharm. Des. 22 (9) (2016) 1177–1193.
[52] D.D. Stenehjem, A.M.S. Hartz, B. Bauer, G.W. Anderson, Novel and emerging strategies in drug delivery for overcoming the blood–brain barrier, Future Med. Chem. 1 (9) (2009) 1623–1641, https://doi.org/10.4155/fmc.09.137.
[53] A. Misra, S. Ganesh, A. Shahiwala, S.P. Shah, Drug delivery to the central nervous system: a review, J. Pharm. Pharm. Sci. 6 (2) (2003) 252–273.
[54] N.J. Abbott, A.A.K. Patabendige, D.E.M. Dolman, S.R. Yusof, D.J. Begley, Structure and function of the blood-brain barrier, Neurobiol. Dis. 37 (1) (2010) 13–25, https://doi.org/10.1016/j.nbd.2009.07.030.
[55] D.R. Groothuis, The blood-brain and blood-tumor barriers: a review of strategies for increasing drug delivery, Neuro Oncol. 2 (1) (2000) 45–59, https://doi.org/10.1093/neuonc/2.1.45.
[56] X. Lin, Tian, Feng Wei, Huang, Wang, Diao, Enhanced brain targeting of temozolomide in polysorbate-80 coated polybutylcyanoacrylate nanoparticles, Int. J. Nanomed. 445 (2011), https://doi.org/10.2147/ijn.s16570.
[57] B. Obermeier, R. Daneman, R.M. Ransohoff, Development, maintenance anddisruption of the blood–brain barrier, Nat. Med. 19 (2013) 1584–1596.
[58] F.G. Dhermain, P. Hau, H. Lanfermann, A.H. Jacobs, M.J. van den Bent, Advanced MRI and PET imaging for assessment of treatment response in patients with gliomas, Lancet Neurol. 9 (2010) 906–920.
[59] O. van Tellingen, B. Yetkin-Arik, M.C. de Gooijer, P. Wesseling, T. Wurdinger, H. E. de Vries, Overcoming the blood-brain tumor barrier for effective glioblastoma treatment, Drug Resist. Updat. 19 (2015) 1–12.
[60] I.S. Chandran, P.M. Prasanna, Blood brain barrier and various strategies for drug delivery to brain, Br. Biomed. Bull. (2014) 504–520. ISSN-2347-5447.
[61] P.K. Pandey, A.K. Sharma, U. Gupta, Blood brain barrier: an overview on strategies in drug delivery, realistic in vitro modeling and in vivo live tracking, Tissue Barriers 4 (1) (2016), e1129476, https://doi.org/10.1080/21688370.2015.1 129476.
[62] S.B. Pehlivan, Nanotechnology-based drug delivery systems for targeting, imaging and diagnosis of neurodegenerative diseases, Pharm. Res. 30 (10) (2013) 2499–2511, https://doi.org/10.1007/s11095-013-1156-7.
[63] A. Schulz, F. Meyer, A. Dubrovska, K. Borgmann, Cancer stem cells and radioresistance: DNA repair and beyond, Cancers (Basel) 11 (6) (2019) 862, https://doi.org/10.3390/cancers11060862. Published 2019 Jun 21.
[64] S. Bao, Q. Wu, R.E. McLendon, et al., Glioma stem cells promote radioresistance by preferential activation of the DNA damage response, Nature 444 (7120) (2006) 756–760, https://doi.org/10.1038/nature05236.
[65] J. Chen, Y. Li, T.-S. Yu, A restricted cell population propagates glioblastoma growth after chemotherapy, Nature 488 (7412) (2012) 522–526, https://doi.org/10.1038/nature11287.
[66] R. Carruthers, A.J. Chalmers, The potential of PARP inhibitors in neuro-oncology 1 (1) (2012) 85–97, https://doi.org/10.2217/cns.12.13.
[67] A.J. Chalmers, Radioresistant glioma stem cells - therapeutic obstacle or promising target? DNA Repair 6 (9) (2007) 1391–1394, https://doi.org/10.1016/j.dnarep. 2007.03.019.
[68] A.J. Chalmers, Overcoming resistance of glioblastoma to conventional cytotoxic therapies by the addition of PARP inhibitors, Anti Cancer Agents Med. Chem. 10 (7) (2010) 520–533, https://doi.org/10.2174/187152010793498627.
[69] M. Zhao, D. van Straten, M.L.D. Broekman, V. Préat, R.M. Schiffelers, Nanocarrier-based drug combination therapy for glioblastoma, Theranostics 10 (3) (2020) 1355–1372, https://doi.org/10.7150/thno.38147.
[70] K.H. Bae, H.J. Chung, T.G. Park, Nanomaterials for cancer therapy and imaging, Mol. Cells 31 (4) (2011) 295–302, https://doi.org/10.1007/s10 059-011-0051-5.
[71] K.K. Jain, A critical overview of targeted therapies for glioblastoma, Front. Oncol. 8 (2018), https://doi.org/10.3389/fonc.2018.00419.
[72] B.M. Alexander, N. Pinnell, P.Y. Wen, A. D'Andrea, Targeting DNA repair and the cell cycle in glioblastoma, J. Neuro-Oncol. 107 (3) (2011) 463–477, https://doi.org/10.1007/s11060-011-0765-4.
[73] B. Kaina, M. Christmann, DNA repair in personalized brain cancer therapy with temozolomide and nitrosoureas, DNA Repair 78 (2019) 128–141.
[74] S. Kesari, S.J. Advani, J.D. Lawson, K.T. Kahle, K. Ng, B. Carter, C.C. Chen, DNA damage response and repair: insights into strategies for radiation sensitization of gliomas, Future Oncol. 7 (11) (2011) 1335–1346.
[75] J.A. Quinn, S.X. Jiang, D.A. Reardon, A. Desjardins, J.J. Vredenburgh, J.N. Rich, S. Gururangan, A.H. Friedman, D.D. Bigner, J.H. Sampson, R.E. McLendon, J. E. Herndon Jr., A. Walker, H.S. Friedman, Phase I trial of temozolomide plus O6-benzylguanine 5-day regimen with recurrent malignant glioma, Neuro-Oncology 11 (5) (2009) 556–561, https://doi.org/10.1215/15228517-2009-007.
[76] J.A. Quinn, S.X. Jiang, D.A. Reardon, A. Desjardins, J.J. Vredenburgh, J.N. Rich, S. Gururangan, A.H. Friedman, D.D. Bigner, J.H. Sampson, R.E. McLendon, J. E. Herndon II, A. Walker, H.S. Friedman, Phase II trial of temozolomide plus o6-benzylguanine in adults with recurrent, temozolomide-resistant malignant glioma, J. Clin. Oncol. 27 (8) (2009) 1262–1267, https://doi.org/10.1200/JCO.2008.18.8417.
[77] J.A. Quinn, A. Desjardins, J. Weingart, et al., Phase I trial of temozolomide plus O6-benzylguanine for patients with recurrent or progressive malignant glioma, J. Clin. Oncol. 23 (2005) 7178–7187.
[78] J.A. Quinn, J. Pluda, M.E. Dolan, et al., Phase II trial of carmustine plus O(6)-benzylguanine for patients with nitrosourea-resistant recurrent or progressive malignant glioma, J. Clin. Oncol. 20 (9) (2002) 2277–2283, https://doi.org/10.1200/JCO.2002.09.084.
[79] J. Weingart, S.A. Grossman, K.A. Carson, et al., Phase I trial of polifeprosan 20 with carmustine implant plus continuous infusion of intravenous O6-benzylguanine in adults with recurrent malignant glioma: new approaches to brain tumor therapy CNS consortium trial, J. Clin. Oncol. 25 (4) (2007) 399–404, https://doi.org/10.1200/JCO.2006.06.6290.

[80] J.E. Adair, S.K. Johnston, M.M. Mrugala, et al., Gene therapy enhances chemotherapy tolerance and efficacy in glioblastoma patients, J. Clin. Invest. 124 (9) (2014) 4082–4092, https://doi.org/10.1172/JCI76739.
[81] M.D. Naidu, R. Agarwal, L.A. Pena, L. Cunha, M. Mezei, M. Shen, D.M. Wilson III, Y. Liu, Z. Sanchez, P. Chaudhary, S.H. Wilson, M.J. Waring, Lucanthone and its derivative hycanthone inhibit apurinic endonuclease-1 (APE1) by direct protein binding, PLoS ONE 6 (9) (2011), e23679.
[82] S.K. Gupta, S.H. Kizilbash, B.L. Carlson, A.C. Mladek, F. Boakye-Agyeman, K. K. Bakken, J.L. Pokorny, M.A. Schroeder, P.A. Decker, L. Cen, J.E. Eckel-Passow, G. Sarkar, K.V. Ballman, J.M. Reid, R.B. Jenkins, R.G. Verhaak, E.P. Sulman, G. J. Kitange, J.N. Sarkaria, Delineation of MGMT hypermethylation as a biomarker for veliparib-mediated temozolomide-sensitizing therapy of glioblastoma, J. Natl. Cancer Inst. (2015), djv369, https://doi.org/10.1093/jnci/djv369.
[83] M. Squatrito, C.W. Brennan, K. Helmy, J.T. Huse, J.H. Petrini, E.C. Holland, Loss of ATM/Chk2/p53 pathway components accelerates tumor development and contributes to radiation resistance in gliomas, Cancer Cell 18 (6) (2010) 619–629, https://doi.org/10.1016/j.ccr.2010.10.034.
[84] I. Dokic, A. Mairani, S. Brons, B. Schoell, A. Jauch, D. Krunic, J. Debus, A. Régnier-Vigouroux, K.-J. Weber, High resistance to X-rays and therapeutic carbon ions in glioblastoma cells bearing dysfunctional ATM associates with intrinsic chromosomal instability, Int. J. Radiat. Biol. 91 (2) (2015) 157–165.
[85] S.E. Golding, E. Rosenberg, B.R. Adams, S. Wignarajah, J.M. Beckta, M. J. O'Connor, K. Valerie, Dynamic inhibition of ATM kinase provides a strategy for glioblastoma multiforme radiosensitization and growth control, Cell Cycle 11 (6) (2012) 1167–1173, https://doi.org/10.4161/cc.11.6.19576.
[86] H.J. Seol, H.Y. Yoo, J. Jin, K.M. Joo, D.-S. Kong, S.J. Yoon, H. Yang, W. Kang, D.-H. Lim, K. Park, J.H. Kim, Nam D.-H. Lee J-Il., Prognostic implications of the DNA damage response pathway in glioblastoma, Oncol. Rep. 26 (2) (2011) 423–430, https://doi.org/10.3892/or.2011.1325.
[87] S. Tribius, A. Pidel, D. Casper, ATM protein expression correlates with radioresistance in primary glioblastoma cells in culture, Int. J. Radiat. Oncol. Biol. Phys. 50 (2) (2001) 511–523, https://doi.org/10.1016/s0360-3016(01)01489-4.
[88] G. Frosina, D. Marubbi, D. Marcello, D. Vecchio, A. Daga, The efficacy and toxicity of ATM inhibition in glioblastoma initiating cells-driven tumor models, Crit. Rev. Oncol. Hematol. 138 (2019) 214–222.
[89] W. Abida, Y.J. Bang, L. Carter, A. Azaro, M. Krebs, S. Im, Y. Chen, N. Buil-Bruna, Y. Li, D. Eato, C. Stephens, G. Ross, M. Pass, J. Rodon, E. Dean, Abstract A094: phase I modular study of AZD0156, a first-in-class oral selective inhibitor of ataxia telangiectasia mutated protein kinase (ATM), in combination with Olaparib (AToM study, module 1) [abstract], in: proceedings of the AACR-NCI-EORTC international conference: molecular targets and cancer therapeutics; Oct 26-30; Philadelphia, PA. Philadelphia (PA): AACR, Mol. Cancer Ther. 17 (1 Suppl) (2018). Abstract nr A094.
[90] N. Bertrand, J. Wu, X. Xu, N. Kamaly, O.C. Farokhzad, Cancer nanotechnology: the impact of passive and active targeting in the era of modern cancer biology, Adv. Drug Deliv. Rev. 66 (2014) 2–25, https://doi.org/10.1016/j.addr.2013.11.009.
[91] A. Giese, R. Bjerkvig, M.E. Berens, M. Westphal, Cost of migration: invasion of malignant gliomas and implications for treatment, J. Clin. Oncol. 21 (8) (2003) 1624–1636, https://doi.org/10.1200/jco.2003.05.063.
[92] S.Y. Tzeng, J.J. Gree, Therapeutic nanomedicine for brain cancer, Ther. Deliv. 4 (6) (2013) 687–704, https://doi.org/10.4155/tde.13.38.
[93] J. Shi, P.W. Kantoff, R. Wooster, O.C. Farokhzad, Cancer nanomedicine: progress, challenges and opportunities, Nat. Rev. Cancer 17 (1) (2017) 20–37, https://doi.org/10.1038/nrc.2016.108.
[94] W. Gu, C. Wu, J. Chen, Y. Xiao, Nanotechnology in the targeted drug delivery for bone diseases and bone regeneration, Int. J. Nanomed. 8 (2013) 2305–2317.
[95] L. Dang, J. Liu, F. Li, L. Wang, D. Li, B. Guo, X. He, F. Jiang, C. Liang, B. Liu, S. A. Badshah, B. He, J. Lu, C. Lu, A. Lu, G. Zhang, Targeted delivery dystems for molecular therapy in skeletal disorders, Int. J. Mol. Sci. 17 (3) (2016) 428.
[96] A.G. Arranja, V. Pathak, T. Lammers, Y. Shi, Tumor-targeted nanomedicines for cancer theranostics, Pharmacol. Res. 115 (2017) 87–95.
[97] V.K. Chaturvedi, A. Singh, V.K. Singh, M.P. Singh, in: Cancer Nanotechnology: A New Revolution for Cancer Diagnosis and Therapy 1530, Publications.Uu.Se, 2018, pp. 41–195.
[98] Z. Li, S. Tan, S. Li, Q. Shen, K. Wang, Cancer drug delivery in the nano era: an overview and perspectives (review), Oncol. Rep. 38 (2017) 611–624.
[99] E. Pérez-Herrero, A. Fernández-Medarde, Advanced targeted therapies in cancer: drug nanocarriers, the future of chemotherapy, Eur. J. Pharm. Biopharm. 93 (2015) 52–79.
[100] L. Bregoli, D. Movia, J.D. Gavigan-Imedio, J. Lysaght, J. Reynolds, A. Prina-Mello, Nanomedicine applied to translational oncology: a future perspective on cancer treatment, Nanomed. Nanotechnol.Biol. Med. 12 (2016) 81–103.
[101] M. Rizwanullah, S. Amin, S.R. Mir, K.U. Fakhri, M.M.A. Rizvi, Phytochemical based nanomedicines against cancer: current status and future prospects, J. Drug Target. 26 (2018) 731–752.
[102] N. Couto, S. Caja, J. Maia, M.C.S. Moraes, B. Costa-Silva, Exosomes as emerging players in cancer biology, Biochimie 155 (2018) 2–10.
[103] D.W. Greening, S.K. Gopal, R. Xu, R.J. Simpson, W. Chen, Exosomes and their roles in immune regulation and cancer, Semin. Cell Dev. Biol. 40 (2015) 72–81.
[104] W. Lim, H.S. Kim, Exosomes as therapeutic vehicles for cancer, Tissue Eng. Regen. Med. 16 (2019) 213–223.
[105] K. Letchford, H. Burt, A review of the formation and classification of amphiphilic block copolymer nanoparticulate structures: micelles, nanospheres, nanocapsules and polymersomes, Eur. J. Pharm. Biopharm. 65 (2007) 259–269.
[106] S. Parveen, S.K. Sahoo, Polymeric nanoparticles for cancer therapy, J. Drug Target. 16 (2008) 108–123.
[107] R.H. Prabhu, V.B. Patravale, M.D. Joshi, Polymeric nanoparticles for targeted treatment in oncology: current insights, Int. J. Nanomedicine 10 (2015) 1001–1018.
[108] M. Chang, F. Zhang, T. Wei, T. Zuo, Y. Guan, G. Lin, W. Shao, Smart linkers in polymer-drug conjugates for tumor-targeted delivery, J. Drug Target. 24 (2016) 475–491.
[109] I. Ekladious, Y.L. Colson, M.W. Grinstaff, Polymer–drug conjugate therapeutics: advances, insights and prospects, Nat. Rev. Drug Discov. 18 (2019) 273–294.
[110] X. Pang, X. Yang, G. Zhai, Polymer-drug conjugates: recent progress on administration routes, Expert Opin. Drug Deliv. 11 (2014) 1075–1086.
[111] F. Yang, C. Jin, S. Subedi, C.L. Lee, Q. Wang, Y. Jiang, J. Li, Y. Di, D. Fu, Emerging inorganic nanomaterials for pancreatic cancer diagnosis and treatment, Cancer Treat. Rev. 38 (2012) 566–579.
[112] M. Yezhelyev, R. Yacoub, R. O'Regan, Inorganic nanoparticles for predictive oncology of breast cancer, Nanomedicine 4 (2009) 83–103.
[113] A. Mukerjee, A.P. Ranjan, J.K. Vishwanatha, Combinatorial nanoparticles for cancer diagnosis and therapy, Curr. Med. Chem. 19 (2012) 3714–3721.
[114] J. Xu, K. Liao, H. Jiang, W. Zhou, Research progress of novel inorganic nanometre materials carriers in nanomedicine for cancer diagnosis and treatment 46 (2018) S492–S502.
[115] C. Greulich, J. Diendorf, T. Simon, G. Eggeler, M. Epple, M. Köller, Uptake and intracellular distribution of silver nanoparticles in human mesenchymal stem cells, Acta Biomater. (2011), https://doi.org/10.1016/j.actbio.2010.08.003.
[116] D. Furtado, M. Björnmalm, S. Ayton, A.I. Bush, K. Kempe, F. Caruso, Overcoming the blood-brain barrier: the role of nanomaterials in treating neurological diseases, Adv. Mater. 30 (46) (2018) 1–66.
[117] M. Kristensen, B. Brodin, Routes for drug translocation across the blood-brain barrier: exploiting peptides as delivery vectors, J. Pharm. Sci. 106 (2017) 2326–2334, https://doi.org/10.1016/j.xphs.2017.04.080.
[118] R.W. Chakroun, P. Zhang, R. Lin, P. Schiapparelli, A. Quiñones-Hinojosa, H. Cui, Nanotherapeutic systems for local treatment of brain tumors, Wiley Interdiscip. Rev. Nanomed. Nanobiotechnol. (2017), https://doi.org/10.1002/wnan.1479.
[119] A.M. Sonabend, A.S. Carminucci, B. Amendolara, et al., Convection-enhanced delivery of etoposide is effective against murine proneural glioblastoma, Neuro-Oncology 16 (9) (2014) 1210–1219, https://doi.org/10.1093/neuonc/nou026.
[120] D.A. Reardon, J.N. Rich, H.S. Friedman, D.D. Bigner, Recent advances in the treatment of malignant astrocytoma, J. Clin. Oncol. 24 (8) (2006) 1253–1265, https://doi.org/10.1200/JCO.2005.04.5302.
[121] P. Kumari, B. Glosh, S. Biswas, Nanocarriers for cancer-targeted drug delivery, J. Drug Target. 24 (3) (2015) 179–191.
[122] Y. Çırpanlı, E. Allard, C. Passirani, E. Bilensoy, L. Lemaire, S. Çalış, J.-P. Benoit, Antitumoral activity of camptothecin-loaded nanoparticles in 9L rat glioma model, Int. J. Pharm. 2011 (403) (2011) 201–206, https://doi.org/10.1016/j.ijpharm.2010.10.015.
[123] L. Nam, C. Coll, L.C.S. Erthal, C. de la Torre, D. Serrano, R. Martínez-Máñez, M. J. Santos-Martínez, E. Ruiz-Hernández, Drug delivery nanosystems for the localized treatment of glioblastoma multiforme, Materials (Basel) 11 (5) (2018) 779, https://doi.org/10.3390/ma1050779.
[124] A. Shivinsky, T. Bronshtein, T. Haber, M. Machluf, The effect of AZD2171- or sTRAIL/Apo2L-loaded polylactic-co-glycolic acid microspheres on a subcutaneous glioblastoma model, Biomed. Microdevices 17 (2015) 69.
[125] M. Irani, G.M.M. Sadeghi, I. Haririan, The sustained delivery of temozolomide from electrospun PCL-diol-b-PU/gold nanocompsite nanofibers to treat glioblastoma tumors, Mater. Sci. Eng. C Mater. Biol. Appl. 75 (2017) 165–174, https://doi.org/10.1016/j.msec.2017.02.029.
[126] S. Ni, X. Fan, J. Wang, H. Qi, X. Li, Biodegradable implants efficiently deliver combination of paclitaxel and temozolomide to glioma C6 cancer cells in vitro, Ann. Biomed. Eng. 42 (1) (2014) 214–221, https://doi.org/10.1007/s10439-013-0903-6.
[127] R. Ramachandran, V.R. Junnuthula, G.S. Gowd, et al., Theranostic 3-dimensional nano brain-implant for prolonged and localized treatment of recurrent glioma, Sci. Rep. 7 (2017) 43271, https://doi.org/10.1038/srep43271.
[128] L. Steffens, A.M. Morás, P.R. Arantes, et al., Electrospun PVA-dacarbazine nanofibers as a novel nano brain-implant for treatment of glioblastoma: in silico and in vitro characterization, Eur. J. Pharm. Sci. 2020 (143) (2020), 105183, https://doi.org/10.1016/j.ejps.2019.105183.
[129] R. Tavakoli, S. Vakilian, F. Jamshidi-Adegani, S. Sharif, A. Ardeshirylajimi, M. Soleimani, Prolonged drug release using PCL–TMZ nanofibers induce the apoptotic behavior of U87 glioma cells, Int. J. Polym. Mater. Polym. Biomater. 67 (15) (2018) 873–878, https://doi.org/10.1080/00914037.2017.1393677.
[130] Y. Tseng, C. Su, S. Yang, Y. Huang, W. Lee, Y. Wang, S. Liu, S. Liu, Advanced interstitial chemotherapy combined with targeted treatment of malignant glioma in rats by using drug-loaded nanofibrous membranes, Retrieved from, Oncotarget 7 (2016) 59902–59916, https://www.oncotarget.com/article/10989/text/.
[131] L.S. Ashby, K.A. Smith, B. Stea, Gliadel wafer implantation combined with standard radiotherapy and concurrent followed by adjuvant temozolomide for treatment of newly diagnosed high-grade glioma: a systematic literature review 14 (1) (2016) 225, https://doi.org/10.1186/s12957-016-0975-5.
[132] P. De Bonis, C. Anile, A. Pompucci, et al., Acta Neurochir. 154 (8) (2012) 1371–1378, https://doi.org/10.1007/s00701-012-1413-2.
[133] J.C. Rocha, F.F. Busatto, L.K. de Souza, J. Saffi, Influence of nucleotide excision repair on mitoxantrone cytotoxicity, DNA Repair (Amst) 42 (2016) 33–43, https://doi.org/10.1016/j.dnarep.2016.04.005.

[134] A.M. Al-Abd, A. Khedr, S.G. Atteiah, F.A. Al-Abbasi, Intra-tumoral drug concentration mapping within solid tumor micro-milieu using in-vitro model and doxorubicin as a model drug, Saudi Pharm J. 28 (6) (2020) 754–762, https://doi.org/10.1016/j.jsps.2020.05.001.
[135] J.N. Bruce, R.L. Fine, P. Canoll, J. Yun, B.C. Kennedy, S.S. Rosenfeld, et al., Regression of recurrent malignant gliomas with convection-enhanced delivery of topotecan, Neurosurgery 69 (2011) 1272–1279.
[136] A. Mehta, C.U. Awah, A.M. Sonabend, Topoisomerase II poisons for glioblastoma; existing challenges and opportunities to personalize therapy, Front. Neurol. 9 (2018) 1–11, https://doi.org/10.3389/fneur.2018.00459.
[137] T. Kato, A. Natsume, H. Toda, et al., Efficient delivery of liposome-mediated MGMT-siRNA reinforces the cytotoxity of temozolomide in GBM-initiating cells, Gene Ther. 17 (11) (2010) 1363–1371, https://doi.org/10.1038/gt.2010.88.
[138] T. Tsujiuchi, A. Natsume, K. Motomura, G. Kondo, M. Ranjit, R. Hachisu, I. Sugimura, S. Tomita, I. Takehara, M. Woolley, N.U. Barua, S.S. Gill, A. S. Bienemann, Y. Yamashita, S. Toyokuni, T. Wakabayashi, Preclinical evaluation of an O(6)-methylguanine-DNA methyltransferase-siRNA/liposome complex administered by convection-enhanced delivery to rat and porcine brains, Am. J. Transl. Res. 6 (2) (2014) 169–178.
[139] S.J. Liu, T.C. Yang, S.T. Yang, Y.C. Chen, Y.Y. Tseng, Biodegradable hybrid-structured nanofibrous membrane supported chemoprotective gene therapy enhances chemotherapy tolerance and efficacy in malignant glioma rats 46 (sup2) (2018) 515–526, https://doi.org/10.1080/21691401.2018.1460374.
[140] K. Bouzinab, H.S. Summers, Stevens MFG, Delivery of temozolomide and N3-propargyl analog to brain tumors using an apoferritin nanocage, ACS Appl. Mater. Interfaces 12 (11) (2020) 12609–12617, https://doi.org/10.1021/acsami.0c01514.
[141] F.M. Kievit, K. Wang, T. Ozawa, Nanoparticle-mediated knockdown of DNA repair sensitizes cells to radiotherapy and extends survival in a genetic mouse model of glioblastoma, Nanomedicine 13 (7) (2017) 2131–2139, https://doi.org/10.1016/j.nano.2017.06.004.
[142] S.M. Chowdhury, C. Surhland, Z. Sanchez, Graphene nanoribbons as a drug delivery agent for lucanthone mediated therapy of glioblastoma multiforme, Nanomedicine 11 (1) (2015) 109–118, https://doi.org/10.1016/j.nano.2014.08.001.
[143] H.H. Pang, C.Y. Huang, Y.W. Chou, Bioengineering fluorescent virus-like particle/RNAi nanocomplexes act synergistically with temozolomide to eradicate brain tumors, Nanoscale 11 (17) (2019) 8102–8109, https://doi.org/10.1039/c9nr01247h.
[144] H. Liu, Y. Cai, Y. Zhang, et al., Development of a hypoxic radiosensitizer-prodrug liposome delivery DNA repair inhibitor Dbait combination with radiotherapy for glioma therapy, Adv. Healthc. Mater. (2017), https://doi.org/10.1002/adhm.201601377.
[145] H.O. King, et al., RAD51 is a selective DNA repair target to radiosensitize glioma stem cells 8 (2017) 125–139.
[146] Y.R. Lawrence, M.V. Mishra, M. Werner-Wasik, D.W. Andrews, T.N. Showalter, J. Glass, et al., Improving prognosis of glioblastoma in the 21st century: who has benefited most? Cancer 118 (2012) 4228–4234.
[147] J.W. Taylor, D. Schiff, Treatment considerations for MGMT-unmethylated glioblastoma 15 (2014) 1–6, https://doi.org/10.1007/s11910-014-0507-z.
[148] M.S. Bobola, S.H. Tseng, A. Blank, M.S. Berger, J.R. Silber, Role of O6-methylguanine-DNA methyltransferase in resistance of human brain tumor cell lines to the clinically relevant methylating agents temozolomide and streptozotocin, Clin. Cancer Res. 2 (1996) 735–741.
[149] S. Ma, S. Egyházi, T. Ueno, et al., O6-methylguanine-DNA-methyltransferase expression and gene polymorphisms in relation to chemotherapeutic response in metastatic melanoma, Br. J. Cancer 89 (8) (2003) 1517–1523, https://doi.org/10.1038/sj.bjc.6601270.
[150] V.L. Thibado, Methods to Increase Temozolomide Sensitivity in Glioblastoma Multiforme: Manipulating PARP-1 and MGMT, Northern Michigan University, Ann Arbor, 2011 [M.S.].
[151] M. Medová, D.M. Aebersold, Y. Zimmer, The molecular crosstalk between the MET receptor tyrosine kinase and the DNA damage response-biological and clinical aspects, Cancers 6 (1) (2013) 1–27, https://doi.org/10.3390/cancers6010001.
[152] M. Fakhoury, Drug delivery approaches for the treatment of glioblastoma multiforme, Artif. Cells Nanomed. Biotechnol. 44 (6) (2016) 1365–1373, https://doi.org/10.3109/21691401.2015.1052467.
[153] Y. Matsumoto, et al., Vascular bursts enhance permeability of tumour blood vessels and improve nanoparticle delivery, Nat. Nanotechnol. 11 (2016) 533–538.
[154] R. Molinaro, et al., Biomimetic proteolipid vesicles for targeting inflamed tissues, Nat. Mater. 15 (2016) 1037–1046.
[155] A. Parodi, et al., Synthetic nanoparticles functionalized with biomimetic leukocyte membranes possess cell-like functions, Nat. Nanotech. 8 (2012) 61–68.
[156] C.Y. Tay, Reality check for nanomaterials-mediated therapy with 3D biomimetic culture systems, Adv. Funct. Mater. 26 (2016) 4046–4065 (2016).
[157] Y. Qiu, et al., Magnetic forces enable controlled drug delivery by disrupting endothelial cell-cell junctions, Nat. Commun. 8 (2017) 15594.
[158] M.I. Setyawati, et al., Titanium dioxide nanomaterials cause endothelial cell leakiness by disrupting the homophilic interaction of VE-cadherin, Nat. Commun. 4 (2013) 1673.
[159] M.I. Setyawati, C.Y. Tay, B.H. Bay, D.T. Leong, Gold nanoparticles induced endothelial leakiness depends on particle size and endothelial cell origin, ACS Nano 11 (2017) 5020–5030.
[160] C.Y. Tay, M.I. Setyawati, D.T. Leong, Nanoparticle density: a critical biophysical regulator of endothelial permeability, ACS Nano 11 (2017) 2764–2772.
[161] J. Wang, L. Zhang, F. Peng, X. Shi, D.T. Leong, Targeting endothelial cell junctions with negatively charged gold nanoparticles, Chem. Mater. 30 (2018) 3759–3767.
[162] X. Ding, et al., Defect engineered bioactive transition metals dichalcogenides quantum dots, Nat. Commun. 10 (2019) 41.
[163] L. Li, et al., Actively targeted deep-tissue imaging and photothermal-chemotherapy of breast cancer by antibody-functionalized drug-loaded X-ray responsive bismuth sulfide@mesoporous silica core-shell nanoparticles, Adv. Funct. Mater. 28 (2018) 1704623.
[164] F. Peng, et al., Silicon-nanowire-based nanocarriers with ultrahigh drug loading capacity for in vitro and in vivo cancer therapy, Angew. Chem. Int. Ed. 52 (2013) 1457–1461.
[165] M.I. Setyawati, V.M. Mochalin, D.T. Leong, Tuning endothelial permeability with functionalized nanodiamonds, ACS Nano 10 (2016) 1170–1181 (2016).
[166] F. Peng, et al., Nanoparticles promote in vivo breast cancer cell intravasation and extravasation by inducing endothelial leakiness, Nature 14 (2019) 279–286.
[167] A. Hafeez, I. Kazmi, Dacarbazine nanoparticle topical delivery system for the treatment of melanoma, Sci. Rep. 7 (2017) 16517.
[168] M.I. Setyawati, C.Y. Tay, D. Docter, R.H. Stauber, D.T. Leong, Understanding and exploiting nanoparticles' intimacy with the blood vessel and blood, Chem. Soc. Rev. 44 (2015) 8174–8199 (2015).
[169] C.H. Ryu, W.S. Yoon, K.Y. Park, et al., Valproic acid downregulates the expression of MGMT and sensitizes temozolomide-resistant glioma cells, J. Biomed. Biotechnol. 987495 (2012), https://doi.org/10.1155/2012/987495.
[170] E. Beltrán-Gracia, A. López-Camacho, I. Higuera-Ciapara, J.B. Velázquez-Fernández, A.A. Vallejo-Cardona, Nanomedicine review: clinical developments in liposomal applications, CancerNanotechnol. 10 (1) (2019), https://doi.org/10.1186/s12645-019-0055-y.
[171] V. Laquintana, A. Trapani, N. Denora, F. Wang, J.M. Gallo, G. Trapani, New strategies to deliver anticancer drugs to brain tumors 6 (2009) 1017–1032.
[172] S.K. Tan, A. Jermakowicz, A.K. Mookhtiar, C.B. Nemeroff, S.C. Schürer, N. G. Ayad, Drug repositioning in glioblastoma: a pathway perspective, Front. Pharmacol. 9 (2018) 218, https://doi.org/10.3389/fphar.2018.00218.
[173] L.P. Ganipineni, F. Danhier, V. Préat, Drug delivery challenges and future of chemotherapeutic nanomedicine for glioblastoma treatment, J. Control. Release 10 (281) (2018) 42–57, https://doi.org/10.1016/j.jconrel.2018.05.00 8.
[174] X.X. Hu, P.P. He, G.B. Qi, Y.J. Gao, Y.X. Lin, C. Yang, P.P. Yang, H. Hao, L. Wang, H. Wang, Transformable nanomaterials as an artificial extracellular matrix for inhibiting tumor invasion and metastasis, ACS Nano 11 (4) (2017) 4086–4096, https://doi.org/10.1021/acsnano.7b00781.
[175] B. Auffinger, A.L. Tobias, Y. Han, G. Lee, D. Guo, M. Dey, M.S. Lesniak, A. U. Ahmed, Conversion of differentiated cancer cells into cancer stem-like cells in a glioblastoma model after primary chemotherapy, Cell Death Differ. 21 (7) (2014) 1119–1131, https://doi.org/10.1038/cdd.2014.31.
[176] H.S. Friedman, T. Kerby, H. Calvert, Temozolomide and treatment of malignant glioma, Clin. Cancer Res. 6 (2000) 2585–2597.
[177] A.O. Sasmita, Y.P. Wong, A.P.K. Ling, Biomarkers and therapeutic advances in glioblastoma multiforme, Asia Pac. J. Clin. Oncol. 14 (1) (2018) 40–51, https://doi.org/10.1111/ajco.12756.

CURRÍCULO LATTES

Jeferson Gustavo Henn

Endereço para acessar este CV: http://lattes.cnpq.br/0078772412119199
ID Lattes: **0078772412119199**
Última atualização do currículo em 15/10/2023

Farmacêutico generalista graduado pela Universidade de Santa Cruz do Sul - UNISC, mestre em Patologia (genética aplicada) pela Universidade Federal de Ciências da Saúde de Porto Alegre - UFCSPA e doutorando em Biociências também pela UFCSPA. Atua nas áreas de biologia celular do câncer, nanotecnologia aplicada a sistemas de drug delivery, engenharia de polímeros, farmacologia, toxicologia, ensaios in vitro e in vivo de atividades antitumoral, cicatrizante, anti-inflamatória, citotóxica, genotóxica e gastroprotetora, desenvolvimento de métodos de análises de compostos naturais por HPLC e fitoquímica. Possui também conhecimentos em rotinas de farmácia hospitalar e drogaria, com experiência em sistemas de controle de estoque de medicamentos e materiais hospitalares, além de ter atuado nas áreas de desenvolvimento comunitário, comunicação e relações interculturais. **(Texto informado pelo autor)**

Identificação

Nome	Jeferson Gustavo Henn
Nome em citações bibliográficas	HENN, J. G.;HENN, J.G.;HENN, JEFERSON GUSTAVO;HENN, JEFERSON G.;GUSTAVO HENN, JEFERSON
Lattes iD	http://lattes.cnpq.br/0078772412119199
Orcid iD	https://orcid.org/0000-0001-8229-1785

Endereço

Endereço Profissional	Fundação Universidade Federal de Ciências da Saúde de Porto Alegre, Departamento de Farmacologia e Toxicologia, Laboratório de Genética Toxicológica. Rua Sarmento Leite, 245, prédio 3, sala 714 Centro Histórico 90050170 - Porto Alegre, RS - Brasil Telefone: (51) 33038861

Formação acadêmica/titulação

2017	Doutorado em andamento em BIOCIÊNCIAS. Fundação Universidade Federal de Ciências da Saúde de Porto Alegre, UFCSPA, Brasil. com **período sanduíche** em Technological University of the Shannon: Midlands Midwest (Orientador: Michael Nugent). Título: Avaliação da eficácia da temozolomida acoplada a ferrocenos no tratamento de glioblastomas Orientador: Dinara Jaqueline Moura. Bolsista do(a): Coordenação de Aperfeiçoamento de Pessoal de Nível Superior, CAPES, Brasil.
2014 - 2016	Mestrado em Patologia. Fundação Universidade Federal de Ciências da Saúde de Porto Alegre, UFCSPA, Brasil. Título: Desenvolvimento de um extrato hidroetanólico das folhas de Plantago australis (Kunth) Rahn padronizado em verbascosídeo e determinação de sua segurança toxicológica, Ano de Obtenção: 2016. Orientador: Dinara Jaqueline Moura. Coorientador: Jenifer Saffi. Bolsista do(a): Coordenação de Aperfeiçoamento de Pessoal de Nível Superior, CAPES, Brasil.
2006 - 2012	Graduação em Farmácia. Universidade de Santa Cruz do Sul, UNISC, Brasil. Título: Avaliação da atividade gastroprotetora de Tripodanthus acutifolius (Ruiz & Pavón) Tieghem em ratos Wistar. Orientador: Chana de Medeiros da Silva.

Formação Complementar

2021 - 2021	Boas Práticas Clínicas. (Carga horária: 40h). Instituto Evandro Chagas, IEC, Brasil.
2019 - 2019	Revisão de literatura para consultores InnVitro. (Carga horária: 20h). INNVITRO PESQUISA & DESENVOLVIMENTO S/S LTDA, INNVITRO, Brasil.
2019 - 2019	Citometria de Fluxo aplicada a ensaios pré-clínicos. (Carga horária: 40h). Instituto Carlos Chagas/FIOCRUZ, ICC/FIOCRUZ, Brasil.
2015 - 2015	Extensão universitária em I Curso de toxicidade genética. (Carga horária: 50h). Fundação Universidade Federal de Ciências da Saúde de Porto Alegre, UFCSPA, Brasil.
2015 - 2015	Biossegurança em instituições de atenção à saúde. (Carga horária: 8h). Associação Nacional de Biossegurança, ANBIO, Brasil.
2014 - 2014	Extensão universitária em IV Estudo da sinalização celular no câncer. (Carga horária: 15h). Universidade Federal do Rio Grande do Sul, UFRGS, Brasil.
2014 - 2014	Língua Francesa - nível A2.3. (Carga horária: 27h). Aliança Francesa - Porto Alegre, AFPOA, Brasil.
2014 - 2014	Escola de Altos Estudos em Toxicologia. (Carga horária: 30h). Universidade Federal do Rio Grande do Sul, UFRGS, Brasil.
2007 - 2007	Extensão universitária em Projeto Rondon - edição 2007. (Carga horária: 450h). Universidade de Santa Cruz do Sul, UNISC, Brasil.
2007 - 2007	Extensão universitária em Dévelop. Communautaire, Relations Interculturelles. (Carga horária: 645h). Cégep Marie-Victorin, CÉGEP M-V, Canadá.
2007 - 2007	Curso de Francês - Projeto Rondon 2007. (Carga horária: 27h). Universidade de Santa Cruz do Sul, UNISC, Brasil.

Atuação Profissional

Abbott Ireland, AI, Irlanda.

Vínculo institucional

2022 - Atual	Vínculo: Celetista, Enquadramento Funcional: Technical Support Scientist, Carga horária: 39

Technological University of the Shannon: Midlands Midwest, TUS, Irlanda.

Vínculo institucional

2021 - Atual	Vínculo: Colaborador, Enquadramento Funcional: Pesquisador visitante
Outras informações	Materials Research Institute

Vínculo institucional

2021 - 2022	Vínculo: Celetista, Enquadramento Funcional: Pharmacy Technician, Carga horária: 19
Outras informações	Faculty of Science & Health

Vínculo institucional

2020 - 2021	Vínculo: Bolsista, Enquadramento Funcional: Bolsista de doutorado-sanduíche, Regime: Dedicação exclusiva.
Outras informações	Materials Research Institute

INNVITRO PESQUISA & DESENVOLVIMENTO S/S LTDA, INNVITRO, Brasil.

Vínculo institucional

2019 - Atual	Vínculo: Autônomo, Enquadramento Funcional: Consultor
Outras informações	Consultoria na área de toxicologia, realizando revisões bibliográficas para o cálculo de doses diárias permitidas (PDE) para indústrias farmacêuticas.

Fundação Universidade Federal de Ciências da Saúde de Porto Alegre, UFCSPA, Brasil.

Vínculo institucional

2021 - Atual	Vínculo: Pesquisador, Enquadramento Funcional: Doutorando, Regime: Dedicação exclusiva.

Vínculo institucional

2017 - 2020	Vínculo: Bolsista, Enquadramento Funcional: Pesquisador (doutorado - CAPES/FAPERGS), Regime: Dedicação exclusiva.
Outras informações	Bolsa suspensa durante período de doutorado-sanduíche

Vínculo institucional

2014 - 2016	

Vínculo: Bolsista, Enquadramento Funcional: Mestrando - CAPES, Regime: Dedicação exclusiva.

Atividades

11/2017 - Atual	Pesquisa e desenvolvimento, Departamento de Farmacologia e Toxicologia, Laboratória de Genética Toxicológica. Linhas de pesquisa Biologia celular do câncer Nanotecnologia
03/2014 - Atual	Pesquisa e desenvolvimento, Departamento de Farmacologia e Toxicologia, Laboratória de Genética Toxicológica. Linhas de pesquisa Farmacognosia Farmacologia Química de produtos naturais Genética toxicológica
2015 - 2019	Estágios , Departamento de Farmacociências. Estágio realizado Disciplinas de Toxicologia (Farmácia e Biomedicina), Bioquímica e Genética Toxicológica (Toxicologia Analítica), Farmacognosia (Farmácia) e Ensaios Pré-clínicos (Química Medicinal).
2015 - 2016	Conselhos, Comissões e Consultoria, Reitoria, Conselho Universitário. Cargo ou função Membro titular do Conselho Universitário - gestão 2015/2017.

DIMED SA, PANVEL FARMÁCIAS, Brasil.

Vínculo institucional

2016 - 2017	Vínculo: Celetista, Enquadramento Funcional: Farmacêutico, Carga horária: 44

Walmart Brasil - Farmácia BIG, WMB, Brasil.

Vínculo institucional

2013 - 2014	Vínculo: , Enquadramento Funcional: Farmacêutico Responsável Técnico, Carga horária: 44

Fundação Estadual de Produção e Pesquisa em Saúde, FEPPS, Brasil.

Vínculo institucional

2012 - 2013	Vínculo: Estágio, Enquadramento Funcional: Estagiário, Carga horária: 40
Outras informações	Seção de Microbiologia de Águas e Alimentos da FEPPS/IPB/LACEN-RS

Hospital Santa Cruz - SCS, HSC, Brasil.

Vínculo institucional

2013 - 2013	Vínculo: , Enquadramento Funcional: Farmacêutico Substituto, Carga horária: 44

Vínculo institucional

2010 - 2012	Vínculo: Celetista, Enquadramento Funcional: Atendente de Farmácia, Carga horária: 40

Ediberto de Oliveira Machado & Cia. Ltda, REDE AGAFARMA, Brasil.

Vínculo institucional

2008 - 2010	Vínculo: Celetista, Enquadramento Funcional: Atendente de farmácia, Carga horária: 30

Universidade de Santa Cruz do Sul, UNISC, Brasil.

Vínculo institucional

2006 - 2007	Vínculo: Bolsista, Enquadramento Funcional: Monitor - Laboratórios de Ensino de Química, Carga horária: 8

Prefeitura Municipal de Sinimbu, PMS, Brasil.

Vínculo institucional

2006 - 2007	Vínculo: Estagiário, Enquadramento Funcional: Atendente em Farmácia Municipal, Carga horária: 32

Linhas de pesquisa

1.	Farmacognosia
2.	Farmacologia

3. Química de produtos naturais
4. Genética toxicológica
5. Biologia celular do câncer
6. Nanotecnologia

Projetos de pesquisa

2013 - Atual

Desenvolvimento de um extrato padronizado de Plantago australis em verbascosídeo e determinação do potencial cicatrizante, anti-inflamatório e da sua segurança toxicológica
Projeto certificado pelo(a) coordenador(a) Dinara Jaqueline Moura em 21/05/2014.
Descrição: Este projeto tem como objetivo elaborar um extrato padronizado de P. australis, em verbascosídeo, e determinar o potencial cicatrizante e anti-inflamatório deste extrato em modelos in vitro e in vivo. Também serão conduzidos os ensaios biológicos in vitro com células gliais N9, para avaliação da atividade anti-inflamatória, com células de queratinócitos (HaCaT), para avaliação da atividade cicatrizante. Paralelamente serão realizados ensaios in vitro para determinação do potencial mutagênico. Os ensaios toxicológicos in vivo complementarão os ensaios biológicos e incluirão as avaliações farmacológicas (anti-inflamatória e cicatrizante) e os ensaios de toxicidade aguda, toxicidade de doses repetidas e genotoxicidade utilizando ratos Wistar.
Situação: Em andamento; Natureza: Pesquisa.
Alunos envolvidos: Mestrado acadêmico: (3) .

Integrantes: Jeferson Gustavo Henn - Integrante / Dinara Jaqueline Moura - Coordenador / jenifer saffi - Integrante / Nathalia Denise de Moura Sperotto - Integrante / Valéria Flores Péres - Integrante / Rodrigo Moisés Veríssimo - Integrante / STEFFENS, LUIZA - Integrante.
Financiador(es): Fundação de Amparo à Pesquisa do Estado do Rio Grande do Sul - Auxílio financeiro.

Projetos de extensão

2007 - 2007

Projeto Rondon - RS / UNISC / Jeunesse Canada Monde
Descrição: Trabalho voluntário em projetos assistenciais no Brasil e Canadá. Vivência de novas culturas pelo convívio com irmãos de acolhida canadenses em famílias locais, com aprendizado das línguas francesa, inglesa e oportunidade de ensinar o idioma português. Viagens de estudo e reflexão a diversos pontos do Rio Grande do Sul e Canadá.
Situação: Concluído; Natureza: Extensão.
Alunos envolvidos: Graduação: (9) .

Integrantes: Jeferson Gustavo Henn - Integrante / Adriana Silveira da Motta - Integrante / Andressa Pens Lazzari - Integrante / Marluce Purper - Integrante / Patrícia Lucinha Rechia Fighera - Integrante / Cássio Vieira Rosa - Integrante / Joel Eduardo Haas de Oliveira - Integrante / Emerson Vogt - Integrante / Mateus Antunes Pereira - Integrante / Cristiana Verônica Mueller - Coordenador.

Revisor de periódico

2019 - Atual

Periódico: JOURNAL OF BIOMEDICAL MATERIALS RESEARCH PART B-APPLIED BIOMATERIALS

Idiomas

Português Compreende Bem, Fala Bem, Lê Bem, Escreve Bem.
Francês Compreende Razoavelmente, Fala Razoavelmente, Lê Bem, Escreve Razoavelmente.
Inglês Compreende Bem, Fala Bem, Lê Bem, Escreve Bem.
Alemão Compreende Razoavelmente, Fala Pouco, Lê Bem, Escreve Pouco.
Espanhol Compreende Razoavelmente, Fala Pouco, Lê Bem, Escreve Pouco.

Prêmios e títulos

2016 Menção honrosa - XXXI Reunião Anual da Federação de Sociedades de Biologia Experimental, Federação de Sociedades de Biologia Experimental.
2015 Destaque, categoria "Trabalhos relacionados à pesquisa" - I Mostra de trabalhos de ensino, pesquisa e extensão, Universidade Federal de Ciências da Saúde de Porto Alegre.
2014 Convocação para vaga em Residência Multiprofissional Integrada em Saúde: área de concentração em Intensivismo, Urgência e Emergência, APESC - Hospital Santa Cruz.
2013

Convocação para vaga em Residência Integrada Multiprofissional em Saúde: área de concentração em Controle de Infecção Hospitalar, Hospital de Clínicas de Porto Alegre. **2012**

Orador da turma de formandos do Curso de Farmácia 2012/2, Universidade de Santa Cruz do Sul. **2012**

Honra ao mérito por atingir a nota 8.861, considerada a melhor média geral da turma de formandos do Curso de Farmácia 2012/2, Universidade de Santa Cruz do Sul. **2012**

Aprovação em Concurso Público para o cargo de Farmacêutico, Prefeitura Municipal de Santa Cruz do Sul.

Produções

Produção bibliográfica

Citações

Web of Science

Total de trabalhos:10 Total de citações:98
Fator H:5

Henn, Jeferson Gustavo; Henn, J. G.; Henn, Jeferson G. Data: 14/10/2023

SCOPUS

Total de trabalhos:12 Total de citações:115

Henn, Jeferson Gustavo; Henn, J. G.; Henn, Jeferson G. Data: 14/10/2023

Outras

Total de trabalhos:16 Total de citações:164

Henn, Jeferson Gustavo; Henn, J.G.; Henn, Jeferson Data: 14/10/2023

Artigos completos publicados em periódicos

Ordenar por

Ordem Cronológica

1. **HENN, JEFERSON GUSTAVO**; BERNARDES FERRO, MATHEUS ; LOPES ALVES, GABRIEL ANTONIO ; PIRES PEÑA, FLÁVIA ; DE OLIVEIRA, JOÃO VITOR RAUPP ; DE SOUZA, BÁRBARA MÜLLER ; DA SILVA, LEONARDO FONSECA ; RAPACK JACINTO SILVA, VICTÓRIA ; SILVA PINHEIRO, ANA CAROLINA ; STEFFENS REINHARDT, LUIZA ; MORÁS, ANA MOIRA ; NUGENT, MICHAEL ; DA ROSA, RICARDO GOMES ; SILVEIRA AGUIRRE, TANIRA ALESSANDRA ; MOURA, DINARA JAQUELINE . Development and characterization of a temozolomide-loaded nanoemulsion and the effect of ferrocene pre and co-treatments in glioblastoma cell models. Pharmacological Reports JCR, v. x, p. x, 2023.

2. STEFFENS REINHARDT, LUIZA ; MOIRA MORÁS, ANA ; **GUSTAVO HENN, JEFERSON** ; RICARDO ARANTES, PABLO ; BERNARDES FERRO, MATHEUS ; BRAGANHOL, ELIZANDRA ; OLIVEIRA DE SOUZA, PRISCILA ; DE OLIVEIRA MERIB, JOSIAS ; RAMOS BORGES, GABRIELA ; SILVEIRA DALANHOL, CAROLINA ; COX HOLANDA DE BARROS DIAS, MABILLY ; NUGENT, MICHAEL ; JAQUELINE MOURA, DINARA . Nek1-inhibitor and temozolomide-loaded microfibers as a co-therapy strategy for glioblastoma treatment. INTERNATIONAL JOURNAL OF PHARMACEUTICS JCR, v. 617, p. 121584, 2022.

Citações: WEB OF SCIENCE ® 3 | 3

3. DE LIMA, TIELIDY A. DE M. ; de Lima, Gabriel Goetten ; Chee, Bor Shin ; **HENN, JEFERSON G.** ; CORTESE, YVONNE J. ; MATOS, MAILSON ; HELM, CRISTIANE V. ; MAGALHÃES, WASHINGTON L. E. ; NUGENT, MICHAEL J. D. . Characterization of Gels and Films Produced from Pinhão Seed Coat Nanocellulose as a Potential Use for Wound Healing Dressings and Screening of Its Compounds towards Antitumour Effects. Polymers JCR, v. 14, p. 2776, 2022.

Citações: WEB OF SCIENCE ® 1 | 2

4. REINHARDT, LUIZA STEFFENS ; **HENN, JEFERSON GUSTAVO** ; MORÁS, ANA MOIRA ; DE MOURA SPEROTTO, NATHALIA DENISE ; FERRO, MATHEUS BERNARDES ; CAO, ZHI ; ROEHE, ADRIANA VIAL ; PETRY, ADRIANA UBIRAJARA SILVA ; NUGENT, MICHAEL ; MOURA, DINARA JAQUELINE . Plantago australis Hydroethanolic Extract-Loaded Formulations: Promising Dressings for Wound Healing. BRAZILIAN JOURNAL OF PHARMACOGNOSY JCR, v. 31, p. 91-101, 2021.

Citações: WEB OF SCIENCE ® 5 | 5

5. MORÁS, A.M. ; **HENN, J.G.** ; STEFFENS REINHARDT, L. ; LENZ, G. ; MOURA, D.J. . Recent developments in drug delivery strategies for targeting DNA damage response in glioblastoma. LIFE SCIENCES JCR, v. 287, p. 120128, 2021.

Citações: WEB OF SCIENCE ™ 6 | 7

6. FAVERZANI, JÉSSICA LAMBERTY ; STEINMETZ, ALINE ; DEON, MARION ; MARCHETTI, DESIRÉE PADILHA ; GUERREIRO, GILIAN ; SITTA, ANGELA ; DE MOURA COELHO, DANIELLA ; LOPES, FRANCIELE FATIMA ; NASCIMENTO, LEOPOLDO VINICIUS MARTINS ; STEFFENS, LUIZA ; **HENN, JEFERSON GUSTAVO** ; FERRO, MATHEUS BERNARDES ; BRITO, VERÔNICA BIDINOTTO ; WAJNER, MOACIR ; MOURA, DINARA JAQUELINE ; VARGAS, CARMEN REGLA . L-carnitine protects DNA oxidative damage induced by phenylalanine and its keto acid derivatives in neural cells: a possible pathomechanism and adjuvant therapy for brain injury in phenylketonuria. METABOLIC BRAIN DISEASE JCR, v. 36, p. 1957-1968, 2021.

Citações: WEB OF SCIENCE ™ 2 | 2

7. TONELLI, AMANDA M. ; VENTURINI, JANIO ; ARCARO, SABRINA ; **HENN, JEFERSON G.** ; MOURA, DINARA J. ; VIEGAS, ALEXANDRE DA CAS ; BERGMANN, CARLOS P. . Novel core-shell nanocomposites based on TIO 2 -covered magnetic Co 3 O 4 for biomedical applications. JOURNAL OF BIOMEDICAL MATERIALS RESEARCH PART B: APPLIED BIOMATERIALS JCR, v. 108, p. 1879-1887, 2020.

Citações: WEB OF SCIENCE ™ 9 | 13

8. DE MOURA SPEROTTO, NATHALIA DENISE ; STEFFENS, LUIZA ; VERÍSSIMO, RODRIGO MOISÉS ; **HENN, JEFERSON GUSTAVO** ; PÉRES, VALÉRIA FLORES ; VIANNA, PRISCILA ; CHIES, JOSÉ ARTUR BOGO ; ROEHE, ADRIANA ; SAFFI, JENIFER ; MOURA, DINARA JAQUELINE . Wound healing and anti-inflammatory activities induced by a Plantago australis hydroethanolic extract standardized in verbascoside. JOURNAL OF ETHNOPHARMACOLOGY JCR, v. 225, p. 178-188, 2018.

Citações: WEB OF SCIENCE ™ 33 | 37

9. **HENN, JEFERSON GUSTAVO**; STEFFENS, LUIZA ; SPEROTTO, NATHALIA DENISE DE MOURA ; DE SOUZA PONCE, BETÂNIA ; VERÍSSIMO, RODRIGO MOISÉS ; BOARETTO, FERNANDA BRIÃO MENEZES ; HASSEMER, GUSTAVO ; PÉRES, VALÉRIA FLORES ; SCHIRMER, HELENA ; PICADA, JAQUELINE NASCIMENTO ; SAFFI, JENIFER ; MOURA, DINARA JAQUELINE . Toxicological evaluation of a standardized hydroethanolic extract from leaves of Plantago australis and its major compound, verbascoside. JOURNAL OF ETHNOPHARMACOLOGY JCR, v. 229, p. 145-156, 2018.

Citações: WEB OF SCIENCE ™ 18 | 21

10. BALDISSERA, G. ; SPEROTTO, N.D.M. ; ROSA, H.T. ; **HENN, J.G.** ; PERES, V.F. ; MOURA, D.J. ; ROEHRS, R. ; DENARDIN, E.L.G. ; DAL LAGO, P. ; NUNES, R.B. ; SAFFI, J. . Effects of crude hydroalcoholic extract of Syzygium cumini (L.) Skeels leaves and continuous aerobic training in rats with diabetes induced by a high-fat diet and low doses of streptozotocin. JOURNAL OF ETHNOPHARMACOLOGY JCR, v. 194, p. 1012-1021, 2016.

Citações: WEB OF SCIENCE ™ 21 | 25

Capítulos de livros publicados

1. STEFFENS, LUIZA ; de Barros Dias, Mabilly Cox Holanda ; Arantes, Pablo Ricardo ; **HENN, JEFERSON GUSTAVO** ; NUGENT, MICHAEL ; MOURA, DINARA JAQUELINE . Nanopolymeric systems to improve brain cancer treatment outcomes. In: Amit Nayak; Kunal Pal; Indranil Banerjee; Samarendra Maji; Upendranath Nanda. (Org.). Advances and Challenges in Pharmaceutical Technology. 1ed.: Elsevier, 2021, v. , p. 355-394.
2. Seba, Viviane ; Silva, Gabriel ; Chee, Bor Shin ; **HENN, JEFERSON GUSTAVO** ; de Lima, Gabriel Goetten ; CAO, ZHI ; Marins, Mozart ; NUGENT, MICHAEL . Stimuli-responsive biopolymeric systems for drug delivery to cancer cells. In: Hriday Bera, Buddhadev Layek, Jagdish Singh. (Org.). Tailor-Made and Functionalized Biopolymer Systems. 1ed.: Elsevier, 2021, v. , p. 663-704.
3. REINHARDT, LUIZA STEFFENS ; Arantes, Pablo Ricardo ; **HENN, JEFERSON GUSTAVO** ; MOURA, DINARA JAQUELINE . Bionanocomposites for In Situ Drug Delivery in Cancer Therapy: Early and Late Evaluations. In: Amit Kumar Nayak; Md Saquib Hasnain. (Org.). Materials Horizons: From Nature to Nanomaterials. 1ed.: Springer Singapore, 2021, v. , p. 145-165.

Resumos publicados em anais de congressos

1. LOPES, G. A. ; FERRO, M. B. ; **HENN, JEFERSON G.** ; ROSA, R. G. ; MOURA, D. J. ; AGUIRRE, T. A. S. . Desenvolvimento de nanoemulsões contendo temozolomida e ferroceno como alternativa para o tratamento de glioblastoma. In: Congresso UFCSPA: conectando saúde e sociedade, 2019, Porto Alegre. Congresso UFCSPA: conectando saúde e sociedade. Recife: Even3, 2019. v. 1. p. 232-233.
2. FERRO, MATHEUS BERNARDES ; **HENN, JEFERSON GUSTAVO** ; STEFFENS, LUIZA ; ALVES, GABRIEL ANTONIO LOPES ; ROSA, RICARDO GOMES DA ; AGUIRRE, TANIRA ; MOURA, DINARA JAQUELINE . INFLUÊNCIA DE NANOEMULSÕES DE NÚCLEO LIPÍDICO CONTENDO COMPOSTOS DE FERROCENOS NA VIABILIDADE DE CÉLULAS DE GLIOBLASTOMA TRATADAS COM TEMOZOLOMIDA. In: Anais do Congresso UFCSPA: conectando saúde e sociedade, 2019, UFCSPA. Anais do(a) Anais do Congresso UFCSPA: conectando saúde e sociedade. Recife: Even3, 2019. v. 1.
3. REINHARDT, L. S. ; **HENN, JEFERSON G.** ; MORAS, A. M. ; SPEROTTO, N. D. M. ; FERRO, M. B. ; CAO, Z. ; NUGENT, M. ; MOURA, DINARA J. . Caracterização e avaliação da atividade cicatrizante de nanofibras poliméricas contendo extrato hidroetanólico de Plantago australis. In: Congresso UFCSPA: conectando saúde e sociedade, 2019, Porto Alegre. Congresso UFCSPA: conectando saúde e sociedade. Recife: Even3, 2019. v. 1. p. 706-707.
4. SEVERO, J. E. ; SILVA, C. M. ; **HENN, J. G.** . Avaliação da atividade Gastroprotetora de Tripodanthus acutifolius (Ruiz & Pavón) Tieghem em ratos Wistar. In: IV Salão de Ensino e de Extensão, 2013, Santa Cruz do Sul. Anais do Salão de Ensino e de Extensão. Santa Cruz do Sul: EDUNISC, 2013. v. 3.

Apresentações de Trabalho

1.

LOPES, G. A. ; FERRO, M. B. ; **HENN, J. G.** ; ROSA, R. G. ; MOURA, D. J. ; AGUIRRE, T. A. S. . Desenvolvimento de nanoemulsões contendo temozolomida e ferroceno como alternativa para o tratamento de glioblastoma. 2019. (Apresentação de Trabalho/Congresso).

2. FERRO, M. B. ; **HENN, J. G.** ; REINHARDT, L. S. ; LOPES, G. A. ; ROSA, R. G. ; AGUIRRE, T. A. S. ; MOURA, D. J. . Influência de nanoemulsões de núcleo lipídico contendo compostos de ferrocenos na viabilidade de células de glioblastoma tratadas com temozolomida. 2019. (Apresentação de Trabalho/Congresso).
3. REINHARDT, L. S. ; **HENN, J. G.** ; MORAS, A. M. ; SPEROTTO, N. D. M. ; FERRO, M. B. ; CAO, Z. ; NUGENT, M. ; MOURA, D. J. . Caracterização e avaliação da atividade cicatrizante de nanofibras poliméricas contendo extrato hidroetanólico de Plantago australis. 2019. (Apresentação de Trabalho/Congresso).
4. FERRO, M. B. ; REINHARDT, L. S. ; **HENN, J.G.** ; MORAS, A. M. ; SPEROTTO, N. D. M. ; CAO, Z. ; NUGENT, M. ; MOURA, D. J. . Plantago australis hydroethanolic extract electrospun nanofibers for wound healing. 2019. (Apresentação de Trabalho/Outra).
5. REINHARDT, L. S. ; MORAS, A. M. ; ARANTES, P. R. ; **HENN, J.G.** ; BRAGANHOL, E. ; SOUZA, P. O. ; DIAS, M. C. H. B. ; CAO, Z. ; NUGENT, M. ; MOURA, D. J. . Nek1-inhibitor and temozolomide-loaded nanofibers as a co-therapy strategy for glioblastoma treatment. 2019. (Apresentação de Trabalho/Outra).
6. **HENN, J.G.**; FERRO, M. B. ; REINHARDT, L. S. ; LOPES, G. A. ; ROSA, R. G. ; AGUIRRE, T. A. S. ; MOURA, D. J. . Influence of nanoemulsions containing ferrocene compounds on the viability of glioblastoma cells treated with temozolomide. 2019. (Apresentação de Trabalho/Outra).
7. **HENN, J.G.**. Metodologias bioanalíticas. 2018. (Apresentação de Trabalho/Conferência ou palestra).
8. **HENN, J.G.**; ROSA, R. G. ; POLETTO, F. ; MOURA, D.J. . Influence of ferrocene compounds on the viability of glioblastoma cells treated with temozolomide. 2018. (Apresentação de Trabalho/Outra).
9. **HENN, J.G.**. Estudo toxicológico e farmacológico do extrato hidroetanólico de Plantago australis e de seu marcador, verbascosídeo. 2018. (Apresentação de Trabalho/Seminário).
10. **HENN, JEFERSON GUSTAVO**; POLETTO, F. ; ROSA, R. G. ; MOURA, DINARA JAQUELINE . Influência de ferrocenos na viabilidade de células de glioblastoma tratadas com temozolomida. 2018. (Apresentação de Trabalho/Outra).
11. ROSA, H. T. ; REINHARDT, L. S. ; **HENN, J. G.** ; SCHUCHMANN, E. T. ; IMMICH, B. F. ; SAFFI, J. ; MOURA, D. J. . Fanconi anemia: recent remarks and model of study using lymphoblastoid cells from patients. 2016. (Apresentação de Trabalho/Outra).
12. VERÍSSIMO, RODRIGO MOISÉS ; SPEROTTO, N.D.M. ; **HENN, J.G.** ; SAFFI, J. ; MOURA, D.J. . Avaliação da atividade anti-inflamatória de um extrato hidroetanólico de Plantago australis (Kunth) Rahn e seu composto verbascosídeo, em modelos in vitro. 2016. (Apresentação de Trabalho/Outra).
13. VERISSIMO, R. M. ; SPEROTTO, N. D. M. ; **HENN, J. G.** ; PERES, V. F. ; SAFFI, J. ; MOURA, D. J. . Atividade cicatrizante do extrato etanólico de Plantago major e seu marcador analítico verbascosídeo. 2015. (Apresentação de Trabalho/Outra).
14. **HENN, J. G.**; PONCE, B. S. ; SPEROTTO, N. D. M. ; VERISSIMO, R. M. ; PERES, V. F. ; SAFFI, J. ; MOURA, D. J. . Desenvolvimento de um extrato etanólico padronizado de Plantago major L. em verbascosídeo e determinação de sua segurança toxicológica. 2015. (Apresentação de Trabalho/Outra).
15. PONCE, B. S. ; **HENN, J. G.** ; SPEROTTO, N. D. M. ; VERISSIMO, R. M. ; PERES, V. F. ; SAFFI, J. ; MOURA, D. J. . Avaliação da citotoxicidade do extrato etanólico de Plantago major L. padronizado em verbascosídeo. 2015. (Apresentação de Trabalho/Outra).
16. VERISSIMO, R. M. ; **HENN, J. G.** ; SPEROTTO, N. D. M. ; PERES, V. F. ; SAFFI, J. ; MOURA, D. J. . Desenvolvimento e padronização de extratos etanólicos das folhas de Plantaginaceae. 2014. (Apresentação de Trabalho/Outra).
17. SEVERO, J. E. ; SILVA, C. M. ; **HENN, J. G.** . Avaliação da atividade gastroprotetora de Tripodanthus acutifolius (Ruiz & Pavón) Tieghem em ratos Wistar. 2013. (Apresentação de Trabalho/Outra).

Produção técnica

Entrevistas, mesas redondas, programas e comentários na mídia

1. MOTTA, A. S. ; LAZZARI, A. P. ; ROSA, C. V. ; MUELLER, C. V. ; VOGT, E. ; **HENN, J.G.** ; OLIVEIRA, J. E. H. ; PURPER, M. ; PEREIRA, M. A. ; FIGHERA, P. L. R. . Uma experiência que 'vale a pena'. 2008. (Programa de rádio ou TV/Entrevista).

Demais tipos de produção técnica

1. **HENN, J.G.**; REINHARDT, L. S. ; MORAS, A. M. . Metodologias bioanalíticas. 2018. (Curso de curta duração ministrado/Extensão).
2. **HENN, JEFERSON GUSTAVO**; SILVA, A. O. . Cultura 3D (Método comercial e home-made). 2018. (Curso de curta duração ministrado/Outra).
3. **HENN, J.G.**; REINHARDT, L. S. ; MORAS, A. M. . Micronúcleo. 2018. (Curso de curta duração ministrado/Extensão).

Eventos

Participação em eventos, congressos, exposições e feiras

1. AIT Postgraduate Poster Event.Evaluation of the efficacy of lipid core nanoemulsions containing temozolomide coupled to ferrocenes in the treatment of glioblastomas. 2020. (Outra).
2. IV Encontro do PPG Biociências. 2019. (Encontro).
3.

IV Encontro do PPG Biociências.Influence of nanoemulsions containing ferrocene compounds on the viability of glioblastoma cells treated with temozolomide. 2019. (Encontro).

4. Seminars in Biomedical Sciences 2019. 2019. (Seminário).
5. UFCSPA Acolhe 2019. Monitoria. 2019. (Feira).
6. III Encontro do PPG Biociências da UFCSPA & Encontro de Pesquisa em Biologia Celular.Influência de ferrocenos na viabilidade de células de glioblastoma tratadas com temozolomida. 2018. (Encontro).
7. III Encontro do PPG Biociências da UFCSPA e Encontro de Pesquisa em Biologia Celular. 2018. (Encontro).
8. UFCSPA Acolhe 2018. Monitoria. 2018. (Feira).
9. VI Fundamental aspects of DNA repair and mutagenesis, VI FARM-DNA. 2018. (Encontro).
10. Cellularised Scaffolds, Co-cultures and Bioreactors for Engineering the Vascular Wall: Potential for Tissue Regeneration?. 2015. (Seminário).
11. Curso de língua e cultura tcheca. 2015. (Outra).
12. Fosfoetanolamina: a polêmica da droga anticâncer. 2015. (Outra).
13. I Jornada acadêmica do curso de Toxicologia Analítica da UFCSPA. 2015. (Outra).
14. IX Congresso brasileiro de biossegurança. 2015. (Congresso).
15. Soluções para Preparo de Amostras e Separações cromatográficas. 2015. (Outra).
16. Toxicologia em debate: acidentes em massa. 2015. (Outra).
17. X Jornada do Programa de Pós-Graduação em Patologia. 2015. (Outra).
18. 5ª Jornada Científica e III Seminário Científico e Tecnológico/FEPPS. 2012. (Outra).
19. Genética e Toxicologia Forense. 2010. (Oficina).
20. Radiofármacos. 2010. (Outra).
21. Intercâmbio Cultural Brasil-Canadá 2007.Relações Comunitárias e Comunicação Intercultural. 2007. (Outra).
22. Programme international éducatif Québec / Brésil - 2007.Guia de aprendizagens - Certificado de estudos colegiais em desenvolvimento Comunitário e relações interculturais. 2007. (Outra).
23. Injetáveis na Prática. 2006. (Outra).
24. Tendências do Mercado Farmacêutico. 2006. (Oficina).
25. VI Semana Acadêmica do Curso de Farmácia: "Amplie seus conhecimentos: promova saúde". 2006. (Outra).

Organização de eventos, congressos, exposições e feiras

1. MOURA, D.J. ; SAFFI, J. ; **HENN, J.G.** ; REINHARDT, L. S. ; MORAS, A. M. ; GLORIA, H. C. E. ; NASCIMENTO, L. V. M. . II Curso de Toxicidade Genética: curso de verão. 2018. (Outro).
2. MOURA, D.J. ; SAFFI, J. ; VILLELA, I. V. ; MACHADO, M. S. ; **HENN, J.G.** ; MORAS, A. M. ; JUCHEM, A. L. M. . Curso Teórico-Prático para Utilização de Métodos Alternativos ao Uso de Animais in vitro para Avaliação do Potencial Genotóxico de Substâncias Químicas ? Avaliação de Micronúcleos in vitro OECD 487. 2018. (Outro).
3. MORAS, A. M. ; VIAU, C. M. ; MOURA, D. J. ; BUSATTO, F. F. ; ROSA, H. T. ; **HENN, J. G.** ; SAFFI, J. ; REINHARDT, L. S. . I Curso de toxicidade genética: causas, consequências e ensaios pré-clínicos. 2015. (Outro).
4. ALMEIDA, L. M. E. ; BRIXNER, B. ; GOMES, R. R. ; **HENN, J. G.** ; HORN, C. ; KITTEL, C. S. ; OLIVEIRA, I. L. ; SILVA, C. L. A. ; SILVA, D. C. L. ; TWORKOWSKI, C. S. ; WALTER, F. Z. ; ZIMMER, E. . IX Semana Acadêmica do Curso de Farmácia:. 2009. (Outro).
5. ALMEIDA, L. M. E. ; BRIXNER, B. ; GOMES, R. R. ; **HENN, J. G.** ; HORN, C. ; KITTEL, C. S. ; NIETIEDT, J. ; OLIVEIRA, I. L. ; SILVA, C. L. A. ; SILVA, D. C. L. ; TWORKOWSKI, C. S. ; WALTER, F. Z. ; ZIMMER, E. . VIII Semana Acadêmica do Curso de Farmácia:. 2008. (Outro).

Orientações

Orientações e supervisões concluídas

Trabalho de conclusão de curso de graduação

1. Matheus Bernardes Ferro. Simulação in vitro de um protocolo clínico para o tratamento de glioblastoma utilizando temozolomida em combinação com ferroceno. 2023. Trabalho de Conclusão de Curso. (Graduação em Farmácia) - Fundação Universidade Federal de Ciências da Saúde de Porto Alegre. Orientador: Jeferson Gustavo Henn.
2. Jucelaine Kulmann de Medeiros. Avaliação da citotoxicidade de extrato de Maytenus ilicifolia em células de hepatocarcinoma humano. 2019. Trabalho de Conclusão de Curso. (Graduação em Farmácia) - Fundação Universidade Federal de Ciências da Saúde de Porto Alegre. Orientador: Jeferson Gustavo Henn.

Iniciação científica

1. Matheus Bernardes Ferro. Preparação de nanoemulsões de núcleo lipídico contendo temozolomida acoplada a ferrocenos para o tratamento de glioblastomas. 2019. Iniciação Científica. (Graduando em Farmácia) - Fundação Universidade Federal de Ciências da Saúde de Porto Alegre, Conselho Nacional de Desenvolvimento Científico e Tecnológico. Orientador: Jeferson Gustavo Henn.
2. Betânia de Souza Ponce. Desenvolvimento de um extrato padronizado de Plantago major L. em ácidos triterpênicos e determinação do potencial cicatrizante, anti-inflamatório e da sua segurança toxicológica. 2015. Iniciação Científica. (Graduando em Biomedicina) - Fundação Universidade Federal de Ciências da Saúde de Porto Alegre. Orientador: Jeferson Gustavo Henn.

3. Rodrigo Moises Veríssimo. Determinação do potencial cicatrizante e anti-inflamatório de um extrato padronizado de Plantago major L. em ácidos triterpênicos. 2014. Iniciação Científica. (Graduando em Biomedicina) - Fundação Universidade Federal de Ciências da Saúde de Porto Alegre, Conselho Nacional de Desenvolvimento Científico e Tecnológico. Orientador: Jeferson Gustavo Henn.

Educação e Popularização de C & T

Cursos de curta duração ministrados

1. **HENN, J.G.**; REINHARDT, L. S. ; MORAS, A. M. . Metodologias bioanalíticas. 2018. (Curso de curta duração ministrado/Extensão).
2. **HENN, J.G.**; REINHARDT, L. S. ; MORAS, A. M. . Micronúcleo. 2018. (Curso de curta duração ministrado/Extensão).

Organização de eventos, congressos, exposições e feiras

1. MOURA, D.J. ; SAFFI, J. ; **HENN, J.G.** ; REINHARDT, L. S. ; MORAS, A. M. ; GLORIA, H. C. E. ; NASCIMENTO, L. V. M. . II Curso de Toxicidade Genética: curso de verão. 2018. (Outro).
2. MORAS, A. M. ; VIAU, C. M. ; MOURA, D. J. ; BUSATTO, F. F. ; ROSA, H. T. ; **HENN, J. G.** ; SAFFI, J. ; REINHARDT, L. S. . I Curso de toxicidade genética: causas, consequências e ensaios pré-clínicos. 2015. (Outro).

Página gerada pelo Sistema Currículo Lattes em 11/11/2023 às 10:16:05

Imprimir currículo